ORNL/CDIAC-138
NDP-080

Carbon Dioxide, Hydrographic, and Chemical Data Obtained During the Nine *R/V Knorr* Cruises Comprising the Indian Ocean CO_2 Survey

(WOCE Sections I8SI9S, I9N, I8NI5E, I3, I5WI4, I7N, I1, I10, and I2; December 1, 1994 – January 19, 1996)

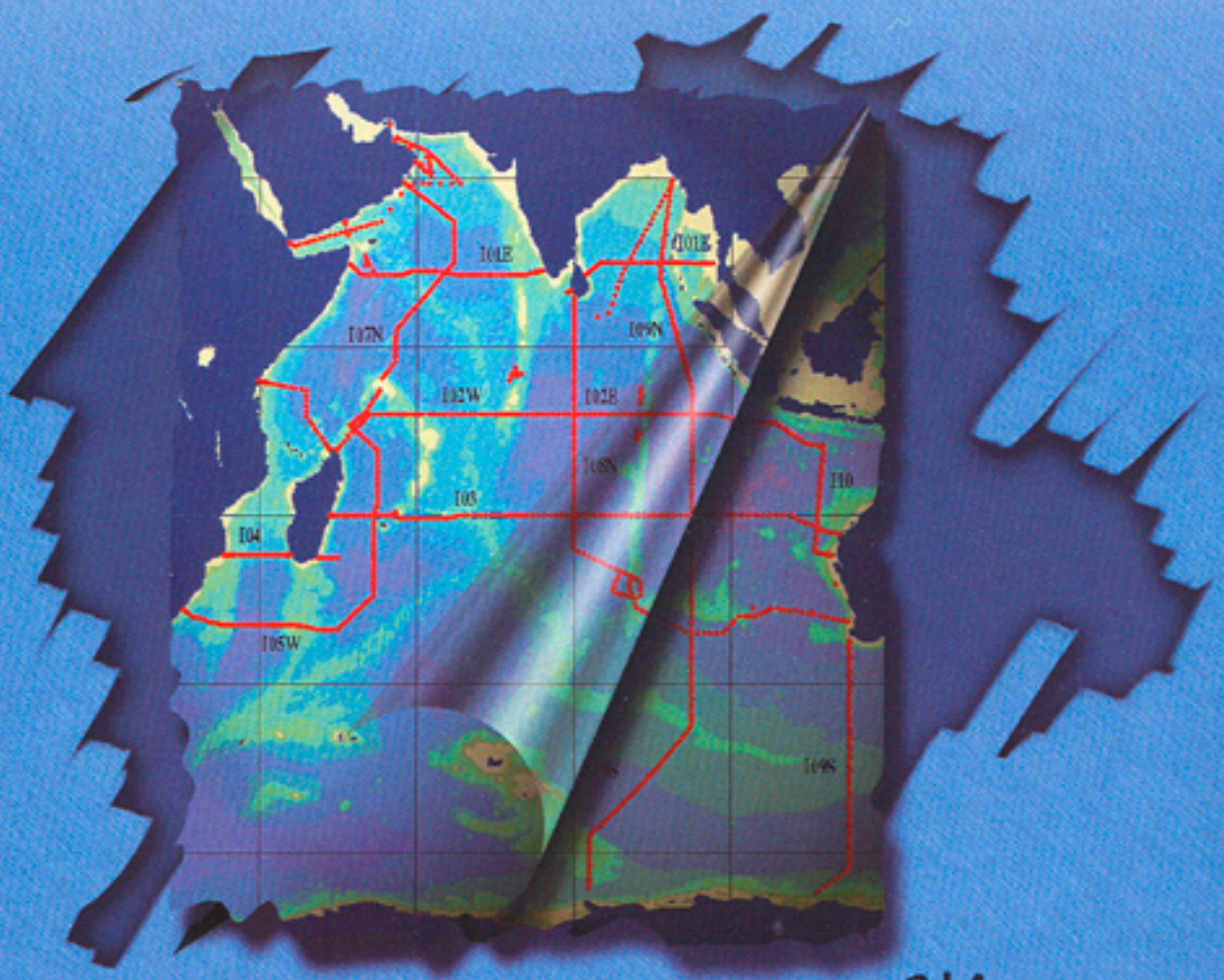

WOCE

JGOFS

CDIAC

CONTENTS

LIST OF FIGURES v

LIST OF TABLES vii

ACRONYMS ix

ABSTRACT xi

PART 1: OVERVIEW 1

1. BACKGROUND INFORMATION 3

2. DESCRIPTION OF THE EXPEDITION 5

2.1 R/V *Knorr*: Technical Details and History 5

2.2 The Indian Ocean CO_2 Survey Cruises Information 7

2.3 Brief Cruise Summary 11

3. DESCRIPTION OF VARIABLES AND METHODS 15

3.1 Hydrographic Measurements 15
3.1.1 SIO/ODF Methods and Instrumentation 15
3.1.2 WHOI Methods and Instrumentation 18
3.1.3 Underway Measurements 19

3.2 Total Carbon Dioxide Measurements 19

3.3 Total Alkalinity Measurements 25

3.4 Carbon Data Synthesis and Analysis 29

3.5 Radiocarbon Measurements 29

4. DATA CHECKS AND PROCESSING PERFORMED BY CDIAC 30

5. HOW TO OBTAIN THE DATA AND DOCUMENTATION 34

6. REFERENCES 35

PART 2: CONTENT AND FORMAT OF DATA FILES 39

7. FILE DESCRIPTIONS **41**

7.1 ndp080.txt (File 1) **42**

7.2 IOstainv.for (File 2) **42**

7.3 i*dat.for (File 3) **43**

7.4 i*sta.dat (Files 4–12) **44**

7.5 i*.dat (File 13–21) **45**

APPENDIX A: List of CO_2 Measurement Group Members Participating in the Indian Ocean CO_2 Survey of 1994–1996 Aboard the R/V *Knorr* **A-1**

APPENDIX B: Reprint of Pertinent Literature **B-1**
Johnson, K. M., A. G. Dickson, G. Eischeid, C. Goyet, P. R. Guenther, R. M. Key, F. J. Millero, D. Purkerson, C. L. Sabine, R. G. Schotle, D. W. R. Wallace, R. J. Wilke, and C. D. Winn. 1998. Coulometric total carbon dioxide analysis for marine studies: Assessment of the quality of total inorganic carbon measurements made during the U.S. Indian Ocean CO_2 Survey 1994–1996. *Marine Chemistry* 63:21–37.

APPENDIX C: Reprint of Pertinent Literature **C-1**
Millero, F. J., A. G. Dickson, G. Eischeid, C. Goyet, P. R. Guenther, K. M. Johnson, K. Lee, E. Lewis, D. Purkerson, C. L. Sabine, R. Key, R. G. Schottle, D. R. W. Wallace, and C. D. Winn. 1998. Total alkalinity measurements in the Indian Ocean during the WOCE hydrographic program CO2 survey cruises 1994–1996. *Marine Chemistry* 63:9–20.

APPENDIX D: Reprint of Pertinent Literature **D-1**
Sabine, C. L., R. M. Key, K. M.. Johnson, F. J. Millero, J. L. Sarmiento, D. R. W. Wallace, and C. D. Winn. 1999. Anthropogenic CO_2 inventory of the Indian Ocean. *Global Biogeochemical Cycles* 13:179–98.

APPENDIX E: Reprint of Pertinent Literature **E-1**
Key R. M., and P. D. Quay. 2002. U.S. WOCE Indian Ocean Survey: Final Report for Radiocarbon. Technical Report. Princeton University, Princeton, N.J.

LIST OF FIGURES

Figure

1 The cruise track during the R/V *Knorr* expeditions in the Indian Ocean along WOCE Sections I8SI9S, I9N, I8NI5E, I3, I5WI4, I7N, I1, and I2 4

2 Sampling depths at all hydrographic stations occupied during the R/V *Knorr* Indian Ocean survey along WOCE Section I9N 21

3 Example of ODV station mode plot: measurements vs depth for Stations 172–174 of Section I9N 31

4 Distribution of the TCO_2 and TALK in seawater along WOCE Section I9N 32

5 Property-property plots for all stations occupied during the R/V *Knorr* cruise along WOCE Section I9N 33

LIST OF TABLES

Table

1 Technical characteristics of R/V *Knorr* 6

2 Dates, ports of call, expedition codes (EXPOCODEs), and names of chief scientists during Indian Ocean CO_2 survey cruises 7

3 WOCE measurement programs and responsible institutions during Indian Ocean CO_2 survey cruises 8

4 Principal investigators and senior at-sea personnel responsible for the WOCE measurement programs during Indian Ocean CO_2 survey cruises 9

5 Personnel responsible for carbonate system parameter measurements, number of CTD stations, and number of TCO_2 and TALK analyses made during Indian Ocean CO_2 survey cruises 10

6 Required WHP accuracy for deep water analyses 17

7 The short-term precision of the nutrient analyses for Indian Ocean Section I2 18

8 Certified salinity, TALK, and TCO_2 for CRM supplied for Indian Ocean CO_2 survey 23

9 Precision of discrete TCO_2 analyses during Indian Ocean CO_2 survey 23

10 Mean difference and standard deviation of the differences between at-sea TCO_2 by coulometry and on-shore TCO_2 by manometry on aliquots of the same sample from Indian Ocean CO_2 survey, and mean replicate precision of the manometric analyses 24

11 Mean analytical difference (ΔTALK) between analyzed and certified TALK for CRM used during Indian Ocean CO_2 survey 27

12 Mean analytical difference (ΔTALK) between analyzed and certified TALK for each section during Indian Ocean CO_2 survey 28

13 Final count of carbonate system parameter (CSP) analyses during Indian Ocean CO_2 survey 29

14 Content, size, and format of data files 41

ACRONYMS

A/D	analog-to-digital
ADCP	acoustic Doppler current profiler
ALACE	autonomous Lagrangian circulation explorer
BOD	biological oxygen demand
BNL	Brookhaven National Laboratory
^{14}C	radiocarbon
CALFAC	calibration factor
CDIAC	Carbon Dioxide Information Analysis Center
CFC	chlorofluorocarbon
CO_2	carbon dioxide
CTD	conductivity, temperature, and depth sensor
CRM	certified reference material
d.f.	degree of freedom
DIW	deionized water
DOE	U.S. Department of Energy
EEZ	Exclusive Economic Zone
emf	electro-magnetic fields
EXPOCODE	expedition code
FSI	Falmouth Scientific Instruments
fCO_2	fugacity of CO_2
FTP	file transfer protocol
GO	General Oceanics
GMT	Greenwich mean time
GPS	global positioning system
Hcl	hydrochloric acid
IAPSO	International Association for the Physical Sciences of the Ocean
IMET	Improved METeorology
I/O	input-output
JGOFS	Joint Global Ocean Flux Study
kn	knots
LADCP	lowered ADCP
LDEO	Lamont-Doherty Earth Observatory
MATS	Miami University alkalinity titration systems
NBIS	Neil Brown Instrument system
NCSU	North Carolina State University
NDP	numeric data package
NOAA	National Oceanic and Atmospheric Administration
nm	nautical mile
NSF	National Science Foundation
ODF	Ocean Data Facility
ONR	Office of Naval Research
OSU	Oregon State University
PC	personal computer
PI	principal investigator
POC	particulate organic carbon
PMEL	Pacific Marine Environmental Laboratory

PU	Princeton University
QA	quality assurance
QC	quality control
R/V	research vessel
RSMAS	Rosenstiel School of Marine and Atmospheric Sciences
SIO	Scripps Institution of Oceanography
SOMMA	single-operator multiparameter metabolic analyzer
SSW	standard seawater
TAMU	Texas A&M University
TALK	total alkalinity
TCO_2	total carbon dioxide
TD	to-deliver
UH	University of Hawaii
UM	University of Miami
UW	University of Washington
VFC	voltage to frequency converter
WHOI	Woods Hole Oceanographic Institution
WHPO	WOCE Hydrographic Program Office
WOCE	World Ocean Circulation Experiment
WHP	WOCE Hydrographic Program

ABSTRACT

Johnson K. M., A. G. Dickson, G. Eischeid, C. Goyet, P. R. Guenther, R. M. Key, K. Lee, E. R. Lewis, F. J. Millero, D. Purkerson, C. L. Sabine, R. G. Schottle, D. W. R. Wallace, R. J. Wilke, and C. D. Winn. *2002. Carbon Dioxide, Hydrographic and Chemical Data Obtained During the Nine R/V Knorr Cruises Comprising the Indian Ocean CO_2 Survey (WOCE Sections I8SI9S, I9N, I8NI5E, I3, I5WI4, I7N, I1, I10, and I2; December 1, 1994–January 22, 1996)*, Ed. A. Kozyr. ORNL/CDIAC-138, NDP-080. Carbon Dioxide Information Analysis Center, Oak Ridge National Laboratory, U.S. Department of Energy, Oak Ridge, Tennessee, 59 pp. **doi: 10.3334/CDIAC/otg.ndp080**

This document describes the procedures and methods used to measure total carbon dioxide (TCO_2) and total alkalinity (TALK) at hydrographic stations taken during the R/V *Knorr* Indian Ocean cruises (Sections I8SI9S, I9N, I8NI5E, I3, I5WI4, I7N, I1, I10, and I2) in 1994–1996. The measurements were conducted as part of the World Ocean Circulation Experiment (WOCE). The expedition began in Fremantle, Australia, on December 1, 1994, and ended in Mombasa, Kenya, on January 22, 1996. During the nine cruises, 12 WOCE sections were occupied.

Total carbon dioxide was extracted from water samples and measured using single-operator multiparameter metabolic analyzers (SOMMAs) coupled to coulometers. The overall precision and accuracy of the analyses was ± 1.20 μmol/kg. The second carbonate system parameter, TALK, was determined by potentiometric titration. The precision of the measurements determined from 962 analyses of certified reference material was ± 4.2 μmol/kg. This work was supported by grants from the National Science Foundation, the U. S. Department of Energy, and the National Oceanographic and Atmospheric Administration.

The R/V *Knorr* Indian Ocean data set is available as a numeric data package (NDP) from the Carbon Dioxide Information Analysis Center (CDIAC). The NDP consists of 18 oceanographic data files, two FORTRAN 77 data retrieval routine files, a readme file, and this printed documentation, which describes the contents and format of all files as well as the procedures and methods used to obtain the data. Instructions for accessing the data are provided.

Keywords: carbon dioxide; TCO_2; total alkalinity; coulometry; gas chromatography; World Ocean Circulation Experiment; Indian Ocean; hydrographic measurements; carbon cycle.

PART 1:

OVERVIEW

1. BACKGROUND INFORMATION

The World Ocean Circulation Experiment (WOCE) Hydrographic Program (WHP) was a major component of the World Climate Research Program. The primary WOCE goal was to understand the general circulation of the global ocean well enough to be able to model its present state and predict its evolution in relation to long-term changes in the atmosphere. The impetus for the carbon system measurements arose from concern over the rising atmospheric concentrations of carbon dioxide (CO_2). Increasing atmospheric CO_2 may intensify the earth's natural greenhouse effect and alter the global climate.

The carbon measurements, which were carried out on the U.S. WOCE Indian Ocean cruises, were supported as a core component of the Joint Global Ocean Flux Study (JGOFS). This coordinated effort received support in the United States from the U.S. Department of Energy (DOE), the National Oceanic and Atmospheric Administration (NOAA), and the National Science Foundation (NSF). Goals were to estimate the meridional transport of inorganic carbon in a manner analogous to the estimates of oceanic heat transport (Bryden and Hall 1980; Brewer, Goyet, and Drysen 1989; Holfort et al. 1998; Roemmich and Wunsch 1985) and to build a database suitable for carbon-cycle modeling and the estimation of anthropogenic CO_2 in the oceans. The global data set includes approximately 23,000 stations. Wallace (2001) recently reviewed the goals, conduct, and initial findings of the survey.

This report discusses the CO_2 science team effort to sample the entire Indian Ocean for inorganic carbon (Fig. 1). The total CO_2 (TCO_2) and total alkalinity (TALK) were measured in the water column and the fugacity of CO_2 (fCO_2) in the surface waters [see Sabine and Key (1998) for a description of the fCO_2 methods and data]. The TCO_2 analytical systems were furnished and set up by Brookhaven National Laboratory under the supervision of D. W. R. Wallace and K. M. Johnson, and the alkalinity titrators were furnished and set up by the University of Miami under the supervision of F. J. Millero. During the survey, certified reference material (CRM) was used to ensure measurement accuracy. All shipboard measurements followed standard operating procedures (DOE 1994). This report focuses on TCO_2 and TALK measurements. Because the team shared equipment throughout all nine cruises and so much material, including quality assessments of the data, has already appeared in the refereed literature, the report will be limited to a brief summary. Published documentation appears in appendices.

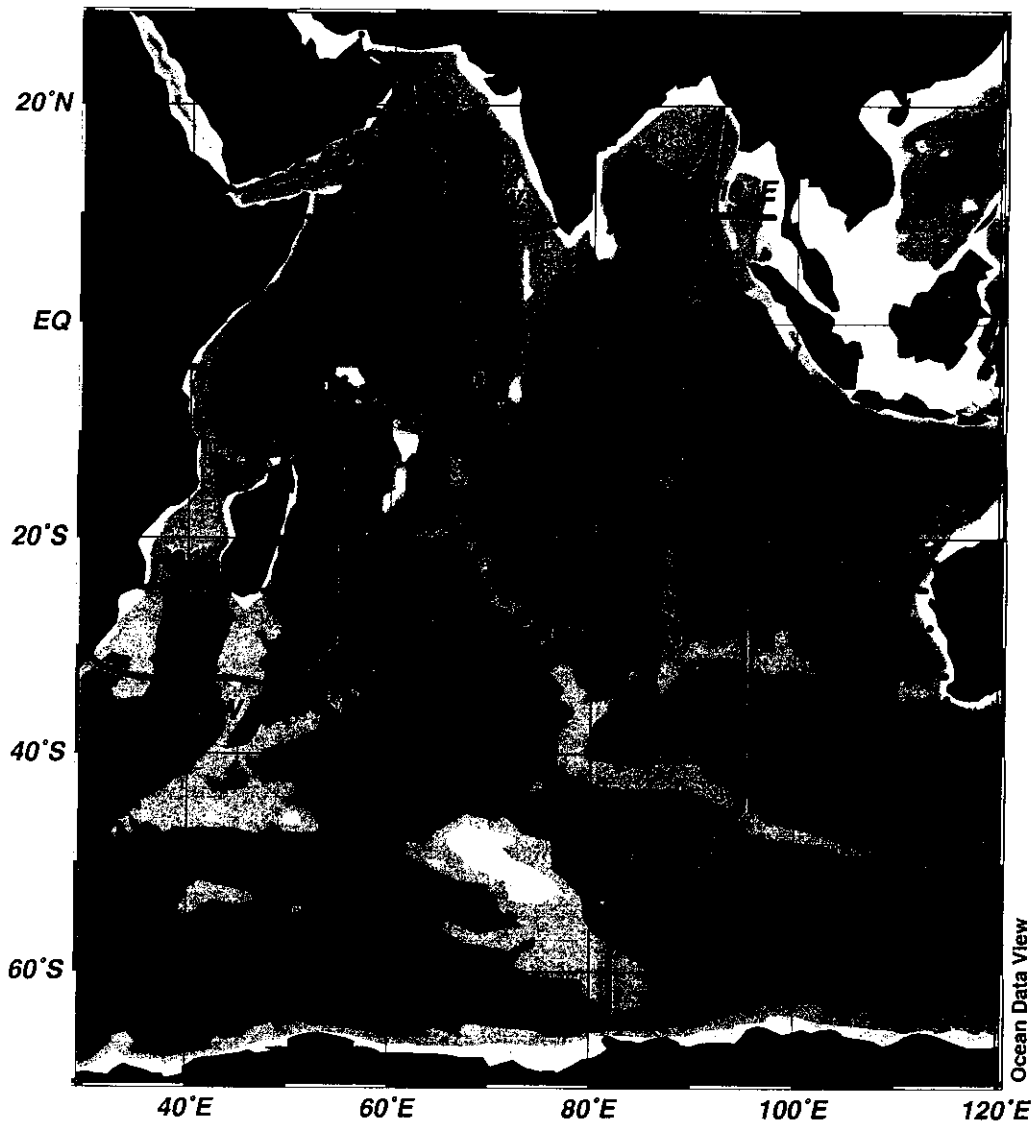

Fig. 1. The cruise tracks during the R/V *Knorr* expeditions in the Indian Ocean along WOCE Sections I8SI9S, I9N, I8NI5E, I3, I5WI4, I7N, I1, I10, and I2.
This figure was made using the Ocean Data View program (Schlitzer 2001).

2. DESCRIPTION OF THE EXPEDITION

2.1 R/V *Knorr:* Technical Details and History

The R/V *Knorr*, built in 1969 by the Defoe Shipbuilding Company in Bay City, Michigan, is owned by the U.S. Navy. It was turned over to the Woods Hole Oceanographic Institution in 1971 for operation under a charter agreement with the Office of Naval Research. It was named for E. R. Knorr, a hydrographic engineer and cartographer who in 1860 held the title of Senior Civilian and Chief Engineer Cartographer of the U.S. Navy Office. Its original length and beam were 245 and 46 ft, respectively. Beginning on February 6, 1989, it underwent a major midlife retrofit or "jumbo-izing" at the McDermott Shipyard in Amelia, Louisiana. A midsection was added to the ship to stretch its length by 34 ft, to 279 ft, and fore and aft azimuthing propulsion systems were added to make it one of the most maneuverable and stable ships in the oceanographic fleet. By the time it was returned to the Woods Hole Oceanographic Institution in late 1991, the retrofit had taken 32 months. The P6 Section was the vessel's first scientific cruise after the retrofitting. The R/V *Knorr* was designed for a wide range of oceanographic operations and possesses antiroll tanks and a strengthened bow for duty in icy waters. Like its sister ship, the R/V *Melville*, it is used for ocean research and routinely carries scientists from many different countries. Table 1 provides a list of technical characteristics of the R/V *Knorr*, while Table 2 provides individual cruise information, parameters measured, and responsible personnel with their institutional affiliations.

Table 1. Technical characteristics of R/V *Knorr*

Ship name:	R/V *Knorr*		
Call sign:	KCEJ		
Basic dimensions:			
Gross registered tonnage	2518 T	Displacement	2958 l ton
Overall length	279 ft	Beam	46 ft
Draught (maximum)	16.5 ft	Service speed	12 kn
Maximum speed	14.5 kn	Minimum speed	0.1 kn
Main deck clear length	126 ft		
Personnel:			
Crew	24		
Scientists	34		
Main engine:	4 × Mak6M 322 = 4 × 1000 kW at 750 rpm		
Propulsion:	Twin lips diesel-electric, azimuthing stern thrusters, 1500 SHP		
Bow thruster:	Lips retractable azimuthing 900 SHP		
Fuel capacity:	160,500 gal		
Maximum cruise duration:	60 days (12,000 nm)		
Nautical equipment :	Integrated navigation system		
	Potable water generator		
	2 instrument hangars		
	Winches: 1 heavy-duty trawl with 30,000 ft of ½-in. wire		
	2 hydrographic, both with 30,000 ft of hydrowire		
	Hydraulic cranes on the starboard side aft and midships		
	Scientific storage space of 1,320 ft^2		
	Portable van space		
	Machine shop		
	Fume hoods		
	Uninterruptible power supply		
	Air conditioning		
	Library/lounge		
	3680 ft^2 of laboratory space for multidisciplinary research		

2.2 The Indian Ocean CO_2 Survey Cruises Information

Ship name:	R/V *Knorr*
Cruise/Leg:	WOCE Sections I8SI9S, I9N, I8NI5E, I3, I5WI4, I7N, I1, I10, and I2
Ports of call:	Fremantle Australia (start), and Mombasa, Kenya (end)
Dates:	December 1, 1994 – January 22, 1996
TALK instrumentation:	F. J. Millero, RSMAS
TCO_2 instrumentation:	D. W. R. Wallace and K. M. Johnson, Brookhaven National Laboratory (BNL)
Reference material:	A. D. Dickson, SIO
Funding support:	DOE, NSF
Chief scientist:	See Table 2

Table 2. Dates, ports of call, expedition codes (EXPOCODEs), and names of chief scientists during Indian Ocean CO_2 survey cruises

Section	Start date	Finish date	From	To	EXPOCODE	Chief scientist (affiliated institution)[a]
I8SI9S	12/01/94	01/19/95	Fremantle	Fremantle	316N145_5	M. McCartney (WHOI)
I9N	01/24/95	03/06/95	Fremantle	Colombo	316N145_6	A. Gordon (LDEO)
I8NI5E	03/10/95	04/16/95	Colombo	Fremantle	316N145__7	L. Talley (SIO)
I3	04/20/95	06/07/95	Fremantle	Port Louis	316N145_8	W. Nowlin (TAMU)
I5WI4	06/11/95	07/11/95	Port Louis	Port Louis	316N145_9	J. Toole (WHOI)
I7N	07/15/95	08/24/95	Port Louis	Muscat	316N145_10	D. Olson (RSMAS)
I1	08/29/95	10/18/95	Muscat	Singapore	316N145_11,12	J. Morrison (NCSU)
Dry Dock	10/19/95	11/05/95	Dampier			
I10	11/06/95	11/24/95	Dampier	Singapore	316N145_13	N. Bray (SIO)
I2	11/28/95	01/22/96	Singapore	Mombasa	316N145_14,15	G. Johnson (PMEL)

[a]Participating institutions:

LDEO Lamont-Doherty Earth Observatory
NCSU North Carolina State University
PMEL Pacific Marine Environmental Laboratory
RSMAS Rosenstiel School of Marine and Atmospheric Science
SIO Scripps Institution of Oceanography
WHOI Woods Hole Oceanographic Institution

The extent and nature of the complete measurement program and the responsible institutions for each cruise are summarized in Table 3.

Table 3. WOCE measurement programs and responsible institutions during Indian Ocean CO_2 survey cruises

Program	Section/Cruise								
	I8SI9S	I9N	I8NI5E	I3	I5WI4	I7N	I1	I10	I2
	Responsible institution[a]								
CTD[b] /Rosette	WHOI	ODF	ODF	ODF	ODF	ODF	WHOI	ODF	WHOI
Bottle Oxygen	WHIO	ODF	ODF	ODF	ODF	ODF	WHOI	ODF	WHOI
Bottle Salts	WHOI	ODF	ODF	ODF	ODF	ODF	WHOI	ODF	WHOI
Nutrients	OSU	ODF	ODF	ODF	ODF	ODF	OSU	ODF	OSU
CFCs[c]	LDEO	UM	LDEO	SIO	UW	UM	UW	UM	PMEL
He[d] /Tr[e]	LDEO	WHOI	WHOI	WHOI	WHOI	UM	WHOI	WHOI	WHOI
Deep He/Tr				LDEO	LDEO		UM	WHOI	LDEO
^{14}C[f]	UW	PU	PU	PU	PU	PU	PU	PU	PU
ADCP[g]	UH	UH	UH	OSU	UH	UH	SIO	SIO	UH
TCO_2, TALK	BNL	PU	UH	RSMAS	BNL	UH	SIO	SIO	UH

[a]Participating institutions:

BNL	Brookhaven National Laboratory
LDEO	Lamont-Doherty Earth Observatory
NCSU	North Carolina State University
PMEL	Pacific Marine Environmental Laboratory
ODF	Ocean Data Facility (SIO)
OSU	Oregon State University
PU	Princeton University
RSMAS	Rosenstiel School of Marine and Atmospheric Science (UM)
SIO	Scripps Institution of Oceanography, University of California, San Diego
TAMU	Texas A&M University
UH	University of Hawaii
UM	University of Miami
UW	University of Washington
WHOI	Woods Hole Oceanographic Institute

[b]conductivity, temperature, and depth sensor
[c]chlorofluorocarbons
[d]helium
[e]tritium
[f]carbon-14
[g]acoustic Doppler current profiler

The principal investigators (PIs) and the senior technical staff for the WOCE measurements program are summarized in Table 4.

Table 4. Principal investigators and senior at-sea personnel responsible for WOCE measurement programs during Indian Ocean CO_2 survey cruises

Program	Responsible personnel (Institution)
CTD/Rosette	James Swift (SIO/ODF), John Toole (WHOI), Frank Delahoyde (SIO/ODF), Carl Mattson (SIO/ODF), Marshall Swartz (WHOI), Laura Goepfert (WHOI)
Bottle oxygen	James Swift (SIO/ODF), John Toole (WHOI), George Knapp (WHOI), John Boaz (SIO/ODF)
Bottle salts	James Swift (SIO/ODF), John Toole (WHOI), George Knapp (WHOI)
Nutrients	Louis Gordon (OSU), James Swift (SIO/ODF), Marie-Claude Beaupre (ODF), Joe Jennings (OSU)
CFCs	John Bullister (PMEL), Rana Fine (RSMAS), William Smethie (LDEO), Mark Warner (UW), Ray Weiss (SIO), Kevin Sullivan (RSMAS), Frederick A. Van Woy (SIO)
He/Tr	William Jenkins (WHOI), Peter Schlosser (LDEO), Zafer Top (RSMAS), Peter Landry (WHOI)
^{14}C	Robert Key (PU)
ADCP	Teri Chereskin (SIO), Peter Hacker (UH), Eric Firing (UH), Mike Kosro (OSU)
TCO_2, TALK	See Table 5

Table 5 contains a summary of the personnel responsible for the discrete carbonate system measurements.

Table 5. Personnel responsible for carbonate system parameter measurements, number of CTD stations, and number of TCO_2 and TALK analyses made during Indian Ocean CO_2 survey cruises

Section	Institution	PI(s)	Group leader	Stations (No.)	TCO_2 (No.)	TALK (No.)
I8SI9S	BNL	D. Wallace K. Johnson	K. Johnson	147	2184	1910
I9N	PU	R. Key C. Sabine	C. Sabine	131	2511	2504
I8NI5E	UH	C. Winn	C. Winn	166	2419	2421
I3	RSMAS	F. Millero	D. Purkerson	120	1734	1810
I5WI4	BNL	D. Wallace K. Johnson	R. Wilke	136	1991	1831
I7N	UH	C. Winn	R. Schottle	156	2235	2577
I1	WHOI	C. Goyet	G. Eischeid	158	2400	2387
I10	PU	R. Key C. Sabine	C. Sabine	61	927	926
I2	UH	C. Winn	R. Schottle	168	2562	2562
Total				1244	18963	18928

A complete list of the CO_2 measurement team members and their home and sponsoring institutions appears in Appendix A.

2.3 Brief Cruise Summary

Unlike other CO_2 survey cruises where a single institution was responsible for all phases of the work, these cruises were a group effort in which the measurement groups used the same ship and instrumentation for a 14-month period. BNL supplied two single-operator multiparameter metabolic analyzers (SOMMA) systems [S/N 004(I) and 006(II)] that were certified at BNL. A complete back-up system (S/N 023) was supplied by WHOI. The alkalinity titrators were supplied by RSMAS. Preparation began with a 4-day workshop held in September 1994 at RSMAS under the direction of and in the laboratory of F. J. Millero. Cruise participants and group leaders from BNL, LDEO, SIO, RSMAS, PU, WHOI, and UH were instructed in the use of the alkalinity titrators by F. J. Millero and D. Campbell and in the use of the SOMMA-coulometer systems by K. M. Johnson and R. W. Wilke. The day after Thanksgiving the BNL and RSMAS TCO2 groups left for Australia. Setup of the alkalinity and coulometric titration systems began on November 28, 1994. The I8SI9S cruise began on December 1, 1994.

The first of the nine cruises on the R/V *Knorr* was the longest continuous cruise during the survey. It occupied a series of CTD stations along two north-south tracks essentially proceeding from Australia to the ice edge (I8S) along 90° E and then back again to Australia (I9S) at approximately 110° E. Station spacing ranged from 5 to 40 nautical miles (nm). Testing and selection of the best of the available titration systems and components was completed during I8S. The alkalinity and especially the coulometric titration systems benefitted from this "shake-out" period. Components damaged during transit were identified and repaired or replaced. By the beginning of the I9S, operations were more or less routine. Except for one approximately 12-h period when high winds of ~60 knots (kn) made sampling impossible, work proceeded pretty much on schedule during the 50-day cruise. During the cruise the ability of a team of four marine mammal and bird observers onboard from PMEL, under the direction of C. Tynan, to remain in the cold weather and identify whales that were little more than blips on the horizon amazed all participants of the expedition. Both Christmas and New Year holidays were celebrated aboard the ship. The fine Christmas dinner was highlighted by the appearance of three humpback whales, who put on a spectacular display, jumping and passing under and about the ship. The ship docked in Fremantle, to the relief of the CO_2 team members, on January 19, 1995, after 147 stations were occupied. Measurement crews were exchanged, and the new team brought along some badly needed spare parts and components.

The ship departed Fremantle for I9N on January 24 with A. Gordon as Chief Scientist and a CO_2 measurement group from PU. This section was basically a northward continuation of I8S. The weather was perfect during all 43 days of the cruise. The participants celebrated the equator crossing on February 14. This cruise ended on March 5 in Colombo, Sri Lanka, with 131 stations logged. During the stopover, the carrier gas supply for the coulometric titrators was shifted from bottled high purity nitrogen to a calibration gas generator (Peak Scientific), which supplied CO_2-free carrier gas for the remaining of the cruises.

I8NI5E began in Colombo on March 10 with L. Talley as chief scientist and a CO_2 measurement group from UH on board. No problems were noted for the sampling program, and the weather remained excellent for most of this leg. The ship track proceeded southward from Sri Lanka along 88° E to 24° S, then angled southeastward to the junction of the Ninety-East Ridge and Broken Ridge. Next, the ship followed a 1987 section along approximately 32° S. This zonal section included the Central Indian Basin, and crossed the northward flow of deep water just west of Australia. Due to the good weather, some extra sampling was carried out, and by the time the ship docked in Fremantle on April 15, 166 stations had been occupied. On station 296, the rosette accidentally hit bottom at 3630 m, but the cast was successfully completed. A postcruise inspection showed no apparent damage to the equipment. This cruise included sampling for particulate organic

carbon (POC) in the surface waters near the equator. POC samples were also taken at 65 stations for $^{13}C/^{12}C$ analyses. Between April 15 and 23, measurement crews were exchanged and spare parts inventories were updated.

On April 23, the R/V *Knorr* departed Fremantle for section I3 with W. Nowlin as chief scientist and a CO_2 measurement group from RSMAS. The ship had to detour almost immediately back to Fremantle for a medical emergency. The injured analyst was able to rejoin the ship in Port Louis, Mauritius. In addition to the CTD work, this cruise included the deployment of current meters, drifters, and autonomous Lagrangian circulation explorer (ALACE) floats. The cruise track ran along 20° S from Australia to Mauritius to Madagascar, crossing the West Australian Basin, Ninety-East Ridge, Central Indian Basin, and Central Indian Ridge before veering southward to 22° S around Rodrigues Island. After this, it proceeded to the east coast of Mauritius, where a 2-day port stop was made in Port Louis. Returning to sea, the ship continued sampling westward along 20° S from the continental shelf to Madagascar. Weather was characterized by southeasterly winds of 10–20 kn, mostly sunny skies, occasional rain squalls, and 4–6 ft swells with slightly higher winds and seas in mid-May. The *Knorr* returned to Port Louis, Mauritius, on June 5 with 120 stations logged.

The next cruise, I4I5W, began on June 11 with J. Toole as chief scientist and a CO_2 measurement group from BNL on board. This leg focused on major circulation features of the southwest region of the Indian Ocean, including the region where the Agulhas Current originates and where dense waters filtering through fractures in the Southwest Indian Ridge form a northward deep boundary current east of Madagascar. The cruise track formed a closed box to aid in deducing the absolute circulation. A stop was made in Durban, South Africa, on June 21 to pick up a replacement drum of CTD wires. Attempts were also made to repair the ship's bow thruster, which had failed very early in the leg; although the repair was not successful, the lack of a bow thruster had no effect on the scientific work. The R/V *Knorr* departed Durban on June 22 and began I5W including reoccupation of stations where data had been taken in 1987. Bad weather was experienced on June 30 when wind gusts of 40–50 kn and high seas slowed winch operations. As the ship moved across the Madagascar Basin toward port, station spacing was decreased to 20 nm. When the ship arrived in port on July 11,136 stations had been occupied—20 more than planned.

After four days in port, the R/V *Knorr* departed on I7N with D. Olson as chief scientist and a CO_2 measurement group from UH. The director of the U.S. WOCE office, Piers Chapman, was aboard and served as a salt analyst during the section. I7N was designed to define the water mass properties and transports across the Mascarene Basin and to measure water mass properties and baroclinic structure on a short section across the Amirante Passage, located between the Mascarene and Somali Basins. It included a cross-equatorial section and a reoccupation of stations previously sampled to confirm water mass flows. This work included sampling along 65° E in the central Arabian Basin. The concluding phase of the cruise was a deep line of stations up the center of the Gulf of Oman. The last station of this phase was in the Strait of Hormuz, and it identified inflows of Arabian (Persian) Gulf water into the Arabian Basin. The cruise terminated on August 24 in Muscat, Oman, with 156 stations occupied.

After a 5-day layover, the R/V *Knorr* departed Muscat on I1 with J. Morrison as chief scientist and a CO_2 measurement group from WHOI. I1 was the northernmost Indian Ocean section. It enclosed the Arabian Sea and Bay of Bengal, which are important sources of salt and fresh water, respectively. The *Knorr* proceeded from Muscat to the southern end of the Red Sea and then to the coast of Somali, where the zonal section started at a nominal latitude of 8° N. The section crossed the Arabian Sea, in part to study the carbon transport in and out of the Arabian Sea, and ended on the continental shelf of India. After a brief port stop in Colombo, Sri Lanka, on September 28–30, the leg continued from the Sri Lankan shelf across the Bay of Bengal to the Myanmar continental shelf. CTD problems caused considerable difficulty for the scientific party and resulted in a

somewhat noisy hydrographic data set compared to data obtained from the other sections. After the last station on the Myanmar shelf, the *Knorr* deadheaded to Singapore, arriving on October 16 with 158 stations logged. I1 was not only the northernmost section, it was clearly the most adventurous. ALACE float deployments had to be canceled in the territorial waters of India because the Indian observer on board refused to allow them, and then the threat of pirates caused the cancellation of a planned section across the Gulf of Aden. In the vicinity of Colombo, the ship had to be escorted by four Sri Lankan gunboats, and planned stops at stations over the Trincomalee Canyon could not be taken because of the threat of attack by the Tamil Tigers. Nevertheless, the *Knorr* was able to coordinate scientific activities and physical oceanographic measurements with the nearby R/V *Meteor* (F. Schott, chief scientist) in an area of German current meter moorings near Socotra. Sampling during I1 enabled comparison of bottle and TCO_2 data with earlier JGOFS results and *Meteor* Pegasus and *Knorr* lowered acoustic Doppler current profiler (LADCP) horizontal velocities. From Singapore, the *Knorr* proceeded to Dampier, Australia, where it was placed in dry dock from October 19 until November 5.

With the R/V *Knorr* back in the water, the I10 CO_2 measurement group from PU arrived. This group was required to do some additional work not normally part of the crew exchange routine. During the dry dock period, the CO_2 instrumentation had been depowered, and the measurement group had to repower and check the instrumentation. Some minor repairs were required for the coulometric titrators, including the replacement of one or two solenoid valves (the only valves replaced during the cruises). In addition, the sample pipettes and coolant lines were dismounted and cleaned of algal growth.

The R/V *Knorr* departed Dampier, Australia, on November 11 with N. Bray as chief scientist. WOCE Section I10 was set to run from Shark Bay, Western Australia, to the Indonesian Exclusive Economic Zone (EEZ) 120 nm south of Sunda Strait. However, constraints imposed by the Indonesian government caused the endpoint to be moved from the Sunda Strait to near central Java. The *Knorr* was not granted permission to enter the EEZ of Indonesia, and concluding stations had to be taken along the boundary of the EEZ. These restrictions prevented full resolution of the South Java current. Throughout the Indian Ocean survey, bottle casts were normally made to within 5–20 m of the bottom; however, on I10 four stations over the Java Trench this could not be done. Instead, the casts were made to the maximum CTD depth of 6000 m. The quality of the bottle data was considered to be excellent throughout with very few mis-trips. ALACE floats were also released during this cruise. A festive Thanksgiving was celebrated aboard the ship, and after the last station (1075), the *Knorr* steamed to Singapore, arriving on November 28, with 61 stations logged.

The R/V *Knorr* departed Singapore on December 2 for the last Indian Ocean WOCE section, I2, with G. Johnson as chief scientist and the UH CO_2 measurement group aboard. Again, clearance for work in the Indonesian EEZ was not available, and after a 3-day steam, work commenced with a reoccupation of the final station of the I10 Section (station 1075). The *Knorr* skirted the Indonesian EEZ and moved westward, crossing the Ninety-East Ridge and the Chagos-Laccadive Ridge. The ship continued at approximately 8° S until it made a brief port call in Diego Garcia from December 28–30. At this point, the chief scientist departed the ship and was replaced by Bruce Warren, accompanied by two Kenyan observers. The *Knorr* returned to the 8° S line, passing the crest of the Central Indian Ridge and then the Mascarene Plateau before it turned southwestward and crossed the Amirante Passage on the way to the northern tip of Madagascar. Rounding the tip, the ship headed northwest toward Africa, making a dogleg to avoid the Tanzanian EEZ. After completing the final Indian Ocean Survey station 1244, it proceeded to Mombasa, arriving on January 22, 1996, with 168 stations logged.

For inorganic carbon, the principal analytical problems for the cruise centered on the breakage of glass components in the alkalinity titrators; resupply; accumulation of bubbles in the acid lines of the alkalinity titrators; damaged coulometric cathode electrodes; algal growth in the

sample lines, baths, pipettes, and alkalinity cells; wide swings in laboratory temperature (19–33°C), and the failure of the TCO_2 glassware drying oven. Fortunately, glassware drying oven was repaired. Temperature swings (21–29°C) were also noted for the salinometer and nutrient laboratories. The most vexing problem for the inorganic carbon analysts was the failure of the refrigerated baths used by both the alkalinity and coulometric titration systems. The baths had to be constantly jury-rigged so that one bath did the work of two, repaired by ship's technicians when possible, or replaced when possible. The two groups used almost 12 different baths, and by the time the work ended, not one could be considered in reliable condition. Some were never repaired, while others were repaired and used for the North Atlantic survey in 1997.

3. DESCRIPTION OF VARIABLES AND METHODS

3.1 Hydrographic Measurements

During the survey, responsibility for hydrographic and bottle data was divided between ODF and WHOI. Each of these groups uses or may use different procedures. Hence, the hydrographic measurements are described in separate sections. Because the greater number of the cruises were made under the auspices of SIO/ODF, the bulk of the methods description is provided in Sect. 3.1.1. Information specific to WHOI is given in Sect. 3.1.2; in this section however, the discussion is limited to significant differences between the SIO/ODF and WHOI operations or methods. Unless otherwise stated in Sect. 3.1.2, material presented in Sect. 3.1.1 applies to all cruises. Sect. 3.1.3 contains a brief description of the underway measurements common to all cruises.

3.1.1 SIO/ODF Methods and Instrumentation

Hydrographic measurements consisted of salinity, dissolved oxygen, and nutrient (nitrite, nitrate, phosphate, and silicate) samples collected from Niskin bottles filled during CTD/rosette casts, and temperature, pressure, salinity, and dissolved oxygen from the CTD. At 5- to 40-nm intervals, depending on the topography, hydrographic casts were made to within 5–20 m of the bottom with a 36-bottle Rosette frame belonging to ODF. This unit consisted of a 36-bottle frame, thirty six 10-L bottles, and a 1016 General Oceanics (GO) 36-place pylon. The GO pylon was used in conjunction with an ODF-built deck unit and power supply. The underwater components comprising the CTD included an ODF-modified Neil Brown Instrument Systems (NBIS) Mark III CTD with conductivity, pressure, oxygen, and temperature sensors. The underwater package also consisted of a SeaTech transmissometer, an LADCP, a Sensormedics dissolved oxygen sensor, a Falmouth Scientific Instruments (FSI) secondary PRT sensor, a Benthos altimeter, and a Benthos pinger. The CTD was mounted horizontally along the bottom of the frame, while the LADCP was vertically mounted inside the bottle rings. The system was suspended from and powered by a three-conductor 0.322-in. electromechanical cable. The Rosette was deployed from the starboard side using either the port side Markey CTD or the starboard side Almon Johnson winch. Standard CTD practices (i.e., soaking the conductivity and O_2 sensors in distilled water between casts and protecting the sensors against sunlight and wind by storing the rosette in the hanger between casts) were observed throughout the cruises. Regular CTD maintenance included the replacement of O-rings when needed, bottle inspections, and a regular cleaning of the transmissometer windows. At the beginning of each station the time, position, and bottom depth were logged. The CTD sensors were powered and control was transferred to the CTD acquisition and control system in the ship's laboratory. The CTD was lowered to within 10 m of the bottom if bottom returns were adequate. Continuous profiles of horizontal velocity from the sea surface to the bottom were made for most CTD/rosette casts using the LADCP.

The CTD's control and acquisition system displayed real-time data [pressure, depth, temperature, salinity (conductivity), oxygen, and density] on the video display of a SunSPARC LX computer. A video recorder was provided for real-time analog backup. The Sun computer system included a color display, a keyboard, a trackball, a 2.5-GB disk, 18 RS-232 ports, and an 8-mm cartridge tape. Two additional Sun systems were networked for display, backup, and processing. Two HP 1200 C color ink-jet printers provided hard copy. The ODF data acquisition software not only acquired the CTD data but also processed it so that the real-time data included preliminary sensor corrections and calibration models for pressure, temperature, and conductivity. The sampling

depths were selected using down-cast data. Bottles were tripped on the up-cast. Bottles on the rosette were identified with a serial number and the pylon tripping sequence, 1–36, where the first (deepest) bottle tripped was no. 1. For shallow-depth stations, fewer than 36 bottles were closed.

After the CTD was on deck, the acquisition system, the CTD, the pylon, and video recording were turned off and the sensor protective measures were completed before sampling began. If a full suite of samples was drawn, the sampling order was CFCs, ^{3}He, O_2, TCO_2, TALK, ^{14}C, ^{3}H, nutrients, and salinity. Only salinity, O_2, and nutrients were measured at every station. A deck log was kept to document the sampling sequence and to note anomalies (e.g., status of bottle valves, leaks, etc.). One member of the sampling crew was designated the "sample cop," and it was his or her responsibility to maintain this log and to ensure that the sampling order was followed. Oxygen sampling included measurement of the temperature, which proved useful for determining leaking or mis-tripped bottles. Following the cruises, WHP quality flags were assigned according to the WOCE Operations Manual (Joyce and Corry 1994) to each measured quantity.

The principal ODF CTD (no. 1) was calibrated for pressure and temperature at the ODF Calibration Facility (La Jolla, Calif.) in December 1994 prior to the five consecutive WOCE Indian Ocean sections beginning with I9N and ending with I7N. The CTD was also calibrated postcruise in September 1995 prior to the I10 cruise. Pre- and postcruise laboratory calibrations were used to generate tables of corrections, which were applied by the CTD data. At sea, bottle salinity and oxygen data were to calibrate or check the CTD sensors. Additional details concerning calibration and the CTD data processing can be obtained from the chief scientists' cruise reports at the WHPO web site: http://whpo.uscd.edu/.

Bottle **salinity** samples were collected in 200-mL Kimax high alumina borosilicate bottles, sealed with custom-made plastic insert thimbles and Nalgene screw caps. Salinity was determined after equilibration in a temperature-controlled laboratory, usually within 8–20 h of collection. Salinity was measured with two ODF-modified Guildline Autosal Model 8400A salinometers, normally at 21 or 24°C, depending on the prevailing temperature of the salinometer laboratory. The salinometers included interfaces for computer-aided measurements (e.g., acquiring the measurements, checking for consistency, logging results, and prompting the analyst). The salinometers were standardized with International Association for the Physical Sciences of the Ocean (IAPSO) Standard Seawater (SSW) Batches P-124, P-126, or P-128 using at least one fresh vial per cast (usually 36 samples). The accuracy of the determination was normally 0.002 relative to the SSW batch used. PSS-78 was then calculated for each sample (UNESCO 1981). On some stations (e.g., on Section I5EI8N), bottle salinity exhibited small offsets (0.002–0.004) compared to the corresponding CTD results and bottle salinity from nearby stations, and corrections of this magnitude need to be applied to the bottle salinity. Errors of this magnitude have no practical effect on the calculated TCO_2 or TALK values. Hence, bottle salinity is sufficiently accurate to express inorganic carbon results in μmol/kg.

Bottle **oxygen** was determined by rinsing 125-mL iodine flasks twice and then filling to overflowing (3x-bottle volume) with a draw tube. Sample temperature was measured immediately with a thermometer imbedded in the draw tube. The Winkler reagents were added; and the flask was stoppered, shaken, and then shaken again 20 min later to ensure that the dissolved O_2 was completely fixed. Oxygen was determined within 4 h of collection using a whole-bottle modified Winkler titration following the technique of Carpenter (1965) and incorporating the modifications of Culberson et al. (1991) on an SIO/ODF-designed automated oxygen titrator. A Dosimat 665 burette driver fitted with a 1.0-mL burette was used to dispense thiosulfate solution (50 g/L). Standards prepared from preweighed potassium iodate (0.012N) were run each time the automated titrator was used, and reagent blanks were determined by analyzing distilled water. The final oxygen results were converted to μmol/kg using the in situ temperature. Bottle volumes were precalibrated at SIO. Laboratory temperature stability during the sections was considered poor, varying from 22 to 28°C

over short time periods; and therefore, portable fans were used by ODF analysts to maintain temperature.

Phosphate, nitrate, nitrite, and **silicate** samples were collected in 45-mL high-density polypropylene, narrow-mouth, screw-capped centrifuge tubes which were cleaned with 10% hydrochloric acid (HCl) and then rinsed three times with sample before filling. The samples were analyzed on an ODF-modified four-channel Technicon AutoAnalyzer II, usually within 1 h of the cast, in a temperature-controlled laboratory. If the samples were stored for longer than 1 h prior to analysis, they were stored at 2–6°C (for no more than 4 h). The AutoAnalyzer incorporates the method of Armstrong, Stearns, and Strickland (1967) for silicate, this same method as modified for nitrate and nitrite, and the method of Bernhardt and Wilhelms (1967) for phosphate. The last method is described by Gordon and coworkers (Atlas et al. 1971; Hager et al. 1972; and Gordon et al. 1992). Standards were analyzed at the beginning and end of each group of sample analyses, with a set of secondary intermediate concentrations prepared by diluting preweighed primary standards. Replicates were also drawn at each station for measurement of short-term precision. For reagent blanks, deionized water (DIW) from a Barnstead Nanopure deionizer fed from the ship's potable water supply was analyzed. An aliquot of deep seawater was run with each set of samples as a substandard. The primary standard for silicate was Na_2SiF_6; and for nitrate, nitrite, and phosphate the standards were KNO_3, $NaNO_2$, and KH_2PO_4, respectively. Chemical purity ranged from 99.97% ($NaNO_2$) to 99.999% (KNO_3).

Most hydrographic data sets met or exceeded the WHP requirements. Some exceptions for silicate were noted when differences between overlapping stations on I3 (Station 548) and I4I5W (Stations 705 and 574) approached 3%; these silicate data (Stations 702–707) were corrected by adding 3% to the original results. Instrument problems also caused difficulties for the nitrite and silicate analyses on many of the I2 cruise stations. Silicate problems were noted at some 30% of these stations, with errors typically being on the order of 2–4%. This required considerable post-cruise evaluation and workup before the desired between-station precision for deep water values of 1% was attained. However, users of the I2 silicate data are urged to use caution or to contact the analysts for assistance. Because of the difficulties with the nutrient analyses on the I2 cruise, the post-cruise I2 precision is given in Table 7 as a "worst case" for comparison with the WHP standards shown in Table 6. Short-term precision is the absolute mean difference between replicates analyzed within a sample run; the standard deviation of the differences is also shown. The authors know of no remaining CTD problems, that would affect the quality of the carbonate system data.

Table 6. Required WHP accuracy for deep water analyses

Parameter	Required accuracy
Salinity	0.002 relative to SSW analysed
Oxygen	1% (2 μmol/kg)
Nitrate	1% (0.3–0.4 μmol/L)
Phosphate	1% (0.02–0.03 μmol/L)
Silicate	1% (1–5 μmol/L)

Table 7. The short-term precision of the nutrient analyses for Indian Ocean Section I2

Parameter	Difference (μmol/L)	± St. Dev.
Nitrate	0.123	0.093
Phosphate	0.015	0.009
Silicic Acid	0.440	0.260

3.1.2 WHOI Methods and Instrumentations

Unless otherwise stated procedures are as decribed in Sect. 3.1.1, above. For the hydrographic work on I8SI9S, I1, and I2, the R/V *Knorr* was outfitted with equipment belonging to both WHOI and SIO/ODF. For the I8SI9S section a NBIS CTD was used. For I1, four CTDs were available. The primary sensors were two new FSI CTDs belonging to WHOI with a Sensormedics oxygen sensors, a titanium pressure transducer, and a temperature monitor. The secondary sensors were two NBIS Mark-III CTDs (WHOI Nos. 9 and 12) also with a Sensormedics oxygen sensor, a titanium pressure transducer, and a temperature monitor. The MKIII CTDs experienced failures early during I1 (Stations 858 and 864), and the bulk of the hydrography was carried out using the FSI (Nos. 1338 and 1344) CTDs . Usually, the frame was set up with the two CTDs—one configured to send data up the wire and one configured to record data internally. Electrical modifications had to be made to the CTDs and the deck controllers before CTD data dropouts were eliminated and the confirmation of bottle closure from the pylon was restored.

For the CTDs, a FSI DT-1050 deck unit was initially used to demodulate the data, but this unit was replaced for most of the cruise with an EG&G MK-III deck unit. These units fed serial data to two personal computers (PCs) running EG&G CTD acquisition software, with one displaying graphical output and the other a running data listing. After each station, the CTD data were forwarded to another set of PCs running EG&G postprocessing and software modified by WHOI (Millard and Yang 1993) in which the data were centered into 2 dbar bins for data quality control, which included fitting to bottle salinity and oxygen results.

The CTDs were calibrated before and after the cruise for temperature and pressure at WHOI by M. Swartz and M. Plueddemann. Both calibrations were consistent, but the data set for I1 was considered to be only of fair quality because noise levels in the data set are somewhat larger than typical for other CTDs. For example, this data set has a salt noise level of 0.002 which is 2 times larger than the norm. Residuals between the bottle and profile data range from 0.001 to 0.004. For a detailed discussion of the CTD calibration and problems experienced at sea during I1, consult the chief scientist's cruise report on the WHPO web site.

For I2, WHOI CTD No. 9, a WHOI-modified NBIS MK-IIIb, was used. The CTD incorporated a Sensormedics oxygen sensor, titanium pressure transducer, and temperature sensor, which were calibrated in November 1995 immediately before the cruise. On most stations, one of the FSI CTDs was used in the memory mode and downloaded after station sampling to provide independent or backup CTD traces. An FSI Ocean Temperature Module was also attached to the MK-III and CTDs. The Mark-III CTD data were acquired using an NBIS Mark-III deck unit/display that provided demodulated data to two PCs, as described for the Section I1 cruise. A PC was also devoted to recovering the data from the FSI CTDs. Post-cruise calibration, including dunk

tests of the CTDs, was completed in April and May of 1996 in the WHOI calibration laboratory. The procedure of Millard and Yang (1993) was used to correct the pressure temperature sensor calibration post-cruise to eliminate down/up pressure historesis. Multiple regression fits of the CTD data to the bottle data were used to calibrate the oxygen and conductivity sensors. See the chief scientist's report on the WHPO web site for further details.

Bottle **salinity** samples were collected in 200-mL glass bottles with removable polyethylene inserts and caps. Then they were removed to a temperature-controlled van at 23°C and analyzed on a Guildline Autosal Model 8400B salinometer (WHOI No. 11). The salinometer was standardized once a day using IAPSO SSW (128, dated July 18, 1995). The accuracy was ~0.002. A complete description of the WHOI measurement techniques is given by Knapp, Stalcup, and Stanley (1990).

Bottle **oxygen** was determined according to procedures given by Knapp, Stalcup, and Stanley (1990). WHOI used a modified Winkler technique similar to that described by Strickland and Parsons (1972). The oxygen reagents and bi-iodate standard were prepared at WHOI in August 1994. There was no evidence that the reagents or standard deteriorated during the 17 months they were aboard the Knorr. Standardization of the thiosulphate titrant was made daily. The accuracy of the method was 0.5%, or approximately 1.0 μmol/kg.

The nutrients were analyzed as described in Sect. 3.1.1 (see also Gordon et al. 1994).

3.1.3 Underway Measurements

Navigational data (heading, speed, time, date, and position) were acquired from the ship's Magnavox MX global positioning system (GPS) receiver via RS-232 and logged automatically at 1-min intervals on a SunSPARC station. Underway bathymetry was logged manually at 5-min intervals from the hull-mounted 12-kHz echo sounder and a Raytheon recorder corrected according to methods described by Carter (1980). These data were merged with the navigation data to provide a time-series of underway position, course, speed, and bathymetry data that were used for all station positions, depths, and vertical sections. The Improved METeorology (IMET) sensors logged meteorological data—which included air temperature, barometric pressure, relative humidity, sea surface temperature, and wind speed and direction—at 1-min intervals. Underway shipboard measurements were made throughout the work to document the horizontal velocity structure along the cruise tracks using a 150-kHz hull-mounted acoustic Doppler current profiler (ADCP) manufactured by RD Instruments. The ADCP was mounted at a depth of 5 m below the sea surface.

Underway chemical measurements in water and air included salinity, pCO_2 (PU and SIO), pN_2O (SIO), and CH_4 (SIO). Two different systems were used for pCO_2; the PU group used a rotating disk equilibrator and infrared detector, while the Scripps group used a shower type equilibrator and gas chromatograph for the detection of CO_2. The pCO_2 measurements, including a comparison of the shower and disk equilibrator results, were described by Sabine and Key (1998). A thermosalinograph (manufactured at FSI) was mounted on the bow approximately 3 m below the surface for underway salinity, which was calibrated against surface CTD and bottle salinity values after the cruise (Sabine and Key 1998). The CFC groups periodically analyzed air for CFCs using sampling lines from the bow and stern of the ship.

3.2 Total Carbon Dioxide Measurements

TCO_2 was determined on 18,963 samples using two automated single-operator multiparameter metabolic analyzers (SOMMA) with coulometric detection of the CO_2 extracted from acidified samples. A description of the SOMMA-coulometry system and its calibration can be found

in Johnson et al. 1987; Johnson and Wallace 1992; and Johnson et al. 1993. A schematic diagram of the SOMMA analytical sequence and a complete description of the sampling and analytical methods used for discrete TCO_2 on the Indian Ocean WOCE sections appear in Appendix B (Johnson et al. 1998). Further details concerning the coulometric titration can be found in Huffman (1977) and Johnson, King, and Sieburth (1985). The measurements for the Indian Ocean Survey were made on two systems provided by BNL (S/Ns 004 and 006) and a backup by WHOI (S/N 023).

TCO_2 samples were collected from approximately every other station [~ 60 nm intervals, 50% of the stations (Fig. 2)] in 300-mL glass biological oxygen demand (BOD) bottles. They were immediately poisoned with 200 μL of a 50% saturated solution of $HgCl_2$, thermally equilibrated at 20°C for at least 1 h, and analyzed within 24 h of collection (DOE Handbook of Methods 1994). Certified reference material (CRM) samples were routinely analyzed, usually at the beginning and end of the coulometer cell lifetime, according to DOE (1994). As an additional check of internal consistency, duplicate samples were usually collected on each cast at the surface and from the bottom waters. These duplicates were analyzed on the same system within the run of cast samples from which they originated, but the analyses were separated in time usually by ~3 h. Periodically, replicate samples were also drawn for shipboard analysis at sea using coulometry and for later analysis on shore at SIO by manometry. The latter samples, typically designated as the "Keeling samples," consisted of two 500-mL replicate samples collected at two depths (four samples total per station). These were analyzed only if both replicates survived the storage and the return journey to SIO.

Seawater introduced from an automated "to-deliver" (TD) pipette into a stripping chamber was acidified, and the resultant CO_2 from continuous gas extraction was dried and coulometrically titrated on a model 5011 UIC coulometer. The coulometer was adjusted to give a maximum titration current of 50 mA, and it was run in the counts mode [the number of pulses or counts generated by the coulometer's voltage-to-frequency converter (VFC)] during the time the titration was displayed and acquired by the computer. In the coulometer cell, the acid (hydroxyethylcarbamic acid) formed from the reaction of CO_2 and ethanolamine was titrated coulometrically (electrolytic generation of OH^-) with photometric endpoint detection. The product of the time and the current passed through the cell during the titration was related by Faraday's constant to the number of moles of OH^- generated and thus to the moles of CO_2 that reacted with ethanolamine to form the acid. The age of each titration cell was logged from its birth (time that electrical current was applied to the cell) until its death (time when the current was turned off). The age was measured from birth (chronological age) and in mass of carbon (mgC) titrated since birth (carbon age). The systems were controlled with PCs equipped with RS232 serial ports for the coulometer and the barometer, a 24-line digital input/output (I/O) card for the solid state relays and valves, and an analog-to-digital (A/D) card for the temperature, conductivity, and pressure sensors. These sensors monitored the temperature of the sample pipette, gas sample loops, and, in some cases, the coulometer cell. The controlling software was written in GWBASIC Version 3.20 (Microsoft Corp., Redmond, Wash.), and the instruments were driven from an options menu appearing on the PC monitor.

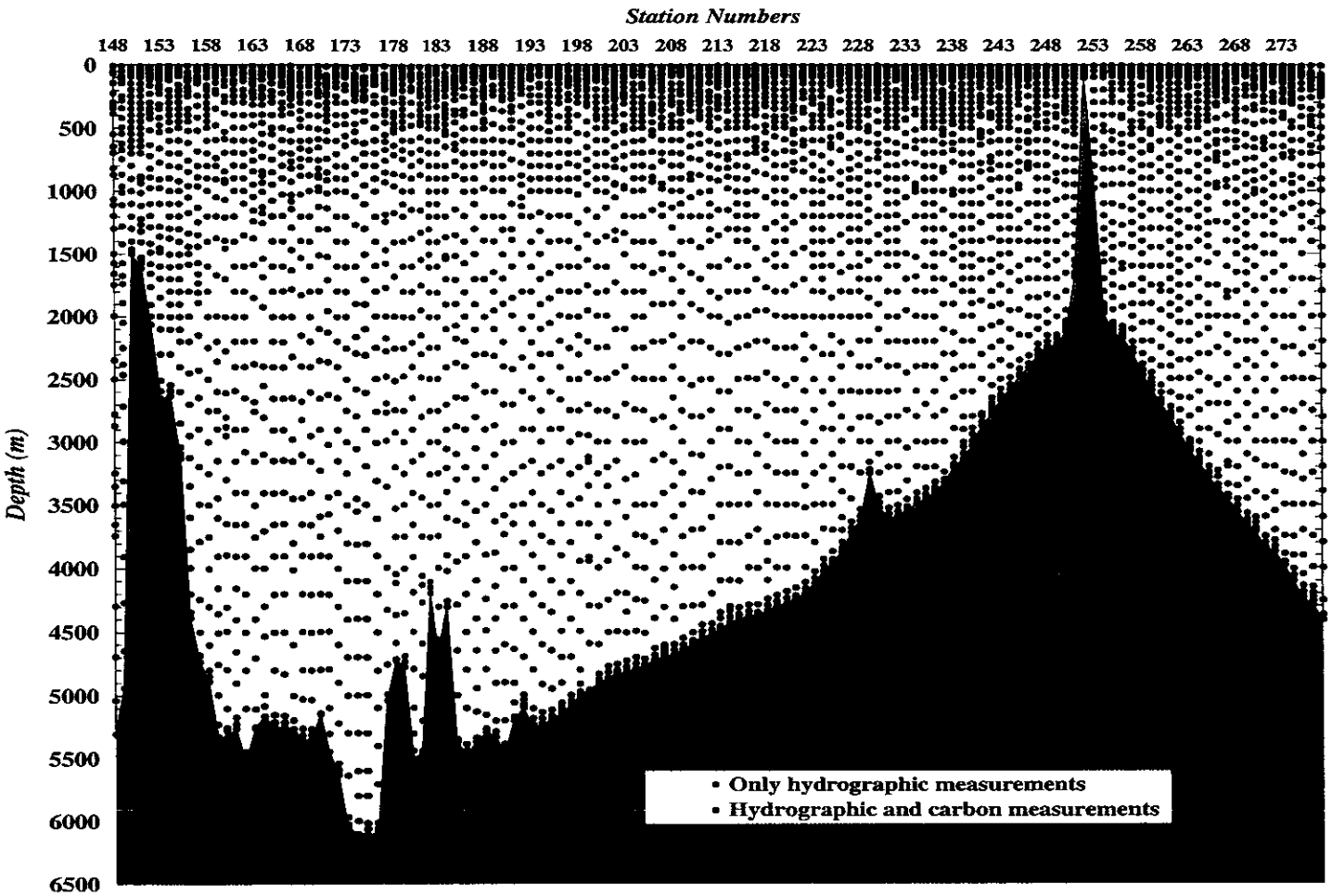

Fig. 2. Sampling depths at all hydrographic stations occupied during the R/V *Knorr* Indian Ocean survey along WOCE Section I9N.

The TD volume (V_{cal}) of the sample pipettes was determined gravimetrically prior to the cruise and periodically during the cruise by collecting aliquots of deionized water dispensed from the pipette into pre-weighed serum bottles which were sealed and re-weighed on shore. The apparent weight of water collected (W_{air}), corrected to the mass in vacuo (M_{vac}), was divided by the density of the calibration fluid at the calibration temperature to give V_{cal}. The sample volume (V_t) at the pipette temperature was calculated from the expression

$$V_t = V_{cal} [1 + a_v (t - t_{cal})] ,$$

where a_v is the coefficient of volumetric expansion for Pyrex-type glass (1×10^{-5}/°C), and t is the temperature of the pipette at the time of a measurement. V_{cal} for the Indian Ocean CO2 survey cruises and a chronology of the pipette volume determinations appear in Appendix B.

The coulometers were electronically calibrated at BNL prior to the cruises and recalibrated periodically during the cruises (Sections I8SI9S and I5WI4) to check the factory calibration as described in Johnson et al. (1993) and DOE (1994). The results for the electronic intercepts (Int_{ec}) and slopes ($Slope_{ec}$) are given in Appendix B. For all titrations, the micromoles of carbon titrated (M) was

$$M = [Counts / 4824.45 - (Blank \times T_t) - (Int_{ec} \times T_i)] / Slope_{ec} ,$$

where 4824.45 (counts/μmol) was the scaling factor obtained from the factory calibration, T_t was the length of the titration in minutes, *Blank* is the system blank in μmol/min, and T_i the time of continuous current flow in minutes.

The SOMMA-coulometry systems were calibrated daily with pure CO_2 (calibration gas) by titrating the mass of CO_2 contained in two stainless steel gas sample loops of known volume and by analyzing CRM samples supplied by Dr. Andrew Dickson of the SIO. The ratio of the calculated (known) mass of CO_2 contained in the gas sample loops to the mass determined coulometrically was the CALFAC (~1.004). A complete history of the calibration results appears in Appendix B. For water and CRM samples, TCO_2 concentration in μmol/kg was

$$TCO_2 = M \times CALFAC \times [1 / (V_t \times \rho)] \times d_{Hg} ,$$

where ρ is the density of seawater in g/mL at the analytical t and S calculated from the equation of state given by Millero and Poisson (1981), and d_{Hg} is the correction for sample dilution with bichloride solution (for the cruises d_{Hg} = 1.000666).

System 006 was equipped with a conductance cell (Model SBE-4, Sea-Bird Electronics, Bellevue, Wash.) for the determination of salinity as described by Johnson et al. (1993). Whenever possible, SOMMA and CTD salinities were compared to identify mis-trips or other anomalies, but the bottle salinities (furnished by the chief scientist) have been used to calculate ρ throughout.

Three CRM batches were used for the Indian Ocean Survey. The certified TCO_2 concentrations were determined by vacuum-extraction/manometry in the laboratory of C. D. Keeling at SIO and are given in Table 8.

Table 8. Certified salinity, TALK, and TCO_2 for CRM supplied for Indian Ocean CO_2 survey

Batch	Salinity	TCO_2 (µmol/kg)	TALK (µmol/kg)
23	33.483	1993.10	2212.70
26	33.258	1978.34	2176.60
27	33.209	1988.10	2214.90

Optimal cell and platinum electrode configurations, according to criteria given in Appendix B, were selected on the first section (I8S) and were used on all subsequent cruises.

The quality control-quality assurance (QC-QA) of the coulometric TCO_2 determinations was assessed from analyses of 983 CRM samples during the nine Indian Ocean CO_2 survey cruises. For both coulometric titration systems (004 and 006) the average ΔTCO_2 (measurement minus CRM value) for the whole survey was −0.86 µmol/kg and the standard deviation was ±1.21 µmol/kg. A cruise-by-cruise breakdown of the accuracy and precision of the CRM analyses is given in Appendix B.

The small mean difference between the analyzed and certified TCO_2 and the very high precision (±1.21 µmol/kg) of the differences indicates that the two systems gave very accurate and virtually identical results over the entire survey (see also Fig. 6 in Appendix B).

The second phase of the QC-QA procedure was an assessment of sample precision, which is presented in Table 9. The sample precision was determined from duplicate samples analyzed on each system during sections I8SI9S at the beginning of the survey and I4I5W about half way through the survey. The pooled standard deviation (S_p^2), shown in Table 9, is the square root of the pooled variance according to Youden (1951) where K is the number of samples with one replicate analyzed on each system, n is the total number of replicates analyzed from K samples, and n − K is the degree of freedom (d.f.) for the calculation. Precision was calculated this way because TCO_2 was analyzed on two different systems, and an estimate of sample precision independent of the analytical system was required. Hence S_p^2 is the most conservative estimate of precision and includes all sources of random and systematic error (bias). Bias between systems would increase the imprecision of the measurements, but the excellent agreement between the S_p^2 values for natural seawater samples (Table 9) and the high precision of the CRM differences confirms the virtually uniform response, accuracy, and high precision of both systems during the survey. This finding confirms that the precision of the TCO_2 analyses during the Indian Ocean CO_2 survey was ±1.20 µmol/kg.

Table 9. Precision of discrete TCO_2 analyses during Indian Ocean CO_2 survey

Section	S_p^2 (K, n, d.f)
I8SI9S	1.26 (15, 30,15)
I4I5W	0.91 (21, 42, 21)
CRM	1.21

The next phase of the QC-QA procedure was the comparison of replicate samples analyzed at sea and in the shore-based laboratory. Samples from every cruise were analyzed at sea by

continuous gas extraction/coulometry, and later, after storage, duplicate samples were analyzed on shore by vacuum extraction/manometry. The results of the analyses are summarized in Table 10.

Table 10. Mean Difference [$\Delta TCO_{2(S-SIO)}$] and standard deviation of the differences [$S.D._{(S-SIO)}$] between at-sea TCO_2 by coulometry and on-shore TCO_2 by manometry on aliquots of the same sample from Indian Ocean CO_2 survey, and the mean replicate precision [$S.D._{(SIO)}$] of the manometric analyses

Section	Pairs Analyzed (n)	$\Delta TCO_{2(S-SIO)}$ (μmol/kg)	$S.D._{(S-SIO)}$ (μmol/kg)	$S.D._{(SIO)}$[a] (μmol/kg)
I8SI9S	23	-4.14	1.80	0.82
I9N	24	-1.96	1.67	0.80
I8NI5E	17	-4.80	2.87	1.31
I3	29	-3.29	1.26	0.82
I4I5W	16	-2.95	1.40	1.30
I7N	13	-5.37	1.92	1.40
I1	26	-5.59	1.38	1.05
I10	8	-4.94	1.52	1.28
I2	10	-4.42	1.50	0.83
n	166	9	9	9
Mean		-4.16	1.70	1.07
S.D.		1.21	0.49	0.25

[a]Each on-shore TCO_2 by manometry is always the mean of two analyses (see text).

In general, the reproducibility and the uniformity of the data as a whole, and specifically, the high precision of the manometric analyses shown in Table 10, indicate that the collection and return of the "Keeling samples" was successfully performed by each of the measurement groups. Poor sampling or storage techniques would probably have been manifested in a much higher imprecision for the on-shore replicate analyses and in the differences between the at-sea and on-shore analyses. However, the negative mean difference (-4.16 ± 1.21, n = 9) for the Indian Ocean sections was greater than the mean difference for WOCE sections in other oceans (-1.36 ± 1.37 μmol/kg, n = 22). The accuracy of the CRM analyses, the tendency for the coulometric analyses to give slightly lower results, and the reproducibility of the at-sea and on-shore differences are similar everywhere, but the magnitude of the Indian Ocean difference is clearly the largest observed to date. Even if the consistent and slightly negative difference for the CRM is taken into account (-0.86 μmol/kg), the at-sea coulometric measurements are approximately 2 μmol/kg lower than the manometric method. A suite of samples from the 1997 North Atlantic sections remains to be analyzed. Until these analyses are completed and a thorough statistical evaluation of the entire CO_2 survey data set is made, the explanation of the at-sea and on-shore differences, including those found for the Indian Ocean, is not possible.

An additional step in the QA-QC was also undertaken. Inspection of Fig. 1 shows points where the cruise tracks cross or nearly cross. The agreement between TCO_2 measurements made at these crossover locations (± 100 km) on different cruises was examined by assuming that the temporal and spatial variations in deep-ocean TCO_2 are small relative to the measurement accuracy and precision. Hence, deep ocean waters should have the same TCO_2 at different times in the absence of internal vertical motion, and because deep ocean motion probably occurs along constant density surfaces (isopycnals), the comparisons of TCO_2 measurements were made with reference to density and not depth. Appendixes B and D (Johnson at al. 1998 and Sabine et al. 1999) give a complete description of the statistical procedures used to make the crossover comparisons. Briefly, crossover points were selected for comparison of water samples collected below 2500 m. A smooth curve was fit through the TCO_2 data as a function of the density anomaly referenced to 3000 dbar (σ-3) using Cleveland's LOESS smoother (Cleveland and Devlin 1988). A separate fit was performed for the data collected at each of the two intersecting crossover points, but the same tension parameter was used for all of the crossover points so that the smoothing function was consistently applied to all crossover locations. The difference between the two smoothed curves was evaluated at 50 evenly spaced points covering the density range where the two data sets overlapped. A mean and standard deviation for the 50 comparisons was calculated for each crossover point. For TCO_2, differences never exceeded 3 μmol/kg, and the overall mean and standard deviation of the differences was -0.78 ± 1.74 μmol/kg. The latter differences were consistent with the overall precision of the CRM analyses (± 1.2 μmol/kg).

Tables 8–10 show an internally consistent TCO_2 data set for the Indian Ocean with excellent accuracy with respect to the CRM certified values, consistently good precision, no analytical bias between the coulometric titration systems, and crossover agreement to within the precision of the method. However, the agreement between the at-sea and on-shore analyses is not as good as for earlier WOCE sections from other oceans (i.e., the Pacific and the South Atlantic). Based on the accuracy of the CRM analyses and the high precision of the sample analyses, the TCO_2 data were not corrected in any way and were deemed to meet survey criteria for accuracy and precision.

3.3 Total Alkalinity Measurements

Total alkalinity was measured on 18,928 samples using two closed-cell automated potentiometric titration systems (hereafter designated as MATS) developed at the University of Miami. The MATS are described by Millero et al. (1993) and by Millero et al. (1998). The latter reprinted in Appendix C of this document, completely describes the Indian Ocean Survey TALK measurements and results. Briefly, the MATS consisted of three parts: a water-jacketed, fixed-volume (about 200 mL determined to ± 0.05 mL) closed Plexiglass sample cell, a Metrohm model 665 Dosimat titrator, and a pH meter (Orion, Model 720A), the last two controlled by a PC. The titration cell was similar to those used by Bradshaw and Brewer (1988), but had a greater volume to improve the precision of the measurements. The cell was equipped with flush-mounted fill and drain valves to increase the reproducibility of the cell volume. The cell, titrant burette, and sample container were held at a temperature of 25 ± 0.01 °C using a constant temperature bath (e.g., Neslab, Model RTE 221).

A Lab Windows C program was used to run the titrators, record the volume of titrant added, and record the measured electromagnetic fields (emf) of the electrodes through RS232 serial interfaces. Two electrodes were used in each cell: a ROSS glass pH electrode (Orion, Model 810100) and a double-junction Ag/AgCl reference electrode (Orion, Model 900200). The specific electrodes used during the Indian Ocean survey were selected after careful screening for non-

Nernstian behavior. Only those electrodes which gave TCO_2 results in good agreement with TCO_2, as determined coulometrically, were used (Sect. 3.2).

Seawater samples were titrated by adding increments of HCl until the carbonic acid endpoint of the titration was exceeded. During a titration, the emf readings were monitored until they were stable (± 0.09 mV). Sufficient volume of acid was added to increase the emf by preassigned increment (~13 mV) in order to give an even distribution of data points over the course of a full titration, which consists of 25 data points. A single titration takes about 20 min. A FORTRAN computer program based on those developed by Dickson (1981) and by Johansson and Wedborg (1982) was used to calculate the carbonate parameters. The pH and pK of the acids used in the program are on the seawater scale, and the dissociation constants for carbonic acid were taken from Dickson and Millero (1987). For further details see Appendix C and DOE (1994).

The titrant (acid) used throughout the cruises was prepared prior to the cruise, standardized, and stored in 500-mL borosilicate glass bottles for use in the field. The 0.25-M HCl acid solution was prepared by dilution of 1-M HCl in 0.45-M NaCl to yield a solution with total ionic strength similar to that of seawater of salinity 35.0 ($I \approx 0.7$ M). The acid was standardized by coulometry (Taylor and Smith 1959; Marinenko and Taylor 1968), and was also checked by independent titration in A. Dickson's laboratory at SIO. The independent determinations agreed to ± 0.0001 M, which corresponds to an uncertainty in TALK of ~ 1 μmol/kg. The Dosimat titrator burettes were calibrated with Milli-Q water at 25 °C to ± 0.0005 mL.

While CRM samples were available to the TCO_2 analysts from the beginning of the measurement program in 1990, the Indian Ocean cruises were the first to have a certified alkalinity standard as well. Hence, the accuracy of the method was checked in the laboratory by analyzing CRM samples from batches 23, 24, 26, 27, 29, and 30 and comparing the analyzed values with the certified TALK determined by A. Dickson at SIO (in the same manner as for TCO_2). These results are summarized in Table 11 (see also Appendix C). The mean difference between the MATS measurements in the laboratory and the certified TALK values was -0.8 μmol/kg for CRM samples with a concentration range approximately one-half as large as the range of a typical seawater profile. The excellent agreement indicated that the CRM concept for alkalinity was valid and that the methodology for TALK was ready for the Indian Ocean survey. The results for the at-sea measurements of the CRM samples have been extracted from Table 2 of Appendix C, summarized, and are given in Table 12.

Table 11. Mean analytical difference (ΔTALK) between analyzed and certified TALK for CRM used during Indian Ocean CO_2 survey

Batch	Salinity	Certified values		MATS mean TALK (μmol/kg)	ΔTALK (MATS - CRM) (μmol/kg)
		TCO_2 (μmol/kg)	TALK (μmol/kg)		
23	33.483	1993.10	2212.7	2213.7	1.0
24	33.264	1987.53	2215.5	2215.8	0.3
26	33.258	1978.34	2176.6	2175.1	-1.5
27	33.209	1988.10	2214.9	2214.3	-0.6
29	33.701	1902.33	2184.8	2182.3	-2.5
30	33.420	1988.78	2201.9	2200.5	-1.4
Range	0.492	90.77	38	40.7	3.5
Mean					-0.8

The analytical differences are for the most part within the precision of the measurements (~ 2–5 μmol/kg) except for the I7N Section. The larger at-sea differences were attributed to operator error or procedures and to uncertainties in the volume of cells, especially after repairs due to leakage, breakage, or repositioning the electrodes after changing the inner filling solutions. Variations between different MATS systems used on a single cruise were corrected using the adjustments required to reproduce the values assigned for the CRM (see Table 11). The at-sea sample titrations were corrected using the results of the at-sea CRM analyses. For TALK, the calibration factor (CF) used to correct the at sea measurements was

$$CF = TALK\ (meas., CRM) - CRM\ (certified\ value),$$

and the corrected TALK (TALKc) was

$$(TALKc) = TALK\ (meas., Spl) \times [\ CRM / (CRM + CF)],$$

where CRM was the certified TALK and Spl was the measured sample TALK.

The overall precision of TALK determinations during the Indian Ocean survey was ± 4.2 μmol/kg. The precision of the potentiometric pH and TCO_2 measurements are given in Table 3 of Appendix C.

Table 12. Mean analytical difference (ΔTALK) between analyzed and certified TALK for each section during Indian Ocean CO_2 survey

Batch	Section	Certified TALK (μmol/kg)	MATS mean TALK (μmol/kg)	S.D. (n) (μmol/kg)	ΔTALK (MATS-CRM) (μmol/kg)
23	I8SI9S	2212.7	2221.5	5.1 (49)	8.8
23	I9N	2212.7	2216.2	3.3 (138)	3.5
23	I8NI5E	2212.7	2211.6	4.9 (80)	-1.1
23	I3	2212.7	2215.4	1.4 (65)	2.7
26	I3	2176.6	2178.0	1.2 (30)	1.4
26	I5WI4	2176.6	2182.6	3.8 (79)	6.0
26	I7N	2176.6	2184.0	5.7 (59)	7.4
27	I7N	2214.9	2221.5	3.1 (8)	6.6
23	I7N	2212.7	2222.4	7.4 (10)	9.7
27	I1	2214.9	2219.4	3.9 (244)	4.5
27	I10	2214.9	2212.9	4.0 (62)	-2.0
27	I2	2214.9	2219.4	4.5 (67)	4.5
n				891	12

TALK was also checked at the crossover locations of two cruises in the same way as TCO_2. The agreement between the corrected TALK measurements made at the crossover locations (± 100 km) on different cruises was examined by assuming that the temporal and spatial variations of the deep-ocean TALK were small relative to measurement accuracy and precision. Hence, deep ocean waters should have the same TALK at different times in the absence of internal vertical motion, and because deep ocean motion probably occurs along constant-density surfaces (isopycnals), the comparisons of TALK measurements were made with reference to density and not depth. Appendixes C and D give a description of the statistical procedures used to make the crossover comparisons. For water samples collected below 2500 m, a smooth curve was fit through the TALK data as a function of the density anomaly referenced to 3000 dbar ($\sigma 3$) using Cleveland's LOESS smoother (Cleveland and Devlin 1988). A separate fit was performed on the data collected at each of the two intersecting crossover points, with the same tension parameter being used for all of the crossovers so that the smoothing function was consistently applied. The difference between the two smoothed curves was evaluated at 50 evenly-spaced points covering the density range where the two data sets overlapped. Mean and standard deviations for the differences at the 50 points were calculated for each crossover point. For TALK, differences never exceeded 6 μmol/kg, and the overall mean and standard deviation of the differences was 2.1 ± 2.1 μmol/kg. The latter were consistent with the overall precision of the CRM analyses (± 4 μmol/kg).

Table 13 is a final summation of the inorganic carbon analytical work completed during the Indian Ocean CO_2 survey from 1994 to 1996.

Table 13. Final count of carbonate system parameter (CSP) analyses during Indian Ocean CO_2 survey

Parameters	No. of CSP determinations		
	Discrete	CRM	Total
TCO_2	18,963	983	19,946
TALK	18,928	949	19,877
Total	37,891	1,932	39,823

3.4 Carbon Data Synthesis and Analysis

In accordance with one of the stated goals of the program, an evaluation of the data set with respect to estimated anthropogenic CO_2 distributions in the Indian Ocean has been completed and published by Sabine et al. (1999) (see Appendix D). The document is appended to this report as Appendix D. Additional crossover comparisons of the survey data with data gathered in the 1980s and in 1993 by French scientists are included. Briefly, the sequestering of anthropogenic CO_2 has been estimated by comparing the Indian Ocean survey results with the Indian Ocean GEOSECS expedition data from 1977 to 1978. Although CRM samples were not available for evaluating the earlier data, statistical methods were used to fit these data and correct for calibration offsets so that they could be compared with the current survey data. The data analysis was complicated by regions of pronounced denitrification (Arabian basin) and other regional variations that had to be considered and quantified. In summary, the estimate of the anthropogenic inventory was relatively small in the Indian and Southern Oceans, with anthropogenic carbon uptake lower by a factor of 2 compared to that of the Atlantic Ocean. Importantly, discrepancies between model and data-based estimates were found especially for the Southern Ocean where carbon uptake appears to have been traditionally overestimated by the extant circulation models. (See Appendix D for further details.) The initial data synthesis work indicates that the survey data will provide an important baseline with respect to future studies and that the spatial distribution of anthropogenic carbon can be an important tool for understanding model-based carbon uptake estimates and the response of models to atmospheric increases in CO_2.

3.5 Radiocarbon Measurements

Full information on the radiocarbon measurement method, instrumentation, and results can be found in Appendix E of this document.

4. DATA CHECKS AND PROCESSING PERFORMED BY CDIAC

An important part of the numeric data packaging process at the Carbon Dioxide Information Analysis Center (CDIAC) involves the quality assurance (QA) of data before distribution. Data received at CDIAC are rarely in a condition that would permit immediate distribution, regardless of the source. To guarantee data of the highest possible quality, CDIAC conducts extensive QA reviews that involve examining the data for completeness, reasonableness, and accuracy. The QA process is a critical component in the value-added concept of supplying accurate, usable data for researchers.

The following information summarizes the data processing and QA checks performed by CDIAC on the data obtained during the R/V *Knorr* cruise along WOCE Sections I8SI9S, I9N, I8NI5E, I3, I5WI4, I7N, I1, I10, and I2 in the Indian Ocean.

1. The final carbon-related data were provided to CDIAC by the ocean carbon measurement PIs listed in Table 5. The final hydrographic and chemical measurements and the station information files were provided by the WOCE Hydrographic Program Office (WHPO) after quality evaluation. A FORTRAN 90 retrieval code was written and used to merge and reformat all data files.

2. Every measured parameter for each station was plotted vs depth (pressure) to identify questionable outliers using the Ocean Data View (ODV) software (Schlitzer 2001) Station Mode (Fig. 3).

3. The section plots for every parameter were generated using the ODV's Section Mode in order to map a general distribution of each property along all Indian Ocean sections (Fig. 4).

4. To identify "noisy" data and possible systematic, methodological errors, property-property plots for all parameters were generated (Fig. 5), carefully examined, and compared with plots from previous expeditions in the Indian Ocean.

5. All variables were checked for values exceeding physical limits, such as sampling depth values that are greater than the given bottom depths.

6. Dates, times, and coordinates were checked for bogus values (e.g., values of MONTH < 1 or > 12; DAY < 1 or > 31; YEAR < 1994 or > 1996; TIME < 0000 or > 2400; LATITUDE < -70.000 or > 60.000; LONGITUDE < 19.000 or > 119.000.

7. Station locations (latitudes and longitudes) and sampling times were examined for consistency with maps and cruise information supplied by PIs.

8. The designation for missing values, given as -9.0 in the original files, was changed to -999.9 for the consistency with other oceanographic data sets.

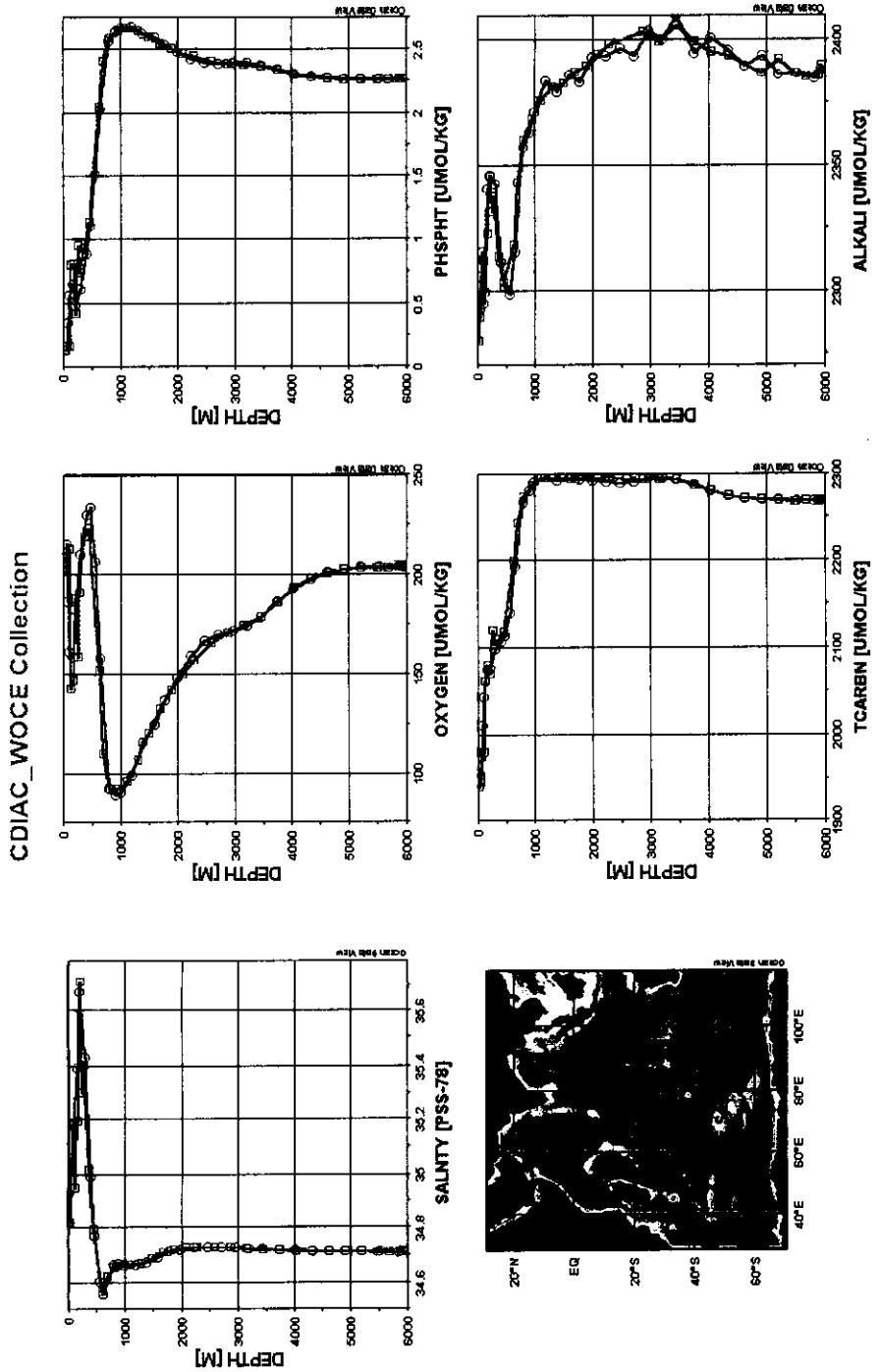

Fig. 3. Example of ODV station mode plot: Measurements vs depth for Stations 172–174 of Section I9N.

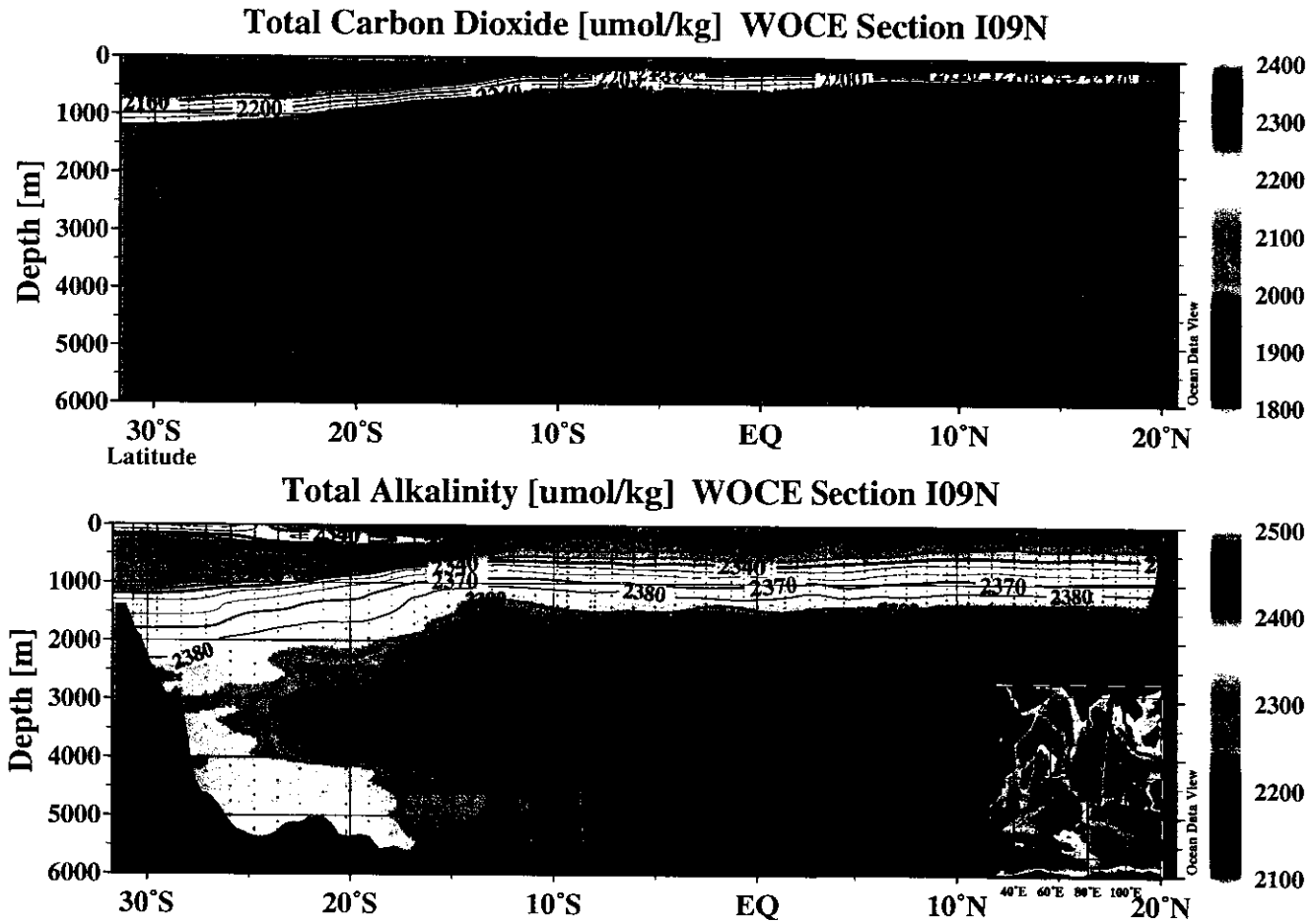

Fig. 4. Distribution of the TCO_2 and TALK in seawater along WOCE Section I9N.

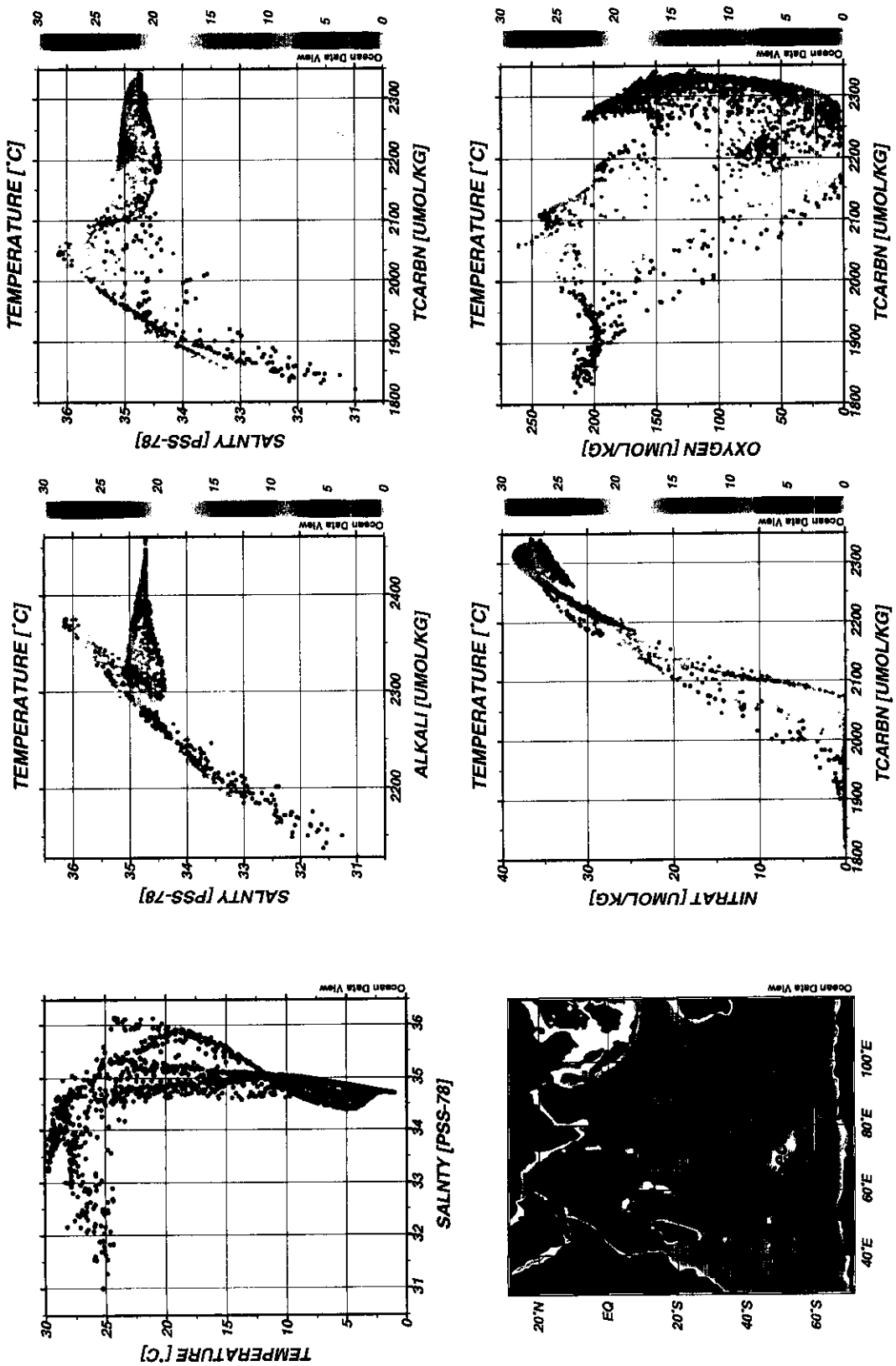

Fig. 5. Property-property plots for all stations occupied during the R/V *Knorr* cruise along WOCE Section I9N.

5. HOW TO OBTAIN THE DATA AND DOCUMENTATION

This database (NDP-077) is available free of charge from CDIAC. The complete documentation and data can be obtained from the CDIAC oceanographic Web site (http://cdiac.ornl.gov/oceans/doc.html), through CDIAC's online ordering system (http://cdiac.ornl.gov/pns/how_order.html), or by contacting CDIAC.

The data are also available from CDIAC's anonymous file transfer protocol (FTP) area via the Internet. Please note that your computer needs to have FTP software loaded on it (this is built in to most newer operating systems). Use the following commands to obtain the database.

ftp cdiac.ornl.gov or >ftp 160.91.18.18
Login: "anonymous" or "ftp"
Password: your e-mail address
ftp> cd pub/ndp080/
ftp> dir
ftp> mget (files)
ftp> quit

Contact information:

Carbon Dioxide Information Analysis Center
Oak Ridge National Laboratory
P.O. Box 2008
Oak Ridge, Tennessee 37831-6335
U.S.A.

Telephone: (865) 574-3645

Telefax: (865) 574-2232

E-mail: cdiac@ornl.gov

Internet: http://cdiac.ornl.gov/

6. REFERENCES

Armstrong, F. A. J., C. R. Stearns, and J. D. H. Strickland. 1967. The measurement of upwelling and subsequent biological processes by means of the Technicon Autoanalyzer and associated equipment. *Deep-Sea Research* 14:381–9.

Atlas, E. L., S. W. Hager, L. I. Gordon, and P. K. Park. 1971. *A Practical Manual for Use of the Technicon AutoAnalyzer® in Seawater Nutrient Analyses* (revised). Technical Report 215, Reference 71-22, Oregon State University, Department of Oceanography, Oreg.

Bernhardt, H. and A. Wilhelms. 1967. The continuous determination of low level iron, soluble phosphate and total phosphate with the AutoAnalyzer. *Technicon Symposia* 1:385–9.

Bradshaw, A. L. and P. G. Brewer. 1988. High precision measurements of alkalinity and total carbon dioxide in seawater by potentiometric titration: 1. Presence of unknown protolyte (s). *Marine Chemistry* 28:69–86.

Brewer, P. G., C. Goyet, and D. Dyrssen. 1989. Carbon dioxide transport by ocean currents at 25° N latitude in the Atlantic Ocean. *Science* 246:477–79.

Bryden, H. L., and M. M. Hall. 1980. Heat transport by ocean currents across 25° N latitude in the North Atlantic Ocean. *Science* 207:884.

Carpenter, J. H. 1965. The Chesapeake Bay Institute technique for the Winkler dissolved oxygen method. *Limnology and Oceanography* 10:141–3.

Carter, D. J. T. 1980. *Computerized Version of Echo-sounding Correction Tales (3rd Ed.).* Marine Information and Advisory Service, Institute of Oceanographic Sciences, Wormley, Godalming, Surrey, U.K.

Cleveland, W. S. and S. J. Devlin. 1988. Locally-weighted regression: an approach to regression analysis by local fitting. *Journal of American Statistical Association* 83:596–610.

Culberson, C. H., G. Knapp, M. Stalcup, R. T. Williams, and F. Zemlyak. 1991. *A comparison of methods for the determination of dissolved oxygen in seawater.* WHP Office Report, WHPO 91-2. WOCE Hydrographic Program Office, Woods Hole, Mass. U.S.A.

Dickson, A. G. 1981. An exact definition of total alkalinity and a procedure for the estimation of alkalinity and total CO_2 from titration data. *Deep-Sea Research* 28:609–23.

Dickson, A. G. and F. J. Millero. 1987. A comparison of the equilibrium constants for the dissociation of carbonic acid in seawater media. *Deep-Sea Research* 34:1733–43.

DOE (U.S. Department of Energy). 1994. *Handbook of Methods for the Analysis of the Various Parameters of the Carbon Dioxide System in Seawater.* Version 2.0. ORNL/CDIAC-74.

A. G. Dickson and C. Goyet (eds.). Carbon Dioxide Information Analysis Center, Oak Ridge National Laboratory, Oak Ridge, Tenn., U.S.A.

Gordon, L. I., J. C. Jennings, Jr., A. A. Ross, and J. M. Krest. 1992. *A suggested protocol for continuous flow automated analysis of seawater nutrients (phosphate, nitrate, nitrite and silicic acid) in the WOCE Hydrographic Program and the Joint Global Ocean Fluxes Study.* Grp. Tech. Rpt. 92-1. Chemical Oceanography Group, Oregon State University, College of Oceanography, Oregon, U.S.A.

Gordon, L. I., J. C. Jennings, Jr., A. A. Ross, and J. M. Krest. 1994. *A suggested protocol for continuous flow automated analysis of seawater nutrients (phosphate, nitrate, nitrite and silicic acid) in the WOCE Hydrographic Program and the Joint Global Ocean Fluxes Study.* In WOCE Operations Manual. WHP Office Report WHPO 91-1. WOCE Report No. 68/91. Revision 1. Woods Hole, Mass., U.S.A.

Hager, S. W., E. L. Atlas, L. I. Gordon, A. W. Mantyla, and P. K. Park. 1972. A comparison at sea of manual and autoanalyzer analyses of phosphate, nitrate, and silicate. *Limnology and Oceanography* 17:931–7.

Huffman, E. W. D., Jr. 1977. Performance of a new automatic carbon dioxide coulometer. *Microchemical Journal* 22:567–73.

Johansson, O., and M. Wedborg. 1982. On the evaluation of potentiometric titrations of seawater with hydrochloric acid. *Oceanology Acta* 5:209–18.

Johnson, K. M., A. E. King, and J. McN. Sieburth. 1985. Coulometric TCO_2 analyses for marine studies: An introduction. *Marine Chemistry* 16:61–82.

Johnson, K. M., P. J. Williams, and L. Brandstroem, and J. McN. Sieburth. 1987. Coulometric TCO_2 analysis for marine studies: Automation and calibration. *Marine Chemistry* 21:117–33.

Johnson, K. M., and D. W. R. Wallace. 1992. *The single-operator multiparameter metabolic analyzer for total carbon dioxide with coulometric detection.* DOE Research Summary No. 19. Carbon Dioxide Information Analysis Center, Oak Ridge National Laboratory, Tenn., U.S.A.

Johnson, K. M., K. D. Wills, D. B. Butler, W. K. Johnson, and C. S. Wong. 1993. Coulometric total carbon dioxide analysis for marine studies: Maximizing the performance of an automated gas extraction system and coulometric detector. *Marine Chemistry* 44:167–87.

Johnson, K. M., A. G. Dickson, G. Eischeid, C. Goyet, P. R. Guenther, R. M. Key, F. J. Millero, D. Purkerson, C. L. Sabine, R. G. Schotle, D. W. R. Wallace, R. J. Wilke, and C. D. Winn. 1998. Coulometric total carbon dioxide analysis for marine studies: Assessment of the quality of total inorganic carbon measurements made during the U.S. Indian Ocean CO_2 Survey 1994–1996. *Marine Chemistry* 63:21–37.

Joyce, T., and C. Corry. 1994. *Requirements for WOCE Hydrographic Programme Data Reporting*. Report WHPO 90-1, WOCE Report No. 67/91, WOCE Hydrographic Programme Office, Woods Hole, Mass. U.S.A. pp. 52-55. Unpublished Manuscript.

Knapp, G. P., M. C. Stalcup, and R. J. Stanley. 1990. *Automated oxygen and salinity determination*. WHOI Technical Report No. WHOI-90-35. Woods Hole Oceanographic Institution, Woods Hole, Mass., U.S.A.

Marinenko, G. and J. K. Taylor. 1968. Electrochemical equivalents of benzoic and oxalic acid. *Analytical Chemistry* 40:1645–51.

Millard, R. C., Jr. 1982. *CTD calibration and data processing techniques at WHOI using the practical salinity scale*. Proceedings Int. STD Conference and Workshop, Mar. Tech. Soc., La Jolla, Calif., p. 19.

Millard, R. C. and K. Yang. 1993. *CTD calibration and processing methods used at Woods Hole Oceanographic Institution*. Woods Hole Oceanographic Institution Technical Report. WHOI 93-44. Woods Hole Oceanographic Institution, Woods Hole, Mass., U.S.A.

Millero, F. J., and A. Poisson. 1981. International one-atmosphere equation of state for seawater. *Deep-Sea Research* 28:625–29.

Millero, F. J., J. Z. Zhang, K. Lee, and D. M. Campbell. 1993. Titration alkalinity of seawater. *Marine Chemistry* 44:153–60.

Millero, F. J., A. G. Dickson, G. Eischeid, C. Goyet, P. R. Guenther, K. M. Johnson, K. Lee, E. Lewis, D. Purkerson, C. L. Sabine, R. Key, R. G. Schottle, D. R. W. Wallace, and C. D. Winn. 1998. Assessment of the quality of the shipboard measurements of total alkalinity on the WOCE Hydrographic Program Indian Ocean CO_2 survey cruises 1994–1996. *Marine Chemistry* 63:9–20.

Roemmich, D., and C. Wunsch. 1985. Two transatlantic sections: Meridional circulation and heat flux in the subtropical North Atlantic Ocean. *Deep-Sea Research* 32:619–64.

Sabine, C. L. and R. M. Key. 1998. *Surface water and atmospheric underway carbon data obtained during the world ocean circulation experiment Indian Ocean survey cruises (R/V Knorr, December 1994–January 1996)*. ORNL/CDIAC-103, NDP-064, Carbon Dioxide Information Analysis Center, Oak Ridge National Laboratory, Oak Ridge, Tenn., U.S.A.

Sabine, C. L., R. M. Key, K. M.. Johnson, F. J. Millero, J. L. Sarmiento, D. R. W. Wallace, and C. D. Winn. 1999. Anthropogenic CO_2 inventory of the Indian Ocean. *Global Biogeochemical Cycles* 13:179–98.

Schlitzer, R. 2001. Ocean Data View. http://www.awi-bremerhaven.de/GEO/ODV. Online publication. Alfred-Wegener-Institute for Polar and Marine Research. Bremerhaven, Germany.

Taylor, J. K. and S. W. Smith. 1959. Precise coulometric titration of acids and bases. *Journal of Research of the National Bureau of Standards* 63A:153–9.

UNESCO. 1981. Background papers and supporting data on the practical salinity scale, 1978. *UNESCO Technical Papers in Marine Science*, No. 37: p. 144.

Wallace, D. W. R. 2002. Storage and transport of excess CO_2 in the oceans: The JGOFS/WOCE Global CO_2 survey. In J. Church, G. Siedler, and J. Gould (eds.). *Ocean Circulation and Climate*, Academic Press, (in press).

Youden, W. J. 1951. *Statistical Methods for Chemists*. Wiley, New York.

PART 2:

CONTENT AND FORMAT OF DATA FILES

7. FILE DESCRIPTIONS

This section describes the content and format of each of the 21 files that constitute this NDP-080 (see Table 14). Because CDIAC distributes the data set in several ways (via the Web, CDIAC's online ordering system, or anonymous FTP), each of the 21 files is referenced by both an ASCII file name, which is given in lowercase, bold-faced type (e.g., **ndp080.txt**), and a file number. The remainder of this section describes (or lists, where appropriate) the contents of each file.

Table 14. Content, size, and format of data files

File number, name, and description	Logical records	File size in bytes
1. **ndp080.txt**: A detailed description of the cruise network, the two FORTRAN 90 data-retrieval routines, and the eighteen oceanographic data files	2,091	128,813
2. **IOstainv.for**: A FORTRAN 90 data-retrieval routine to read and print **i*sta.dat** (Files 4–12)	44	1,411
3. **IOdat.for:** A FORTRAN 90 data-retrieval routine to read and print **i*.dat** (Files 13–21)	58	2,407
4–12. **i08si09ssta.dat**	156	12,573
i09nsta.dat	139	11,340
i08ni05esta.dat	175	14,260
i03sta.dat	140	11,390
i05wi04sta.dat	145	11,688
i07nsta.dat	159	12,949
i01sta.dat	167	13,650
i10sta.dat	70	5,684
i02sta.dat: A listing of the station locations, sampling dates, and sounding bottom depths for each station of the WOCE Sections I8SI9S, I9N, I8NI5E, I3, I5WI4, I7N, I1, I10, and I2	177	14,420
13–21. **i08si09s.dat**	4,566	898,494
i09n.dat	4,537	892,942
i08ni05e.dat	5,477	1,078,087
i03.dat	4,017	790,348
i05wi04.dat	4,028	792,411

i07n.dat	5,128	1,009,334
i01.dat	4,601	905,550
i10.dat	1,748	343,395
i02.dat:	5,567	1,095,817
Hydrographic, carbon dioxide, and chemical data from all stations occupied on WOCE Sections I8SI9S, I9N, I8NI5E, I3, I5WI4, I7N, I1, I10, and I2		
Total	43,190	8,046,963

7.1 ndp080.txt (File 1)

This file contains a detailed description of the data set, the two FORTRAN 90 data-retrieval routines, and the 18 oceanographic data files. It exists primarily for the benefit of individuals who acquire this database as machine-readable data files from CDIAC.

7.2 IOstainv.for (File 2)

This file contains a FORTRAN 90 data-retrieval routine to read and print **i*sta.dat** (Files 4–12). The following is a listing of this program. For additional information regarding variable definitions, variable lengths, variable types, units, and codes, please see the description for **i*sta.dat** in Sect. 7.4.

```
c**********************************************************************
c* This is a Fortran 90 retrieval code to read and format the
c* station inventory during the R/V Knorr Cruises along the WOCE
c* Sections I8SI9S, I9N, I8NI5E, I3, I5WI4, I7N, I1, I10, and I2
c* in the Indian Ocean
c**********************************************************************

c*Defines variables*

       INTEGER  stat, cast, depth
       REAL latdcm, londcm
       CHARACTER expo*10, sect*4, date*10, time*4
       OPEN (unit=1, file='i*sta.dat')
       OPEN (unit=2, file='i*sta.data')
       write (2, 5)

c*Writes out column labels*

 5     format (1X,'EXPOCODE',8X,'SECT',2X,'STNBR',2X,'CAST',9X,
     2 'DATE',2X,'TIME',2X,'LATITUDE',2X,'LONGITUDE',2X,'DEPTH',/)

c*Sets up a loop to read and format all the data in the file*

       read (1, 6)
 6     format (////////)
```

```
7       CONTINUE
        read (1, 10, end=999) expo, sect, stat, cast, date, time,
     1 latdcm, londcm, depth

10      format (1X, A10, 6X, A4, 3X, I4, 5X, I1, 3X, A10, 2X, A4, 3X,
     1 F7.3, 3X, F8.3, 3X, I4)

        write (2, 20) expo, sect, stat, cast, date, time,
     1 latdcm, londcm, depth

20      format (1X, A10, 6X, A4, 3X, I4, 5X, I1, 3X, A10, 2X, A4, 3X,
     1 F7.3, 3X, F8.3, 3X, I4)

        GOTO 7
999     close(unit=5)
        close(unit=2)
        stop
        end
```

7.3 i*dat.for (File 3)

This file contains a FORTRAN 90 data-retrieval routine to read and print **i*.dat** (Files 13–21). The following is a listing of this program. For additional information regarding variable definitions, variable lengths, variable types, units, and codes, please see the description for **i*.dat** in Sect. 7.5.

```
c*********************************************************************
c* FORTRAN 90 data retrieval routine to read and print the files
c* named "i*.dat" (Files 13-21)
c*********************************************************************
        CHARACTER qualt*15, bot*6
        INTEGER sta, cast, samp
        REAL pre, ctdtmp, ctdsal, ctdoxy, theta, sal, oxy, silca
        REAL nitrat, nitrit, phspht, cfc11, cfc12, tcarb, alkali
        REAL delc14, c14er, delc13
        OPEN (unit=1, file='i08si09s.dat')
        OPEN (unit=2, file='i08si09s.data')
        write (2, 5)

c*Writes out column labels*

 5      format (2X,'STNNBR',2X,'CASTNO',2X,'SAMPNO',2X,'BTLNBR',2X,
     1  'CTDPRS',2X,'CTDTMP',2X,'CTDSAL',2X,'CTDOXY',3X,'THETA',4X,
     2  'SALNTY',2X,'OXYGEN',2X,'SILCAT',2X,'NITRAT',2X,'NITRIT',2X,
     3  'PHSPHT',3X,'CFC-11',3X,'CFC-12',2X,'TCARBN',2X,'ALKALI',2X,
     4  'DELC14',2X,'C14ERR',2X,'DELC13',10X,'QUALT1',/,
     5  36X,'DBAR',2X,'ITS-90',2X,'PSS-78',1X,'UMOL/KG',
     6  2X,'ITS_90',4X,'PSS-78',1X,5('UMOL/KG',1X),1X,'PMOL/KG',2X,
     7  'PMOL/KG',1X,2('UMOL/KG',1X),1X,3('/MILLE',2X),13X,'*',/,
     8  25X,'*******',17X,2('*******',1X),10X,6('*******',1X),1X,
     9  '*******',2X,4('*******',1X),8X,"********",15X,'*')

c*Sets up a loop to read and format all the data in the file*

        read (1, 6)
```

```
 6      format (//////////)

 7      CONTINUE
        read (1, 10, end=999) sta, cast, samp, bot, pre, ctdtmp,
     1 ctdsal, ctdoxy, theta, sal, oxy, silca, nitrat, nitrit,
     2 phspht, cfc11, cfc12, tcarb, alkali, delc14, c14er, delc13,
     3 qualt

10      format (4X, I4, 7X, I1, 6X, I2, 2X, A6, 1X, F7.1, 1X, F7.4,
     1 1X, F7.4, 1X, F7.1, 1X, F7.4, 1X, F9.4, 1X, F7.1, 1X, F7.2,
     2 1X, F7.2, 1X, F7.2, 1X, F7.2, 1X, F8.3, 1X, F8.3, 1X, F7.1,
     3 1X, F7.1, 1X, F7.1, 1X, F7.1, 1X, F7.1, 1X, A15)

        write (2, 20) sta, cast, samp, bot, pre, ctdtmp,
     1 ctdsal, ctdoxy, theta, sal, oxy, silca, nitrat, nitrit,
     2 phspht, cfc11, cfc12, tcarb, alkali, delc14, c14er, delc13,
     3 qualt

20      format (4X, I3, 7X, I1, 6X, I2, 2X, A6, 1X, F7.1, 1X, F7.4,
     1 1X, F7.4, 1X, F7.1, 1X, F7.4, 1X, F9.4, 1X, F7.1, 1X, F7.2,
     2 1X, F7.2, 1X, F7.2, 1X, F7.2, 1X, F8.3, 1X, F8.3, 1X, F7.1,
     3 1X, F7.1, 1X, F7.1, 1X, F7.1, 1X, F7.1, 1X, A15)


        GOTO 7
999     close(unit=1)
        close(unit=2)
        stop
        end
```

7.4 i*sta.dat (Files 4–12)

These files, **i08si09ssta.dat, i09nsta.dat, i08ni05esta.dat, i03sta.dat, i05wi04sta.dat, i07nsta.dat, i01sta.dat, i10sta.dat**, and **i02sta.dat**, provide station inventory information for each station occupied during the R/V *Knorr* cruises along WOCE Sections I8SI9S, I9N, I8NI5E, I3, I5WI4, I7N, I1, I10, and I2. Each line in the files contains an expocode, section number, station number, cast number, sampling date (month/date/year), sampling time, latitude, longitude, and sounding depth. The files are sorted by station number and can be read by using the following FORTRAN 90 code (contained in **IOstainv.for**, File 2):

```
        INTEGER  stat, cast, depth
        REAL latdcm, londcm
        CHARACTER expo*10, sect*4, date*10, time*4

        read (1, 10, end=999) expo, sect, stat, cast, date, time,
     1 latdcm, londcm, depth

10      format (1X, A10, 6X, A4, 3X, I4, 5X, I1, 3X, A10, 2X, A4, 3X,
     1 F7.3, 3X, F8.3, 3X, I4)
```

Stated in tabular form, the contents include the following:

Variable	Variable type	Variable width	Starting column	Ending column
expo	Character	10	2	11
sect	Character	4	18	21
stat	Numeric	4	25	28
cast	Numeric	1	34	34
date	Character	10	38	47
time	Character	4	50	53
latdcm	Numeric	7	57	63
londcm	Numeric	8	67	74
depth	Numeric	4	78	81

The variables are defined as follows:

expo expedition code of the cruise

sect WOCE section number

stat station number

cast cast number

date sampling date (month/day/year)

time sampling time [Greenwich mean time (GMT)]

latdcm latitude of the station (in decimal degrees; negative values indicate the Southern Hemisphere)

londcm longitude of the station (in decimal degrees; negative values indicate the Western Hemisphere)

depth sounding depth of the station (in meters)

7.5 i*.dat (Files 13–21)

These files,**i08si09s.dat, i09n.dat, i08ni05e.dat, i03.dat, i05wi04.dat, i07n.dat, i01.dat, i10.dat,** and **i02.dat,** provide hydrographic, carbon dioxide, and chemical data for all stations occupied during the R/V *Knorr* cruises along WOCE Sections I8SI9S, I9N, I8NI5E, I3, I5WI4, I7N, I1, I10, and I2. Each line consists of station number, cast number, sample number, bottle number, CTD pressure, CTD temperature, CTD salinity, CTD oxygen, potential temperature, bottle salinity, bottle oxygen, silicate, nitrate, nitrite, phosphate, CFC-11, CFC-12, TCO_2, TALK, $\Delta^{14}C$, ^{14}C error, $\Delta^{13}C$, and data-quality flags. The files are sorted by station number and pressure and can be read by using the following FORTRAN 90 code (contained in **i*dat.for,** File 3):

```
      CHARACTER qualt*15, bot*6
      INTEGER sta, cast, samp
      REAL pre, ctdtmp, ctdsal, ctdoxy, theta, sal, oxy, silca
      REAL nitrat, nitrit, phspht, cfc11, cfc12, tcarb, alkali
      REAL delc14, c14er, delc13

      read (1, 10, end=999) sta, cast, samp, bot, pre, ctdtmp,
     1 ctdsal, ctdoxy, theta, sal, oxy, silca, nitrat, nitrit,
     2 phspht, cfc11, cfc12, tcarb, alkali, delc14, c14er, delc13,
     3 qualt

10    format (4X, I4, 7X, I1, 6X, I2, 2X, A6, 1X, F7.1, 1X, F7.4,
     1 1X, F7.4, 1X, F7.1, 1X, F7.4, 1X, F9.4, 1X, F7.1, 1X, F7.2,
     2 1X, F7.2, 1X, F7.2, 1X, F7.2, 1X, F8.3, 1X, F8.3, 1X, F7.1,
     3 1X, F7.1, 1X, F7.1, 1X, F7.1, 1X, F7.1, 1X, A15)
```

Stated in tabular form, the contents include the following:

Variable	Variable type	Variable width	Starting column	Ending column
sta	Numeric	4	5	8
cast	Numeric	1	16	16
samp	Numeric	2	23	24
bot	Character	6	27	32
pre	Numeric	7	34	40
ctdtmp	Numeric	7	42	48
ctdsal	Numeric	7	50	56
ctdoxy	Numeric	7	58	64
theta	Numeric	7	66	72
sal	Numeric	9	74	82
oxy	Numeric	7	84	90
silca	Numeric	7	92	98
nitrat	Numeric	7	100	106
nitrit	Numeric	7	108	114
phspht	Numeric	7	116	122
cfc11	Numeric	8	124	131
cfc12	Numeric	8	133	140
tcarb	Numeric	7	142	148
alkali	Numeric	7	150	156
delc14	Numeric	7	158	164
c14er	Numeric	7	166	172
delc13	Numeric	7	174	180
qualt	Character	15	182	196

The variables are defined as follows:

sta	station number
cast	cast number
samp	sample number
bot[a]	bottle number
pre	CTD pressure (dbar)
ctdtmp	CTD temperature (°C)
ctdsal[a]	CTD salinity [on the Practical Salinity Scale (PSS)]
ctdoxy[a]	CTD oxygen (μmol/kg)
theta	potential temperature (°C)
sal[a]	bottle salinity (on the PSS)
oxy[a]	oxygen concentration (μmol/kg)
silca[a]	silicate concentration (μmol/kg)
nitrat[a]	nitrate concentration (μmol/kg)
nitrit[a]	nitrite concentration (μmol/kg)
phspht[a]	phosphate concentration (μmol/kg)
cfc11[a]	chlorofluorocarbon 11 (pmol/kg)
cfc12[a]	chlorofluorocarbon 12(pmol/kg)
tcarb[a]	total carbon dioxide concentration (μmol/kg)
alkali[a]	total alkalinity (μmol/kg)
delc14[a]	radiocarbon delta ^{14}C (per mille)
c14er	error of delta ^{14}C (percent)
delc13[a]	is the radiocarbon delta ^{13}C (per mille);
qualt	15-digit character variable that contains data-quality flag codes for parameters underlined with asterisks (*******) in the file header

[a]Variables that are underlined with asterisks in the data file's header indicate they have a data-quality flag. Data-quality flags are defined as follows:

1	=	sample for this measurement was drawn from water bottle but analysis was not received
2	=	acceptable measurement
3	=	questionable measurement
4	=	bad measurement
5	=	not reported
6	=	mean of replicate measurements
7	=	manual chromatographic peak measurement
8	=	irregular digital chromatographic peak integration
9	=	sample not drawn for this measurement from this bottle

APPENDIX A:

List of CO_2 measurement group members participating in the Indian Ocean CO_2 Survey aboard the R/V *Knorr* in 1994–1996

Appendix A

List of CO_2 measurement group members participating in the Indian Ocean CO_2 Survey aboard the R/V *Knorr* in 1994–1996

(CO_2 group leaders for each section are given in Table 4 in the text)

Section	Name	Sponsoring institute	Affiliation (if known)
I8SI9S	Haynes, Charlotte H Haynes, Elizabeth M Wysor, Brian S.	BNL BNL BNL	WDNR RU SHC
I9N	Dorety, Art Kozyr, Alex Suntharalingam, Parv	PU PU PU	PU ORNL/CDIAC PU
I8NI5E	Parks, Justine Popp, Brian Schottle, R.	UH UH UH	SIO UH UH
I3	Aicher, Jennifer Edwards, Christopher Krenisky, Joann	RSMAS RSMAS RSMAS	RSMAS RSMAS RSMAS
I4I5W	Lewis, Ernie Pikanowski, Linda Zotz, Michelle	BNL BNL BNL	BNL SHML BNL
I7N	Adams, Angela Angeley, Kelly Phillips, Jennifer	UH UH UH	UH UHH
I1	Amaoka, Toshitaka Okuda, Kozo Ording, Philip	WHOI WHOI WHOI	GSEESHU GSEESHU WHOI
I10	Boehme, Sue Markham, Marion Mcdonald, Gerard	PU PU PU	RU PU PU
I2	Admas, Angela Cipolla, Cathy Phillips, Jennifer	UH UH UH	UH GSOURI UHH

Participating institutions:

BNL	Brookhaven National Laboratory
ORNL/CDIAC	Oak Ridge National Laboratory/Carbon Dioxide Information Analysis Center
GSEESHU	Graduate School of Environmental and Earth Science, Hokkaido University
GSOURI	Graduate School of Oceanography, University of Rhode Island
PU	Princeton University
RSMAS	Rosenstiel School of Marine and Atmospheric Science, University of Miami
RU	Rutgers University
SHC	South Hampton College
SHML	Sandy Hook Marine Laboratory
SIO	Scripps Institution of Oceanography
UH	University of Hawaii, Honolulu
UHH	University of Hawaii at Hilo
WDNR	Wisconsin Department of Natural Resources
WHOI	Woods Hole Oceanographic Institution

APPENDIX B:

REPRINT OF PERTINENT LITERATURE

Johnson, K. M., A. G. Dickson, G. Eischeid, C. Goyet, P. R. Guenther, R. M. Key, F. J. Millero, D. Purkerson, C. L. Sabine, R. G. Schotle, D. W. R. Wallace, R. J. Wilke, and C. D. Winn. 1998. Coulometric total carbon dioxide analysis for marine studies: Assessment of the quality of total inorganic carbon measurements made during the U.S. Indian Ocean CO_2 Survey 1994–1996. *Marine Chemistry* 63:21–37.

ELSEVIER

Marine Chemistry 63 (1998) 21–37

MARINE CHEMISTRY

Coulometric total carbon dioxide analysis for marine studies: assessment of the quality of total inorganic carbon measurements made during the US Indian Ocean CO_2 Survey 1994–1996

Kenneth M. Johnson [a,*], Andrew G. Dickson [b], Greg Eischeid [c], Catherine Goyet [c], Peter Guenther [b], Robert M. Key [d], Frank J. Millero [e], David Purkerson [e], Christopher L. Sabine [d], Rolf G. Schottle [f], Douglas W.R. Wallace [a], Richard J. Wilke [a], Christopher D. Winn [f]

[a] *Department of Applied Science, Brookhaven National Laboratory, Upton, NY 11973, USA*
[b] *Scripps Institution of Oceanography, University of California, San Diego, La Jolla San Diego, CA 92093, USA*
[c] *Woods Hole Oceanographic Institution, Woods Hole, MA 02543, USA*
[d] *Geology Department, Princeton University, Princeton, NJ 08544, USA*
[e] *Rosenstiel School of Marine and Atmospheric Sciences, University of Miami, Miami, FL 33149, USA*
[f] *Department of Oceanography, University of Hawaii, Honolulu, HI 96822, USA*

Received 8 January 1998; accepted 6 May 1998

Abstract

Two single-operator multiparameter metabolic analyzers (SOMMA)-coulometry systems (I and II) for total carbon dioxide (TCO_2) were placed on board the R/V Knorr for the US component of the Indian Ocean CO_2 Survey in conjunction with the World Ocean Circulation Experiment-WOCE Hydrographic Program (WHP). The systems were used by six different measurement groups on 10 WHP Cruises beginning in December 1994 and ending in January 1996. A total of 18,828 individual samples were analyzed for TCO_2 during the survey. This paper assesses the analytical quality of these data and the effect of several key factors on instrument performance. Data quality is assessed from the accuracy and precision of certified reference material (CRM) analyses from three different CRM batches. The precision of the method was 1.2 μmol/kg. The mean and standard deviation of the differences between the known TCO_2 for the CRM (certified value) and the CRM TCO_2 determined by SOMMA-coulometry were -0.91 ∓ 0.58 ($n = 470$) and -1.01 ∓ 0.44 ($n = 513$) μmol/kg for systems I and II, respectively, representing an accuracy of 0.05% for both systems. Measurements of TCO_2 made on 12 crossover stations during the survey agreed to within 3 μmol/kg with an overall mean and standard deviation of the differences of -0.78 ∓ 1.74 μmol/kg ($n = 600$). The crossover results are therefore consistent with the precision of the CRM analyses. After 14 months of nearly continuous use, the accurate and the virtually identical performance statistics for

* Corresponding author. Tel.: +1-516-344-5668; Fax: +1-516-344-3246

PII: S0304-4203(98)00048-6

the two systems indicate that the cooperative survey effort was extraordinarily successful and will yield a high quality data set capable of fulfilling the objectives of the survey.

Keywords: total carbon dioxide (TCO_2); single-operator multiparameter metabolic analyzers (SOMMA) coulometry; marine studies

1. Introduction

Between 1990 and 1997 an international effort was made to determine the global oceanic distribution of inorganic carbon in conjunction with the World Ocean Circulation Experiment (WOCE) Hydrographic Programme (WHP). This effort is referred to as the Global Survey of CO_2 in the oceans, and it is an integral part of the Joint Global Ocean Flux Study (JGOFS). The goals of this survey are to:

1. Accurately determine the oceanic distribution of dissolved inorganic carbon,
2. Quantify the uptake of anthropogenic carbon dioxide by the oceans to better predict future atmospheric carbon dioxide levels,
3. Provide a global description of anthropogenic carbon dioxide in the oceans to aid development of a 3-dimensional model of the oceanic carbon cycle,
4. Characterize the transport of carbon dioxide between the ocean and the atmosphere and the large scale (e.g., meridional) transports of carbon dioxide within the ocean.

The survey has acquired a global data set of profile measurements of dissolved carbon dioxide parameters on both zonal and meridional oceanographic transects throughout the world's oceans. With reference to program goals, Bates et al. (1996) found that for mixed layer waters the average rate of increase in CO_2 concentration due to the uptake of anthropogenic CO_2 was 1.7 μmol/kg/yr (< 0.1%). This rate of increase establishes a natural target for the accuracy of the TCO_2 measurements. The distribution of this 'excess' CO_2 signal is not uniform spatially, and it is masked by variability in CO_2 concentrations arising from natural biological and physicochemical processes. Hence, the goals of the program imply that measurements must be extremely accurate (0.1% or better) and spatially extensive. A large part of the US contribution to this survey has been conducted by a team of investigators supported by the US Department of Energy (DOE). This team has developed certified reference materials (Dickson, 1990), instrumentation (Johnson and Wallace, 1992), a set of standard operating procedures (DOE, 1994) and, to a large extent, shared a common approach to the measurement program.

This paper presents the DOE team effort which sampled the Indian Ocean for inorganic carbon during the course of approximately 1 year. All the measurements were made aboard a single research vessel during sequential cruises which allowed the investigators to share equipment and procedures to an unprecedented extent. This paper concentrates on estimating the accuracy of the shipboard determinations of the total dissolved inorganic carbon concentration of seawater. This parameter was established at the onset of the survey as the primary carbonate system parameter because its concentration should change in response to anthropogenic CO_2 uptake and it had the highest potential for measurement accuracy. Our results highlight some factors which affect the accuracy of this measurement. The Indian Ocean Survey aboard the R/V Knorr encompassed the cruise legs shown in Fig. 1 in the sequence given in Table 1. Fig. 1 also gives the location of the crossover

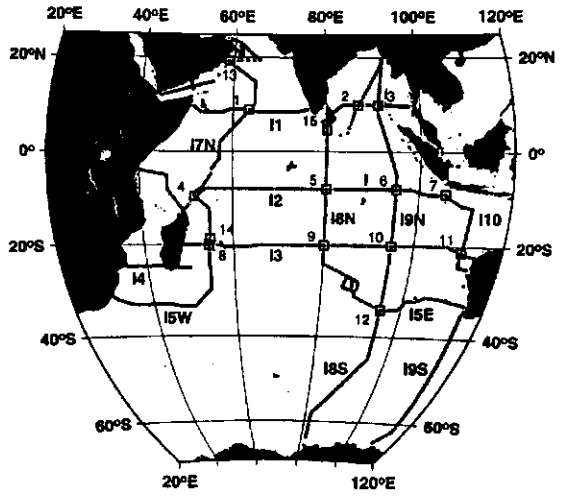

Fig. 1. The cruise tracks for the nine legs of the US Indian Ocean WOCE Survey 1994–1996. Crossover points between the various legs are marked with a square and numbered. These intersection points and crossovers are referred to in Table 4.

Table 1
Approximate dates and ports of call for the 9 legs of the Indian Ocean CO_2 Survey, and the measurement groups responsible for the determination of the carbonate system parameters

Leg	Dates		From	To	Group	Duration (days)
	Start	End				
I8SI9S	12/1/94	1/19/95	Fremantle	Fremantle	BNL	50
I9N	1/24/95	3/6/95	Fremantle	Colombo	Princeton U.	42
I8NI5E	3/10/95	4/16/95	Colombo	Fremantle	U. of Hawaii	38
I3	4/20/95	6/7/95	Fremantle	Port Louis	U. of Miami	49
I5WI4	6/11/95	7/11/95	Port Louis	Port Louis	BNL	31
I7N	7/15/95	8/24/95	Port Louis	Matrah	U. of Hawaii	41
I1	8/29/95	10/18/95	Matrah	Singapore	WHOI	51
Dry Dock	10/19/95	11/5/95	Singapore			17
I10	11/6/95	11/24/95	Singapore	Singapore	Princeton U.	19
I2	11/28/95	1/19/96	Singapore	Mombasa	U. of Hawaii	53

Abbreviations: BNL, Brookhaven National Laboratory; U, University; WHOI, Woods Hole Oceanographic Institution.

points (cruise track intersections) where comparisons of the reproducibility of the TCO_2 analyses were made. The six survey groups measured two water column carbonate system parameters, total dissolved carbon dioxide (TCO_2) and total alkalinity (TA), and assisted with the operation of an underway pCO_2 (surface) system. This paper focuses on TCO_2 by coulometry, while the total alkalinity (TA) and partial pressure of CO_2 (pCO_2) measurements are the subject of companion papers and reports (Millero et al., 1998; Sabine and Key, 1998).

2. Materials and methods

2.1. Preparations

The total carbon dioxide concentration (TCO_2) was determined using two single-operator multiparameter metabolic analyzers (SOMMA) each connected to a Model 5011 coulometer (UIC, Joliet, IL 60434). Descriptions of the SOMMA-coulometer system and its calibration can be found in the works of Johnson (1995), Johnson and Wallace (1992), and Johnson et al. (1987, 1993). A schematic diagram of the SOMMA is shown in Fig. 2, and further details concerning the coulometric titration can be found in the works of Huffman (1977) and Johnson et al. (1985). Briefly, seawater fills an automated to-deliver sample pipette. The contents of the pipette are pneumatically injected into a stripping chamber containing approximately 1.2 cm^3 of 8.5% (v/v) phosphoric acid, and the resultant CO_2 is extracted, dried, and coulometrically titrated. Calibration is performed by titrating known masses of pure CO_2 and checked by analyzing certified reference material (CRM). The coulometers were adjusted to give a maximum titration current of 50 mA, and they were run in the counts mode (the number of pulses or counts generated by the coulometer's voltage to frequency converter during the titration is displayed). In the coulometer cell, the acid (hydroxyethylcarbamic acid) formed from the reaction of CO_2 and ethanolamine is titrated coulometrically (electrolytic generation of OH^-) with photometric endpoint detection. The systems were equipped with conductance cells (Model SBE-4, Sea-Bird Electronics, Bellevue, WA) for measuring salinity as described by Johnson et al. (1993).

The DOE supported the construction of nine SOMMA-coulometer systems for the US CO_2 Survey Measurement Groups in the early 1990's (Johnson and Wallace, 1992), and two of these systems from the DOE instrument pool were set up aboard the R/V Knorr in Fremantle, Australia on November 28, 1994. Before they were shipped to Australia, the temperature sensors were calibrated, the glassware was chemically cleaned and gravimetrically calibrated, the gas sample loop volumes were calibrated according to the procedure of Wilke et al. (1993), the coulometers were electronically cali-

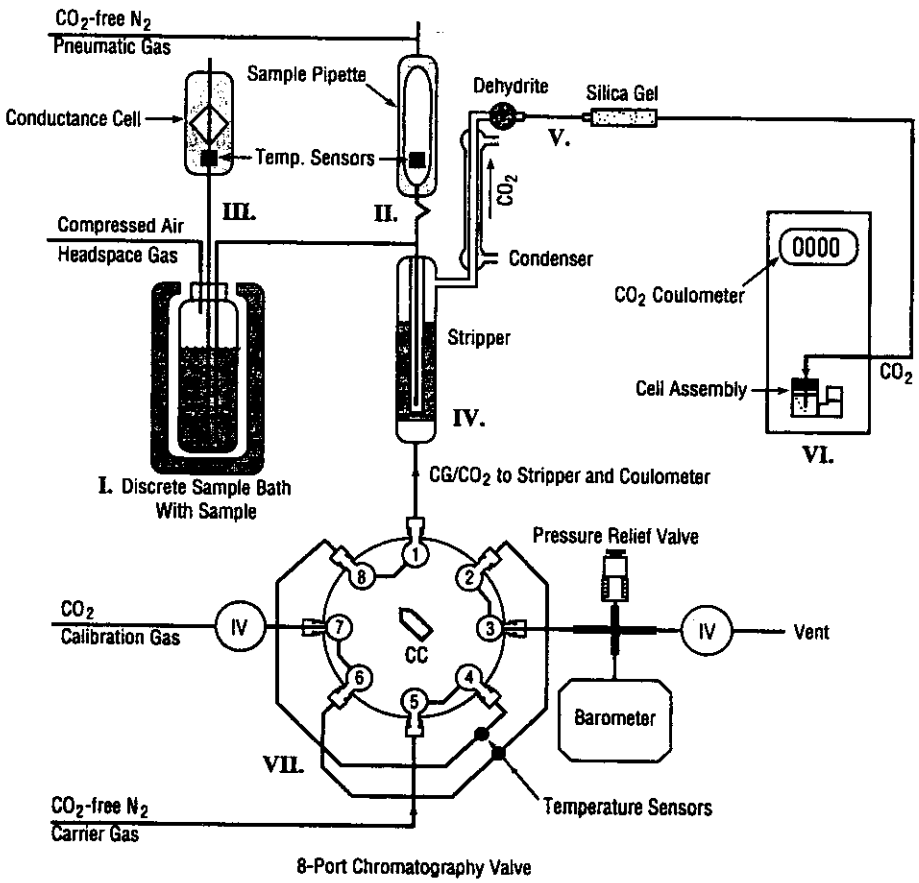

Fig. 2. SOMMA-coulometer system schematic. Carbon dioxide extracted from a water sample (I) or from volume-calibrated gas sample loops filled at a known pressure and temperature is degassed from the stripper (IV), dried (V), and coulometrically titrated (VI). The water sample is pneumatically injected from the pipette (II) into the stripper, and the pure CO_2 contained in the gas loops is delivered to the stripper from an 8-port chromatography valve (VII) equipped with pressure and temperature sensors. Salinity is measured using a conductance cell (III) integrated into the SOMMA chassis. The pipette and conductance cell are thermostatted and equipped with temperature sensors.

brated (Johnson et al., 1993; DOE, 1994), and system accuracy was verified with CRM at Brookhaven National Laboratory (BNL). The same two systems (hereafter called I and II) were used by all measuring groups. A backup system (from Woods Hole Oceanographic Institution) was onboard but was not used. Pre-cruise preparations also included a training session for participants at the University of Miami in September 19–23, 1994.

Referring to Fig. 2, the analytical gases included UHP nitrogen (99.998%) for carrier and pneumatic gases, compressed air for the headspace gas, and analytical grade CO_2 (99.995%) from Scott Specialty Gases (South Plainfield, NJ) for the calibration gas. The survey began with the use of compressed gases, but prior to leg I8N in April 1995, a N_2 generator (TOC Model 1500, Peak Scientific, Chicago, IL) was placed into service. The generator provided N_2 (99.9995%, hydrocarbons < 0.1 ppm, CO_2 < 1.0 ppm) for carrier and pneumatic gases to both systems for the remainder of the survey. Unless otherwise stated, all other reagents remain as described by Johnson et al. (1993).

The BNL measurement group supplied 7 side-arm type glass titration cells (UIC, PN 200-034), 7 silver electrodes (PN 101-033), and 5 rubber cell

caps (PN 192-005). A platinum electrode (PN 101-034), temperature sensor (PN LM34CH, National Semiconductor, Santa Clara, CA), and a teflon inlet tube were mounted in each cap. Together, the cell and cap comprise the cell assembly shown in Fig. 3. For this paper, each cell assembly is assigned an 'age' or lifetime which is measured in minutes (chronological age) or by the mass of carbon titrated in mg C (carbon age) from the time when current is first applied to the assembly (cell birth) until the current is turned off (cell death). The software continuously records the chronological and carbon ages.

2.2. Selection of cell assemblies

The performance of individual cell assemblies (Fig. 3) varies widely (K.M. Johnson, unpublished data). Unacceptable assemblies exhibit high blanks, prolonged blank determinations (> 2 h), reduced accuracy or precision, or become noisy early in their lifetime. Acceptable assemblies stabilize quickly (within 60 min) and function well for periods exceeding 24 h. Cell behavior will be discussed elsewhere, but our experience suggests several factors play a role: quality of the reagents; quality (purity) of the carrier gases; damage to the platinum electrode; and perhaps the porosity of the cell frit. Therefore, a systematic effort was made at the beginning of leg I8SI9S to select satisfactorily performing cell assemblies using pretested reagents and carrier gas sources known to be uncontaminated. During this first leg, the assemblies on hand were evaluated for conformance to the following empirical criteria.

(1) Cell assemblies should attain a blank of $\lesssim$ 0.005 μmol C/min within 90 min of cell birth. Satisfactory assemblies usually exhibit a 15–25% decline in the blank with each successive determination.

(2) The gas calibration factor, which is the ratio of an accurately known mass of CO_2 to the mass of this gas determined coulometrically, should be 1.004 ∓ 0.0015 (recoveries of ~ 99.6%).

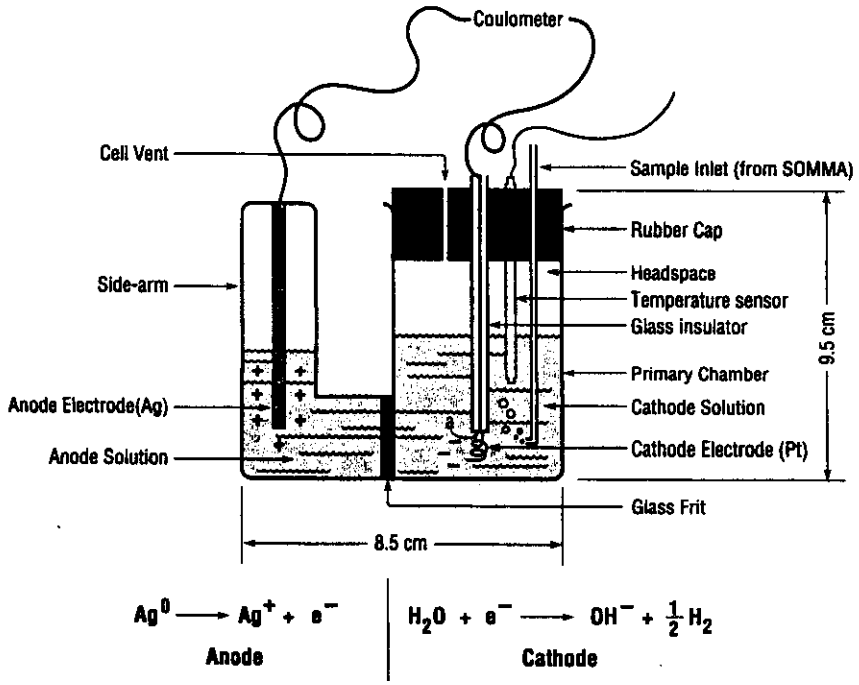

Fig. 3. The titration cell assembly and the cathodic and anodic half reactions for the coulometric titration of the H^+ from the acid formed by the reaction of CO_2 and ethanolamine.

(3) Titrations of CO_2 extracted from gas sample loops (gas calibration) or pipettes of 20 cm^3 (sample analysis) should take 9–12 min.

(4) Cell assemblies, which repeatedly exhibit titrations longer than 20 min (no endpoint) before their carbon age reached 30 mg C titrated, were considered defective. An occasional failure to attain an endpoint after the carbon age exceeds 30 mg C was interpreted to mean that the cell frit required cleaning with 6 N HNO_3 and retesting.

Based on these criteria, three assemblies (2 primary and a third as backup) were found to be acceptable during the first leg, and these assemblies were used throughout the survey (at the midpoint of the survey an additional assembly was placed into service).

2.3. At-sea operations

The following TCO_2 sampling and measurement practices were followed throughout the survey.

(1) The daily sequence of analytical operations for each system as described in the SOMMA operator's manual (Johnson, 1995) consisted of changing the cells and drying agents, determining the blank, running test seawater samples, calibrating the system using pure CO_2 (gas calibration), analyzing samples, and analyzing certified reference material (CRM) at the beginning and end of the cell lifetime.

(2) A complete deep vertical profile for TCO_2 and TA consisted of 36 samples. A lesser number of samples were drawn at shallower stations. Complete profiles were taken at every other station, and if time permitted, additional truncated profiles (0–1000 m) were taken. TCO_2 samples always coincided with ^{14}C samples. Samples were drawn from 10-l Niskin bottles according to DOE (1994).

(3) Samples for TCO_2 were collected in 300 cm^3 BOD-type glass bottles. They were poisoned with a saturated $HgCl_2$ solution (200–400 μl) upon collection. The appropriate correction factors for dilution were applied by the measurement groups according to DOE (1994).

(4) Sample bottles were rinsed and then allowed to overflow by at least 1/2 volume before poisoning. Prior to April 1995, a glass stopper was inserted into the full BOD bottle. After April 1995, a headspace of approximately 4 cm^3 was created before poisoning and stoppering. This was done in a reproducible manner by squeezing the filling tube shut before withdrawing it from the bottle. This change was made to ensure that no $HgCl_2$ was displaced by the stopper, and to allow for water expansion. The gas–liquid phase ratio was approximately 1.3%. A correction (± 0.5 μmol/kg) for the reequilibration of the liquid with the gas phase was applied by the measurement groups according to DOE (1994).

(5) To estimate sample precision, duplicate samples were normally collected at surface, mid depth, and at the deepest depth. The duplicate analyses were interspersed with the analysis of the other profile samples with a minimum of 2 h and up to 12 h between duplicate analyses. Because the duplicate analyses were separated in time, these data could potentially detect drift (decreased precision) as the cell aged. Every effort was made to run each station profile on a single cell assembly, and to limit the cell lifetime to $\lesssim 35$ mg C.

(6) Although salinity was determined by the SOMMA-coulometer systems, post-cruise sample density was calculated using bottle salinities supplied by the chief scientists. However, SOMMA-based salinities were often compared to the real-time CTD salinities to spot bottle mistrips during the taking of the vertical profiles. The agreement between SOMMA-based and CTD salinities was ± 0.02 or better.

(7) To monitor the volume of the SOMMA pipettes, they were periodically filled with deionized water at known temperatures, and their output collected in preweighed serum bottles. The bottles were sealed immediately and stored until they were reweighed at BNL on a model R300S (Sartorius, Göttingen, Germany) balance. The mass of water corrected for buoyancy was used to calculate the to-deliver pipette volume (V_{cal}, Eq. (3)) according to DOE (1994).

(8) After use, cells were cleaned with deionized water followed by an acetone rinse of the glass frit. Before reuse, they were dried at 55°C for at least 12 h. Cell caps and the platinum electrodes were thoroughly washed with deionized water and dried at 55°C for at least 6 h before reuse.

(9) Duplicate samples from approximately 3000 m and 20 m were regularly collected for shore-based

reference analyses of TCO_2 by vacuum extraction/manometry by C.D. Keeling at the Scripps Institution of Oceanography (SIO). Between 2 and 5% of the samples analyzed at sea will be analyzed at SIO and reported elsewhere.

2.4. Calculation of results

For the coulometric determination, the mass of carbon titrated from CO_2 extracted from the gas sample loops or a water sample in μmol of carbon is given by M according to:

$$M = [\text{Counts}/4824.45 - (\text{Blank} \times t_t) - (\text{Int}_{ec} \times t_i)]/\text{Slope}_{ec}, \quad (1)$$

where Counts is the coulometer display, i.e., the number of pulses accumulated by the coulometer's voltage to frequency circuit (VFC); 4824.45 (counts/μmol) is a scaling factor derived from the factory calibration of the VFC and the value of the Faraday (96,485.309 C/mol); Blank is the system blank in μmol/min; t_t is the length of the titration in minutes; Int_{ec} is the intercept from the electronic calibration of the coulometer; t_i is the duration (min) of continuous current flow, and Slope_{ec} is the slope from electronic calibration (Johnson et al., 1993; DOE, 1994). Electronic calibration serves as a check of the factory calibration. If the coulometer was perfectly calibrated, the slope and intercept would be 1 and 0, respectively. Typically, minor deviations from the theoretical slope (0.998–0.999) and intercept (0.001–0.01) are observed. The water sample TCO_2 concentration in μmol/kg is calculated from:

$$TCO_2 = M \times \text{Calibration Factor} \times (1/(V_T p))D + \Delta TCO_2, \quad (2)$$

where V_T is the sample volume (to-deliver volume of the SOMMA pipette) calculated from:

$$V_T = V_{cal}[1 + a_v(T - T_{cal})], \quad (3)$$

and T is the analytical temperature; V_{cal} is the calibrated volume of the pipette at the calibration temperature, T_{cal}; a_v is the coefficient of volumetric expansion for Pyrex glass (1.0×10^{-5}/deg). In Eq. (2), Calibration Factor is the gas calibration factor (see Eq. (4)); p is the density of seawater from the seawater equation of state (Millero and Poisson, 1981) at the sample salinity and T; D is the correction due to dilution of the sample with $HgCl_2$ preservative; ΔTCO_2 is the correction for the repartitioning of CO_2 into the sample headspace according to DOE (1994). Note that correction factors D and ΔTCO_2 (Eq. (2)) are not incorporated into the SOMMA software and were applied post cruise by the individual measurement groups.

The gas calibration factor (Calibration Factor) is the ratio of:

$$M_{calc}/M, \quad (4)$$

where M_{calc} is the mass of CO_2 contained in the gas sample loop calculated according to DOE (1994), and M is the coulometric determination of that same mass from Eq. (1).

2.5. Assessment of analytical accuracy

Analytical accuracy was assessed by analyzing certified reference materials (CRMs). The CRMs are filtered seawater poisoned with $HgCl_2$. They are prepared in 500 cm^3 bottles at the Scripps Institution of Oceanography (SIO) according to procedures given by Dickson (1990). The certified TCO_2 value is obtained by analyzing a representative number of samples by vacuum extraction/manometry in the laboratory of C.D. Keeling at SIO. For this paper, the term analytical difference refers to the difference between the analyzed (by coulometry) and the certified value of the CRM (by manometry), i.e., at-sea accuracy is estimated from the analyzed TCO_2-certified TCO_2 differences.

2.6. Data distribution

The complete data set has been submitted to the Carbon Dioxide Information Analysis Center (CDIAC) at the Oak Ridge National Laboratory (ORNL). CDIAC will issue a final data report which will detail the procedures for retrieving the data. The overall accuracy given below is considered final at this time, and the estimated precision is expected to remain unchanged. The CDIAC web address is http://cdiac.esd.ornl.gov.

3. Results

During the survey, approximately 18,828 separate samples (not counting duplicates) for TCO_2, and 983 CRM were analyzed on the two systems (A. Kozyr, personal communication, November 1997).

3.1. To-deliver pipette volume

Some 103 gravimetric determinations of the sample pipette volume were made on 28 separate occasions during the survey (14 on each system). Four of the determinations were rejected; two because they were exactly 1 cm^3 too high with respect to the survey mean (likely due to failure to correctly note the tare weight determined prior to the cruise), and two because they were inexplicably 0.3% lower than the survey mean volumes (probably due to faulty sealing and evaporation). There were no results from leg I8N because the gravimetric samples were collected incorrectly. Volume determinations should have been made at the start, middle, and at the end of each leg, or at least at the beginning and end of each leg. However, for a variety of reasons, this was not always the case. In order to consistently assign a pipette volume to each leg, a leg-specific volume (V_{cal}) was obtained by averaging the volume determinations made closest to the beginning and end of the leg along with any made during that leg. Table 2 presents the results for V_{cal}, and the chronological order of the pipette determinations used to calculate V_{cal} are plotted in Fig. 4a for system I and Fig. 4b for

Table 2
The leg-specific to-deliver pipette volume (V_{cal}) and the calibration temperature (T_{cal}) for SOMMA-coulometer systems I and II during the Indian Ocean Survey 1994–1996

Leg	n	V_{cal} (cm^3)	S.D. (±cm^3)	R.S.D. (%)	T_{cal} (C)	Determinations averaged (legs)
System I						
I8SI9S	2	21.4609	0.0037	0.02	20.00	see text, $8S9S_e$
I9N	9	21.4543	0.0112	0.05	20.97	$8S9S_e$, $9N_e$
Gas generator introduced as CG source						
I8NI5E	9	21.4443*	0.0021	0.01	20.97	$9N_e$, 3_m
I3	15	21.4471	0.0042	0.02	20.57	$9N_e$, 3_m, 4_s
Gas generator output pressure adjusted from 5 to 10 psi						
I5WI4	10	21.4506*	0.0023	0.01	19.93	$5W4_{s,e}$
I7N	8	21.4506	0.0032	0.02	20.36	$7N_{s,m,e}$
I1	5	21.4462	0.0074	0.03	20.12	$7N_e$, 1_e
Pipette dismounted, cleaned, and recalibrated						
I10	5	21.4460	0.0110	0.05	20.08	10_e
I2	8	21.4482	0.0091	0.04	20.08	10_e, $2_{s,e}$
System II						
I8SI9S	18	21.6388	0.0068	0.03	20.24	$8S9S_{s,e}$
I9N	9	21.6360	0.0163	0.08	20.49	$8S9S_e$, $9N_e$
Gas generator introduced as CG source						
I8NI5E	8	21.6239	0.0080	0.04	20.56	$9N_e$, 3_m
I3	14	21.6243	0.0068	0.03	20.31	$9N_e$, 3_m, 4_s
Gas generator output pressure adjusted from 5 to 10 psi						
I5WI4	11	21.6293	0.0068	0.03	19.97	$5W4_{s,e}$
I7N	8	21.6194*	0.0048	0.02	20.05	$7N_{s,m,e}$
I1	4	21.6156	0.0035	0.02	20.00	$7N_e$, 1_e
Pipette dismounted, cleaned, and recalibrated						
I10	4	21.6269*	0.0017	0.01	19.95	10_e
I2	9	21.6270	0.0028	0.01	19.94	10_e, $2_{s,e}$

The subscripts (s, m, or e) for the pipette volume determinations averaged to calculate V_{cal} signify determinations made at the start, middle, or end of a leg, respectively. Values of V_{cal} which are significantly different from the V_{cal} of the preceding leg are denoted by the asterisk.

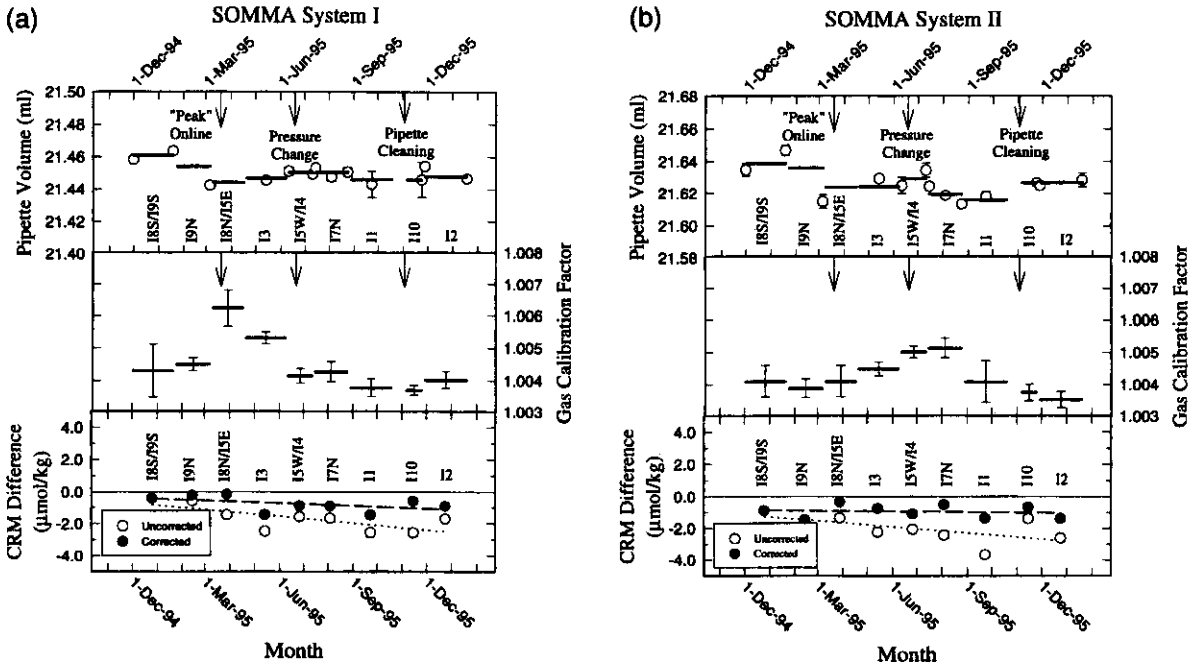

Fig. 4. The temporal record of the analytical performance of SOMMA-coulometer system I (Fig. 4a) and II (Fig. 4b) during the Indian Ocean Survey 1994–1996. The top section of the three-part graphs shows the leg-specific pipette volumes, V_{cal}, as horizontal lines corresponding to the duration of the individual legs, and the relative chronological order of the means of the individual pipette determinations from which V_{cal} was calculated as open circles placed before, in the middle of, or following the horizontal lines representing V_{cal} (see text and Table 2 for details). The middle section depicts the mean gas calibration factors for each leg (horizontal lines), and the bottom section shows the mean analytical differences for the CRM analyses assuming a constant pipette volume (V_{cal} for leg I8S) for the duration of the survey (open circles) vs. the leg-specific V_{cal} (closed circles). The error bars through the plot symbols represent the S.D. of the determinations. Procedural changes (introduction of the gas generator, pressure adjustments, and cleaning) which may have affected pipette volume are indicated by the arrows.

system II. This averaging increases the number of determinations used to calculate V_{cal}, and ensures that V_{cal} is based on at least two sets of determinations, separated in time, for all legs except the initial leg (I8SI9S) and leg I10 after the pipette was cleaned. Table 2 and Fig. 4a and b show the timing of events which could conceivably have affected pipette volume. For I8SI9S, the pipette volumes were determined in the laboratory prior to the cruise; however, the volume of system I had to be empirically redetermined at-sea because its pipette was broken during transit. This was done as follows: after replacing the pipette, V_{cal} was determined by simultaneously analyzing a replicate from a single seawater sample on systems I and II. Because V_{cal} was well known for system II, the TCO_2 concentration determined on system II was used to calculate the pipette volume of system I by rearranging Eq. (2) to solve for V_T and letting V_T be equal to V_{cal} for the subsequent analyses on system I during leg I8SI9S. As Table 2 shows, numerous volume determinations were made for both systems I and II on succeeding legs.

For I10, data from the prior leg could not be used to calculate V_{cal} because leg I10 took place after the pipettes had been dismounted for cleaning, which may have altered their volumes. On legs I5WI4 and I7N, replicate volume determinations were made at the beginning, middle, and end of the leg by the same measuring group so that V_{cal} for these legs do not include results from preceding or succeeding legs. The survey mean pipette volumes and their standard deviations for systems I and II are 21.4502 $\pm$ 0.0032 cm^3 at 20.25°C ($n = 43$) and 21.6261 $\pm$ 0.0028 cm^3 at 20.14°C ($n = 56$), respectively. The

pooled standard deviation (sp^2) calculated according to Youden (1951) for the 28 sets of gravimetric determinations is ± 0.0042 cm^3. Individually, sp^2 for system I is ± 0.0049 cm^3, and for system II sp^2 is ± 0.0036 cm^3, suggesting a very slightly higher precision for system II.

Significant differences at the 95% confidence level in V_{cal} for comparisons between each leg with the succeeding leg were determined by two-tailed *t*-tests according to Taylor (1990), and are denoted by asterisks in Table 2. For the most part, leg to leg differences in V_{cal} are not significant (significance in 2 of 9 comparisons for each instrument), but it should be noted that for both systems, the differences between the initial leg (I8SI9S) pipette volumes and all leg-specific volumes after leg I9N are significant. In both systems, the to-deliver pipette volume declines slightly with time. However, the decline is not consistent between instruments. In system I, significant decreases in volume appear earlier in the survey and may be correlated with the switch to the N_2 generator and a documented generator outlet pres-

Table 3
A summary of the mean analytical parameters and mean analytical differences for the three batches of CRM analyzed on SOMMA-coulometer systems I and II during the Indian Ocean Survey 1994–1996

Leg	$Slope_{ec}$	Int_{ec}	Calfactor	CRM (batch)	Precision, n ($\pm$ μmol/kg)	Analytical difference const-vp/corr-vp
System I						
I8SI9S	1.0002	0.0008	1.0043	23	1.15 (54)	−0.41/−0.41
I9N	1.0007	0.0013	1.0045	23	0.86 (71)	−0.83/−0.20
I8NI5E[a]	1.0007	0.0013	1.0062	23	1.36 (55)	−1.71/−0.15
I3	1.0007	0.0013	1.0053	23	0.98 (37)	−2.33/−1.31
I3	1.0007	0.0013	1.0053	26	0.98 (20)	−2.77/−1.72
I5WI4[b]	0.9998	−0.0057	1.0041	26	1.31 (41)	−1.83/−0.88
I7N	0.9998	−0.0057	1.0043	23	1.71 (6)	−1.66/−0.69
I7N	0.9998	−0.0057	1.0043	26	1.88 (55)	−1.74/−0.78
I7N	0.9998	−0.0057	1.0043	27	0.88 (8)	−2.91/−1.95
I1	0.9998	−0.0057	1.0038	27	1.10 (64)	−2.82/−1.45
I10[c]	0.9998	−0.0057	1.0037	27	0.72 (32)	−0.58/−0.58
I2	0.9998	−0.0057	1.0040	27	1.11 (27)	−0.57/−0.77
Mean			1.0045		1.17 (470)	−1.68/−0.91
S.D. ($\pm$)			0.0008		0.35	0.92/0.58
System II						
I1SI9S	0.9996	−0.0025	1.0041	23	1.18 (104)	−0.89/−0.89
I9N	0.9996	−0.0025	1.0039	23	0.90 (70)	−1.83/−1.57
I8NI5E[a]	0.9996	−0.0025	1.0041	23	1.14 (59)	−1.73/−0.35
I3	0.9996	−0.0025	1.0045	23	0.85 (35)	−2.14/−0.62
I3	0.9996	−0.0025	1.0045	26	0.69 (13)	−2.44/−1.11
I5WI4[b]	0.9998	0.0045	1.0050	26	0.79 (41)	−2.14/−1.28
I7N	0.9998	0.0045	1.0051	23	0.88 (5)	−3.25/−1.47
I7N	0.9998	0.0045	1.0051	26	0.84 (54)	−2.09/−0.32
I7N	0.9998	0.0045	1.0051	27	0.77 (10)	−2.88/−1.10
I1	0.9998	0.0045	1.0041	27	1.11 (70)	−3.51/−1.38
I10[c]	0.9998	0.0045	1.0038	27	0.65 (28)	−0.66/−0.66
I2	0.9998	0.0045	1.0035	27	1.11 (24)	−1.38/−1.39
Mean			1.0042		0.91 (513)	−2.08/−1.01
S.D. ($\pm$)			0.0005		0.18	0.87/0.44

For each CRM batch analyzed, precision is given as the standard deviation of the mean of (n) analyses. Abbreviations: ec, electronic calibration; calfactor, gas calibration factor; Int, intercept; const-vp, mean analytical difference calculated using a constant pipette volume; corr-vp, mean analytical difference calculated using the leg-specific V_{cal} (Table 2).

[a] Gas Generator introduced as CG source.

[b] Gas generator output pressure adjusted from 5 to 10 psi.

[c] Pipette dismounted, cleaned and recalibrated.

sure adjustment, but this is not the case with system II where dismounting and cleaning of the pipette late in the survey may have had the greatest effect.

3.2. CRM analyses and system accuracy

In addition to the leg-specific pipette volumes, Fig. 4a (system I) and Fig. 4b (system II) show the mean analytical differences (analyzed TCO_2-certified TCO_2) and the mean gas calibration factors for each survey leg. The plots are scaled so that each *Y*-axis spans a similar range in order that the factors controlling system accuracy can be more readily identified. These data are also tabulated and summarized in Table 3. Table 3 shows that the gravimetric volume determinations (Table 2) have detected real changes in V_{cal} during the survey. The mean analytical differences calculated with the corrected pipette volumes (corr-vp, Table 3) are −0.91 and −1.01 μmol/kg for systems I and II, respectively. If the pipette volumes determined at the beginning of the survey (const-vp) were used, the corresponding differences would be −1.61 and −2.08 μmol/kg, showing that the routine determination of pipette volume increased accuracy by a factor of ~2.

Fig. 5 is a bar chart of the mean analytical difference (accuracy) for systems I and II as a function of cell carbon age. Both systems behave very

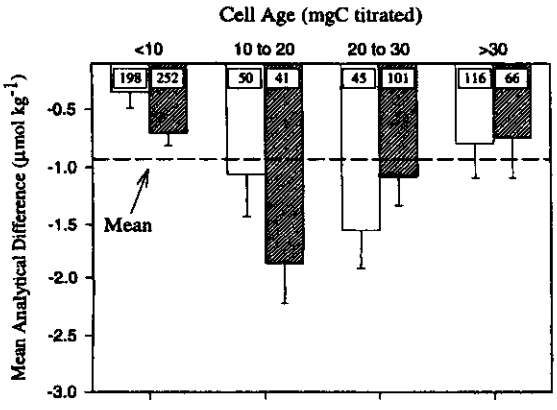

Fig. 5. A plot showing the distribution of mean analytical differences for CRM analyses vs. coulometer cell age for SOMMA-coulometer systems I (open bars) and II (filled bars) during the Indian Ocean Survey 1994–1996. The error bars represent the 95% confidence interval for the mean differences, and the numbers inside the columns are the number of measurements (*n*) used to compute the means.

similarly with the best precision and accuracy early in the cell lifetime (< 10 mg C), increasing differences for cells of intermediate ages (> 10 to < 30 mg C), and smaller differences for carbon ages exceeding 30 mg C which are not significantly different from those at ages < 10 mg C. No corrections based on the analyzed-certified TCO_2 differences or cell age have been applied to the CDIAC data set.

3.3. System repeatability and precision during the survey

For the survey as a whole, the operating conditions and analytical performance of the two SOMMA systems were virtually identical. Survey-wide the mean gas calibration factors of the two systems were nearly identical (1.0045 for system I compared to 1.0042 for II). While both systems yielded slightly negative (~ 1.0 μmol/kg) mean analytical differences (Table 3), the standard deviation of the analytical differences was slightly better on system II (±0.91 μmol/kg) than system I (1.17 μmol/kg). This is consistent with the gravimetric volume determinations where system II also exhibited a slightly higher precision (sp^2 = ±0.0036 cm^3 vs. ±0.0049 cm^3 for system I).

For the CRM analyses, the precision or pooled standard deviation (sp^2) calculated according to Youden (1951) is 1.19 μmol/kg (df = 977). For this calculation, the three batches of CRM analyzed on the two systems are treated as six separate samples with multiple replicates. Because sp^2 includes CRM data measured on both systems on all legs, it applies to both systems on all legs. For water samples, sp^2 was calculated from duplicates analyzed on each system during leg I8SI9S at the start of the survey and leg I5WI4 about half way through the survey. The sp^2 for leg I8SI9S is ±1.26 μmol/kg (df = 15), and for leg I5WI4, sp^2 is ±0.91 μmol/kg (df = 21). These values are consistent with the precision of the CRM analyses given in Table 3. For the survey, the overall precision of the TCO_2 determination is ±1.19 μmol/kg.

Fig. 6 is a plot of the analytical differences by system and CRM batch for the entire survey. The differences, calculated using the parameters in Table 3, reiterate the point that there are no significant

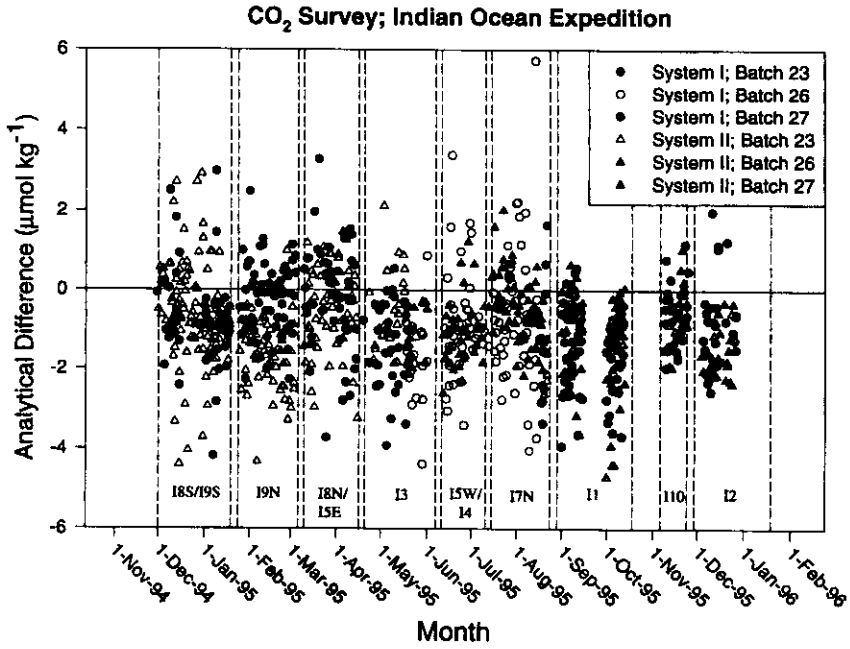

Fig. 6. The analytical differences for the CRM analyses made on SOMMA-coulometer systems I and II during the Indian Ocean Survey 1994–1996 with separate symbols for the results from the two systems and for the three batches of CRM analyzed. The beginning and end of each leg is marked by vertical dashed lines. The respective salinities and certified TCO_2 (μmol/kg) for batches 23, 26, and 27 are 33.483 and 1993.10, 33.258 and 1978.34, 33.209 and 1988.10 μmol/kg.

analytical differences (bias) between systems or between CRM batches.

4. Discussion

The Indian Ocean CO_2 Survey differed from the previous DOE CO_2 Survey efforts in that a single ship was used for all legs, and that the measurement groups shared the same analytical equipment. The latter included the use of a single cache of coulometric reagents (two different lot numbers both of which were tested pre-cruise with CRM), invariant sources of analytical gases, use of the same titration cell assemblies, standard sampling procedures, and standardized software. There was a pre-cruise training session, and all of the participants had prior experience with the sampling and measurement techniques (poisoning, reagent concentrations, standard calculations, glassware calibration, etc.) documented in the DOE Handbook of Methods (DOE, 1994). Thus, an extraordinary effort over several years to ensure analytical quality and uniformity culminated in the procedures used during the Indian Ocean Survey.

An improvement in system accuracy (Table 3) of approximately 1 part in 2000 shows that the effort to gravimetrically determine the pipette volumes on each leg was worthwhile. The volumes of both systems did decrease slightly but significantly with time. Possible explanations include pressure changes in the carrier gas source (system I) or fouling of the glass pipette walls causing altered surface tension or displacement of small amounts of liquid (system II). Because the samples were poisoned with $HgCl_2$, it is unlikely that biological fouling was a problem, but the high quantity of grease used to seal the CRM bottles makes it possible that some of this grease found its way into the pipettes. After cleaning, V_{cal} for leg I10 remained unchanged compared to the preceding leg I1 on system I and increased slightly on system II, but for both systems it was significantly smaller than the V_{cal} determined for the initial leg (I8SI9S). After cleaning, the mean analytical difference for leg I10 (system I and II, $n = 2$) was -0.62 μmol/kg compared to -0.40 μmol/kg on

the initial leg I8S when the instruments were fresh from the laboratory indicating that pipettes were most accurate after cleaning. Whatever the cause of subsequent volume changes, the data confirm the importance of periodically redetermining the volume, and indicate that the procedure is mandatory for the highest accuracy over extended periods of analytical work and/or after major changes in system plumbing. In aggregate, both systems share a small negative analytical difference (-1.0 μmol/kg) for the CRM analyses throughout the survey even after pipette volume corrections have been applied.

The cell accuracy vs. carbon age relationship shown in Fig. 5 is typical of data from previous cruises (K.M. Johnson, unpublished data). The best precision and accuracy is found at a carbon age of 5–10 mg C, a slightly reduced accuracy (usually as lower recoveries of CRM carbon) is observed between 10–30 mg C, gradually increasing recoveries and imprecision after 30 mg C until cell death where cell death is defined as a positive difference ≥ 3.0 μmol/kg. This behavior underlies the recommendation that cell lifetimes be limited to a carbon age of ≤ 35 mg C, i.e., to limit imprecision and because cell death normally occurs at carbon ages ≥ 35 mg C. During the survey, neither CRM or samples were run until the carbon age exceeded 5 mg C. This was accomplished by configuring the software to automatically run a test sample and three consecutive gas calibrations before samples were analyzed. The reasons for the observed cell behavior are not understood, but limiting cell lifetimes from ≥ 5 to ≤ 35 mg C probably helps to limit system drift which might compromise the sample analyses. Although the imprecision associated with cell aging is small and cell failure is rare at carbon ages ≤ 35 mg C, good analytical practice requires that samples should be run in random order rather than systematically in order of depth to avoid systematic biases which might result from any drift associated with cell age.

Fig. 4a and b shows no correlation between the gas calibration factors and the analytical differences after the CRM analyses were corrected for pipette volume changes (Table 3). These data do show that the overall mean gas calibration factor for both systems is nearly the same (1.004), but that the temporal record with respect to gas calibration factor variation is not. Calibration factor variation (R.S.D. = 0.06–0.08%) is greater than the variation in V_{cal} (R.S.D. = 0.03%), and is therefore a potentially more important control on system accuracy. For system I, the highest mean gas calibration factor (poorest recovery of CO_2) was observed on leg I8N, while for system II, the corresponding result occurred months later, on leg I7N (same measurement group, see Table 1). Because the system calibration factors are not correlated with the analytical differences, the observed variations in calibration factors are real, i.e., they document a change in system response shared by the calibration and sample analyses rather than an isolated malfunction of the gas calibration hardware (see Fig. 2).

The reason for gas calibration factor variation is not known. It could conceivably be due to procedures unique to each measurement group, e.g., positioning of the cathode electrode and the gas inlet tube with respect to the coulometer light source and photodetector (Fig. 3), plumbing differences resulting in leaks and small losses of CO_2, or the amount of reagents used to dry the gas stream (Fig. 2). These procedural differences would affect sample determinations and gas calibration results similarly because, as Fig. 2 shows, the calibration gas follows the same route to the coulometer as the CO_2 extracted from samples. Table 3 suggests at least one other possible cause of gas calibration factor variation. The coulometers were electronically calibrated by the BNL group at the start of the survey (I8SI9S) and about half way through the survey on leg I5WI4. Between legs I8SI9S and I5WI4 the coulometer calibration appears to have changed by 0.08% for system I, and by 0.02% for system II. These calibrations were separated by many weeks so the exact magnitude or timing of the shift is not known. Changes in the coulometer's circuitry affecting the electronic slope ($Slope_{ec}$) and intercept (Int_{ec}) would alter the gas calibration factor but would not affect system accuracy because, until recalibration, the previous electronic calibration coefficients represent constants in Eq. (1). In both systems, the sense of the apparent change in electronic calibration coefficients compared to the earlier coefficients is qualitatively consistent with the observed short-lived variation in gas calibration factors, and it is possible that this variation was due to unexplained changes in the coulometer response.

The important point is the efficacy of the gas calibration procedure: corrections to data based solely on the CRM analyses which would usually be applied on a cruise-average basis may mask short term variation or step changes in system response arising from stochastic or procedural changes. The gas calibration procedure, in which known masses of pure CO_2 are regularly analyzed, is an independent check of all system components except pipette volume, and it provides traceable documentation for the subsequent survey results.

The importance of cell assembly selection should be stressed. Investigators have found that the behavior of individual cell assemblies can vary significantly (e.g., D. Chipman, personal communication, July 1996). The factors affecting cell performance are still not yet completely understood. Hence, the use of empirical selection criteria such as those given in Section 2 is recommended. It is beyond the scope of the paper to go into detail, but point 'a' in Fig. 3 illustrates one of the locations for potential problems. A faulty seal where the platinum electrode emerges from the glass insulator could allow infiltration and trapping of the cell solution in the insulator where electrochemical or chemical reactions could take place. Small quantities of this solution (at a pH different from the bulk cell solution) could randomly exchange with the bulk cell solution and cause titration errors. This would be difficult to detect. Assemblies which did not meet the empirical performance criteria in Section 2 were simply not used. The attention to cell assembly testing and selection is believed to a major reason for the success of the Indian Ocean TCO_2 Survey. The survey assemblies were also carefully washed and dried. Drying at 55 ∓ 5°C removes traces of the volatile and reactive cell solution from the rubber caps.

5. Crossover analysis

The agreement between TCO_2 measurements made at similar locations, but on different legs of the survey, were used as a check on the internal consistency of the measurements. Deep measurements were used because of the lower variability in TCO_2 observed in the deep ocean. Because most motion in the ocean interior takes place along surfaces of constant density (isopycnals), comparisons were made along isopycnal surfaces rather than depth.

Table 4
Results of the crossover analysis (see text for details)

Crossover no.	Expedition legs		Stations		TCO_2 difference ∓ S.D. (μmol/kg)
	Late	Early	Late	Early	
1	I1	I7N	927:931	780:784	−2.5 ∓ 0.5
2	I1	I9N	987:990	266:270	−2.7 ∓ 6.3[a]
3	I1	I9N	996:998	233:235	−0.9 ∓ 1.7
4	I2	I7N	1205	728:730	−0.4 ∓ 1.1
5	I2	I8NI5E	1137:1139	320:324	1.5 ∓ 1.5
6	I2	I9N	1094:1096	191:193	−3.0 ∓ 0.7
7	I2	I10	1078	1075	−1.5 ∓ 1.5
8	I5WI4	I3	705	547:549	1.6 ∓ 0.5
9	I3	I8NI5E	498:501	346:348	−2.6 ∓ 0.7
10	I3	I9N	472	169	1.1 ∓ 1.2
11	I10	I3	1039	452:454	1.1 ∓ 0.3
12	I8NI5E	I8SI9S	404:408	9:13	−1.1 ∓ 1.0
13	I1	I7N	861	808	1.3 ∓ 0.4[b]
Mean					−0.78

The TCO_2 difference between legs is calculated by subtracting data from the earlier sampling of a crossover location from that of the later sampling. The station numbers refer to the actual stations used for this analysis.
[a]The LOESS fit diverged significantly from the data.
[b]Not considered reliable due to insufficient data.

Our crossover analysis was performed as follows:

(1) Locations at which different cruise legs intersected were identified as 'crossover points.' These are identified in Table 4 and are plotted on Fig. 1.

(2) Stations located in the immediate proximity of these crossover points, for which TCO_2 data existed, were selected for the comparison. In general, stations located within 100 km of the crossover location were selected.

(3) For water samples collected below 2500 m, smooth curves were fit through the TCO_2 data as a function of the density anomaly referenced to 3000 dbar (sigma 3) using Cleveland's LOESS smoother (Cleveland and Devlin, 1988). A separate fit was performed to the data collected from each of the two intersecting legs. The tension parameter for the smoother was adjusted subjectively to give a 'reasonable' fit to the data at the majority of the crossover locations, and the same value for the tension parameter was used for all of the crossovers. Hence, while the fits to the data may not necessarily represent the best possible at each individual crossover point, the smoothing function has been consistently applied to all crossovers.

(4) For each crossover, the difference between the two smooth curves was evaluated at 50 evenly spaced intervals which covered the density range over which the two data sets overlapped. A mean and a standard deviation of the difference between the two curves was estimated based on these 50 values, and these values are reported in Table 4. An illustration of a typical analysis, the fitted data for crossover 4, is plotted on Fig. 7.

The results of the crossover analysis indicate that absolute leg-to-leg differences are always < 3.0 μmol/kg (Table 4). Note that the comparisons were evaluated consistently such that the fit to data from the earlier leg at each crossover was subtracted from the fit to the later leg's data. Any uncorrected, long-term, monotonic drift in the calibration of the

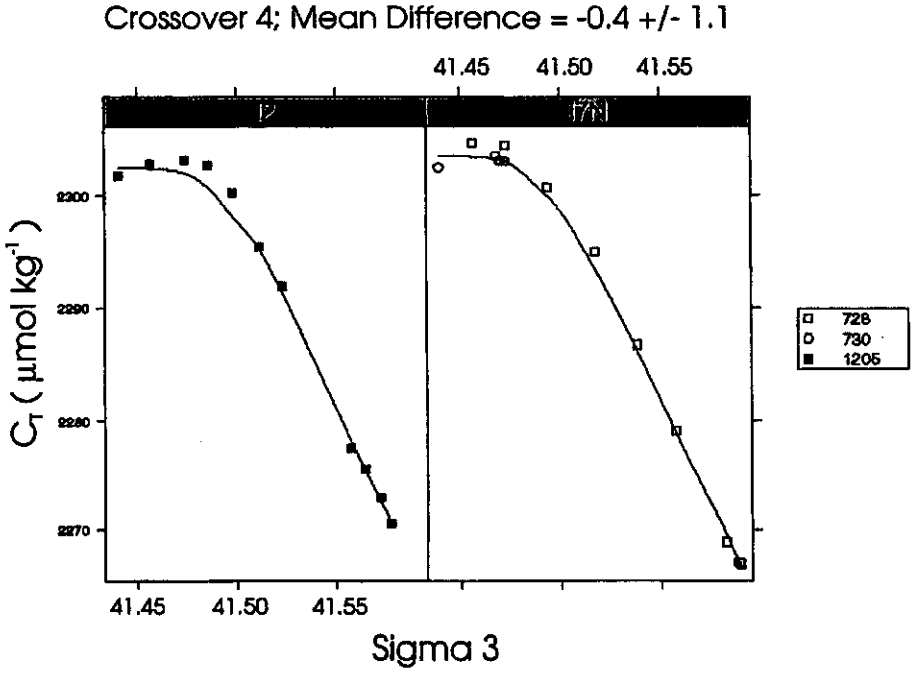

Fig. 7. An example of a crossover analysis using the TCO_2 vs. density fits at crossover location #4. This location was first sampled on leg I7N in July 1995. It was resampled during January 1996 on leg I2. The TCO_2 data from stations within 100 km of the crossover location and depths > 2500 m have been plotted vs. the potential density anomaly referenced to 3000 dbar (sigma 3). The solid curves represent fits to the data using a LOESS smoother (see text). The difference between the fits for the two separate legs was evaluated at 50 density intervals spaced evenly within the overlapping density range of the two legs (see Table 4). The legend shows the station numbers used for the comparison.

SOMMA analyzers over the course of the Indian Ocean expedition would therefore result in a non-zero value for the overall mean of these differences. The overall mean and standard deviation of the differences at crossovers 1–12 is −0.78 (±1.74) μmol/kg, and there was also no significant correlation between the individual differences derived from each crossover and the number of days which separated the crossover samplings. In general, the results of the crossover analysis are quite consistent with the overall precision (±1.2 μmol/kg) of the CRM analyses (see Section 3.3), and confirms that this precision applies to both systems throughout the survey. There is no suggestion in the crossover results of any additional significant sources of error or uncertainty.

6. Conclusions

In summary, personnel aboard the R/V Knorr have been able to use the SOMMA-coulometer system to consistently replicate within analytical error the certified CRM TCO_2 values. They have been able to use these systems to make, counting duplicates and CRM, over 20,000 determinations of TCO_2 during the 14 months of the Indian Ocean Survey without significant instrument down time. The measurement groups have accomplished the following.

(1) They have charted the history of the to-deliver volume of the sample pipettes by gravimetric determinations, and corrected the water sample data for the documented changes in the pipette volumes. The change in system response due to the change in pipette volume corresponded to approximately 1 part in 2000 for TCO_2 on both systems over the 10 months prior to recleaning of the pipettes.

(2) The groups have determined that the survey precision for the TCO_2 analyses, irrespective of which leg or system the water samples were analyzed on, was ±1.2 μmol/kg. The precision of the two instruments was nearly identical and consistent throughout the 14 months of the survey.

(3) They have analyzed nearly 1000 CRM with an overall difference between the analyzed and certified TCO_2 of −1.0 μmol/kg (0.05%) on both systems which demonstrates the equivalency of the two independent instruments, and meets the survey's goal for accuracy.

(4) The measurement groups have documented the influence of factors besides pipette volume which could have affected accuracy including electronic calibration, gas calibration, cell age, and cell assembly selection.

For precision, the pooled standard deviation (sp^2 = 1.2 μmol/kg), calculated according to Youden (1951), is the most conservative estimate of precision because it includes all random analytical errors (sampling, instrumental, and method). The identical accuracy for the CRM analyses on both systems and the results of the crossover analysis (Table 4) indicate that the sp^2 statistic can be used to evaluate survey data sets irrespective of the leg or system the data originated from.

The SOMMA-coulometry systems have allowed several scientific groups in a shared effort to examine carbon inventories and aquatic carbon cycling. For the Indian Ocean Survey, the sensitivity of the TCO_2 determinations defined as the ratio of their precision (1.2 μmol/kg) over the TCO_2 dynamic range (250 μmol/kg) was 0.4% which approaches the 0.1% sensitivity of the salinometers used, and these systems were as reliable as the salinometers. If their reliability is to be improved, the focus should be on understanding the basic behavior of the cell assemblies and the chemical behavior of the cell solutions as they age, so that procedural corrections can be made. The accuracy and precision of the Indian Ocean TCO_2 analyses indicates that these data will be more than adequate for testing applicable oceanographic models, and allow the direct measurement of the CO_2 uptake if and when these lines are resampled.

Acknowledgements

We would like to thank the US Department of Energy's Office of Biological and Environmental Research for their support. The success of the Indian Ocean CO_2 Survey was due to the shared efforts of the DOE Science Team. We thank John Downing for his initial organization of the Science Team and assistance in getting the US CO_2 Survey underway. We thank the chief scientists, scientific staff, and crew aboard the R/V Knorr for their assistance throughout. Dave Chipman and Taro Takahashi are acknowledged for helpful comments and advice. The

instruments used for the survey were produced at the Equipment Development Laboratory (EDL) at the University of Rhode Island's Graduate School of Oceanography under the supervision of Dr. John King and David Butler. This research was performed under the auspices of the United States Department of Energy under Contract No. DE-AC02-98CH10886.

References

Bates, N.R., Michaels, A.F., Knap, A.H., 1996. Seasonal and interannual variability of oceanic carbon dioxide species at the US JGOFS Bermuda Atlantic time-series study (BATS) site. Deep-Sea Research II 43, 347–383.

Cleveland, W.S., Devlin, S.J., 1988. Locally-weighted regression: an approach to regression analysis by local fitting. J. Am. Stat. Assoc. 83, 596–610.

Dickson, A.G., 1990. The oceanic carbon dioxide system: planning for quality data. US JGOFS News 2:2.

DOE, 1994. Handbook of methods for the analysis of the various parameters of the carbon dioxide system in sea water; version 2.0. ORNL/CDIAC-74.

Huffman, E.W.D. Jr., 1977. Performance of a new automatic carbon dioxide coulometer. Microchem. J. 22, 567–573.

Johnson, K.M., 1995. Operator's Manual. Single-Operator Multiparameter Metabolic Analyzer (SOMMA) for Total Carbon Dioxide (C_T) with Coulometric Detection. Version 3.0. Available from K.M. Johnson, Department of Applied Science, Brookhaven National Laboratory, Upton, NY.

Johnson, K.M., Wallace, D.W.R., 1992. The single-operator multiparameter metabolic analyzer for total carbon dioxide with coulometric detection. DOE research summary no. 19. Carbon Dioxide Information Analysis Center, Oak Ridge National Laboratory, TN.

Johnson, K.M., King, A.E., Sieburth, J.McN., 1985. Coulometric TCO_2 analyses for marine studies: an introduction. Mar. Chem. 16, 61–82.

Johnson, K.M., Sieburth, J.McN., Williams, P.J.leB., Bränström, L., 1987. Coulometric TCO_2 analysis for marine studies: automation and calibration. Mar. Chem. 21, 117–133.

Johnson, K.M., Wills, K.D., Butler, D.B., Johnson, W.K., Wong, C.S., 1993. Coulometric total carbon dioxide analysis for marine studies: maximizing the performance of an automated gas extraction system and coulometric detector. Mar. Chem. 44, 167–187.

Millero, F.J., Poisson, A., 1981. International one-atmosphere equation of state for sea water. Deep-Sea Res. 28, 625–629.

Millero, F.J., Dickson, A.G., Eischeid, G., Goyet, C., Guenther, P., Johnson, K.M., Lee, K., Purkerson, D., Sabine, C.L., Key, R., Schottle, R.G., Wallace, D.W.R., Lewis, E.R., Winn, C.D., 1998. Assessment of the quality of the shipboard measurements of total alkalinity on the WOCE Hydrographic Program Indian Ocean CO_2 survey cruises 1994–1996. Mar. Chem. 63, 9–20.

Sabine, C.L., Key, R.M., 1998. Surface water and atmospheric underway carbon data obtained during the world ocean circulation experiment Indian Ocean survey cruises (R/V Knorr, December 1994–January 1996). NDP-064, Carbon Dioxide Information Analysis Center, Oak Ridge National Laboratory, Oak Ridge, TN.

Taylor, J.K., 1990. Statistical techniques for data analysis. Lewis Publishers, Chelsea, 200 pp.

Wilke, R.J., Wallace, D.W.R., Johnson, K.M., 1993. A water-based, gravimetric method for the determination of gas sample loop volume. Anal. Chem. 65, 2403–2406.

Youden, W.J., 1951. Statistical Methods for Chemists. Wiley, New York, 126 pp.

APPENDIX C:

REPRINT OF PERTINENT LITERATURE

Millero, F. J., A. G. Dickson, G. Eischeid, C. Goyet, P. R. Guenther, K. M. Johnson, K. Lee, E. Lewis, D. Purkerson, C. L. Sabine, R. Key, R. G. Schottle, D. R. W. Wallace, and C. D. Winn. 1998. Assessment of the quality of the shipboard measurements of total alkalinity on the WOCE Hydrographic Program Indian Ocean CO2 survey cruises 1994–1996. *Marine Chemistry* 63:9–20.

ELSEVIER

Marine Chemistry 63 (1998) 9–20

MARINE CHEMISTRY

Assessment of the quality of the shipboard measurements of total alkalinity on the WOCE Hydrographic Program Indian Ocean CO_2 survey cruises 1994–1996

Frank J. Millero [a,*], Andrew G. Dickson [b], Greg Eischeid [c], Catherine Goyet [c], Peter Guenther [b], Kenneth M. Johnson [d], Robert M. Key [e], Kitack Lee [f], Dave Purkerson [a], Christopher L. Sabine [e], Rolf G. Schottle [g], Douglas W.R. Wallace [d], Ernie Lewis [d], Christopher D. Winn [g]

[a] *Rosenstiel School of Marine and Atmospheric Science, University of Miami, Miami, FL 33149, USA*
[b] *Scripps Institution of Oceanography, University of California, La Jolla, San Diego, CA 92093, USA*
[c] *Woods Hole Oceanographic Institute, Woods Hole, MA 02543, USA*
[d] *Department of Applied Science, Brookhaven National Laboratory, Upton, NY 111973, USA*
[e] *Department of Geosciences, Princeton University, Princeton, NJ 08544, USA*
[f] *NOAA/AOML, Miami, FL 33149, USA*
[g] *Department of Oceanography, University of Hawaii, Honolulu, HI 96822, USA*

Received 16 January 1998; revised 31 March 1998; accepted 7 April 1998

Abstract

In 1995, we participated in a number of WOCE Hydrographic Program cruises in the Indian Ocean as part of the Joint Global Ocean Flux Study (JGOFS) CO_2 Survey sponsored by the Department of Energy (DOE). Two titration systems were used throughout this study to determine the pH, total alkalinity (TA) and total inorganic carbon dioxide (TCO_2) of the samples collected during these cruises. The performance of these systems was monitored by making closed cell titration measurements on Certified Reference Materials (CRMs). A total of 962 titrations were made on six batches of CRMs during the cruises. The reproducibility calculated from these titrations was ∓ 0.007 in pH, ∓ 4.2 μmol kg^{-1} in TA, and ∓ 4.1 μmol kg^{-1} in TCO_2. The at-sea measurements on the CRMs were in reasonable agreement with laboratory measurements made on the same batches. These results demonstrate that the CRMs can be used as a reference standard for TA and to monitor the performance of titration systems at sea. Measurements made on the various legs of the cruise agreed to within 6 μmol kg^{-1} at the 15 crossover points. The overall mean and standard deviation of the differences at all the crossovers are 2.1 ∓ 2.1 μmol kg^{-1}. These crossover results are quite consistent with the overall reproducibility of the CRM analyses for TA (∓ 4 μmol kg^{-1}) over the duration of the entire survey. The TA results for the Indian Ocean cruises provide a reliable data set that when combined with TCO_2 data can completely characterize the carbonate system.

Keywords: alkalinity; WOCE Hydrographic Program; CO_2

* Corresponding author.

0304-4203/98/$ - see front matter
PII: S0304-4203(98)00043-7

1. Introduction

From 1994 to 1996, a number of cruises were made in the Indian Ocean as part of the World Ocean Circulation Experiment (WOCE) Hydrographic Program to characterize the carbon dioxide system. This survey of CO_2 was an integral part of the Joint Global Ocean Flux Study (JGOFS). The goals of this survey were to: (1) Quantify the uptake of anthropogenic carbon dioxide by the oceans to better predict future atmospheric carbon dioxide levels; (2) Provide a global description of the carbon dioxide in the oceans to aid in the development of a 3-dimensional model of the oceanic carbon cycle; and (3) Characterize the transport of CO_2 across the air–sea interface and the large scale transports of carbon dioxide within the oceans.

To satisfy these goals, it was necessary to make very precise measurements of at least two of the carbonate system parameters (pH; total alkalinity, TA; total carbon dioxide, TCO_2; and the fugacity of carbon dioxide, fCO_2). Within the United States a large part of this survey was conducted by a team of investigators supported by the US Department of Energy. The team selected the measurement of TCO_2 (Johnson et al., 1998) and of TA as the parameters to be measured in the water column and fCO_2 in the atmosphere and surface waters. To insure that the measurements of TCO_2 and TA were as precise and accurate as possible Certified Reference Materials (CRMs) (Dickson, 1990a) were used throughout the studies. The team also developed a set of Standard Operating Procedures [1] (DOE, 1994) and, to a large extent, shared a common approach to the measurement program.

For the studies in the Indian Ocean, the team shared equipment throughout the study. This paper presents the results of this team effort to precisely and accurately determine the total alkalinity during these cruises and the intercomparison between cruises. A companion paper (Johnson et al., 1998) describes the total carbon dioxide measurements.

[1] DOE, 1991. Handbook of methods for the analysis of the various parameters of the carbon dioxide system in sea water, In: Dickson, A.G., Goyet, C. (Eds.), Version 1.0, Unpublished manuscript

2. Methods

The total alkalinity was determined on the JGOFS Indian Ocean cruises by the DOE group using systems described in detail by Millero et al. (1993). The total alkalinity of seawater was evaluated from the proton balance at the alkalinity equivalence point, $pH_{equiv} \sim 4.5$, according to the exact definition of total alkalinity (Dickson, 1981)

$$\begin{aligned} TA = {} & [HCO_3^-] + 2[CO_3^{2-}] + [B(OH)_4^-] \\ & + [OH^-] + [HPO_4^{2-}] + 2[PO_4^{3-}] \\ & + [SiO(OH)_3^-] + [HS^-] \\ & + [NH_3] - [H^+] - [HSO_4^-] \\ & - [HF] - [H_3PO_4] \end{aligned} \quad (1)$$

At any point in the titration, the total alkalinity of seawater can be calculated from the equation

$$\begin{aligned} (W_0 \times TA - W \times C_{HCl})/(W_0 + W) = {} & [HCO_3^-] \\ & + 2[CO_3^{2-}] + [B(OH)_4^-] + [OH^-] + [HPO_4^{2-}] \\ & + 2[PO_4^{3-}] + [SiO(OH)_3^-] + [HS^-] + [NH_3] \\ & - [H^+] - [HSO_4^-] - [HF] - [H_3PO_4] \end{aligned} \quad (2)$$

where W_0 is the mass of the sample to be titrated, C_{HCl} is the concentration of acid titrant, and W is the mass of acid added. In the calculations, volumes of the sample and of the acid were converted to mass using the density of seawater (Millero and Poisson, 1981) and the density of HCl in NaCl (Millero et al., 1977). Direct measurements made on the density of the acid used agreed to within 10 ppm with the equations used in the computer code. At the endpoint (W_2) the total alkalinity is given by

$$TA = W_2 \times C_{HCl}/W_0 \quad (3)$$

The uncertainties in TA associated with acid concentration ($\sim 0.25 \pm 0.0001$ M), mass of acid delivered ($\sim 2.5 \pm 0.0005$ g), and mass of the sample

(~ 200 ± 0.05 g) are ± 1, ± 0.5, and ± 0.5 μmol kg^{-1}, respectively (which gives a probable error of about ± 1 μmol kg^{-1}). By using the same acid, titrators, and acid throughout a given cruise one can obtain a precision that is comparable with this probable error. Discussed below are more details on the components of the titration systems.

2.1. Titration system

The titration systems used to determine TA consist of a Metrohm 665 Dosimat titrator and an Orion 720A pH meter controlled by a personal computer (Millero et al., 1993). Both the acid titrant in a water-jacketed burette and the seawater sample in a water-jacketed cell were controlled to a constant temperature of 25 ± 0.1°C with a Neslab constant temperature bath. The plexiglass water-jacketed cells used for our studies were similar to that used by Bradshaw and Brewer (1988) except a larger volume (about 200 cm^3) was used to improve the precision. These cells have fill and drain valves that increased the reproducibility of the cell volume.

A Lab Windows C program is used to run the titration and record the volume of the added acid and the emf of the electrodes using RS232 interfaces. The titration is made by adding HCl to seawater past the alkalinity end point. A typical titration records the average of ten emf readings after they become stable (± 0.09 mV) and adds enough acid to change the voltage by a pre-assigned increment (~ 13 mV). In contrast to the delivery of a fixed volume of acid, this method gives more data points in the range of a rapid increase in the emf near the endpoint. A full titration (25 points) takes about 20 min.

2.1.1. Electrodes

The electrodes used to measure the emf of the sample during a titration consist of a ROSS glass pH electrode and an Orion double junction Ag, AgCl reference electrode. A number of electrodes were screened to select those to be used in the titrators. Electrodes with non-Nernstian behavior (slopes more than 1.0 mV different from the theoretical value) were discarded. The reliability of the electrodes was evaluated by determining the TA, TCO_2 and pH of Gulf Stream seawater. The titration values of TCO_2 are normally higher than the values measured by coulometry and the values of pH are typically lower than the values obtained by spectrophotometric methods. These differences in TCO_2 and pH are caused by the non-Nernstian behavior of the electrodes (Millero et al., 1993). We selected electrodes which gave values of TCO_2 and pH close to the values determined by coulometric and by spectrophotometric methods, respectively.

2.1.2. Standard acids

The HCl used for this study and for all of our cruises was made in the laboratory, standardized, and stored in 500 cm^3 glass bottles. The ~ 0.25 M HCl solutions were made from 1 M Mallinckrodt standard solutions in 0.45 M NaCl to yield an ionic strength equivalent to that of average seawater (~ 0.7 M). The concentration of HCl was measured using a constant current coulometric technique (Taylor and Smith, 1959; Marinenko and Taylor, 1968). Coulometric analysis of the acids used for these cruises agreed to ± 0.0001 M with the analyses performed independently on the same batches of acids in Dr. A. Dickson's laboratory at Scripps Institution of Oceanography (SIO). The mutual consistency of these acids was also confirmed by comparing the values of TA measured on Gulf Stream seawater using different batches of acids, but using the same titrator and electrodes. The uncertainties in TA associated with acid concentration (± 0.0001 M) is ~ 1 μmol kg^{-1}.

2.1.3. Volume of the cells

The volume of each of the titration cells used at sea was determined by comparing the values of TA obtained for Gulf Stream seawater with open and closed cells in the laboratory. All of the open cell laboratory TA measurements were made with weighed amounts of seawater in a cell with a small head-space. If the volume is correct, the TA from the open and closed cells should be the same, provided that the same acid, titrator, and electrodes are used. At least 10 measurements were made on each cell yielding an average TA that agreed with the assigned value to better than 1 μmol kg^{-1}. If the volume of a

Table 1
Comparison of the total alkalinity of Certified Reference Materials

Batch	SIO	Miami	Δ(S-M)	Cruise
23	2212.7	2213.7	−1.0	I8S/I9S, I9N, I8N /I5E, I3, I7N
24	2215.5	2215.8	−0.3	I8R
26	2176.6	2175.1	1.5	I3, I5W/ I4, I−7N
27	2214.9	2214.3	0.6	I7N, I1, I10, I2
29	2184.8	2182.3	2.5	I8R
30	2201.9	2200.5	1.4	I2

titration cell needed to be adjusted during the cruise (because of broken electrodes, plungers etc.), the volumes were determined from the daily titrations on low-nutrient surface seawater (usually collected before the first station) and Certified Reference Materials (CRMs) provided by Dr. A. Dickson (SIO). Post-cruise calibrations of the cells were made by comparing the values of TA for the Gulf Stream seawater and CRM with open and closed cells. The nominal volumes of all the cells were about 200 cm^3, and the values were determined to ± 0.05 cm^3. The uncertainty in TA associated with this uncertainty in the volume of the cells (± 0.05 cm^3) is 0.5 μmol kg^{-1} obtained for the weighed samples.

2.1.4. Volume of titrant

The volume of HCl delivered to the cell is traditionally assumed to have small uncertainty (Dickson, 1981) and equated to the digital output of the titrator. Calibrations of all the burettes of the Dosimats used were made with Milli-Q water at 25°C. Since the cell volumes are calibrated using standard solutions, errors in the accuracy of volume delivery will be partially canceled and included in the value of cell volumes assigned. The calibration of all the Dosimats used at sea and in the laboratory indicated that the amount of acid delivered (for a typical calculation) was uncertain to ∓ 0.0005 cm^3. This uncertainty in the volume delivered leads to an error in the TA of ∓ 0.5 μmol kg^{-1}. Nevertheless, corrections to the Dosimat reading were made in all of our laboratory TA measurements and calibrations to insure that the assigned value for a different batch of CRM and Gulf Stream water was not affected by the

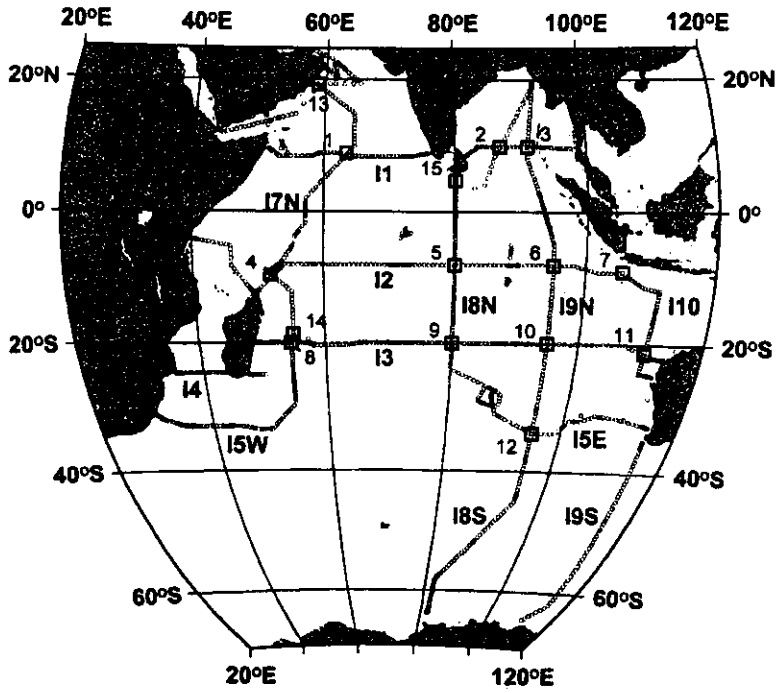

Fig. 1. Cruise tracts of the Indian Ocean Studies showing crossover points.

Table 2
Measurements of pH, TA and TCO_2 of CRM at sea

Cruise	Start date	End date	Batch	Cell	N	TA average	S.D.	TCO_2 average	S.D.	pH average	S.D.
I8S/I9S	12/1/94	1/19/95	23	All	49	2221.5	5.1	2004.5	4.1		
				5	18	2223.3	4.8	2003.8	2.5		
				6	18	2220.8	4.0	2008.0	3.1		
				20	13	2220.0	6.4	2001.4	3.8		
I9N	1/24/95	3/6/95	23	All	138	2216.2	3.3	2000.1	3.5	7.891	0.005
				5	68	2215.0	3.3	1999.1	3.3	7.892	0.004
				6	65	2217.5	3.3	2001.3	3.3	7.891	0.005
				20	5	2214.2	3.1	1996.5	3.5	7.895	0.007
I8N/I5E	3/10/95	4/16/95	23	All	80	2211.6	4.9	1997.0	3.0	7.890	0.006
				5	36	2213.0	5.5	1998.6	3.8	7.890	0.005
				6	44	2210.1	3.6	1996.2	2.6	7.890	0.007
I3	4/20/95	6/7/95	23	All	65	2215.4	1.4	2002.1	1.4	7.894	0.005
				2	33	2215.7	1.3	2000.7	1.4	7.898	0.006
				13	35	2215.0	1.4	2003.6	1.3	7.890	0.004
			26	All	30	2178.0	1.2	1984.8	1.2	7.858	0.004
				2	14	2178.3	1.3	1983.3	1.2	7.862	0.003
				13	16	2177.7	1.2	1986.0	1.1	7.855	0.004
I5W/ I4	6/11/95	7/11/95	26	All	79	2182.6	3.8	1990.2	3.4		
				2	41	2183.3	3.9	1988.0	2.4		
				13	38	2182.0	3.5	1992.9	2.3		
I7N	7/15/95	8/24/95	26	All	59	2184.0	5.7	1984.7	3.4	7.862	0.009
				2	33	2186.2	3.1	1984.3	2.6	7.862	0.009
				13	26	2181.5	7.4	1985.2	4.0	7.858	0.006
			27	All	8	2221.5	3.1	1995.5	1.4	7.916	0.005
				2	4	2221.4	2.4	1994.9	1.4	7.914	0.005
				13	4	2221.5	4.1	1996.0	1.5	7.918	0.006
			23	All	10	2222.4	7.4	2002.0	4.0	7.896	0.006
				2	5	2227.5	5.8	2003.2	4.1	7.897	0.005
				13	5	2216.2	6.4	1999.9	3.9	7.893	0.009
I1	8/29/95	10/18/95	27	All	244	2219.4	3.9	1998.8	5.4	7.906	0.013
				2	123	2220.1	3.2	1995.3	3.2	7.911	0.005
				7	54	2219.6	3.6	1999.7	4.1	7.908	0.013
				13	15	2216.2	4.7	1994.6	4.5	7.909	0.005
				14	52	2217.9	4.5	2006.5	3.6	7.885	0.009
I10	11/6/95	11/24/95	27	All	62	2212.9	4.0	1991.3	2.9	7.912	0.006
				11	30	2212.3	4.5	1989.6	2.4	7.914	0.005
				16	32	2213.5	3.5	1993.1	2.0	7.910	0.006
I8R	9/23/95	10/24/95	29	All	36	2184.2	1.8	1914.8	2.4	8.006	0.006
NOAA Cruise				4	9	2185.5	1.7	1914.5	1.9	8.006	0.005
				17	17	2183.9	1.6	1914.4	2.2	8.007	0.005
				18	10	2183.4	2.1	1915.7	3.1	8.004	0.009
			24	All	10	2216.6	2.3	1998.7	1.7	7.902	0.006
				4	2	2218.5	3.8	1998.6	3.9	7.907	0.004
				17	5	2215.1	0.6	1998.5	1.4	7.902	0.006
				18	3	2217.3	2.6	1998.6	1.7	7.899	0.006
I2	11/28/95	1/19/96	27	All	67	2219.4	4.5	1994.0	2.8	7.916	0.005
				11	36	2219.9	5.7	1993.1	3.3	7.918	0.005

Table 2 (continued)

Cruise	Start date	End date	Batch	Cell	N	TA average	S.D.	TCO_2 average	S.D.	pH average	S.D.
				16	31	2218.9	3.2	1994.7	2.2	7.915	0.006
			30	All	9	2204.6	2.7	1996.8	2.1	7.879	0.004
				11	4	2205.3	2.3	1995.0	2.2	7.880	0.002
				16	5	2204.0	3.0	1998.4	0.8	7.879	0.006

use of different Dosimats. These corrections were also made when calculating the volume of each cell.

2.2. Evaluation of the carbonate parameters

A FORTRAN computer program has been developed to calculate the carbonate parameters (pH, $E*$, TA, TCO_2, and pK_1) in the seawater solutions. The program is patterned after those developed by Dickson (1981), Johansson and Wedborg (1982) and Dickson ([1]; DOE, 1994). The fitting is performed using the STEPIT routine (J.P. Chandler, Oklahoma State University, Stillwater, OK 74074). The STEPIT software package minimizes the sum of squares of residuals by adjusting the parameters $E*$, TA, TCO_2 and pK_1 of carbonic acid. The computer program is based on Eq. (2) and assumes that nutrients such as phosphate, silicate and ammonia are negligible. This assumption is strictly valid only for surface waters. Neglecting the concentration of nutrients in the seawater sample does not affect the accuracy of TA, but must be considered when calculating the carbonate alkalinity ($CA = [HCO_3^-] + 2\,[CO_3^{2-}]$) from TA.

The pH and pK of the acids used in the program are on the seawater scale, $[H^+]_{sw} \sim [H^+] + [HSO_4^-] + [HF]$ (Dickson, 1984). The dissociation constants used in the program were taken from Dickson and Millero (1987) for carbonic acid, from Dickson (1990b) for boric acid, from Dickson and Riley (1979) for HF, from Dickson (1990c) for HSO_4^- and from Millero (1995) for water. The program requires as inputs the concentration of acid, volume of the cell, salinity, temperature, measured emfs (E) and volumes of HCl (V). To obtain a reliable TA from a full titration, at least 25 data points should be collected (9 data points between pH 3.0 to 4.5). The precision of the fit is less than 0.4 μmol kg^{-1} when pK_1 is allowed to vary and 1.5 μmol kg^{-1} when pK_1 is fixed. Our titration program has been compared to the titration programs used by others (Johansson and Wedborg, 1982; Bradshaw and Brewer, 1988) and the values of TA agree to within ± 1 μmol kg^{-1}.

3. Results and discussion

3.1. Laboratory ta measurements of CRMs

The laboratory TA measurements made on the CRMs used throughout this study are summarized in Table 1. The results obtained by both laboratories demonstrate that no systematic differences in TA are found. With the exception of Batch 29, the differences in the measurements of the CRMs between the two laboratories are less that 2 μmol kg^{-1}. Since the Miami measurements were made with the same acid as used at sea, one cannot attribute the differences in Batch 29 to differences in the concentration of the acids (calibrated at SIO). The Miami measurements were also made using the same acid for all the batches of CRM within a one-week period to ensure the internal consistency of its results. The measurements made on the acid concentration in Miami and SIO by a coulometric titration were in agreement to ± 0.0001 M, which is equivalent to an error of ± 1 μmol kg^{-1} in TA.

3.2. At sea measurements of TA, TCO_2, and pH on CRMs

3.2.1. Accuracy of at sea measurements

The tracts of the cruise made during the Indian Ocean studies are shown in Fig. 1. A total of 962 titrations were made on six batches of the CRMs during the cruises (Table 2). A summary of the pH, TA and TCO_2 measurements made on CRMs

Table 3
The overall precision of at sea TA, TCO_2, and pH measurements on the Certified Reference Material

Parameters	Precision (1 σ) (μmol kg^{-1})	Number of measurements
TA	4.2	949
TCO_2	4.1	947
pH	0.007	793[a]

[a]The numbers of the pH measurements were less than for TA and TCO_2 because some values were not recorded.

(Table 3) throughout the cruise is shown in Figs. 2–4. The reproducibility on the six batches of the CRMs used was ±0.007 in pH, ±4.2 μmol kg^{-1} in TA, and ±4.1 μmol kg^{-1} in TCO_2. The at sea TA measurements on the CRMs were in good agreement (~2–4 μmol kg^{-1}) with laboratory measurements made on the same batches at MIAMI and SIO. These small differences (~2–4 μmol kg^{-1}) are well within the overall precision of our measurements and can be attributed to uncertainties in the volume of cells assigned in the laboratory before the cruises. However, the cells used on I7 gave significantly greater errors than the values obtained in the laboratories on the same batch of CRM. These large discrepancies might be attributed to inaccurately assigned volumes of the cells after they were repaired for leakage due to repositioning of a reference electrode after changing the inner filling solution.

3.2.2. *Long term stability of a cell performance*

The at sea TA measurements on the CRMs can be used to examine the long-term stability of the cells used during the cruises. Overall, the TA results obtained using cells for a given cruise did not show any systematic trends. Differences in TA between laboratory and field measurements remained unchanged over the entire period of each cruise. However, inter-cruise variations in TA between laboratory and field results were observed when the same cells were used. For instance, cells 2 and 13 were used for four consecutive cruises over the period of six months. When these two cells were used on the first cruise (I3), the field measurements agreed to within ±2 μmol kg^{-1} with the values obtained in

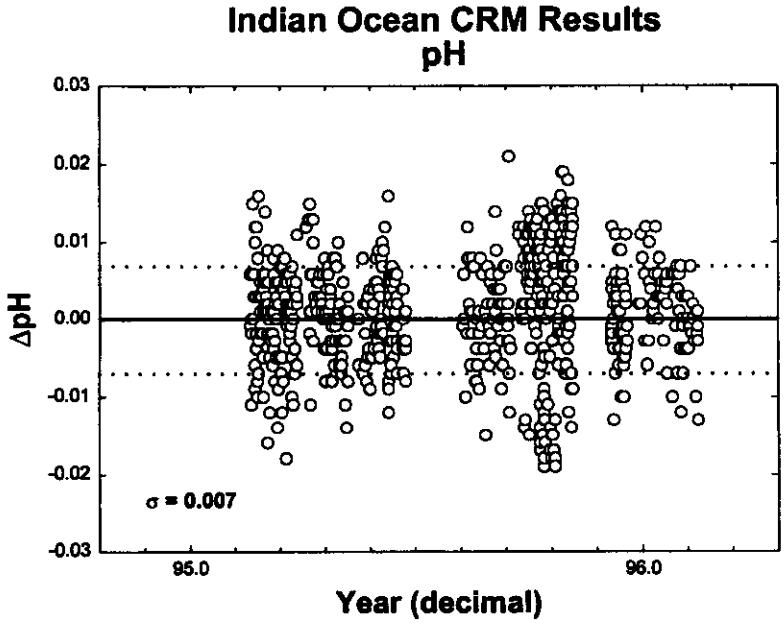

Fig. 2. The reproducibility of the titration pH measurements made on Certified Reference Material on the Indian Ocean Study.

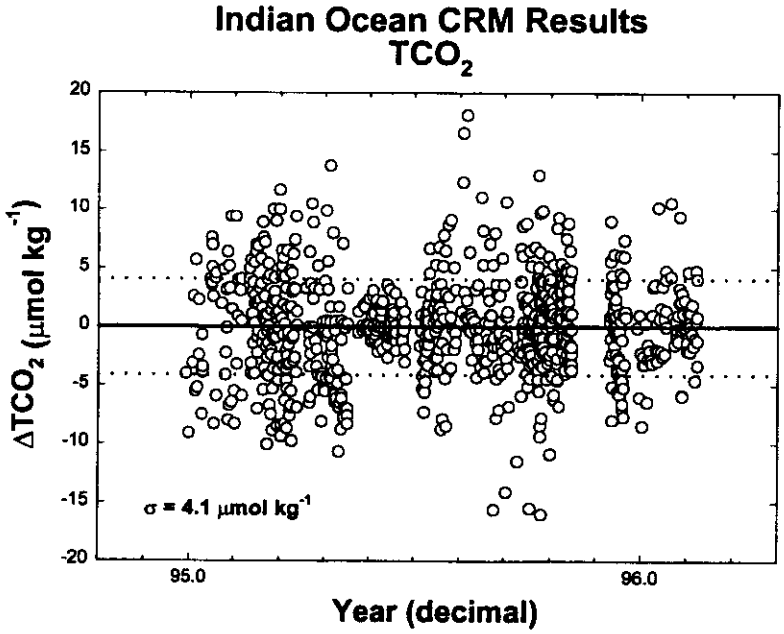

Fig. 3. The reproducibility of the titration TCO_2 measurements made on Certified Reference Material on the Indian Ocean Study.

the laboratory. These small discrepancies are within the precision of our measurements. When the same cells were used for the later cruises, the differences in TA between laboratory and field measurements became significantly larger (9 μmol kg^{-1}). As mentioned in Section 3.2.1, these larger differences can

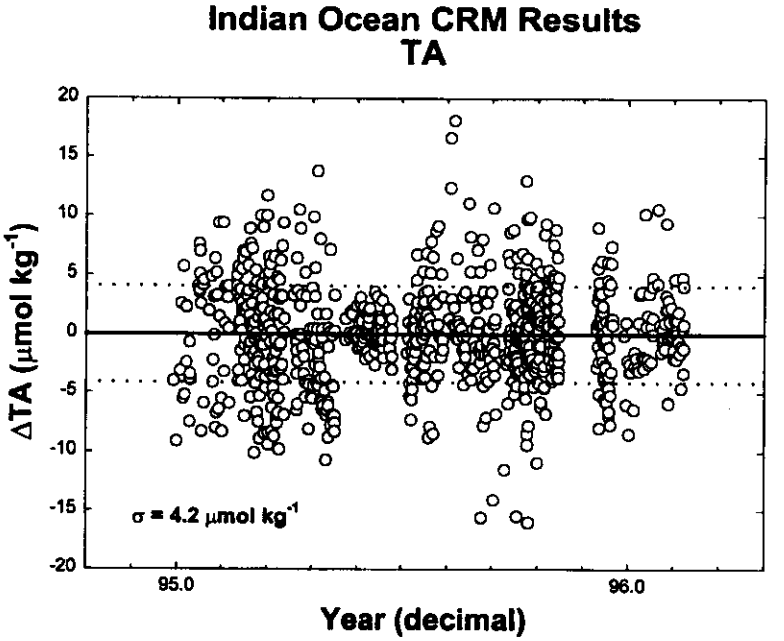

Fig. 4. The reproducibility of the titration TA measurements made on Certified Reference Material on the Indian Ocean Study.

Table 4
Differences between TA measurements made at sea and values measured in the laboratory (SIO)

Cell	I8S/I9S	I9N	I8N/I5E	I3	I5W/I4	I7N	I1	I8R	I10	I2
2				+2.6[a]	+6.7	+9.9[a]	+5.2			
4								0.7		
5	+10.6	+2.3	+0.3							
6	+8.1	+4.8	−2.6							
7							+4.7			
11									−2.6	+4.8[a]
13				+2.1[a]	+6.0	+4.9[a]	+1.3			
14							+3.0			
16									−1.4	+3.7[a]
17								−0.9		
18								−1.4		
20	+7.3	+1.5								

[a]Based on the weighted average on different CRM.

be attributed to changes in the assigned volume of the cells due to repositioning of a reference electrode. These inter-cruise variations in TA can be corrected by normalizing the measured values obtained during the cruises using the corrections required to reproduce the values assigned for the CRMs by SIO (Table 4). This correction was applied using

$$\bar{\Delta} = \mathrm{TA(meas,CRM)} - \mathrm{CRM}) \quad (4)$$

$$\mathrm{TA(corr.)} = \mathrm{TA(meas.)} \times [\mathrm{CRM}/(\mathrm{CRM} + \bar{\Delta})] \quad (5)$$

where CRM is the SIO-certified values.

3.3. Crossover analysis

In order to cross-check our estimates of accuracy of the TA data, which are derived from analyses of CRMs, we examined the agreement between TA measurements made at identical locations on different legs of the Indian Ocean expedition. All of these comparisons have been made after applying the corrections given in Table 4. The implicit assumption is that temporal and spatial gradients of TA concentrations in the deep ocean are small relative to measurement accuracy, so that water sampled at the same location in the deep ocean at two different times should have near-identical values of TA. In practice, vertical gradients of TA can be significant relative to measurement accuracy and there can also be significant vertical motions in the deep ocean. Hence, measurements made at the same geographical location cannot be compared simply on the basis of their common depth. Because most motion in the ocean interior takes place along surfaces of constant den-

Table 5
Crossover results for the TA measurements made in the Indian Ocean

Number	Stations	Legs	ΔTA
1	927,929,931, 780,782,784	I1-I7N	1.7±1.0
2	987,990,266, 268,270	I1-I9N	−2.1±5.9
3	996,998, 233,235	I1-I9Nb	1.2±0.8
4	1205,728, 730	I2-I7N	5.6±2.4
5	1137,1139, 320,324	I2-I9N/I5E	3.4±2.2
6	1094,1096, 191,193	I2-I9N	−3.4±1.4
7	1078,1075	I2-I10	1.8±2.4
8	705,547,549	I5W/I4-I3	0.7±1.7
9	498,499,501, 346,348	I3-I8N/I5E	−0.8±2.3
10	472,169	I3-I9N	−0.8±0.6
11	1039,452,454	I10-I3	−1.0±0.7
12	404,406,408, 9,11,13	I8N/I5E-I8S/I9S	−2.7±3.8
13	861,808	I1-I7N	0.3±0.6
14	709,707	I7N-I5W/I4	2.4±1.7
15	966,968,969, 283,287	I1-I8N/I5E	−4.2±4.5

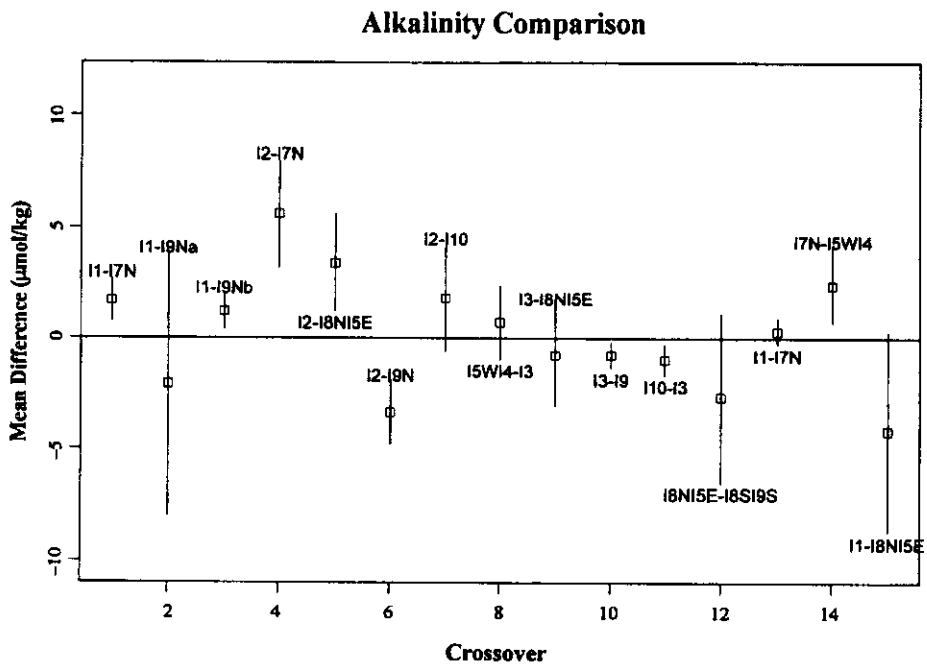

Fig. 5. Summary of the TA reproducibility for crossover points in the Indian Ocean.

sity (isopycnals), it is preferable to compare concentrations using density as the frame of reference rather than depth.

Our crossover analyses were performed as follows.

(1) Locations at which different cruise legs intersected were identified as crossover points. These are identified in Table 5 and Fig. 1.

(2) Stations located in the immediate proximity of these crossover points, for which TA data existed, were selected for the comparison. In general, stations located within 100 km of the crossover location were selected.

(3) For water samples collected below 2500 m, smooth curves were fit through the TA data as a function of the density anomaly referenced to 3000 db (sigma-3) using Cleveland's loess or smoother local regression (Cleveland and Devlin, 1988; Cleveland and Grosse, 1991; Chambers and Hastie, 1991). A separate fit was performed to the data collected from each of the two intersecting legs. The tension parameter for the smoother was adjusted subjectively to give a 'reasonable' fit to the data at the majority of the crossover locations, and the same value for the tension parameter was used for all of the crossovers. Hence, while the fits to the data may not necessarily represent the best possible at each individual crossover point, the smoothing function has been

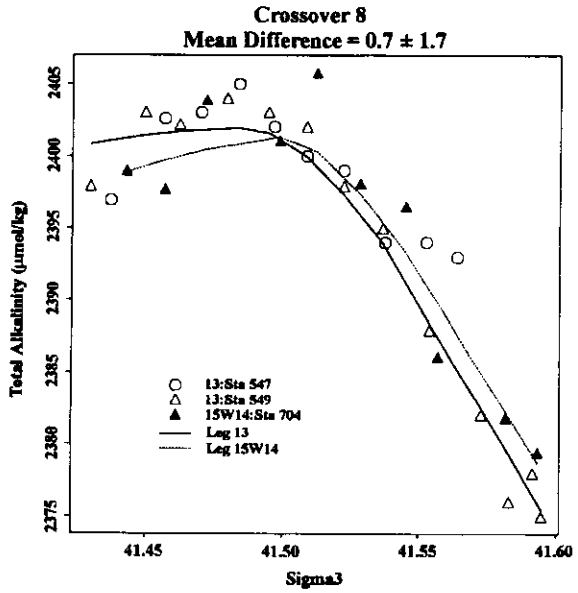

Fig. 6. Results for a typical crossover comparison (I3-I5W/I4) in the Indian Ocean.

applied consistently. It is important to note that the comparison of the data at the crossover points does not depend on the fitting algorithm within the experimental error.

(4) For each crossover, the difference between the two smooth curves was evaluated at 50 evenly spaced intervals that covered the density range over which the two data sets overlapped. A mean and a standard deviation of the difference between the two curves was estimated based on these 50 values, and these values are reported in Table 5 and shown in Fig. 5. An example of the crossover for cruises I3-I5W/I4 is shown in Fig. 6.

The results of the crossover analysis indicate that absolute leg-to-leg differences are always < 6 μmol kg^{-1}. Note that the comparisons were evaluated consistently such that the fit to data from the earlier leg at each crossover was subtracted from the fit to the later leg's data. Any uncorrected, long-term, monotonic drift in the calibration of the titrators over the course of the Indian Ocean expedition would therefore tend to result in a non-zero value for the overall mean of these differences. The overall mean and standard deviation of the differences at all the crossovers are 2.1 ± 2.1 μmol kg^{-1}. In general, the results of the crossover analysis are quite consistent with the overall reproducibility of the CRM analyses (± 4 μmol kg^{-1}) over the duration of the entire Survey.

4. Conclusion

At-sea total alkalinity measurements on the several CRM batches demonstrated that the measurements made by various investigators were precise to about ± 4 μmol kg^{-1}. This level of the precision of at sea measurements was approximately two times worse than that in the laboratory. Differences in the precision between different investigators suggest that the performance of TA measurements was dependent upon the operators. The inter-cruise variations in total alkalinity between laboratory and field results clearly demonstrate that CRMs are an essential component to monitor the performance of titration systems and increase the accuracy for total alkalinity measurements in the field.

Acknowledgements

The authors wish to acknowledge the support of the Department of Energy for their support of the CO_2 studies. The WOCE cruises were supported by the National Science Foundation, as was some of the laboratory work related to the preparation and standardization of Certified Reference Material.

References

Bradshaw, A.L., Brewer, P.G., 1988. High precision measurements of alkalinity and total carbon dioxide in seawater by potentiometric titration: 1. Presence of unknown protolyte(s)?. Mar. Chem. 28, 69–86.

Chambers, J.M., Hastie, T.J., 1991. Stat. Models Sci., 309–376.

Cleveland, W.S., Devlin, S.J., 1988. Locally-weighted regression: an approach to regression analysis by local fitting. J. Am. Statist. Assoc. 83, 596–610.

Cleveland, W.S., Grosse, E., 1991. Computational Methods for Local Regression. Stat. Comput., Vol. 1.

Dickson, A.G., 1981. An exact definition of total alkalinity and a procedure for the estimation of alkalinity and total CO_2 from titration data. Deep-Sea Res. 28, 609–623.

Dickson, A.G., 1984. pH scales and proton-transfer reactions in saline media such as seawater. Geochim. Cosmochim. Acta 48, 2299–2308.

Dickson, A.G., 1990a. The oceanic carbon dioxide system: planning for quality data. US JGOFS News 2 (2), 10.

Dickson, A.G., 1990b. Thermodynamics of the dissociation of boric acid in synthetic seawater from 273.15 to 318.15 K. Deep-Sea Res. 37, 755–766.

Dickson, A.G., 1990c. Standard potential of the (AgCl + 1/2 H_2 = Ag + HCl(aq)) cell and the dissociation of bisulfate ion in synthetic sea water from 273.15 to 318.15 K. J. Chem. Thermodyn. 22, 113–127.

Dickson, A.G., Riley, J.P., 1979. The estimation of acid dissociation constants in sea water media from potentiometric titrations with strong base: I. The ionic production of water– K_W. Mar. Chem. 78, 89–99.

Dickson, A.G., Millero, F.J., 1987. A comparison of the equilibrium constants for the dissociation of carbonic acid in seawater media. Deep-Sea Res. 34, 1733–1743.

DOE, 1994. Handbook of methods for the analysis of the various parameters of the carbon dioxide system in sea water, In: Dickson, A.G., Goyet, C. (Eds.), Version 2, ORNL/CDIAC-74.

Johansson, O., Wedborg, M., 1982. On the evaluation of potentiometric titrations of seawater with hydrochloric acid. Oceanol. Acta 5, 209–218.

Johnson, K.M., Dickson, A.G., Eischeid, G., Goyet, C., Guenther, P., Key, R.M., Millero, F.J., Purkerson, D., Sabine, C.L.,

Schottle, R.G., Wallace, D.R.W., Wilke, R.J., Winn, C.D., 1998. Coulometric total carbon dioxide analysis for marine studies: Assessment of the quality of total inorganic carbon measurements made during the US Indian Ocean CO_2 Survey 1994–1996. Mar. Chem. 63, 21–37.

Marinenko, G., Taylor, J.K., 1968. Electrochemical equivalents of benzoic and oxalic acid. Anal. Chem. 40, 1645–1651.

Millero, F.J., 1995. The thermodynamics of the carbon dioxide system in oceans. Geochim. Cosmochim. Acta 59, 661–677.

Millero, F.J., Poisson, A., 1981. International equation of state of seawater. Deep-Sea Res. 28, 625–629.

Millero, F.J., Laferriere, A., Chetirkin, P.V., 1977. The partial molal volumes of electrolytes in 0.725 m sodium chloride solutions at 25°C. J. Phys. Chem. 81, 1737–1745.

Millero, F.J., Zhang, J.Z., Lee, K., Campbell, D.M., 1993. Titration alkalinity of seawater. Mar. Chem. 44, 153–160.

Taylor, J.K., Smith, S.W., 1959. Precise coulometric titration of acids and bases. J. Res. Natl. Bur. Stds. 63A, 153–159.

APPENDIX D:

REPRINT OF PERTINENT LITERATURE

Sabine, C. L., R. M. Key, K. M.. Johnson, F. J. Millero, J. L. Sarmiento, D. R. W. Wallace, and C. D. Winn. 1999. Anthropogenic CO_2 inventory of the Indian Ocean. Global *Biogeochemical Cycles* 13:179–98.

GLOBAL BIOGEOCHEMICAL CYCLES, VOL. 13, NO. 1, PAGES 179-198, MARCH 1999

Anthropogenic CO_2 inventory of the Indian Ocean

C. L. Sabine,[1] R. M. Key,[1] K. M. Johnson,[2] F. J. Millero,[3] A. Poisson,[4] J. L. Sarmiento,[1] D. W. R. Wallace,[2,5] and C. D. Winn[6,7]

Abstract. This study presents basin-wide anthropogenic CO_2 inventory estimates for the Indian Ocean based on measurements from the World Ocean Circulation Experiment/Joint Global Ocean Flux Study global survey. These estimates employed slightly modified ΔC^* and time series techniques originally proposed by *Gruber et al.* [1996] and *Wallace* [1995], respectively. Together, the two methods yield the total oceanic anthropogenic CO_2 and the carbon increase over the past 2 decades. The highest concentrations and the deepest penetrations of anthropogenic carbon are associated with the Subtropical Convergence at around 30° to 40°S. With both techniques, the lowest anthropogenic CO_2 column inventories are observed south of 50°S. The total anthropogenic CO_2 inventory north of 35°S was 13.6±2 Pg C in 1995. The inventory increase since GEOSECS (Geochemical Ocean Sections Program) was 4.1±1 Pg C for the same area. Approximately 6.7±1 Pg C are stored in the Indian sector of the Southern Ocean, giving a total Indian Ocean inventory of 20.3 ±3 Pg C for 1995. These estimates are compared to anthropogenic CO_2 inventories estimated by the Princeton ocean biogeochemistry model. The model predicts an Indian Ocean sink north of 35°S that is only 0.61-0.68 times the results presented here; while the Southern Ocean sink is nearly 2.6 times higher than the measurement-based estimate. These results clearly identify areas in the models that need further examination and provide a good baseline for future studies of the anthropogenic inventory.

1. Introduction

The current Intergovernmental Panel on Climate Change (IPCC) estimate for the oceanic sink of anthropogenic CO_2 (2.0 ±0.8 Pg C yr^{-1}) is based primarily on ocean models [e.g., *Sarmiento et al.*, 1992; *Sarmiento and Sundquist*, 1992; *Siegenthaler and Sarmiento*, 1993; *Siegenthaler and Joos*, 1992; *Stocker et al.*, 1994], atmospheric models [e.g., *Keeling et al.*, 1989; *Keeling and Shertz*, 1992] or on the oceanic distribution of related species such as $\delta^{13}C$ [*Quay et al.*, 1992]. Although the basic assumptions used in these methods are reasonably well grounded, there will always be room for doubt with indirect approaches. Direct estimates of the oceanic CO_2 sink, however, have been primarily limited by a lack of high-quality data on a global scale.

Two general approaches can be used to estimate the uptake of anthropogenic CO_2 by the oceans. One approach, initially proposed by *Tans et al.* [1990], is to use direct measurements of the air-sea difference in CO_2 partial pressure together with global winds and a gas exchange coefficient to estimate the net transfer of CO_2 into the oceans. These estimates, together with an atmospheric transport model, predicted that the oceanic sink was only 0.3 to 0.8 Pg C yr^{-1}, much smaller than the model predictions. The difficulty with the ΔpCO_2 approach lies both in the large uncertainty in the wind speed dependence of the air-sea gas exchange velocity and in the ability to properly represent the large temporal and spatial variability of the surface ocean pCO_2 because of a lack of seasonal, global data coverage. This estimate has recently been revised to 0.6 to 1.34 Pg C yr^{-1} with the addition of more data and a lateral advection-diffusion transport equation to help with the necessary temporal and spatial interpolations [*Takahashi et al.*, 1997].

A second approach, which avoids many of the problems of temporal variability, is to estimate the inventory of anthropogenic CO_2 stored in the oceans interior based on inorganic carbon measurements. Again, the problem with this approach in the past has been a lack of high-quality global data coverage. As pointed out by *Broecker et al.* [1979] after completion of the last global oceanographic survey, GEOSECS (Geochemical Ocean Sections Program), the precision of ocean carbon measurements at that time was two orders of magnitude smaller than the predicted 0.035% annual increase in surface ocean dissolved inorganic carbon. Nearly 20 years have passed since GEOSECS, and the quality of today's carbon measurements has improved significantly.

This is the first of several papers aimed at estimating the anthropogenic CO_2 inventory of the oceans based on the recent global survey of CO_2 in the oceans. The survey was conducted as part of the JGOFS (Joint Global Ocean Flux Study) in close cooperation with the WOCE-HP (World Ocean Circulation Experiment - Hydrographic Programme). This program was a multiyear effort to collect high-precision inorganic carbon data with the highest possible spatial resolution on a global scale. This paper will focus on anthropogenic CO_2 estimates for the Indian Ocean. Papers will

[1]Department of Geosciences, Princeton University, Princeton, New Jersey.
[2]Oceanographic and Atmospheric Sciences Division, Brookhaven National Laboratory, Upton, New York.
[3]Rosenstiel School of Marine and Atmospheric Science, University of Miami, Miami, Florida.
[4]Laboratoire de Physique et Chimie Marines, Université Pierre et Marie Curie, Paris.
[5]Now at Institut für Meereskunde, Universität Kiel.
[6]Department of Oceanography, University of Hawaii at Manoa, Honolulu, Hawaii.
[7]Now at Hawaii Pacific University, Kaneohe, Hawaii.

Paper number 1998GB900022.
0886-6236/99/1998GB900022$12.00

soon follow with estimates for the other major ocean basins, with the ultimate goal of generating an estimate of the global oceanic anthropogenic CO_2 sink based on direct carbon system measurements. The strength of these calculations lies not only in our ability to directly estimate the magnitude of the oceanic anthropogenic CO_2 sink but also in the fact that these estimates can be directly compared to anthropogenic CO_2 inventories estimated by carbon-cycle ocean general circulation models (GCMs). The two methods described here provide information over different timescales. The combined results place strong constraints on the uptake rate for anthropogenic CO_2 and are useful for identifying weaknesses in the models.

2. Methods

Estimates of the anthropogenic CO_2 inventory are determined from measured values using two different techniques. The first technique, referred to as the "time series" approach, is based on quantifying the increase in total carbon dioxide (TCO_2) since GEOSECS. The second approach quantifies the total anthropogenic CO_2 inventory using a quasi-conservative tracer, ΔC^*. Although the general idea for both techniques has been around for a long time, recent improvements in the estimation of the preserved end-member concentrations together with significant improvements in the accuracy and spatial coverage of global carbon data give us much more confidence in these results. Given the difficulty of isolating the anthropogenic signal from the large TCO_2 background, however, it is relevant to summarize the quality of the carbon data set and the techniques used to estimate the anthropogenic signal.

2.1. Data Quality

Over 20,000 water samples collected between December 1994 and July 1996 as part of the U.S. WOCE Indian Ocean survey were analyzed for both TCO_2 and total alkalinity (TA) using standard coulometric and potentiometric techniques, respectively. Figure 1 shows the locations of the 1352 stations occupied by U.S. WOCE as part of the Indian Ocean survey together with the station locations from the GEOSECS Indian Ocean Survey and the French INDIGO I, II, and III and CIVA1 (WOCE designation I6S) cruises. Details of the WOCE/JGOFS Indian Ocean CO_2 measurement program, including personnel, sampling procedures, measurement protocols and data quality assurance/quality control checks are described elsewhere [*Johnson et al.*, 1998; *Millero et al.*, 1998a]. Calibrations of both the TCO_2 and TA systems were checked approximately every 12 hours by analyzing Certified Reference Material (CRM) samples with known concentrations of TCO_2 and TA [*Dickson*, 1990] (A.G. Dickson, Oceanic carbon dioxide quality control at http://www-mpl.ucsd.edu/people/adickson/CO2_QC/ , 1998). On the basis of these CRM analyses the accuracy of the TCO_2 and TA measurements was estimated to be ±2 and ±4 μmol kg^{-1}, respectively. Primary hydrographic data from the conductivity-temperature-depth/Rosette were collected and analyzed following standard procedures [*Millard*, 1982]. Samples were collected for salinity on every bottle and analyzed with an Autosal salinometer using standard techniques [*UNESCO*, 1981]. Oxygen samples were analyzed with an automated system using a modified Winkler technique [*Culberson et al.*, 1991]. Nutrients were analyzed on a four-channel Technicon AutoAnalyzer II following the methods of *Gordon et al.* [1992]. Chlorofluorocarbon samples were analyzed

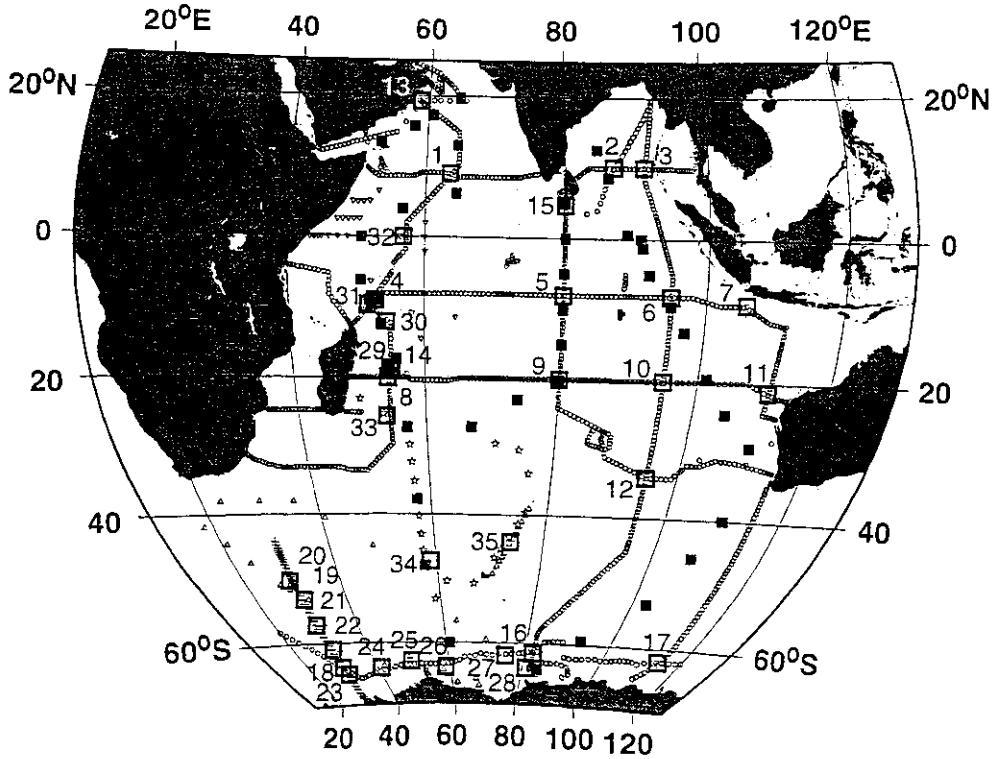

Figure 1. Station locations for WOCE Indian Ocean (circles), CIVA 1/I6S (crosses), INDIGO I (stars), INDIGO II (inverted triangles), INDIGO III (triangles), and GEOSECS (solid squares) Indian Ocean Surveys. Numbered boxes indicate location of crossovers discussed in the text. Map generated using Generic Mapping Tools version 3 [*Wessel and Smith*, 1995].

on a gas chromatograph using the techniques of *Bullister and Weiss* [1988]. Complete details of the analytical protocols and personnel can be obtained from the individual cruise reports available through the WOCE Office.

All of the data available at the time this manuscript was written have been included in the Indian Ocean analysis. For the primary hydrographic and nutrient data this means that the preliminary values available at the conclusion of the cruise were used. While we would prefer to use the final hydrographic data, typical postcruise corrections for the WOCE data sets are well below noise level for these calculations. Preliminary to semifinal chlorofluorocarbon (CFC) data were used to estimate the water age necessary for one of the correction terms in the ΔC^* method. Although postcruise blank corrections can influence the final CFC concentrations, an examination of the existing data (except I8NI5E because data were not available at time of writing) indicated that the CFC-11 and CFC-12 age comparisons as well as comparisons of the data from one leg to the next were reasonably consistent with each other. The calculations were limited to waters with CFC-12 ages of less than 40 years where potential blank corrections are a relatively small fraction of the signal and mixing effects are minimized. The carbon data, which primarily influence the quality of the calculations, have all been calibrated and finalized as discussed briefly below.

Examination of Figure 1 reveals that although the WOCE survey was extensive, a large data gap exists in the southwestern Indian Ocean. To fill in this gap, data from the three French survey legs INDIGO I (February-March 1985), II (April 1986) and III (January-February 1987) as well as the more recent French cruise CIVA1 (February-March 1993 (WOCE designation I6S)) were included in the analysis [*Poisson et al.*, 1988; 1989; 1990]. TCO_2 and TA were analyzed on the INDIGO cruises using standard potentiometric titration techniques developed by *Edmond* [1970]. Potentiometric titrations were also used to analyze the TA samples on CIVA1, but the TCO_2 samples were analyzed using the coulometric techniques of *Johnson et al.* [1985]. The internal consistency of these cruises was examined by comparing carbon values in the deep waters (pressure > 2500 dbars) at the intersections of different legs. The stations selected for each crossover were those with carbon values which were closest to the intersection point. Smooth curves were fit through the data from each cruise as a function of sigma- 3 (density anomaly referenced to 3000 dbars) using Cleveland's loess function [*Cleveland and Devlin*, 1988; *Cleveland et al.*, 1992]. The difference between the curves was evaluated at 50 evenly spaced intervals that covered the density range over which the two data sets overlapped. The mean and standard deviation of the difference in TA and TCO_2 at the 35 intersections identified in Figure 1 are shown in Figure 2. The long-term stability of the WOCE/JGOFS measurements can be estimated from the first 17 crossover results. The mean of the absolute values for the leg-to-leg differences was less than the estimated accuracy for both TCO_2 (1.8 ± 0.8 μmol kg^{-1}) and TA (2.4 ± 1.6 μmol kg^{-1}). Although there is only one reliable crossover point between the WOCE/JGOFS cruises and the CIVA1 (I6S) cruise, the differences for both parameters are within the estimated accuracy of the measurements. Results from the analysis of CRM samples on the CIVA1 cruise also support the quality of the measurements. Some of the older INDIGO cruises, however, did appear to have offsets relative to the WOCE/JGOFS and CIVA1 data. INDIGO I and II alkalinity values averaged 6.5 μmol kg^{-1} high and 6.8 μmol kg^{-1} low, respectively, while the INDIGO III alkalinity values showed no clear offset. The INDIGO TCO_2 values were all consistently high relative to WOCE/JGOFS and CIVA1, with differences of 10.7, 9.4, and 6.4 μmol kg^{-1}, respectively. These offsets are consistent with differences observed between at-sea values and replicate samples run at C.D. Keeling's shore-based TCO_2 facility (P. Guenther, personal communication, 1998). Since the INDIGO cruises were run prior to the introduction of CRMs, these offsets were presumed to be calibration differences, and each leg was adjusted to bring the values in line with the remaining cruises. The dotted boxes in Figure 2 show the original offsets at the crossovers. The solid boxes show the final offsets used in the following calculations. The means of the absolute values for the leg-to-leg differences for all 35 crossover analyses suggest that the final data set is internally consistent to ± 2.2 and 3.0 μmol kg^{-1} for TCO_2 and TA, respectively.

2.2. "Time Series" Calculations

The "time series" method for estimating the increase in the anthropogenic inventory uses measurements of TCO_2 made at a certain point in time to develop a predictive equation based on a multiple linear regression of the observed TCO_2 and simultaneously measured parameters such as temperature, salinity, oxygen, and TA (or silicate). These empirical multiparameter relationships have been shown to hold over large spatial scales, and their use drastically reduces the complicating effects of natural variability in determining temporal trends [*Brewer et al.*, 1995; *Wallace*, 1995; *Brewer et al.*, 1997]. The TCO_2 residuals from such predictive equations can be compared directly with patterns of residuals evaluated using the same predictive equation with TA, oxygen, and hydrographic data collected at different times (e.g., over decadal intervals). Since the uptake of anthropogenic CO_2 will increase the TCO_2 of the waters but will not directly affect the concentrations of the fit parameters, systematic changes in the magnitude and distribution of the TCO_2 residuals over time provide a direct estimate of the oceanic CO_2 inventory change due to the uptake of anthropogenic CO_2. The most comprehensive historical carbon data set for the Indian Ocean is from the GEOSECS expedition. By examining the WOCE data relative to that collected during the 1977-1978 GEOSECS Indian Ocean Survey, the increase in anthropogenic inventory over the last 18 years can be estimated.

2.2.1. GEOSECS fit. All of the GEOSECS data from the Indian Ocean (excluding Gulf of Aden and Red Sea regions) were fit with a single predictive equation as a function of potential temperature (θ), salinity (S), apparent oxygen utilization (AOU), and TA. To minimize the influence of short-term temporal variability, only data from pressures greater than 200 dbars were included in the fit. Despite the large area covered, the GEOSECS TCO_2 values can be predicted from this equation to ± 5.2 μmol kg^{-1} ($R^2 = 0.992$ and $N = 1120$). There is, however, a pattern in the residuals that correlates with observed hydrographic regions in the Indian Ocean (Figure 3).

In an attempt to improve the fit, a categorical variable based on region was added to the regression. The categorical variable differs from the other continuous variables by the fact that it is either applied or not applied depending on whether the sample is located within the region. The regions were defined as follows: 1, Arabian Sea (north of 10°N and west of 78°E); 2, North of 10°S (excluding Arabian Sea); 3, Chemical Front (21°S to 10°S); 4, Central Gyre (35°S to 21°S); and 5, Southern Ocean (south of 35°S)

The addition of the regional variable resulted in a marginal improvement in the fit ($R^2 = 0.993$ and $\sigma = 4.9$ μmol kg^{-1}) but

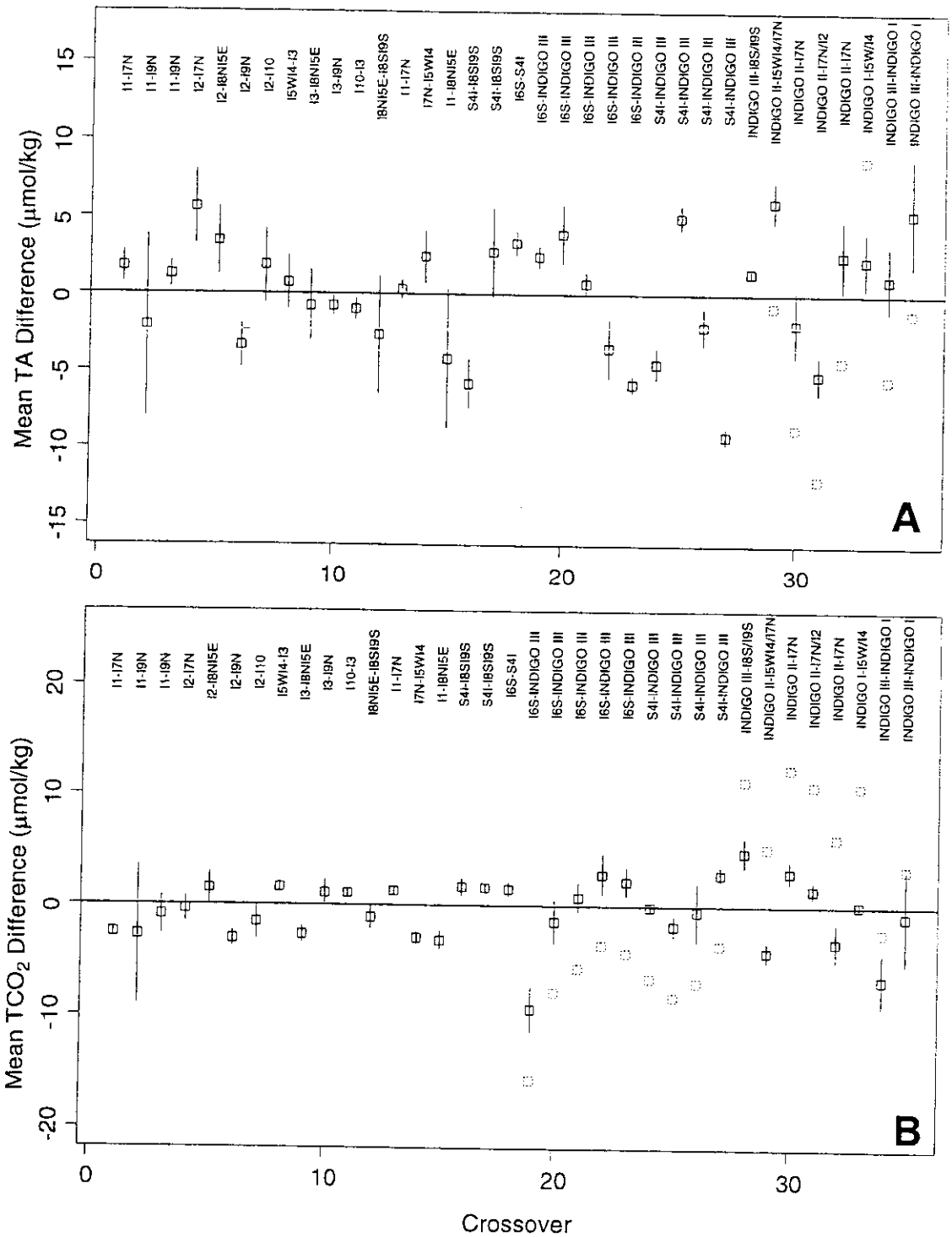

Figure 2. Mean difference between deep water values of (a) TA and (b) TCO_2 for cruise intersections identified in Figure 1. Bars indicate one standard deviation. Dotted boxes indicate difference before adjustment (see explanation in text).

more importantly, removed the regional bias in the predictive equation. The coefficients of the final fit are shown in Figure 4 along with a plot of the measured versus calculated TCO_2 values for all of the points used in the fit. The resulting equation was then used to generate TCO_2 values for each of the WOCE sample locations based on the measured temperature, salinity, oxygen, and TA values. The difference between the measured TCO_2 and the predicted TCO_2 reflects the CO_2 increase in the time between the two cruises. For this work the difference is referred to as "excess CO_2."

The residual method of estimating excess CO_2 was applied to the water column below 200 dbars. The surface waters, however, are dominated by seasonal variability which can bias the residual

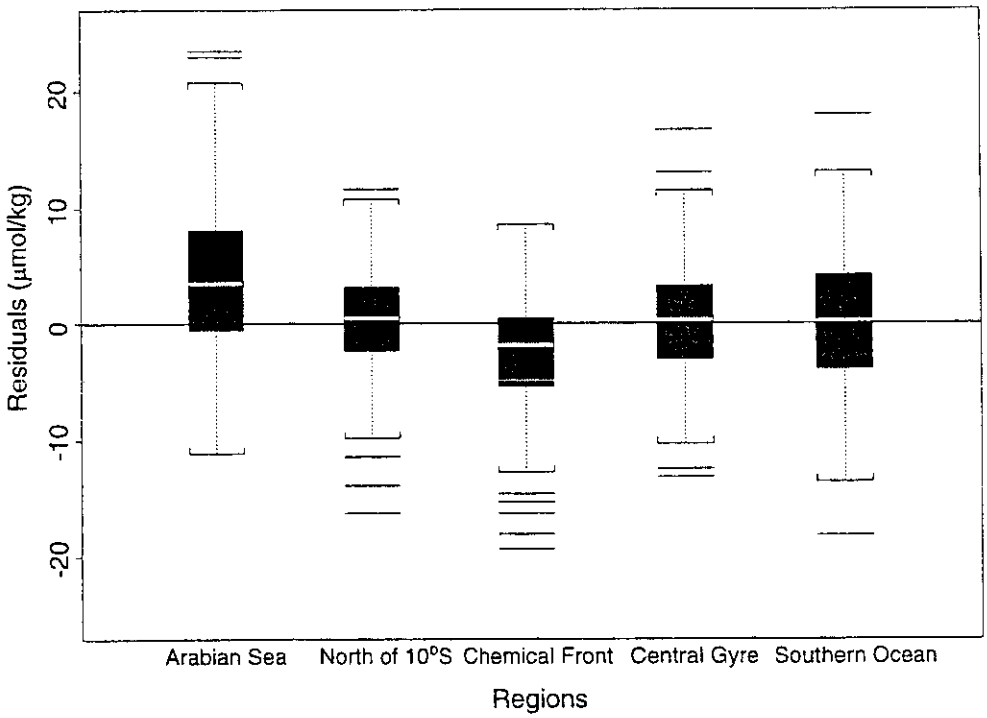

Figure 3. Box and whiskers plot of residuals from a multiple linear regression of GEOSECS Indian Ocean data (pressure > 200 dbars) fit without the regional designator versus oceanographic region: $TCO_2 = 706.5 + 7.7S - 6.68\theta + 0.513TA + 0.7257AOU$. Solid boxes cover the range of ± 1 standard deviation about the mean. White lines within the boxes indicate median values. The whiskers indicate the range of data within the 99% confidence interval. The bars outside the whiskers give the values of outliers in the data set.

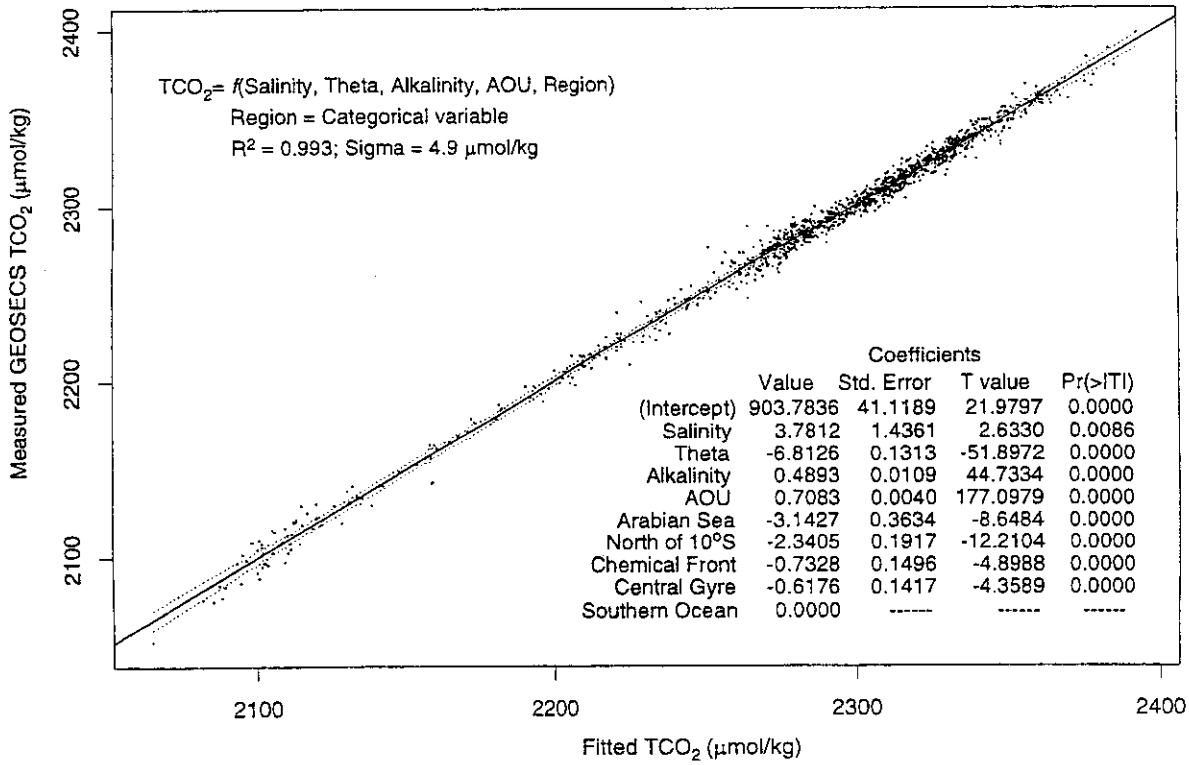

Figure 4. Plot of measured GEOSECS TCO_2 versus the calculated values. Solid line shows 1:1 relationship. The dashed lines indicate the 99% confidence interval for the fit. Text gives coefficients and related statistics. The column labeled "Pr(>|T|)" gives the probability that the T value in the previous column is larger than the T table value in a student T test.

calculations. The excess CO_2 of the surface waters therefore was determined from the difference in the estimated annual mean TCO_2 concentrations between GEOSECS and WOCE. The annual mean TCO_2 concentration was calculated from TA and surface water fCO_2. The surface alkalinity was estimated from the gridded annual mean salinity and temperature values of *Levitus et al.* [1994] and *Levitus and Boyer* [1994] using a multiple linear fit of the WOCE/JGOFS surface (pressure < 60 dbars) TA data to the measured surface temperature and salinity. The 1978 and 1995 surface water fCO_2 concentrations were estimated from the annual mean atmospheric concentration for the 2 years, and the annual mean ΔpCO_2 values estimated from the full correction scheme of *Takahashi et al.* [1997]. The excess TCO_2 values between the surface and 200 dbars were estimated with a linear approximation between the surface and 200 dbars values for each 1° grid box.

2.2.2. Data consistency. One of the major concerns with the time series technique is the necessity of having two data sets that are consistent with each other. This consistency can be well documented for both TCO_2 and TA today through the use of certified reference materials (CRMs) supplied by A. Dickson of Scripps Institute of Oceanography (SIO). Since CRMs were not available at the time of GEOSECS, the only way to infer consistency with the WOCE data set is to assume the deep water carbon distributions have not changed since GEOSECS. The most reliable way to compare the two data sets is to examine the difference between the predicted TCO_2 and the measured TCO_2 (excess CO_2) in deep waters. The basic assumption with this technique is that the correlation between the different hydrographic parameters in the deep waters does not change with time. Given the long residence time of the deep and bottom waters in the ocean, this should be a reasonable assumption. This technique has the advantage that it implicitly accounts for the possibility of real variability in hydrographic properties between the two expeditions which would not be taken into account by simply comparing carbon profiles.

Examination of the excess CO_2 values in waters that should be free of anthropogenic CO_2 (pressures > 2000 dbars and containing no detectable chlorofluorocarbons) revealed that the GEOSECS values were 22.5 ±3 μmol kg^{-1} higher than the comparable WOCE measurements. This difference is comparable to the correction of -18 ± 7 μmol kg^{-1} noted by *Weiss et al.* [1983] to make the TCO_2 measurements consistent with the TA and discrete CO_2 partial pressure measurements based on the *Merbach et al.* [1973] dissociation constants. Additional support for an adjustment of the original GEOSECS data comes from C. D. Keeling's shore-based analysis of TCO_2 samples collected on both the GEOSECS and the WOCE/JGOFS expeditions. *Weiss et al.* [1983] point out that the shore-based analyses of Keeling were systematically smaller than the at-sea measurements by 16.5 ± 5 μmol kg^{-1} during GEOSECS. Similar comparisons between the WOCE/JGOFS at-sea measurements with Keeling's shore-based analyses indicate that the shore-based samples are approximately 5 μmol kg^{-1} higher than the at-sea values (P. Guenther, personal communication, 1998). Together, the GEOSECS-Keeling-WOCE/JGOFS combination suggests an offset of 21.5 μmol kg^{-1} between GEOSECS and WOCE/JGOFS at-sea measurements. It is also important to note that there is no indication of a depth or concentration dependent correction for the GEOSECS data. The shore-based comparison, based only on samples collected at the surface, is within 1 μmol kg^{-1} of the deep comparison described above. On the basis of these results a constant correction of the -22.5 μmol kg^{-1} was applied to the GEOSECS TCO_2 values to improve the consistency of the two data sets.

Ideally, the data used in the time series calculations would cover the same geographic region with as much of a time difference as possible. The trade-off, however, is that the quality and spatial coverage of the older data sets is generally very limited. Given the relatively small area of overlap between the WOCE/JGOFS and INDIGO data sets and the shorter time difference between cruises (9 years versus 18 years for WOCE - GEOSECS), the time series analysis was limited to a comparison between WOCE/JGOFS and GEOSECS in the main Indian Ocean basin.

2.2.3. Evaluation of Errors. An estimate of the random errors associated with the excess CO_2 calculation can be made with a simple propagation of errors based on the fit to the GEOSECS data and the estimated precision of the WOCE/JGOFS data. With a standard deviation of 4.9 μmol kg^{-1} for the GEOSECS fit and an estimated long-term precision of ±2 μmol kg^{-1} in the WOCE/JGOFS TCO_2 values the excess CO_2 error is estimated to be approximately ±5 μmol kg^{-1}. This value compares well with the standard deviation of 3.5 μmol kg^{-1} for the excess CO_2 below the maximum anthropogenic CO_2 penetration depth (pressure > 1500 dbars).

Systematic errors with this technique are very difficult to evaluate. The largest potential systematic error is probably associated with the surface water estimates. Because the same ΔpCO_2 value is used to estimate the TCO_2 for both years, the excess CO_2 (1995 TCO_2 - 1978 TCO_2) is not very sensitive to potential errors associated with the actual ΔpCO_2 values used. The surface estimate is sensitive, however, to the assumption that the ΔpCO_2 has not changed over time (i.e., that the surface ocean increase has kept pace with the atmospheric increase). It is not likely that the surface ocean has increased at a faster rate than the atmosphere, but it is conceivable that the rate is slower. The current assumption results in a total inventory of 0.8 Pg C in the surface layer. If the surface ocean were increasing at half the rate of the atmosphere, the systematic bias in the final inventory would be around 0.4 Pg C. Below the surface layer the most likely systematic error would result from the uncertainty in fitting the GEOSECS data. Systematic errors associated with calibration differences between cruises are potentially quite large, but the analysis and subsequent correction given in section 2.2.2 should remove these biases. The estimated uncertainty for the GEOSECS adjustment was ±3 μmol kg^{-1}. If this value is integrated for the area north of 35°S between 200 m and the average penetration depth of the excess CO_2 (~ 800 m), the potential error would be ±0.9 Pg C. Propagating the errors for the surface and deeper layers gives an estimated error of approximately ±1 Pg C in the total excess CO_2 inventory. Clearly, there are other ways of estimating the potential errors in these calculations, but we feel that this is a reasonable estimate based on the available data.

2.3. ΔC* Calculations

Gruber et al. [1996] developed a method to estimate the total anthropogenic CO_2 inventory which has accumulated in the water column since preindustrial times. Although the details of the calculation are thoroughly discussed by Gruber et al., the basic concept of the calculation can be expressed in terms of the following equation:

$$C_{anth}\left(\frac{\mu mol}{kg}\right) = C_m - \Delta C_{bio} - C_{280} - \Delta C_{dis} \qquad (1)$$

where

C_{anth} anthropogenic carbon concentration;
C_m measured total carbon concentration;
ΔC_{bio} change in TCO_2 as a result of biological activity;
C_{280} TCO_2 of waters in equilibrium with an atmospheric CO_2 concentration of 280 μatm;
ΔC_{dis} air-sea difference in CO_2 concentration expressed in μmol kg^{-1} of TCO_2.

The Gruber et al. technique employs a new quasi-conservative tracer ΔC*, which is defined as the difference between the measured TCO_2 concentration, corrected for biology, and the concentration these waters would have at the surface in equilibrium with a preindustrial atmosphere (i.e., $\Delta C^* = C_m - \Delta C_{bio} - C_{280}$). Rearranging (1) shows that ΔC* reflects both the anthropogenic signal and the air-sea CO_2 difference (i.e., $\Delta C^* = C_{anth} + \Delta C_{dis}$). The air-sea disequilibrium component can then be discriminated from the anthropogenic signal using either information about the water age (e.g., from transient tracers such as CFCs or ^3H-^3He) or the distribution of ΔC* in regions not affected by the anthropogenic transient. The details of this technique will not be covered here except as necessary to explain small modifications that were necessary for use with the WOCE Indian Ocean data set.

2.3.1. Preformed alkalinity equation. The first modification to the *Gruber et al.* [1996] technique involved a recalculation of the preformed alkalinity equation. The preformed alkalinity (Alk^0) of a subsurface water parcel is an estimate of the alkalinity that the water had when it was last at the surface. This value is necessary to determine the equilibrium concentration (C_{280}) of the waters. Gruber et al. generated a single global equation for estimating Alk^0 from salinity and the conservative tracer "PO" ($PO = O_2 + 170*P$) [*Broecker*, 1974] based on the data collected during GEOSECS, South Atlantic Ventilation Experiment, Transient Tracers in the Ocean/North Atlantic Study and Transient Tracers in the Ocean/Tropical Atlantic Study. Given the limited representation of the Indian Ocean in these data and the improved quality of today's measurements, the Gruber et al. fit was examined for a possible bias with respect to the WOCE/JGOFS results. Alk^0 values calculated from the Gruber et al. equation were found to be, on average, 7 ±12 μmol kg^{-1} lower than the WOCE/JGOFS measured surface alkalinity values. Rather than making assumptions about which parameters would provide the best fit to the surface alkalinity data, several possible parameters were tested based on previously noted correlations. Although salinity has been shown to generally correlate very strongly with surface alkalinity [*Brewer et al.*, 1986; *Millero et al.*, 1998b], some areas, such as the high-latitude regions, require additional parameters to fit regional changes in alkalinity. Some investigators have used temperature as an additional variable [e.g., *Chen and Pytkowicz*, 1979; *Chen*, 1990; *Millero et al.*, 1998b]. Others, such as *Gruber et al.* [1996], have used other conservative tracers to compensate for the regional differences. The best fit for the WOCE/JGOFS, INDIGO, and CIVA Indian Ocean data, with pressures less than 60 dbars, is given by (2):

$$Alk^0 = 378.1 + 55.22 \times S + 0.0716 \times PO - 1.236 \times \theta \quad (2)$$

Alk^0 has units of μmol kg^{-1} when salinity (S) is on the practical salinity scale, PO is in μmol kg^{-1}, and potential temperature (θ) is in degrees Celsius. The standard error in the new Alk^0 estimate is ±8.0 μmol kg^{-1} based on 2250 data points. A standard ANOVA analysis of the fit shows that all four terms are highly significant (Table 1). Reevaluating the Alk^0 equation not only removed the 7 μmol kg^{-1} offset of Gruber's equation but also resulted in a 35% reduction in the uncertainty.

Table 1. Results From ANOVA Analysis of Alk^0 Fit.

	Coefficient	Standard Error	T Value	Pr(>|T|)
Intercept	378.1	8.9	42.2715	0.0000
Salinity	55.22	0.23	235.0369	0.0000
PO	0.0716	0.0041	17.4693	0.0000
Theta	-1.236	0.061	-20.3697	0.0000

The column labeled "Pr(>|T|)" gives the probability that the T value in the previous column is larger than the T table value in a student T test. Alk^0 is preformed alkalinity, an estimate of the alkalinity of a parcel of subsurface water when it was last at the surface.

2.3.2. Denitrification Correction. A second modification to the original ΔC* technique was necessary to properly account for the anoxic regions in the northern Indian Ocean. The C_{bio} term in (1) assumes that the remineralization of carbon in the interior of the ocean occurs in proportion to the oxygen uptake based on a standard Redfield type stoichiometry. The ratios used for these calculations were based on the global estimates of *Anderson and Sarmiento* [1994]. *Gruber et al.* [1996] demonstrated that the errors in the ΔC* calculation due to uncertainties in the C:O stoichiometric ratio only become significant for AOU values greater than 80 μmol kg^{-1}. Given that most of the anthropogenic CO_2 is found in relatively shallow waters with low AOU, this error, on average, is small. For some regions of the Arabian Sea, however, oxygen depletion can be quite extensive at relatively shallow depths [*Sen Gupta et al.*, 1976; *Deuser et al.*, 1978; *Naqvi and Sen Gupta*, 1985]. In areas where the waters become anoxic, denitrification can significantly alter the dissolved carbon to oxygen ratio [*Naqvi and Sen Gupta*, 1985; *Anderson and Dyrssen*, 1994; *Gruber and Sarmiento*, 1997]. The dissolved carbon generated by denitrification shows up as high ΔC* values as demonstrated at the northern end of the section in Figure 5a. The distribution of ΔC* values along the density surface σ_θ=26.9-27.0 shows maximum values at both the northern and southern ends of the section. One would expect the uptake of anthropogenic CO_2 to generate the highest values close to the outcrop region in the south, but this surface does not outcrop in the north. Following the methods of *Gruber and Sarmiento* [1997], the denitrification signal can be estimated using the N* tracer. N* is a quasi-conservative tracer which can be used to identify nitrogen (N) excess or deficits relative to phosphorus (P). Using the global equation of *Gruber and Sarmiento* [1997], N* is defined as

$$N^*\left(\frac{\mu mol}{kg}\right) = 0.87(N - 16P + 2.90) \quad (3)$$

Figure 5b shows the magnitude of the denitrification signal along the σ_θ=26.9-27.0 surface. The N* values were converted from nitrogen units to μmol C kg^{-1} based on a denitrification carbon to nitrogen ratio of 106:-104 [*Gruber and Sarmiento*, 1997]. Negative values reflect nitrogen fixation, while positive values indicate denitrification. As expected, the values of N* are essentially zero in the main Indian Ocean basin but show a strong denitrification signal at

middepths in the Arabian Sea. The low N* values at the north end of this surface (Figure 5b) are from the Bay of Bengal and show little or no denitrification in this region. Subtracting a denitrification correction term from the original ΔC^* equation lowers the high ΔC^* values at the northern end of the section leaving the expected maximum near the outcrop region (Figure 5c).

The final definition for ΔC^* as used in this work is given by (4):

$$\Delta C^* = TCO_2^{(meas)} - TCO_2^{(S,\,T,\,Alk^0,\,280)} - \frac{117}{-170}(O_2 - O_2^{(sat)}) - \frac{1}{2}(TA - Alk^0 + \frac{16}{-170}(O_2 - O_2^{(sat)})) - \frac{106}{-104}N^* \quad (4)$$

where $TCO_2^{(meas)}$, TA, and O_2 are the measured concentrations for a given water sample in $\mu mol\ kg^{-1}$. Alk^0 is the preformed alkalinity value as described in section 2.3.1. $O_2^{(sat)}$ is the calculated oxygen saturation value that the waters would have if they were adiabatically raised to the surface. $TCO_2^{(S,\,T,\,Alk^0,\,280)}$ is the TCO_2 value the waters would have at the surface with a TA value equal to Alk^0 and an fCO_2 value of 280 μatm.

2.3.3. Estimation of air-sea disequilibrium. To isolate the anthropogenic CO_2 component from ΔC^*, the air-sea disequilibrium values (ΔC_{dis}) must be determined. *Gruber et al.* [1996] described two techniques for estimating these values on density surfaces. For deeper density surfaces one can assume that the waters far away from the outcrop region are free from anthropogenic CO_2. The mean ΔC^* values in these regions therefore reflect only the disequilibrium value. For shallower surfaces the air-sea disequilibrium can be inferred from the ΔC^*_t tracer.

ΔC^*_t is the difference between C* and the concentration the waters would have in equilibrium with the atmosphere at the time they were last at the surface. The time since the waters were in contact with the surface is estimated from CFC-12 age (τ) and the atmospheric CO_2 concentration history as a function of time ($fCO_2\{t_{sample}-\tau\}$). The atmospheric CO_2 time history from 1750 through 1996 was determined from a spline fit to ice core and measured atmospheric values [*Neftel et al.*, 1994; *Keeling and Whorf*, 1996]. The CFC-12-based ages were determined following the technique described by *Warner et al.* [1996]. The apparent age of the water is determined by matching the CFC-12 partial pressure ($pCFC\text{-}12$) of the waters with the atmospheric CFC-12 concentration history (procedures and atmospheric time history provided by J. Bullister). Although CFCs do not give a perfect representation of the true calendar age of the waters, *Doney et al.* [1997] have shown that the CFC-12 and ^3H-^3He ages in the North Atlantic agree within 1.7 years for ages less than 30 years. *Gruber* [1998] successfully used both CFC and ^3H-^3He ages for his disequilibrium calculations in the Atlantic and has thoroughly discussed the assumptions and caveats associated with these techniques. The disequilibrium values on shallow density surfaces presented here were calculated using CFC-12 ages modified from the ΔC^*_t equation of *Gruber* [1998] to include the denitrification correction:

$$\Delta C^*_t = TCO_2^{(meas)} - TCO_2^{(S,\,T,\,Alk^0,\,fCO_2\{t_{sample}-\tau\})} - \frac{117}{-170}(O_2 - O_2^{(sat)}) - \frac{1}{2}(TA - Alk^0 + \frac{16}{-170}(O_2 - O_2^{(sat)})) - \frac{106}{-104}N^* \quad (5)$$

where $TCO_2^{(S,\,T,\,Alk^0,\,fCO_2\{t_{sample}-\tau\})}$ is the TCO_2 the waters would have at the surface with a TA value of Alk^0 and an fCO_2 value in equilibrium with the atmospheric CO_2 concentration at the time the waters were last at the surface (date of sample collection minus CFC age).

The CFC age method was used for waters with densities less than $\sigma_\theta = 27.25$ and CFC-12 ages less than 40 years. The anthropogenic CO_2 of the waters with pressures less than 150 dbars or densities less than $\sigma_\theta = 25.95$ was determined by subtracting the ΔC^*_t value estimated at each sample location from the corresponding ΔC^* value. Given that the Indian Ocean does not extend into the high northern latitudes, the major outcrop region for Indian Ocean waters below the mixed layer is toward the south. Although other tracers might be used to identify multiple end-members, the CFC-12 ages on each density surface get steadily older toward the north, and the ΔC^*_t values are reasonably constant (see diamonds in Figure 6). This suggests that most of the water in the Indian Ocean is derived from the south or, at least in terms of the air-sea disequilibria, cannot be distinguished from other sources. The ΔC_{dis} term for the main Indian Ocean basin therefore was determined from a mean ΔC^*_t value on each surface. The mean ΔC_{dis} terms were then subtracted from the individual ΔC^* values to determine the anthropogenic component. Table 2 summarizes the ΔC_{dis} values for the density surfaces estimated exclusively from the ΔC^*_t method.

One major exception to the southern source waters is observed in the Arabian Sea. Although none of the surfaces with σ_θ values greater than 26.0 outcrop in the Arabian Sea, a number of higher-density surfaces do outcrop in the Red Sea and Persian Gulf. These outcrops could provide pathways for the introduction of CFCs and anthropogenic CO_2 into the northern Arabian Sea and could reset the disequilibria term. *Wyrtki* [1973] noted that the Red Sea and Persian Gulf waters mix in the Arabian Sea to form the high-salinity North Indian Intermediate Water (NIIW). The ΔC^*_t values in the Arabian Sea do vary significantly and generally have a strong correlation with salinity. The CFC-12 ages also begin to get younger toward the northern end of the Arabian Sea. These high-salinity waters appear to have a higher disequilibria term than the lower-salinity waters that make up the majority of the Indian Ocean intermediate waters.

To account for this phenomenon, the Arabian Sea waters (north of 5°N and west of 78°E) were isolated, and the ΔC^*_t values were fit against salinity with a linear regression. Thus this region was treated as a two-end-member mixing scenario between the high-salinity NIIW and the lower-salinity waters of the main Indian Ocean basin. The ΔC_{dis} values in this region were determined based on the relative contributions of the two end-members using salinity as a conservative tracer. The coefficients for the Arabian Sea fits are given in Table 2. The difference between the high-salinity and lower-salinity disequilibria generally decreased as densities increased (note decreasing slope values in Table 2) to the point where the Arabian Sea disequilibria values were no longer distinguishable from the main Indian Ocean basin values. The additional terms were dropped for surfaces where the two end-member mixing terms resulted in values within the error of the basin-wide mean (Table 2).

As stated previously, the disequilibria term for the deeper, CFC free surfaces was determined directly from the mean ΔC^* value of each density interval. Careful examination of the extent of CFC penetration along the density surface was used to limit data used in

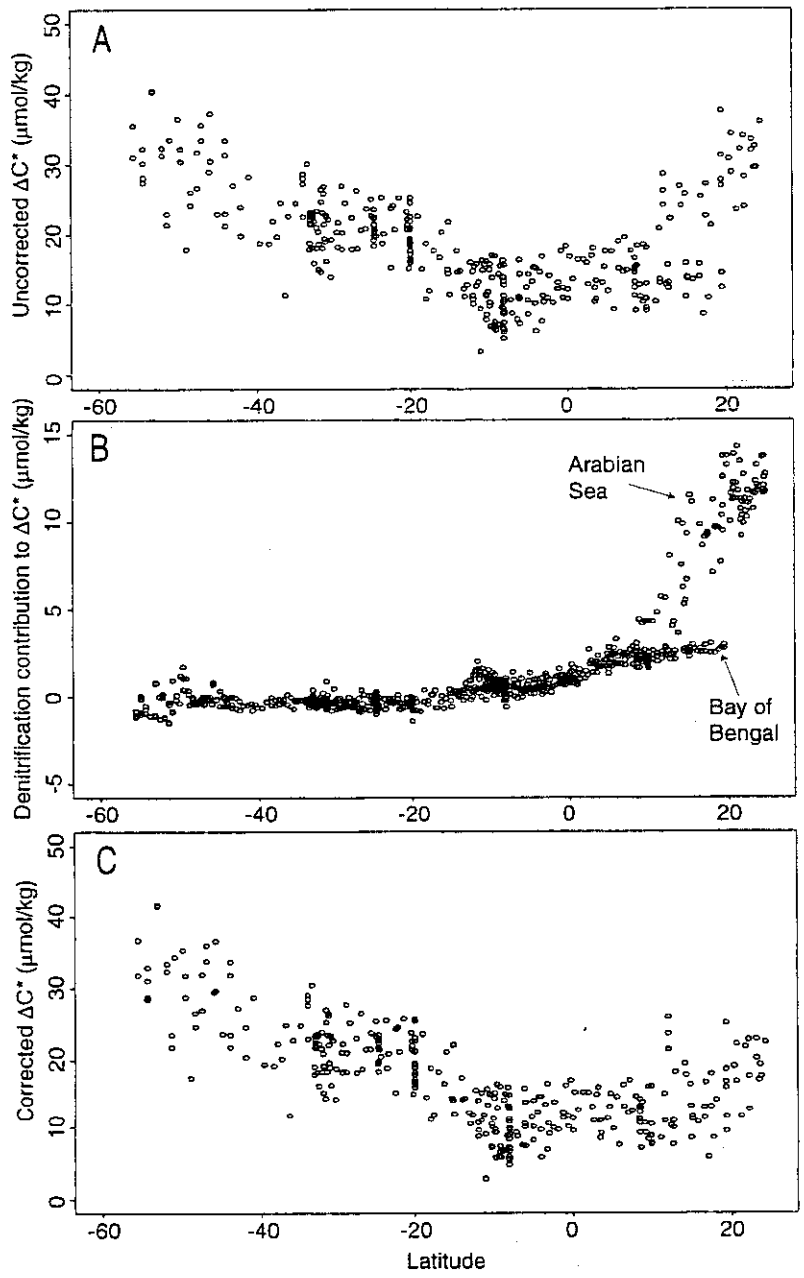

Figure 5. ΔC* values for data on the 26.9 - 27.0 σ_θ surface: (a) calculated without denitrification, (b) denitrification signal put in terms of ΔC*, (c) with denitrification correction (i.e., data in Figure 5a minus the data in Figure 5b).

determining the ΔC_{dis} term. Only regions where CFC concentrations were below a reasonable blank (0.005 pmol kg^{-1}) were considered. The ΔC_{dis} values determined using this method are summarized in the lower half of Table 3 ($\sigma_\theta > 27.5$).

Determination of the ΔC_{dis} values for either shallow or deep surfaces is relatively straightforward using the techniques mentioned above. It is not straightforward, however, to estimate the ΔC_{dis} values for intermediate levels where the CFC ages are relatively old and may be significantly influenced by mixing and yet the waters could have enough anthropogenic CO_2 to influence the estimates based on ΔC*. The effect of using the ΔC* technique in waters that actually have anthropogenic CO_2 would be to overestimate the ΔC_{dis} term and thus underestimate the anthropogenic CO_2. The effect of mixing on the CFC ages, however, generally results in an underestimation of the CFC age which would lead to an underestimation of the ΔC_{dis} term and an overestimation of the anthropogenic CO_2. The CFC age technique has additional problems in waters with σ_θ values greater than 27.25, because the waters with the younger ages are all found in the very high latitudes of the Southern Ocean and generally are not directly venti-

Table 2. Values of ΔC_{dis} Determined on Potential Density (σ_θ) Intervals

Potential Density Range	Main Basin Mean (SDM)	Main Basin Number of Points	Arabian Intercept (SD)	Arabian Slope (SD)	Arabian Number of Points
25.95-26.05	-1.3 (±0.88)	56	-740 (±92)	21.3 (±3)	12
26.05-26.15	-0.7 (±1.21)	42	-745 (±130)	21.4 (±4)	12
26.15-26.25	-3.4 (±0.65)	63	-699 (±76)	20.0 (±2)	11
26.25-26.35	-4.8 (±0.62)	61	-516 (±90)	14.8 (±3)	12
26.35-26.45	-5.6 (±0.48)	83	-316 (±84)	9.1 (±2)	20
26.45-26.55	-7.1 (±0.34)	103	-558 (±87)	15.9 (±2)	21
26.55-26.65	-7.2 (±0.32)	123	-512 (±53)	14.5 (±1)	28
26.65-26.75	-8.9 (±0.27)	152	-397 (±52)	11.2 (±1)	34
26.75-26.85	-9.1 (±0.23)	254	-428 (±66)	12.0 (±2)	28
26.85-26.95	-11.2 (±0.31)	209	-285 (±115)	7.9 (±3)	6
26.95-27.00	-12.2 (±0.35)	104	-	-	-
27.00-27.05	-13.8 (±0.48)	92	-	-	-
27.05-27.10	-15.2 (±0.40)	90	-	-	-
27.10-27.15	-16.3 (±0.47)	84	-	-	-
27.15-27.20	-17.1 (±0.51)	89	-	-	-
27.20-27.25	-19.5 (±0.56)	74	-	-	-

Standard deviations (SD) are given for the slope and intercept terms for the Arabian Sea data. Standard deviation of the mean (SDM, i.e., standard deviation weighted by the number of individual determinations) is given for each main basin estimate. Values of ΔC_{dis} are given in μmol kg^{-1}. Dashes indicate value not determined.

lated in these regions. Therefore the basic assumption that the ΔC_{dis} term can be determined by following the density level to its outcrop and examining the younger waters there is not valid.

As a general rule, the errors associated with the CFC age technique increase at higher density levels, and the errors associated with the ΔC^* technique decrease at higher density levels. To minimize the errors in the final ΔC_{dis} determination, waters with σ_θ values between 27.25 and 27.5 were evaluated using a combination of the two methods mentioned above. The 27.25 cut in the CFC age technique was chosen because this density corresponds

Table 3. Values of ΔC_{dis} Determined on Potential Density (σ_θ) Intervals

Potential Density Range	Mean ΔC^* (SDM)	Number of Points	Mean ΔC^*_t (SDM)	Number of Points	Final Mean ΔC_{dis} (SDM)
27.25-27.30	-2.3 (±0.45)	42	-19.7 (±0.98)	22	-8.3 (±1.13)
27.30-27.35	-4.0 (±0.49)	45	-21.0 (±0.84)	19	-9.1 (±1.06)
27.35-27.40	-5.3 (±0.44)	72	-22.5 (±1.25)	7	-6.8 (±0.69)
27.40-27.45	-7.1 (±0.26)	92	-23.5 (±0.83)	10	-8.7 (±0.54)
27.45-27.50	-7.9 (±0.30)	98	-25.0 (±1.65)	7	-9.0 (±0.51)
27.50-27.55	-9.3 (±0.28)	93	-	-	-9.3 (±0.28)
27.55-27.60	-10.7 (±0.28)	92	-	-	-10.7 (±0.28)
27.60-27.65	-11.3 (±0.34)	125	-	-	-11.3 (±0.34)
27.65-27.70	-13.0 (±0.36)	127	-	-	-13.0 (±0.36)
27.70-27.75	-14.8 (±0.30)	184	-	-	-14.8 (±0.30)
27.75-27.80	-15.3 (±0.24)	349	-	-	-15.3 (±0.24)
>27.80	-18.6 (±0.15)	629	-	-	-18.6 (±0.15)

Standard deviation of the mean given in brackets (SDM, i.e., standard deviation weighted by the number of individual determinations). Values of ΔC_{dis} are given in μmol kg^{-1}. Dashes indicate value not determined.

with the core of the Antarctic Intermediate water and also generally the highest-density water that outcrops in this region [*Wyrtki*, 1973; *Levitus and Boyer*, 1994; *Levitus et al.*, 1994]. To help ensure that the ΔC_{dis} values were determined on waters moving into the main Indian Ocean basin, mean ΔC^*_t values were only estimated from samples north of 35°S with CFC-12 ages less than 40 years. Mean ΔC^* values were also determined on the same density surfaces for samples where CFCs were measured, but concentrations were below 0.005 pmol kg^{-1}. The final mean value used for the ΔC_{dis} correction on each surface was determined from the mean of the combined individual estimates from each method (Table 3).

Examination of the individual and combined means in Table 3 indicates that there is a sizeable spread in the estimates from the two techniques in the overlap region. This difference is maximized since these density levels are pushing the limits of both techniques, and the errors in both estimates serve to increase this difference. Since the number of points available from the CFC age technique generally decreased at greater density levels and the number of points from the ΔC^* technique generally increased at greater density levels, the mean becomes progressively more heavily weighted toward the ΔC^* technique as the density levels increased. Although this is not the ideal solution, we believe that this minimizes the potential errors as much as possible. The technique used to estimate final ΔC_{dis} values in this region could systematically bias the anthropogenic CO_2 inventory estimates. The magnitude of this potential error on the final inventory was estimated to be approximately ±1.8 Pg C by integrating the difference between the two methods over the effected water volume. This estimate represents a maximum potential error since the known limitations of each method work to increase the differences in ΔC_{dis}.

2.3.4. Time adjustment for INDIGO data. One difficulty with combining data from different cruises for a time-dependent calculation like the anthropogenic CO_2 inventory is the issue of getting the data sets referenced to a common time. One of the advantages of the WOCE/JGOFS Indian Ocean survey data is the fact that all of the samples were collected in a little over a year's time. In terms of the CO_2 inventory this is essentially a synoptic data set. The couple of years between the CIVA1 cruise and the WOCE/JGOFS data are also not distinguishable in terms of the anthropogenic increase. The INDIGO data, however, were collected 8-10 years before the WOCE/JGOFS data set and must be adjusted to reflect the anthropogenic uptake during that time. Unfortunately, any correction of this sort can have large errors and potentially bias the results. This problem must be weighed against the errors of ignoring the time difference between cruises or omitting these data entirely. The decision to correct the INDIGO data was based on two factors. First, analysis of the change in anthropogenic inventory between GEOSECS and WOCE (discussed below) indicated that a significant fraction of the total anthropogenic uptake has occurred in the past 2 decades. Second, careful examination of objective maps of anthropogenic CO_2 made prior to the INDIGO correction showed obvious, anomalously low concentrations in the regions strongly dependent on the INDIGO data. Two different adjustment functions were made depending on whether the stations were located in the main Indian Ocean basin or in the Southern Ocean.

North of 30°S, where portions of the INDIGO data were located relatively near WOCE stations, a crossover comparison of the INDIGO anthropogenic CO_2 concentrations as a function of density was made with the WOCE/JGOFS data in that region. The difference between the two data sets was evaluated at σ_θ intervals of 0.05 from the surface to σ_θ = 27.5 and added to the INDIGO data. This correction ranged from approximately 12 μmol kg^{-1} at the surface down to zero at 27.5.

South of 30°S, there were very few WOCE or CIVA1 stations close enough for a proper crossover comparison. It was clear from the northern data, however, that some correction was necessary. Given that the isolines for most properties in the Southern Ocean run east-west, we decided to correct the southern INDIGO data based on a crossover comparison with all results from CIVA1 and WOCE cruises in that region. The average adjustment for the southern stations was approximately 11 μmol kg^{-1} over the same density range. The magnitude of the corrections in both regions is consistent with the expected increase over the time period between cruises.

2.3.5. Evaluation of Errors. Error evaluation is much more difficult for the ΔC^* method than for the time series approach because of potential systematic errors associated with some of the parameters (i.e., the biological correction). The random errors associated with the anthropogenic CO_2 can be determined by propagating through the precision of the various measurements required for the calculation of (4).

$$\begin{aligned}\{\sigma_{C_{anth}}\}^2 = {} & \{\sigma_C\}^2 + \{-\sigma_{C_{eq}}\}^2 \\ & + \{(-R_{CO} - 0.5R_{NO})\sigma_{O_2}\}^2 \\ & + \{(R_{CO} + 0.5R_{NO})\sigma_{O_{2[sat]}}\}^2 \\ & + \{-0.5\sigma_{TA}\}^2 + \left\{\left(-\frac{\partial C_{eq}}{\partial TA} + 0.5\right)\sigma_{Alk^0}\right\}^2 \\ & + \{0.8667\sigma_N\}^2 + \{13.867\sigma_P\}^2 \\ & + \left\{0.8667\left(-P - \frac{N - 16P + 2.9}{120}\right)\sigma_{R_{N:P[nitr]}}\right\}^2 \\ & + \{-0.00111(N - 16P + 2.9)\sigma_{R_{N:P[denitr]}}\}^2 \\ & - \{\sigma_{\Delta C_{dis}}\}^2 \end{aligned} \quad (6)$$

where σ_C = 2 μmol kg^{-1}; $\sigma_{C_{eq}}$ = 4 μmol kg^{-1}; σ_{O_2} = 1 μmol kg^{-1}; $\sigma_{O_{2[sat]}}$ = 4 μmol kg^{-1}; σ_{TA} = 4 μmol kg^{-1}; $\frac{\partial C_{eq}}{\partial TA}$ = 0.842; σ_{Alk^0} = 7.8 μmol kg^{-1}; σ_N = 0.2 μmol kg^{-1}; σ_P = 0.02 μmol kg^{-1}; $\sigma_{R_{N:P[nitr]}}$ = 0.25; and $\sigma_{R_{N:P[denitr]}}$ = 15. The equation for the random error analysis is adapted from *Gruber et al.* [1996] (excluding those terms that involve the C:O Redfield error) with additional terms for the error propagation of the N* correction [*Gruber and Sarmiento*, 1997]. The terms involving the C:O are evaluated separately below because the random errors cannot be isolated from potential systematic errors. The sigma values used in (6) were either taken from the appropriate WOCE cruise reports or from previously determined estimates of *Gruber et al.* [1996] and *Gruber and*

Sarmiento [1997]. The error in the ΔC_{dis} term is taken from the average value for the standard deviation of the mean for the examined surfaces ($\sigma_{\Delta C_{dis}}$ = 0.5 μmol kg^{-1}). The formulation given in (6) results in an estimated error of 6.1 μmol kg^{-1}. This estimate is larger than the standard deviation of the ΔC* values below the deepest anthropogenic CO_2 penetration depth (±2.8 μmol kg^{-1} for pressure > 2000 dbars) suggesting that the propagated errors may be a maximum estimate of the random variability.

The potential systematic errors associated with the anthropogenic CO_2 calculation are much more difficult to evaluate. The random error estimate above includes all terms except those associated with the C:O biological correction. Although other terms involving N:O and N:P corrections potentially have systematic offsets associated with errors in the ratio estimates, the only potentially significant errors involve the C:O corrections [*Gruber et al.*, 1996; *Gruber*, 1998].

There is evidence, however, that the *Anderson and Sarmiento* [1994] stoichiometric ratios must be reasonably close to the actual remineralization ratios observed in the Indian Ocean. Figure 6 is a plot of ΔC^*_t based on CFC-12 ages for the density interval from σ_θ = 27.1 to σ_θ = 27.15. The diamonds are the values calculated from (5). These values represent the preserved air-sea disequilibrium value for the past 40 years and should be constant if the air-sea disequilibrium has not changed over time (i.e., that the surface ocean CO_2 is increasing at the same rate at the atmosphere). A linear regression of the diamonds in Figure 6 yields a slope that is not significantly different from zero. The circles and pluses are the ΔC^*_t values one would get by using a C:O ratio of -0.60 and -0.78 in (5), respectively. These C:O values represent one standard deviation from the *Anderson and Sarmiento* [1994] mean value of -0.69. The -0.60 ratio results in values with a significant positive slope. This slope would imply that the surface ocean CO_2 is increasing much slower than the atmospheric increase. While this is possible, the -0.60 ratio is much larger than historical Redfield estimates and would be very difficult to justify. The -0.78 ratio is more typical of historical estimates but results in a significant negative slope in the ΔC^*_t values with time. A negative slope would imply that carbon is accumulating in the ocean faster than the atmosphere. Neither of these scenarios seems very likely. The fact that none of the ΔC^*_t values on the examined surfaces exhibit a statistically significant slope suggests that the C:O value of -0.69 does accurately represent the remineralization ratio for these waters and supports the methodology of taking a mean value of ΔC^*_t on these density surfaces.

A sensitivity study was also used to evaluate the potential error associated with an incorrect C:O value. Two additional estimates of anthropogenic CO_2 were determined using the -0.60 and -0.78

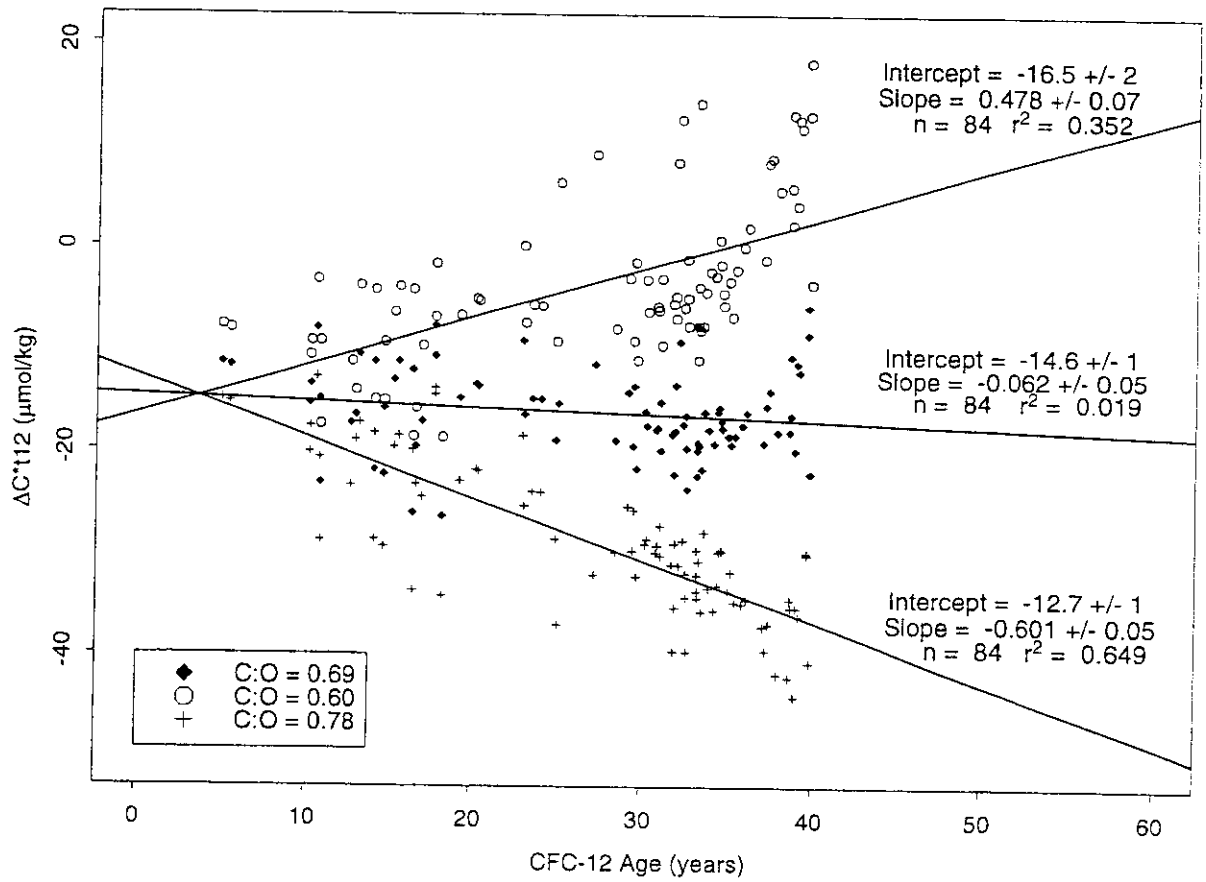

Figure 6. Plot of ΔC^*_t based on CFC-12 ages for the density interval from σ_θ = 27.1 to 27.15 versus CFC-12 age. The diamonds were calculated using the *Anderson and Sarmiento* [1994] C:O (-0.69). The circles and pluses were calculated from C:O of -0.60 and -0.78, respectively. Lines and text give results from a linear regression of the three sets of data.

C:O values. Since the C:O correction applies to both ΔC^* and the ΔC^*_t terms, the disequilibrium values were reevaluated in the same manner as described above. The range of anthropogenic values from these three estimates varied as a function of apparent oxygen utilization (AOU) from 0.0 to 22 with an average difference of only 4.2 μmol kg^{-1}. Because the C:O correction affects both the ΔC^* and ΔC^*_t terms together, much of the systematic error in the final anthropogenic estimate (ΔC^*-ΔC^*_t) cancels out.

2.4. Inventory Estimates

Basin-wide anthropogenic and excess CO_2 concentrations (WOCE/JGOFS - GEOSECS) were evaluated on a 1° grid at 100 m intervals between the surface and 2600 m using the objective mapping techniques of *Sarmiento et al.* [1982]. Total anthropogenic CO_2 was mapped over an area from 20° to 120°E and 70°S to 30°N (excluding areas of land, the Red Sea, the Persian Gulf, and the South China Sea). Because the WOCE/JGOFS data set did not cover much of the Southern Ocean, the excess CO_2 maps were limited to the area north of 35°S. The values at each level were multiplied by the volume of water in the 100 m slab and summed to generate the total anthropogenic or excess CO_2 inventory. The method of integrating mapped surfaces compared very well with the technique of vertically integrating each station and mapping the station integrals.

It is extremely difficult to evaluate a reasonable estimate of the potential errors associated with the inventory estimates. A simple propagation of errors implies that the random errors associated with any individual anthropogenic estimate is approximately ±6.1 μmol kg^{-1}, but these errors should essentially cancel out for an integrated inventory based on nearly 25,000 individual estimates. Systematic errors have by far the largest impact on the inventory estimates. Potential errors as large as ±1.8 Pg C have been estimated for the ΔC_{dis} term. Sensitivity studies with the C:O variations give a range of total inventory estimates of ±2.5 Pg C. Other systematic errors could also be generated from the denitrification term, the terms involving N:O, the time correction for the INDIGO data, and the mapping routines used in the inventory estimates. The magnitude of these errors is believed to be much smaller than the uncertainty in either the C:O correction or the ΔC_{dis} determination. Propagation of the two estimated uncertainties gives an overall error of approximately ±3 Pg C for the total inventory. An error of roughly 15% is comparable to previous error estimates using this technique [*Gruber et al.*, 1996; *Gruber*, 1998]. Errors for regional inventories are assumed to scale to the total.

3. Results and Discussion

The excess CO_2 concentrations for the Indian Ocean range from 0 to 25 μmol kg^{-1}. The most prominent feature in the excess CO_2 distribution, as shown with representative sections in the eastern and western Indian Ocean (Figure 7), is the maximum in concentrations at midlatitudes (~ 40°S). This maximum is coincident with the relatively strong gradient in surface density associated with the Subtropical Convergence and the transition from the high-salinity subtropical gyre waters to the low-salinity Antarctic waters. The outcropping of these density surfaces and subsequent sinking of surface waters provides a pathway for excess CO_2 to enter the interior of the ocean. Relatively high excess CO_2 concentrations can also be observed at the very northern end of the western section (Figure 7a). Although not readily evident from this section, the distribution of concentration gradients indicates that excess CO_2 is entering the northern Indian Ocean from the Persian Gulf and Red Sea regions. This is likely to result from the outcropping of density surfaces in these areas which are not ventilated in the main Indian Ocean basin. The implied Red Sea and Persian Gulf sources of CO_2 are consistent with uptake estimates of anthropogenic CO_2 in these areas as observed by *Papaud and Poisson* [1986]. The third major feature observed in the excess CO_2 distribution is a dramatic shoaling of the excess CO_2 isolines south of approximately 40°S. *Poisson and Chen* [1987] attributed the low anthropogenic CO_2 concentrations in Antarctic Bottom Water to a combination of the pack sea ice blocking air-sea gas exchange and the upwelling of old Weddell Deep Water. This explanation is consistent with the observed excess CO_2 distributions in this study.

The general features observed with excess CO_2 are also observed in the anthropogenic CO_2 distribution (Figure 8). The range of values, however, extends up to 55 μmol kg^{-1}. The maximum depth of the 5 μmol kg^{-1} contour is approximately 1300 m at around 40°S, only 200 m deeper than the maximum depth of the 5 μmol kg^{-1} contour of excess CO_2. The similarity in maximum penetration depth between the 200 year and the 18 year anthropogenic CO_2 accumulation, together with the wide range of depths covered by the 5 μmol kg^{-1} isoline, indicates that the primary pathway for CO_2 to enter the ocean's interior is from movement along isopycnals, not simple diffusion or cross isopycnal mixing from the surface. The 1300 m penetration results from the downwarping of the isopycnals in the region of the Subtropical Convergence. Likewise, the low anthropogenic CO_2 concentrations in the high-latitude Southern Ocean result from the compression and shoaling of isopycnal surfaces in that region. Although the complex oceanography of the Southern Ocean may call into question some of the assumptions regarding mixing and nutrient uptake ratios with these techniques, both the time series excess CO_2 and the ΔC^* anthropogenic CO_2 calculations clearly indicate that the anthropogenic CO_2 concentrations south of approximately 50°S are relatively small.

The distribution of anthropogenic CO_2 determined in this study is similar to the distribution presented by *Chen and Chen* [1989] based on GEOSECS and INDIGO data. Although the penetration depth at 40°S was slightly deeper than observed with this study (1400-1600 m for the 5 μmol kg^{-1} isoline), Chen and Chen also observed a significant shoaling of the anthropogenic CO_2 isolines toward the south. They suggest that anthropogenic CO_2 has only penetrated a few hundred meters into the high-latitude (>50°S) Southern Ocean.

There has been debate in the literature over recent years as to the importance of the Southern Ocean as a sink for anthropogenic CO_2 [e.g., *Sarmiento and Sundquist*, 1992; *Keeling et al.*, 1989; *Tans et al.*, 1990]. Most of the recent data-based estimates, however, indicate a relatively small Southern Ocean sink [*Poisson and Chen*, 1987; *Murphy et al.*, 1991; *Gruber*, 1998; this study]. The lack of observed anthropogenic CO_2 in the Southern Ocean is also qualitatively consistent with $\Delta^{14}C$ estimates which show no measurable storage of bomb ^{14}C in the Southern Ocean since GEOSECS [*Leboucher et al.*, 1998; R. Key, unpublished data, 1998]. Recent studies by *Bullister et al.* [1998], which show evidence of deep CFC penetration in the Southern Ocean, may appear to contradict these low anthropogenic CO_2 estimates, but we believe it is further evidence that one must be careful when inferring anthropogenic carbon distributions from other tracers. One possible explanation of this apparent discrepancy may be the CFC equilibration

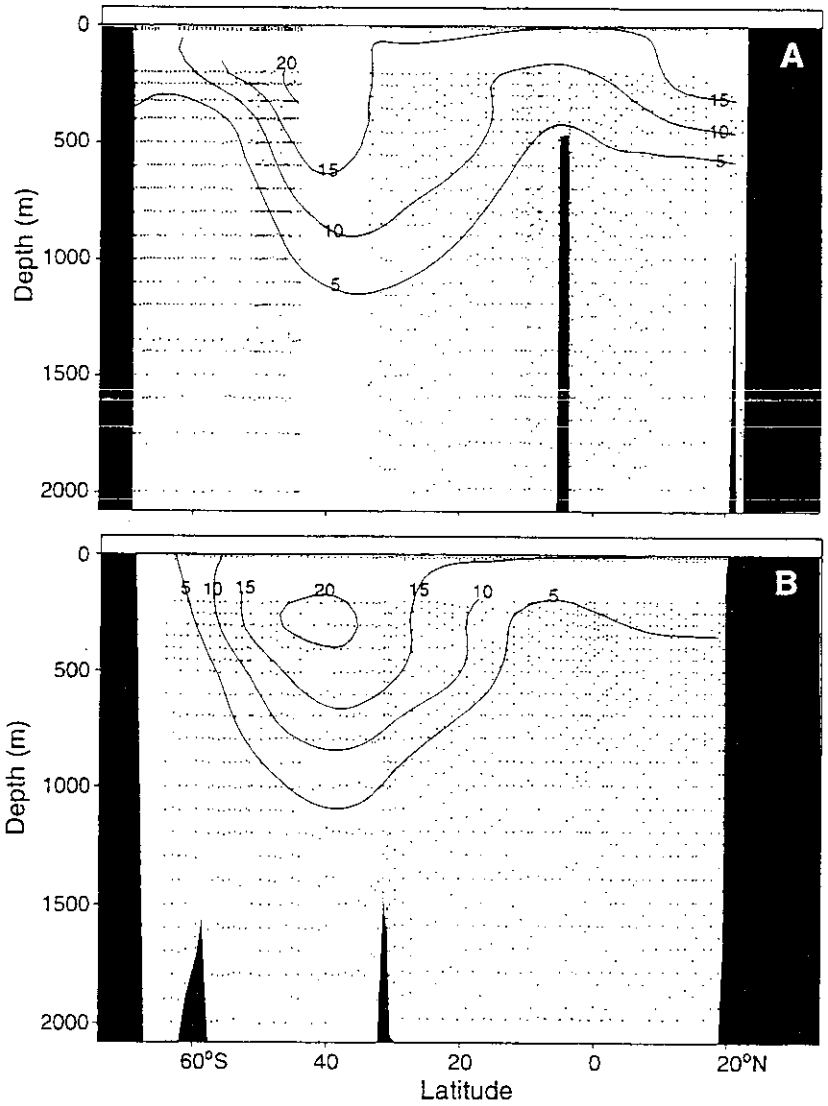

Figure 7. Sections of excess CO_2 along (a) ~57°E and (b) ~92°E. Dots indicate sample locations used in sections. Note that I6S data along 30°E were brought into the line of section for contours south of 40°S in Figure 7a.

rate of days which is significantly faster than the CO_2 equilibration time of months [e.g., *England*, 1995; *Warner and Weiss*, 1985; *Tans et al.*, 1990]. This can become an issue in the Southern Ocean where upwelling and convection may allow the CFCs to equilibrate to a greater extent than the CO_2. Again, we acknowledge the limitations of the methods used in the Southern Ocean, and it is possible that the apparent discrepancy in the CFC penetration versus the CO_2 penetration may also be an issue of detection limits. With a detection limit that is approximately 6 μmol kg^{-1}, it is not possible to say with this technique that the concentration of anthropogenic CO_2 below 500 m at 60°S is zero. However, we can say with some confidence that the concentration is not 10 μmol kg^{-1} or greater. Since there is no natural oceanic source of CFCs and these compounds are not biologically utilized, the ability to detect them is much greater. If mixing has diluted the anthropogenic signal to concentrations just below detection limits, it is possible that carbon measurement based techniques would underestimate the Southern Ocean sink.

The total anthropogenic CO_2 inventory for the main Indian Ocean basin (north of 35°S) was 13.6±2 Pg C in 1995. The increase in CO_2 inventory since GEOSECS was 4.1±1 Pg C for the same area. This represents a nearly 30% increase in the past 18 years relative to the total accumulation since preindustrial times. The relative oceanic increase is very similar to the 31% increase observed in atmospheric concentrations over the same time period [*Keeling and Whorf*, 1996]. This similarity suggests that the oceans, at least for now, are keeping pace with the rise in atmospheric CO_2. Approximately 6.7±1 Pg C are stored in the Indian sector of the Southern Ocean giving a total Indian Ocean inventory (between 20° and 120°E) of 20.3±3 Pg C in 1995.

To put these results in a global perspective, the total inventory for the Indian Ocean is only half that of the Atlantic (40±6 Pg C [*Gruber*, 1998]), but it contains an ocean volume that is nearly 80% of the Atlantic. The main difference between the two oceans, of course, is that the Indian Ocean does not have the high northern latitude sink that the Atlantic has. The big unknown at this point is

the anthropogenic inventory of the Pacific. With nearly 50% of the total ocean volume the Pacific has the potential to be the largest oceanic reservoir for anthropogenic CO_2.

4. Comparison With Princeton Ocean Biogeochemistry Model

Current IPCC anthropogenic estimates are primarily based on global carbon models. Ultimately, these models are necessary to predict the oceanic response to future climate scenarios. It is important, however, to validate these models. One way to compare results is to examine profiles of the average anthropogenic concentrations such as those shown in Figure 9. The model presented here is the Princeton Ocean Biogeochemistry Model (OBM). The Princeton OBM is based on the circulation of *Toggweiler et al.* [1989] with explicit parameterization for the biological and solubility carbon pumps [*Sarmiento et al.*, 1995; *Murnane et al.*, 1998]. On this scale the model-based concentrations for both the total anthropogenic CO_2 and the increase since GEOSECS appear to be reasonably consistent with the data. The primary difference is slightly higher values at middepths in the data-based estimates. A more detailed examination, however, indicates that the regional distribution of the model-based estimates is significantly different than the data-based distribution. Figure 10 presents maps of the vertically integrated excess CO_2 normalized to a unit area. The model shows a consistent decrease in column inventory toward the north. The lowest inventories in the data-based map are in a narrow band just south of the equator. The highest values are found in the southeastern Indian Ocean. Relatively high values are also observed in the Arabian Sea in the regions near the Red Sea and the Persian Gulf. The small patch of lower values immediately outside the Gulf of Aden does not result from low concentrations but rather results from the shallow water depth associated with the mid-ocean ridge in that area. The low values east of there, however, do result from lower concentrations near the southern tip of India. The total model-based inventory for the region north of 35°S is approximately 0.61 times the data-based inventory (Table 4).

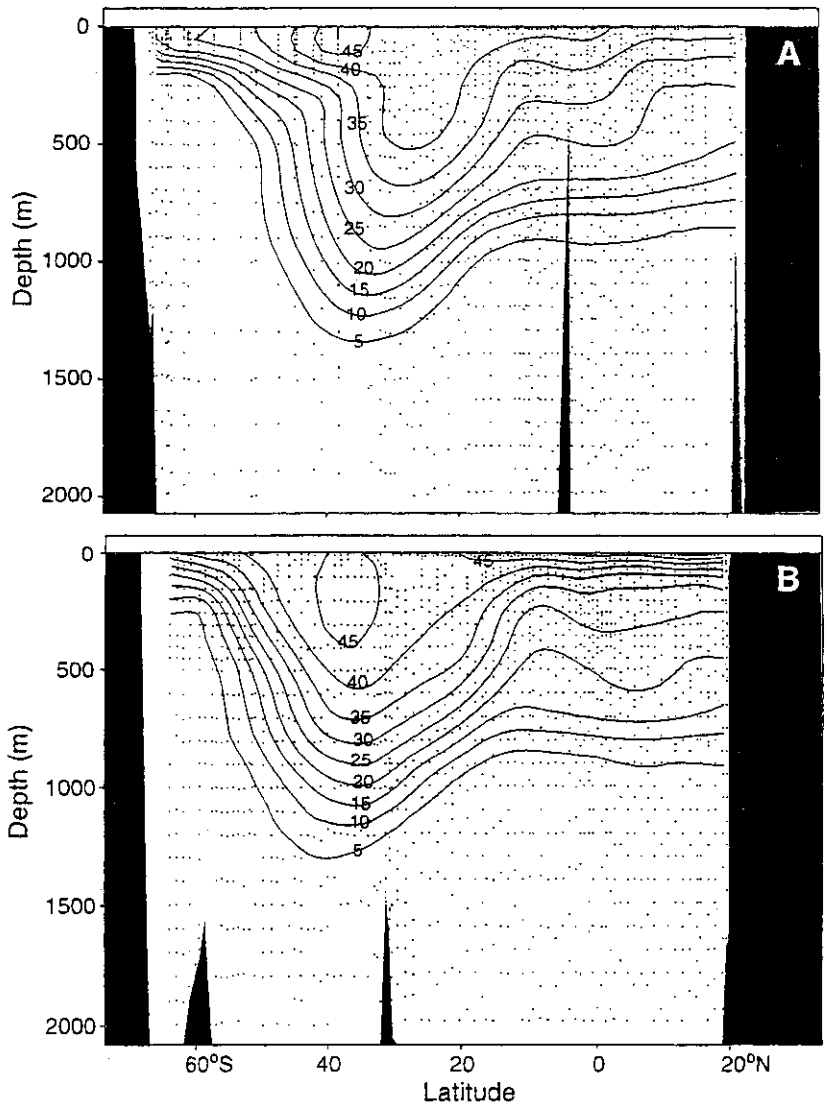

Figure 8. Sections of anthropogenic CO_2 along (a) ~57°E and (b) ~92°E. Dots indicate sample locations used in sections.

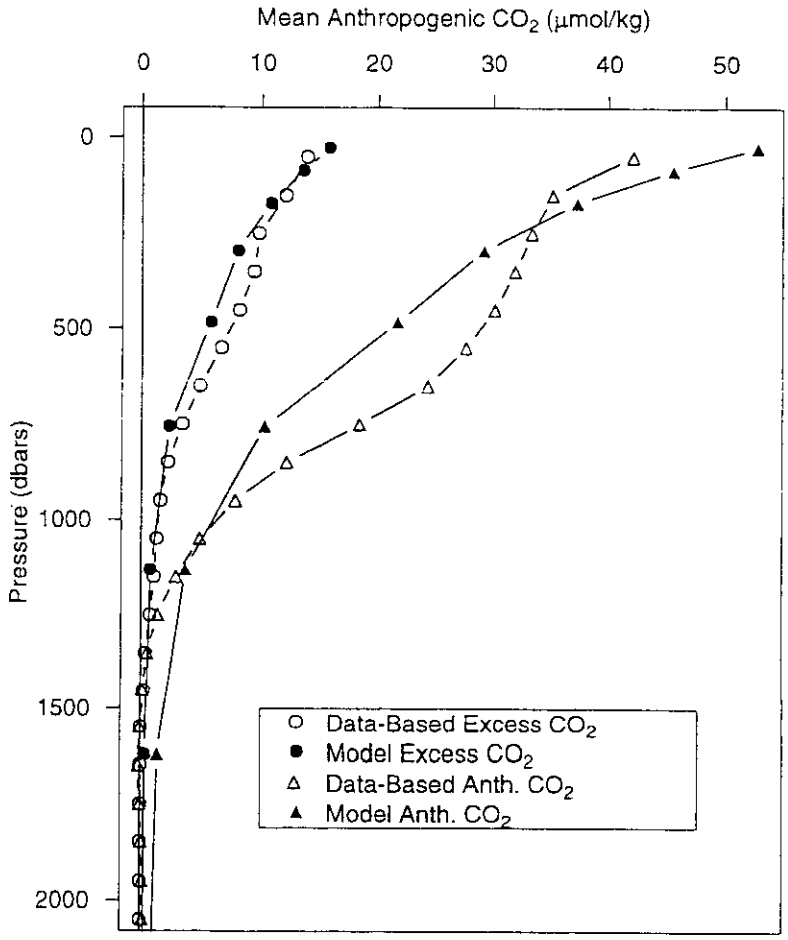

Figure 9. Profile of area weighted mean anthropogenic CO_2 concentrations for model (solid symbols) and data-based (open symbols) estimates for main Indian Ocean basin (north of 35°S). Circles show increase since GEOSECS (1978-1995). Triangles show total increase since preindustrial times.

Figure 11 shows maps of total anthropogenic CO_2 column inventory. As with the excess CO_2, the model predicts decreasing anthropogenic concentrations north of 35°S. The data-based distribution pattern is similar to the data-based excess CO_2 pattern with a minimum inventory band south of the equator and higher values toward the north and south. Similar to the findings with excess CO_2, the model-based anthropogenic inventory north of 35°S is approximately 0.68 times the data-based inventory (Table 4). The largest difference between the data-based results and the model is evident, however, in the Southern Ocean (south of 35°S). In this region the model anthropogenic inventory is nearly 2.6 times the data-based inventory (Table 4). The primary reason for this difference is the presence of a large convective cell in the model at approximately 55°S and 90°E in the Southern Ocean. This is a region of intense, unrealistic convection which pumps relatively high concentrations of anthropogenic CO_2 down in excess of 4000 m. This problem is a known shortcoming with the mixing scheme used in several GCMs [e.g., *England*, 1995] but has never before been quantified in terms of its direct effect on anthropogenic CO_2 storage by the models. It is beyond the scope of this paper to examine the details of the model physics; however, this same general trend of getting too much anthropogenic CO_2 into the Southern Ocean has been observed in comparisons with three other global carbon models with a range of mixing and advective schemes [C. Sabine, unpublished results, 1998]. This cursory comparison with the Princeton OBM clearly demonstrates the diagnostic usefulness of comparing the data distributions with models.

5. Conclusions

Although the general techniques proposed by *Gruber et al.* [1996] and *Wallace* [1995] can be important tools for estimating global anthropogenic CO_2, careful consideration must be used when applying these techniques to new regions. Complicating factors such as those found in the Arabian Sea can influence the quality of the estimates if not properly addressed. An additional term had to be added to the basic ΔC^* calculation to account for denitrification in the Arabian basin. For the excess CO_2 calculations a categorical variable was used to remove regional biases in the GEOSECS fit.

With the above mentioned modifications the anthropogenic inventory of the Indian Ocean was shown to be relatively small, approximately half of that found in the Atlantic. This study provides an important baseline for future studies of the Indian Ocean. The calculations presented here suggest that the oceanic increase in carbon storage (30%) has roughly kept pace with the atmo-

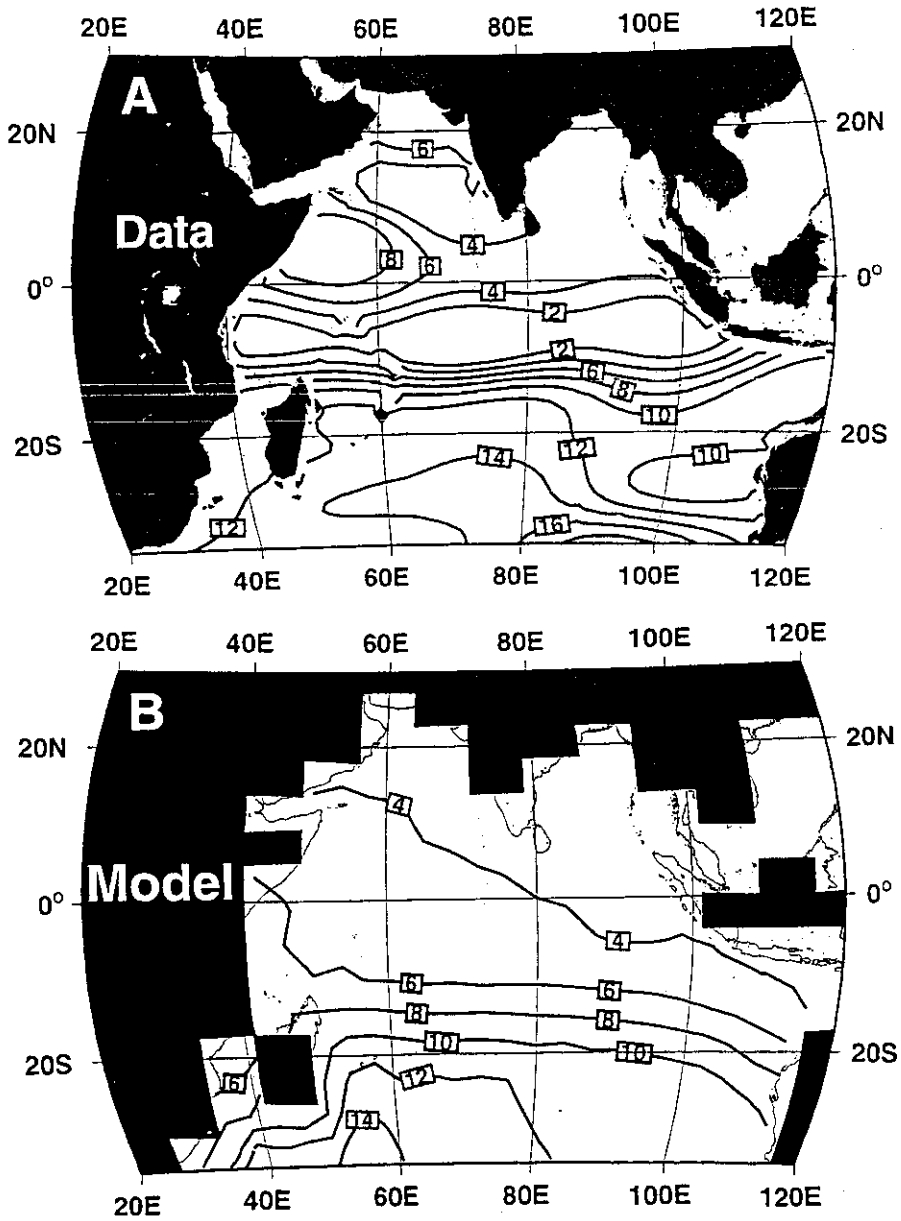

Figure 10. Maps of vertically integrated excess CO_2 based on (a) data and (b) model estimates. Contours are in mol m^{-2}. Solid regions indicate land mask used for inventory estimates. Thin lines in Figure 10b indicate land regions used in Figure 10a.

Table 4. Summary of Data Based and Model Based Inventory Estimates

	Total Anthropogenic CO_2,[α] Pg C	Southern Ocean Anthropogenic CO_2,[β] Pg C	Main Basin Anthropogenic CO_2,[χ] Pg C	Main Basin Excess CO_2,[χ] Pg C	Increase since GEOSECS, %
Data based	20.3±3	6.7±1	13.6±2	4.1±1	29.9
Model based	26.7	17.4	9.3	2.5	26.7

[α]Area between 20°-120°E.
[β]Latitude is < 35°S.
[χ]Latitude is > 35°S.

spheric increase (31%) over the past 18 years. Models predict that this trend is likely to change as atmospheric CO_2 concentrations continue to rise in the future [*Sarmiento et al.*, 1995]. As more CO_2 enters the ocean, the carbonate ion concentration will become depleted. This will decrease the buffering capacity of the ocean and its ability to continue carbon uptake at the current rate. Comparison of future survey cruises in the Indian Ocean with the anthropogenic and total carbon values from this study will allow us to document future changes in ocean chemistry and better understand the oceanic response to global change.

Finally, comparison of the spatial distribution of the anthropogenic carbon can be a powerful tool for understanding the carbon uptake of the models. The methods presented here provide a two-point calibration for examining the response of the models to

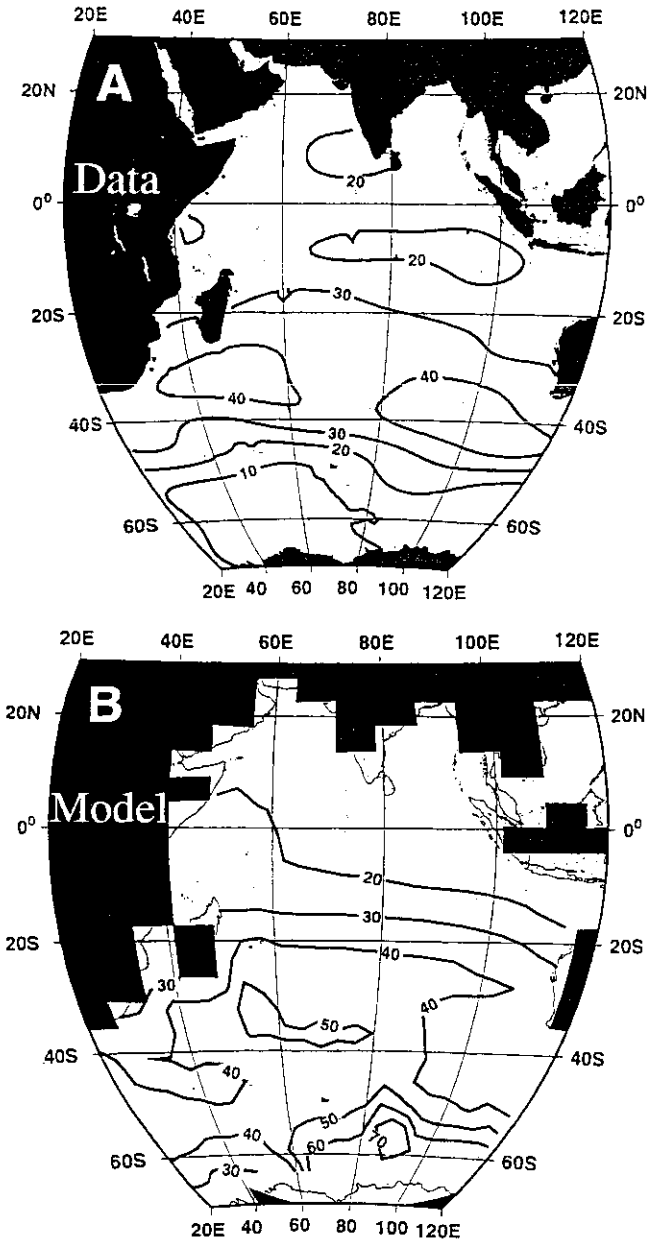

Figure 11. Maps of vertically integrated anthropogenic CO_2 based on (a) data and (b) model estimates. Contours are in mol m^{-2}. Solid regions indicate land mask used for inventory estimates. Thin lines in Figure 11b indicate land regions used in Figure 11a.

observed atmospheric CO_2 increases. The anthropogenic CO_2 data can also be subtracted from the TCO_2 measurements to provide an estimate of the preindustrial TCO_2 distribution. Comparing these estimates with the steady state model distributions can provide insight into whether differences in the model and data-based anthropogenic inventories result from problems with the uptake parameterization or the basic physics and initialization parameters of the model. This paper is just the first step in the interpretation of the WOCE/JGOFS data set. Subsequent papers will analyze additional cruise data as they become available. Together, these analyses will significantly improve our understanding of the global carbon cycle.

Acknowledgments. This work was accomplished with the cooperative efforts of the DOE CO_2 Science Team. We thank B. Warren for organizing the WOCE Indian Ocean expedition, the captain and crew of the R/V Knorr, and the WOCE-HP personnel at sea. We thank the chief scientists (M. McCartney, A. Gordon, L. Talley, W. Nowlin, J. Toole, D. Olson, J. Morrison, N. Bray, and G. Johnson) and the CFC PIs (J. Bullister, R. Fine, M. Warner, and R. Weiss) for giving us access to their preliminary data for use in this publication. We also thank N. Metzl, G. Eischeid, and C. Goyet for providing carbon data and T. Takahashi for providing S4I data and ΔpCO_2 maps. We thank R. Murnane and T. Hughes for providing model results. Strong collaboration, cooperation, and input from N. Gruber and investigators in the NOAA Ocean Atmosphere Carbon Exchange Study (R. Wanninkhof, R. Feely, J. Bullister, and T.-H. Peng) is also acknowledged along with the helpful comments of two anonymous reviewers. This work was primarily funded by DOE grant DE-FG02-93ER61540 with additional support by NSF/NOAA grant OCE-9120306.

References

Anderson, L., and D. Dyrssen, Alkalinity and total carbonate in the Arabian Sea: Carbonate depletion in the Red Sea and Persian Gulf, *Mar. Chem.*, *47*, 195-202, 1994.

Anderson, L.A., and J.L. Sarmiento, Redfield ratios of remineralization determined by nutrient data analysis, *Global Biogeochem. Cycles*, *8*, 65-80, 1994.

Brewer, P.G., A.L. Bradshaw, and R.T. Williams, Measurement of total carbon dioxide and alkalinity in the North Atlantic Ocean in 1981, in *The Changing Carbon Cycle: A Global Analysis*, edited by J.R. Trabalka and D.E. Reichle, pp. 348-370, Springer-Verlag, New York, 1986.

Brewer, P.G., D.M. Glover, C. Goyet, and D.K. Shafer, The *p*H of the North Atlantic Ocean: Improvements to the global model for sound absorption in seawater, *J. Geophys. Res.*, *100*, 8761-8776, 1995.

Brewer, P.G., C. Goyet, and G. Freiderich, Direct observation of the oceanic CO_2 increase revisited, *Proc. Natl. Acad. Sci. U. S. A.*, *94*, 8308-8313, 1997.

Broecker, W.S., 'NO', a conservative water-mass tracer, *Earth Planet. Sci. Lett.*, *23*, 100-107, 1974.

Broecker, W.S., T. Takahashi, H.J. Simpson, and T.-H. Peng, Fate of fossil fuel carbon dioxide and the global carbon budget, *Science*, *206*, 409-418, 1979.

Bullister, J.L., and R.F. Weiss, Determination of CCl_3F and CCl_2F_2 in seawater and air, *Deep Sea Res., Part A*, *35*, 839-853, 1988.

Bullister, J.L., D.P. Wisegrave, W.M. Smethie, and M.J. Warner, The appearance of CFCs and carbon tetrachloride in the abyssal waters of the Samoa Passage, *Eos, Trans. AGU*, *79*, 1998.

Chen, C.-T., Rates of calcium carbonate dissolution and organic carbon decomposition in the North Pacific Ocean, *J. Oceanogr. Soc. Jpn.*, *46*, 201-210, 1990.

Chen, C.-T., and R.M. Pytkowicz, On the total CO_2-titration alkalinity-oxygen system in the Pacific Ocean, *Nature*, *281*, 362-365, 1979.

Chen, D.W., and C.-T. Chen, The anthropogenic CO_2 signals in the Indian Ocean, *J. Environ. Prot. Soc. Repub. China*, *12* (2), 46-65, 1989.

Cleveland, W.S., and S.J. Devlin, Locally-weighted regression: An approach to regression analysis by local fitting, *JASA J. Am. Stat. Assoc.*, *83*, 596-610, 1988.

Cleveland, W.S., E. Grosse, and W.M. Shyu, Local regression models, in *Statistical Models in S*, edited by J.M. Chambers and T.J. Hastie, pp. 309-376, Wadsworth and Brooks, Pacific Grove, California, 1992.

Culberson, C.H., et al., A comparison of methods for the determination of dissolved oxygen in seawater, *WHPO Rep. 91-2*, World Ocean Circ. Exp. Hydrogr. Programme Off., Woods Hole, Massachusetts, 1991.

Dickson, A.G., The ocean carbon dioxide system: Planning for quality data, *US JGOFS News*, 2(2), 2, 1990.

Doney, S.C., W.J. Jenkins, and J. Bullister, A comparison of ocean tracer dating techniques on a meridional section in the eastern North Atlantic, *Deep-Sea Res., Part I*, *44*, 603-626, 1997.

Dueser, W.G., E.H. Ross, and Z.J. Mlodzinska, Evidence for and rate of denitrification in the Arabian Sea, *Deep Sea Res.*, *25*, 431-445, 1978.

Edmond, J.M., High precision determination of titration alkalinity and total carbon dioxide content of seawater by potentiometric titration, *Deep Sea Res.*, *17*, 737-750, 1970.

England, M.H., Using chlorofluorocarbons to assess ocean climate models, *Geophys. Res. Lett.*, *22*, 3051-3054, 1995.

Gordon, L.I., J.C. Jennings Jr., A.A. Ross, and J.M. Krest, A suggested protocol for continuous flow automated analysis of seawater nutrients in the WOCE Hydrographic Programme and the Joint Global Ocean Fluxes Study, *Grp. Tech. Rep. 92-1*, Coll. of Oceanogr., Oregon State Univ., Corvallis, 1992.

Gruber, N., Anthropogenic CO_2 in the Atlantic Ocean, *Global Biogeochem. Cycles*, *12*, 165-191, 1998.

Gruber, N., and J.L. Sarmiento, Global patterns of marine nitrogen fixation and denitrification, *Global Biogeochem. Cycles*, *11*, 235-266, 1997.

Gruber, N., J.L. Sarmiento, and T.F. Stocker, An improved method for detecting anthropogenic CO_2 in the oceans, *Global Biogeochem. Cycles*, *10*, 809-837, 1996.

Johnson, K.M., A.E. King, and J.M. Sieburth, Coulometric TCO_2 analyses for marine studies: An introduction, *Mar. Chem.*, *16*, 61-82, 1985.

Johnson, K.M., et al., Coulometric total carbon dioxide analysis for marine studies: Assessment of the quality of total inorganic carbon measurements made during the US Indian Ocean CO_2 Survey 1994-1996, *Mar. Chem.*, 63, 21-37, 1998.

Keeling, C.D., and T.P. Whorf, Atmospheric CO_2 records from sites in the SIO air sampling network, in *Trends: A Compendium of Data on Global Change*, Carbon Dioxide Inf. Anal. Cent., Oak Ridge Nat. Lab., Oak Ridge, Tenn., 1996.

Keeling, C.D., S.C. Piper, and M. Heimann, A three-dimensional model of atmospheric CO_2 transport based on observed winds, 4, Mean annual gradients and interannual variations, in *Aspects of Climate Variability in the Pacific and the Western Americas*, *Geophys. Monogr. Ser.*, Vol. 55, edited by D.H. Peterson, pp. 305-363, AGU, Washington D.C., 1989.

Keeling, R.F., and S.R. Shertz, Seasonal and interannual variations in atmospheric oxygen and implications for the global carbon cycle, *Nature*, *358*, 723-727, 1992.

Leboucher, V., J. Orr, P. Jean-Baptiste, M. Arnold, P. Monfray, N. Tisnerat-Laborde, A. Poisson, and J. Duplessy, Oceanic radiocarbon between Antarctica and South Africa along WOCE section I6 at 30°E, *Radiocarbon*, in press, 1998.

Levitus, S., and T.P. Boyer, Temperature, in *NOAA Atlas NESDIS 3: World Ocean Atlas 1994*, *NOAA Tech. Rep. 4*, Natl. Environ. Satell. Data and Inf. Serv., Silver Spring, MD, 1994.

Levitus, S., R. Burgett, and T.P. Boyer, Salinity, in *NOAA Atlas NESDIS 3: World Ocean Atlas 1994*, *NOAA Tech. Rep. 3*, Natl. Environ. Satell. Data and Inf. Serv., Silver Spring, MD, 1994.

Merbach, C., C.H. Culberson, J.E. Hawley, and R.M. Pytkowicz, Measurements of the apparent dissociation constants of carbonic acid in seawater at atmospheric pressure, *Limnol. Oceanogr.*, *18*, 897-907, 1973.

Millard, R.C., Jr., CTD calibration and data processing techniques at WHOI using the practical salinity scale, paper presented at International STD Conference and Workshop, Mar. Tech. Soc., La Jolla, Calif., 1982.

Millero, F.J., et al., Total alkalinity measurements in the Indian Ocean during the WOCE Hydrographic Program CO_2 survey cruises 1994-1996, *Mar. Chem.*, *63*, 9-20, 1998a.

Millero, F.J., K. Lee, and M. Roche, Alkalinity as a major variable in the marine carbonate system, *Mar. Chem.*, *60*, 111-130, 1998b.

Murnane, R., J.L. Sarmiento, and C. LeQuere, The spatial distribution of air-sea CO_2 fluxes and the interhemispheric transport of carbon by the oceans, *Global Biogeochem. Cycles*, in press, 1999.

Murphy, P.P., R.A. Feely, R.H. Gammon, K.C. Kelly, and L.S. Waterman, Autumn air-sea disequilibrium of CO_2 in the South Pacific Ocean, *Mar. Chem.*, *35*, 77-84, 1991.

Naqvi, S.W.A., and R. Sen Gupta, "NO" a useful tool for the estimation of nitrate deficits in the Arabian Sea, *Deep Sea Res., Part A*, 32, 665-674, 1985.

Neftel, A., H. Friedli, E. Moor, H. Lotscher, H. Oeschger, U. Siegenthaler, and B. Stauffer, Historical CO_2 record from the Siple station ice core, in *Trends '93: A Compendium of Data on Global Change*, edited by T. Boden et al., *Rep. ORNL/CDIAC-65*, pp. 11-14, Carbon Dioxide Inf. Anal. Cent., Oak Ridge Nat. Lab., Oak Ridge, Tenn., 1994.

Papaud, A., and A. Poisson, Distribution of dissolved CO_2 in the Red Sea and correlation with other geochemical tracers, *J. Mar. Res.*, *44*, 385-402, 1986.

Poisson, A., and C.-T.A. Chen, Why is there little anthropogenic CO_2 in the Antarctic Bottom Water?, *Deep Sea Res., Part A*, *34*, 1255-1275, 1987.

Poisson, A., B. Schauer, and C. Brunet, Les Rapports des campagnes a la mer, MD43/INDIGO 1, in *Les publications de la mission de recherche des Terres Australes et Antarctiques Fancaises*, *Rep. 85-06*, 267 pp., Univ. Pierre et Marie Curie, Paris, France, 1988.

Poisson, A., B. Schauer and C. Brunet, Les Rapports des campagnes a la mer, MD49/INDIGO 2, in *Les publications de la mission de recherche des Terres Australes et Antarctiques Fancaises*, *Rep. 86-02*, 234 pp., Univ. Pierre et Marie Curie, Paris, France, 1989.

Poisson, A., B. Schauer and C. Brunet, Les Rapports des campagnes a la mer. MD53/INDIGO 3, in *Les publications de la mission de recherche des Terres Australes et Antarctiques Fancaises*, *Rep. 87-02*, 269 pp., Univ. Pierre et Marie Curie, Paris, France, 1990.

Quay, P.D., B. Tilbrook, and C.S. Wong, Oceanic uptake of fossil fuel CO_2: Carbon-13 evidence, *Science*, *256*, 74-79, 1992.

Sarmiento, J.L., and E.T. Sundquist, Revised budget for the oceanic uptake of anthropogenic carbon dioxide, *Nature*, *356*, 589-593, 1992.

Sarmiento, J.L., J. Willebrand, and S. Hellerman, Objective analysis of Tritium observations in the Atlantic Ocean during 1971-74, *OTL Tech Rep. 1*, 19 pp., Ocean Tracers Lab., Princeton Univ., Princeton, N. J., 1982.

Sarmiento, J.L., J.C. Orr, and U. Siegenthaler, A perturbation simulation of CO_2 uptake in an ocean general circulation model, *J. Geophys. Res.*, *97*, 3621-3645, 1992.

Sarmiento, J.L., R. Murnane, and C. LeQuere, Air-sea CO_2 transfer and the carbon budget of the North Atlantic, *Philos. Trans. R. Soc. London, Ser. B*, *348*, 211-219, 1995.

Sen Gupta, R., M.D. Rajagopal, and S.Z. Qasim, Relationship between dissolved oxygen and nutrients in the northwestern Indian Ocean, *Indian J. Mar. Sci.*, *5*, 201-211, 1976.

Siegenthaler, U., and F. Joos, Use of a simple model for studying oceanic tracer distributions and the global carbon cycle, *Tellus*, *Ser. B*, *44*, 186-207, 1992.

Siegenthaler, U., and J.L. Sarmiento, Atmospheric carbon dioxide and the ocean, *Nature*, *365*, 119-125, 1993.

Stocker, T.F., W.S. Broecker, and D.G. Wright, Carbon uptake experiments with a zonally-averaged global circulation model, *Tellus*, *Ser. B*, *46*, 103-122, 1994.

Takahashi, T.T., R.A. Feely, R.F. Weiss, R.H. Wanninkhof, D.W. Chipman, S.C. Sutherland, and T.T. Takahashi, Global air-sea flux of CO_2: An estimate based on measurements of sea-air pCO_2 difference, *Proc. Natl. Acad. Sci. U. S. A.*, *94*, 8292-8299, 1997.

Tans, P.P., I.Y. Fung, and T. Takahashi, Observational constraints on the global atmospheric CO_2 budget, *Science*, *247*, 1431-1438, 1990.

Toggweiler, J.R., K. Dickson, and K. Bryan, Simulations of radiocarbon in a coarse-resolution world ocean model, 1. Steady state pre-bomb distributions, *J. Geophys. Res.*, *94*, 8217-8242, 1989.

UNESCO, Background papers and supporting data on the Practical Salinity Scale, *1978 UNESCO Tech. Pap. in Mar. Sci.*, *37*, 1981.

Wallace, D.W.R., Monitoring global ocean inventories, *OOSDP Background Rep. 5*, 54 pp., Ocean Observ. Syst. Dev. Panel, Texas A&M Univ., College Station, Tex., 1995.

Warner, M.J. and R.F. Weiss, Solubilities of chlorofluorocarbons 11 and 12 in water and seawater, *Deep-Sea Res.*, 32, 1485-1497, 1985.

Warner, M.J., J.L. Bullister, D.P. Wisegarver, R.H. Gammon, and R.F. Weiss, Basin-wide distributions of chlorofluorocarbons CFC-11 and CFC-12 in the North Pacific: 1985-1989, *J. Geophys. Res.*, *101*, 20525-20542, 1996.

Weiss, R.F., W.S. Broecker, H. Craig, and D. Spencer, *GEOSECS Indian Ocean Expedition Vol. 5, Hydrographic Data 1977-1978*, 48 pp., Natl. Sci. Found., U.S. Gov. Print. Off., Washington D. C., 1983.

Wessel, P., and W.H.F. Smith, New version of generic mapping tools released, *Eos Trans. AGU*, *76*, 329, 1995.

Wyrtki, K., Physical oceanography of the Indian Ocean, in *Ecological Studies: Analysis and Synthesis*, vol. 3, pp. 18-36, edited by B. Zeitzschel, Springer-Verlag, New York, 1973.

K.M. Johnson, Oceanographic and Atmospheric Sciences Division, Brookhaven National Laboratory, Upton, NY 11973.

R.M. Key, C.L. Sabine, and J.L. Sarmiento, Department of Geosciences, Princeton University, Princeton, NJ 08544. (key@geo.princeton.edu, sabine@geo.princeton.edu, and jls@splash.princeton.edu)

F.J. Millero, Rosenstiel School of Marine and Atmospheric Sciences, University of Miami, 4600 Rickenbacker Cswy., Miami, FL 33149. (fmillero@rsmas.miami.edu)

A. Poisson, Laboratoire de Physique et Chimie Marines, Université Pierre et Marie Curie, 4 Place Jussieu, Tour 24-25, 75720 Paris Cedex 05 France. (apoisson@ccr.jussieu.fr)

D.W.R. Wallace, Abteilung Meereschemie, Institut für Meereskunde an der Universität Kiel, Duesternbrooker Weg 20, D-24105 Kiel, Germany. (dwallace@ifm.uni-kiel.de)

C.D. Winn, Marine Science Program, Hawaii Pacific University, 45-045 Kamehameha Highway, Kaneohe, HI 96744-5297. (cwinn@soest.hawaii.edu)

(Received May 11, 1998; revised November 24, 1998; accepted November 24, 1998.)

APPENDIX E:

REPRINT OF PERTINENT LITERATURE

Key R. M., and P. D. Quay. 2002. U.S. WOCE Indian Ocean Survey: Final Report for Radiocarbon. Technical Report. Princeton University, Princeton, N.J.

U.S. Woce Indian Ocean Survey: Final Report for Radiocarbon

Robert M. Key and Paul D. Quay
July 12, 2002

1.0 General Information

The U.S. WOCE Indian Ocean Survey consisted of 9 cruises covering the period December 1, 1994 to January 22, 1996. All of the cruises used the R/V Knorr operated by the Woods Hole Oceanographic Institute. A total of 1244 hydrographic stations were occupied with radiocarbon sampling on 366 stations. The radiocarbon stations are shown as black dots in Figure 1. To give an indication of the total radiocarbon coverage for the Indian Ocean, the figure includes radiocarbon stations from WOCE sections S4I (Key, 1999; red dots) and I6S (Leboucher, *et al.*, 1999; white dots) and from the earlier GEOSECS (Stuiver and Ostlund, 1983; brown dots) and INDIGO (Bard, *et al.*, 1988; yellow dots) expeditions. Specific summary information on the 9

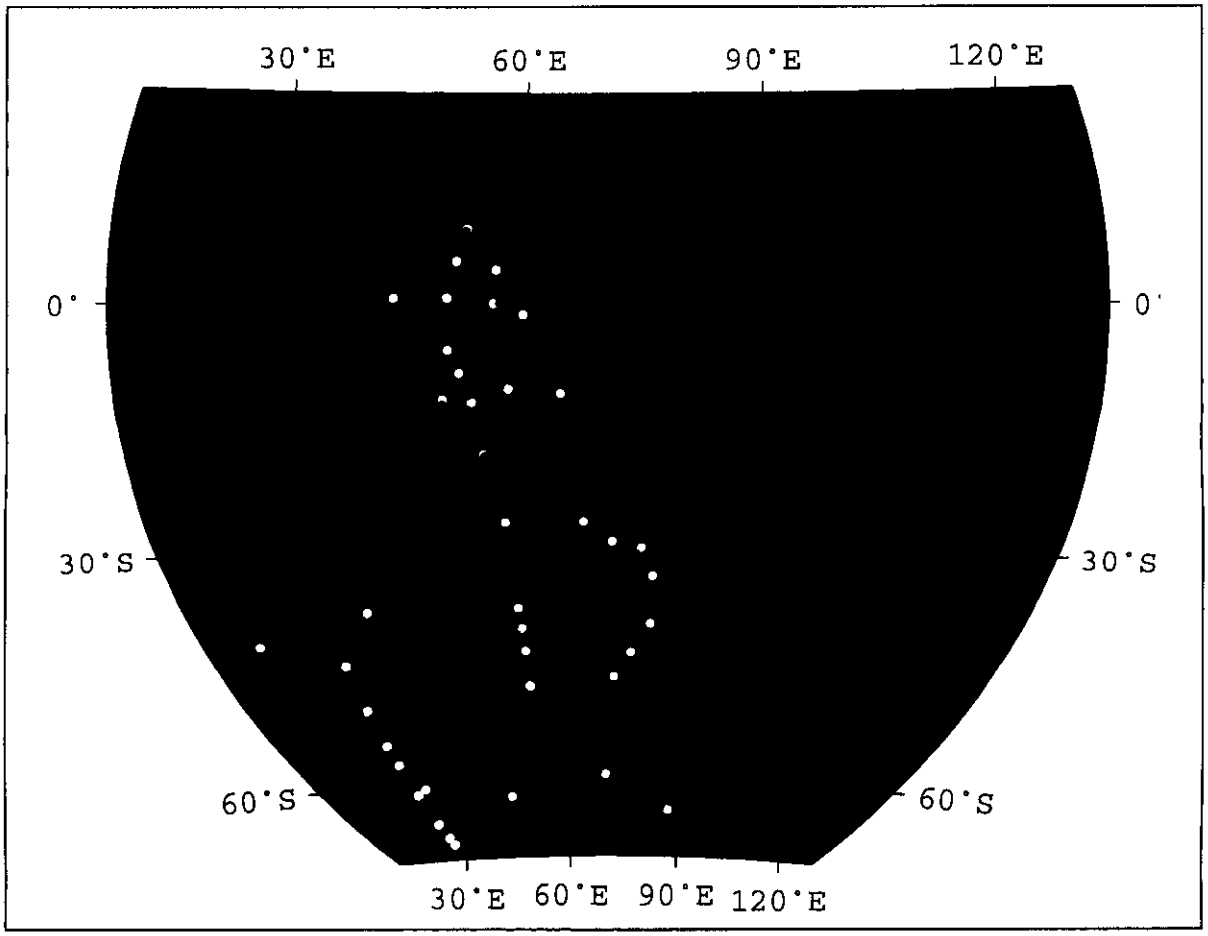

Figure 1: AMS ^{14}C station map for WOCE S4I.

WOCE survey cruises is given in Table 1.

TABLE 1. Summary for Survey Sections

Cruise	Chief Scientist	Start	End	$\Delta^{14}C$ Stations	$\Delta^{14}C$ Samples
I8SI9S	M. McCartney T. Whitworth	12/01/94 Fremantle Australia	01/19/95 Fremantle Australia	26	662
I9N	A. Gordon D. Olson	01/24/95 Fremantle Australia	03/05/95 Colombo Sri Lanka	22	364
I8NI5E	L. Talley M. Baringer	03/10/95 Colombo Sri Lanka	04/15/95 Fremantle Australia	20	414
I3	W. Nowlin B. Warren	04/20/95 Fremantle Australia	06/07/95 Port Louis Mauritius	20	462
I5WI4	J. Toole	06/11/95 Port Louis Mauritius	07/11/95 Port Louis Mauritius	15	361
I7N	D. Olson S. Doney D. Musgrave	07/15/95 Port Louis Mauritius	08/24/95 Muscat Oman	22	373
I1	J. Morrison H. Bryden	08/29/95 Muscat Oman	10/16/95 Singapore	24	426
I10	N. Bray J. Toole	11/11/95 Dampier Australia	11/28/95 Singapore	6	127
I2	G. Johnson B. Warren	12/02/95 Singapore China	01/22/96 Mombasa Kenya	28	651

2.0 Personnel

$\Delta^{14}C$ sampling for cruise I8SI9S was carried out by Melinda Brockington (University of Washington). Personnel for the remainder of the cruises came from the Ocean Tracer Lab (OTL Princeton University) and included G. McDonald, A. Doerty, R. Key, T. Key, and R. Rotter. $\Delta^{14}C$ (and accompanying $\delta^{13}C$) analyses were performed at the National Ocean Sciences AMS Facility (NOSAMS) at Woods Hole Oceanographic Institution. R. Key collected the data from NOSAMS, merged the files with hydrographic data, assigned quality control flags to the $\Delta^{14}C$ and submitted the results to the WOCE office (4/02). R. Key is P.I. for the ^{14}C data. P. Quay (U.W.) and A. McNichol (WHOI/NOSAMS) are P.I.s for the ^{13}C data. In addition to collecting samples the ship-board ^{14}C person was also responsible for operation of the underway pCO_2 system provided by the OTL (Sabine and Key, 1997; Sabine, *et al.*, 2000).

3.0 Results

This $\Delta^{14}C$ data set and any changes or additions supersedes any prior release.

3.1 Hydrography

Hydrographic data from these cruises were submitted to the WOCE office by the chief scientists and are described in various reports which are available from the web site (http://whpo.ucsd.edu/data/tables/onetime/1tim_ind.htm).

3.2 $\Delta^{14}C$

The $\Delta^{14}C$ values described here were originally distributed in the NOSAMS data reports listed in Table 2 and given in full in the References . Those reports included results which had not been through the WOCE quality control procedures. For WOCE applications, this report supersedes the NOSAMS reports.

TABLE 2. NOSAMS Data Report Summary

Cruise	Report
I8SI9S	99-089
I7N I9N	99-144
I1	99-199
I8N	00-218
I3 I5WI4	01-013
I2	02-001

All of the AMS samples from these cruise have been measured using the AMS methods outlined in Key *et al.*, 1996 and citations therein (especially Mcnichol *et al.*, 1994; Osborne *et al.* 1994; and Scheider*et al.* 1995). Table 3 summarizes the number of samples analyzed and the quality control flags assigned for each cruise.Approximately 98% of the samples collected were deemed to be "good" (flagged 2 or 6). Quality flag values were assigned to all $\Delta^{14}C$ measurements using the code defined in Table 0.2 of WHP Office Report WHPO 91-1 Rev. 2 section 4.5.2. (Joyce, *et al.*, 1994). No measured values have been removed from this data set.

TABLE 3. Sample Analysis and QC Summary

Cruise	Samples Analyzed	QC Flag Totals				
		2	3	4	5	6
I8SI9S	662	636	6	8	0	12
I9N	368	354	4	3	4	3
I8NI5E	416	401	6	0	2	7
I3	463	448	5	0	1	9
I5WI4	366	342	3	1	5	15
I7N	383	370	3	0	10	0
I1	430	421	2	2	4	1
I10	127	127	0	0	0	0
I2	655	636	13	2	4	0
Total	3870	3735	42	16	30	47

4.0 Data Summary

Figures 2-6 summarize the $\Delta^{14}C$ data collected during the Indian Ocean survey. Only $\Delta^{14}C$ measurements with a quality flag value of 2 ("good") or 6 ("replicate") are included in the figures. Figure 2 shows the $\Delta^{14}C$ values with 2σ error bars plotted as a function of pressure. The

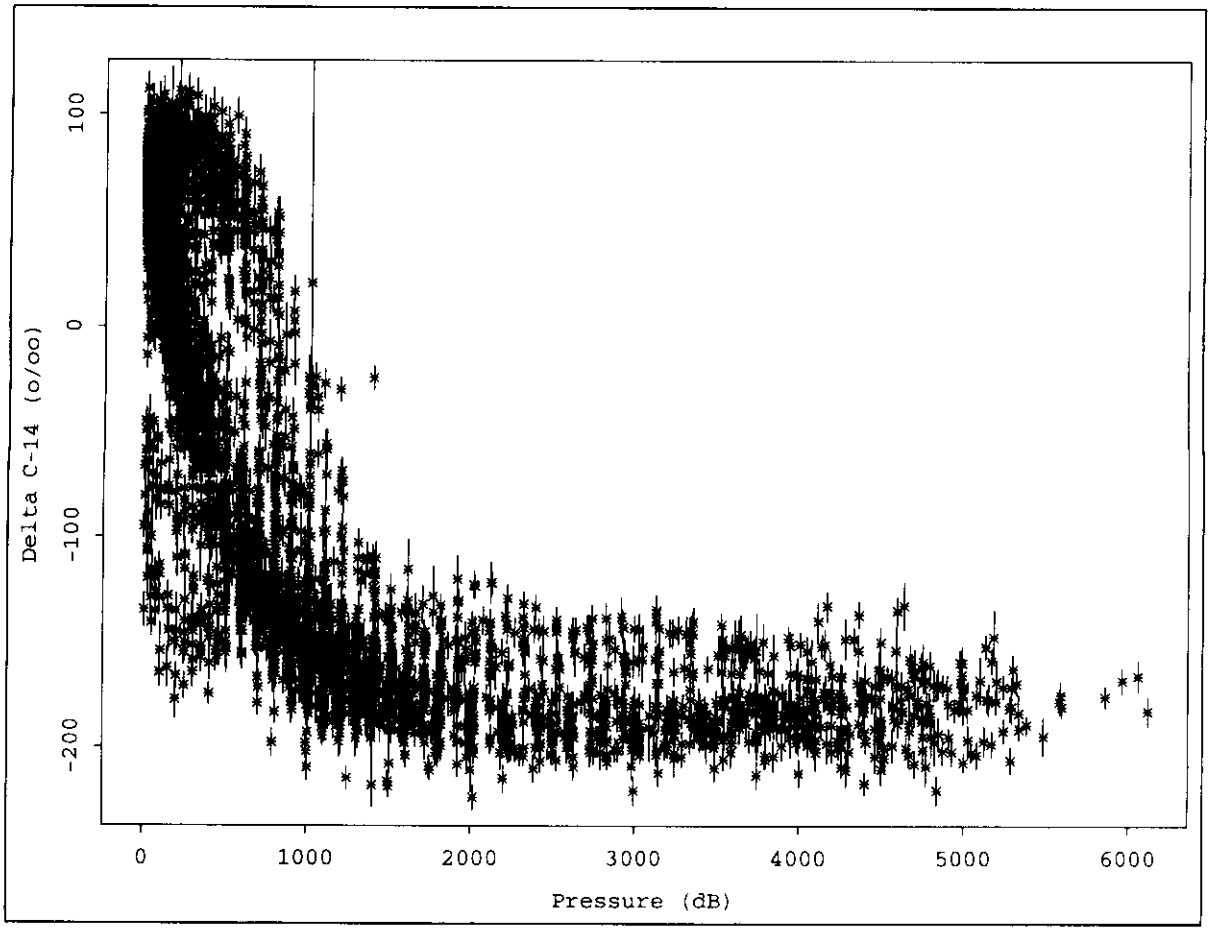

Figure 2: $\Delta^{14}C$ results shown with 2σ error bars.

mid depth $\Delta^{14}C$ minimum which occurs around 2500 meters in the Pacific is not apparent in these data. In fact, there is very little variation in the deep and bottom water other than the previously reported decrease in $\Delta^{14}C$ from south to north. All of the samples collected at a depth greater than 1000 meters have a mean $\Delta^{14}C$ = -165.±25‰ (standard error = 0.5‰ with n=2086). A substantial fraction of this variability is due to the difference between the Southern Ocean and main basin deep waters.

Figure 3 shows the deep (>1000m) $\Delta^{14}C$ values plotted against silicate.The black and red points are from north and south of 35°S, respectively. The straight line shown in the figure is the least squares regression relationship derived by Broecker *et al.* (1995) based on the GEOSECS global data set. According to their analysis, this line ($\Delta^{14}C$ = -70 - Si) represents the relationship between naturally occurring radiocarbon and silicate for most of the ocean. They noted that the technique could not be simply applied at high latitudes as confirmed by this data set.

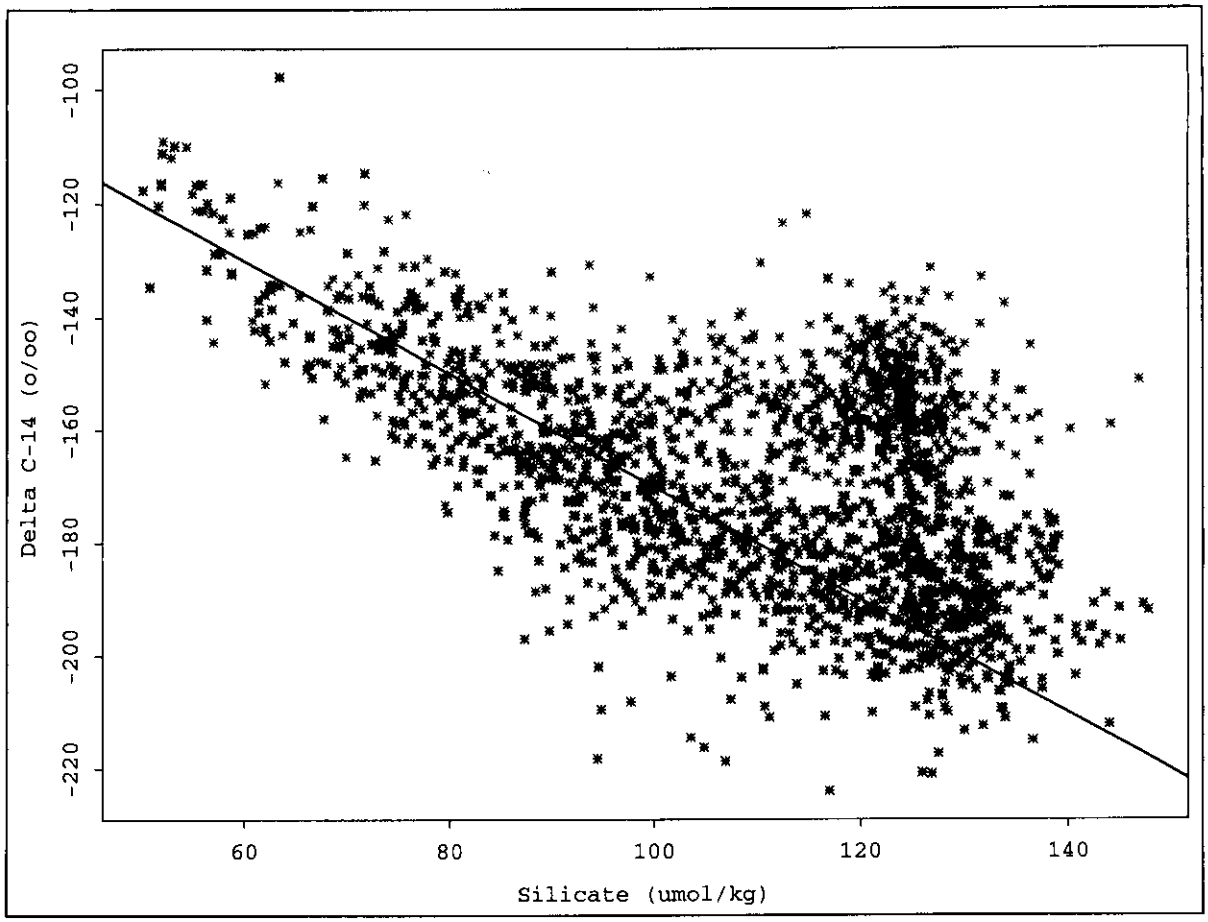

Figure 3: $\Delta^{14}C$ as a function of silicate for samples collected deeper than 1000m. The black points are from north of 35°S and the red points south of 35°. The straight line shows the relationship proposed by Broecker, *et al.*, 1995 ($\Delta^{14}C$ = -70 - Si with radiocarbon in ‰ and silicate in µmol/kg).

Figure 4 shows all of the radiocarbon values plotted against potential alkalinity (defined as [alkalinity + nitrate]*35/salinity). The straight line is the regression fit (^{14}C = -59 - 0.962(PALK - 2320) derived by Rubin and Key (2002) using GEOSECS measurements assumed to have no bomb-produced $\Delta^{14}C$. The value 2320 is the estimated surface ocean mean potential alkalinity. As with Figure 3 the black and red points in Figure 4 indicate measurements taken north and south of 35°S, respectively. Unlike the silicate plot (Figure 3), there is no apparent difference in the relationship for Southern Ocean *vs* Indian Ocean deep waters. The distance a point falls above the regression line is an estimate of the bomb radiocarbon contamination for the sample.

Figures 5-9 show gridded sections of the $\Delta^{14}C$ data. In each figure the water column is divided into upper (0-1000m) and lower (1000-bottom) portions. The data were gridded using the loess method (Chambers *et al.*, 1983; Chambers and Hastie, 1991; Cleveland,1979; Cleveland and Devlin, 1988). The span for the fits was adjusted to be minimum and yet capture the large scale features. The contour interval is 10‰ for the upper water column and 20‰ for intermediate and deep water.

Figure 5 and Figure 6 show the meridional $\Delta^{14}C$ distribution in the eastern and western Indian Ocean. In both figures the distribution pattern is very similar to that seen in the Pacific

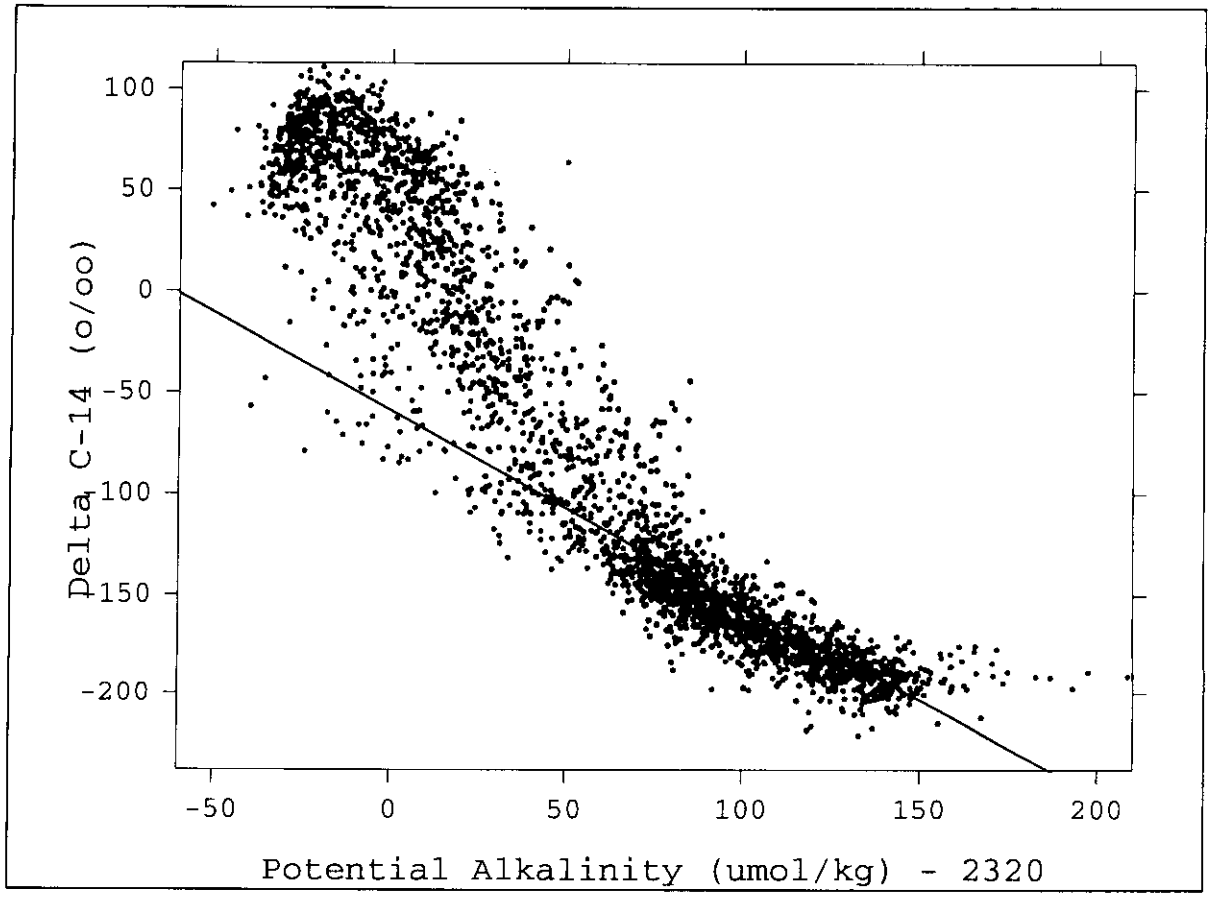

Figure 4: Based on the potential alkalinity method (Rubin and Key, 2002), the samples which plot above the line and have potential alkalinity values less than about 2400 μmole/kg are contaminated with bomb-produced ^{14}C..

Ocean WOCE samples. In the Pacific the maximum $\Delta^{14}C$ values were frequently found in shallow water, but beneath the surface. In the Indian Ocean data a subsurface maximum is not so common. Both sections show intrusion of Circumpolar Deep Water from the south along the bottom and return flow of deep water at 2000-3000m. As with the Pacifiic the middepth waters have the lowest $\Delta^{14}C$ values, however the middepth Indian Ocean waters have significantly higher values that corresponding Pacific waters. This pattern is consistant with a mean ageing of waters from the Atlantic to Indian to Pacific.

Figure 7, Figure 8 and Figure 9 show zonal $\Delta^{14}C$ sections along the WOCE lines I1 (~10°N), I2(~8°S) and I3(~20°S). Except for the western ends, the $\Delta^{14}C$ contours in the upper kilometer are relatively flat. In each section the deep waters of the western basins have somewhat higher $\Delta^{14}C$ than at the same depth in the eastern basins. The strength of this signal decreases from south to north and is almost certainly due to the western basins having a higher fraction of North Atlnatic Deep Water.

Figure 10 shows the meridional distribution of bomb produced $\Delta^{14}C$ (*via* Rubin and Key, 2002) in the eastern and western Indian Ocean. The eastern section used all WOCE samples collected at depths less than 1000m and east of 85°E. The western section uses the same depth range, but samples from west of 75°E. Both sections are contoured and colored in potential density space rather against depth. One might expect *a priori* that the distributions would differ north of the

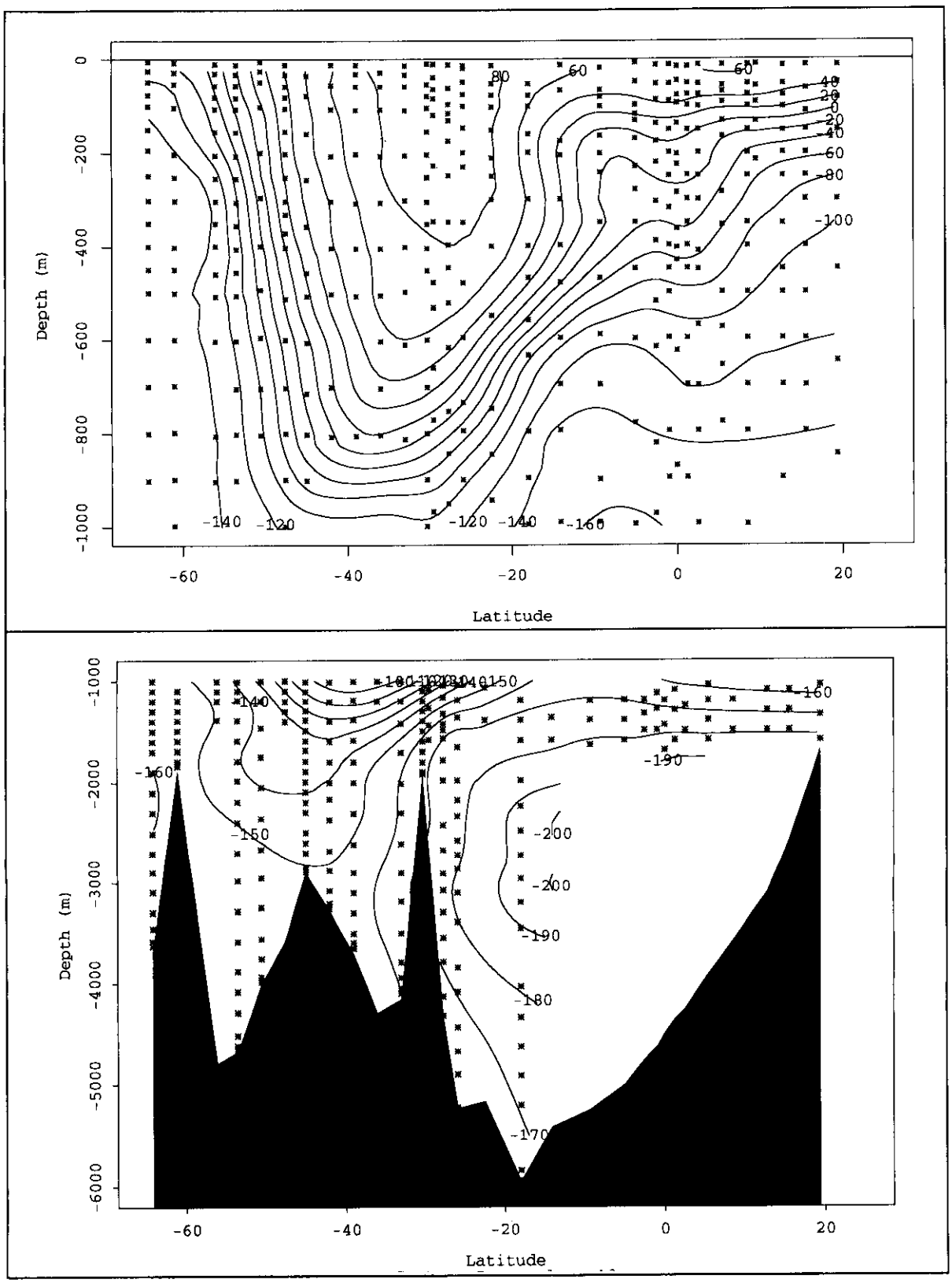

Figure 5: $\Delta^{14}C$, along I8S and I9N in the eastern Indian Ocean.

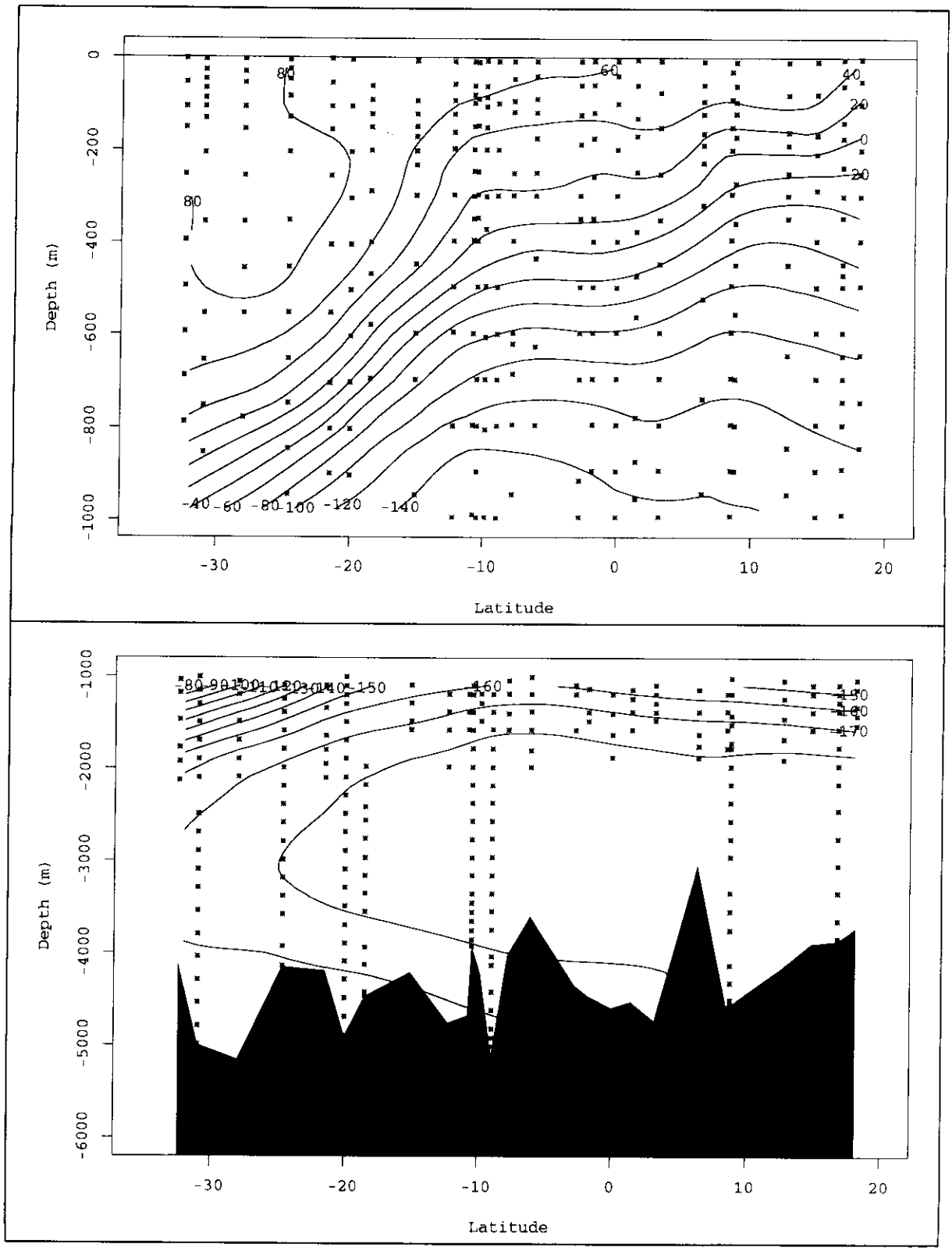

Figure 6: $\Delta^{14}C$ along I7 in the western Indian Ocean.

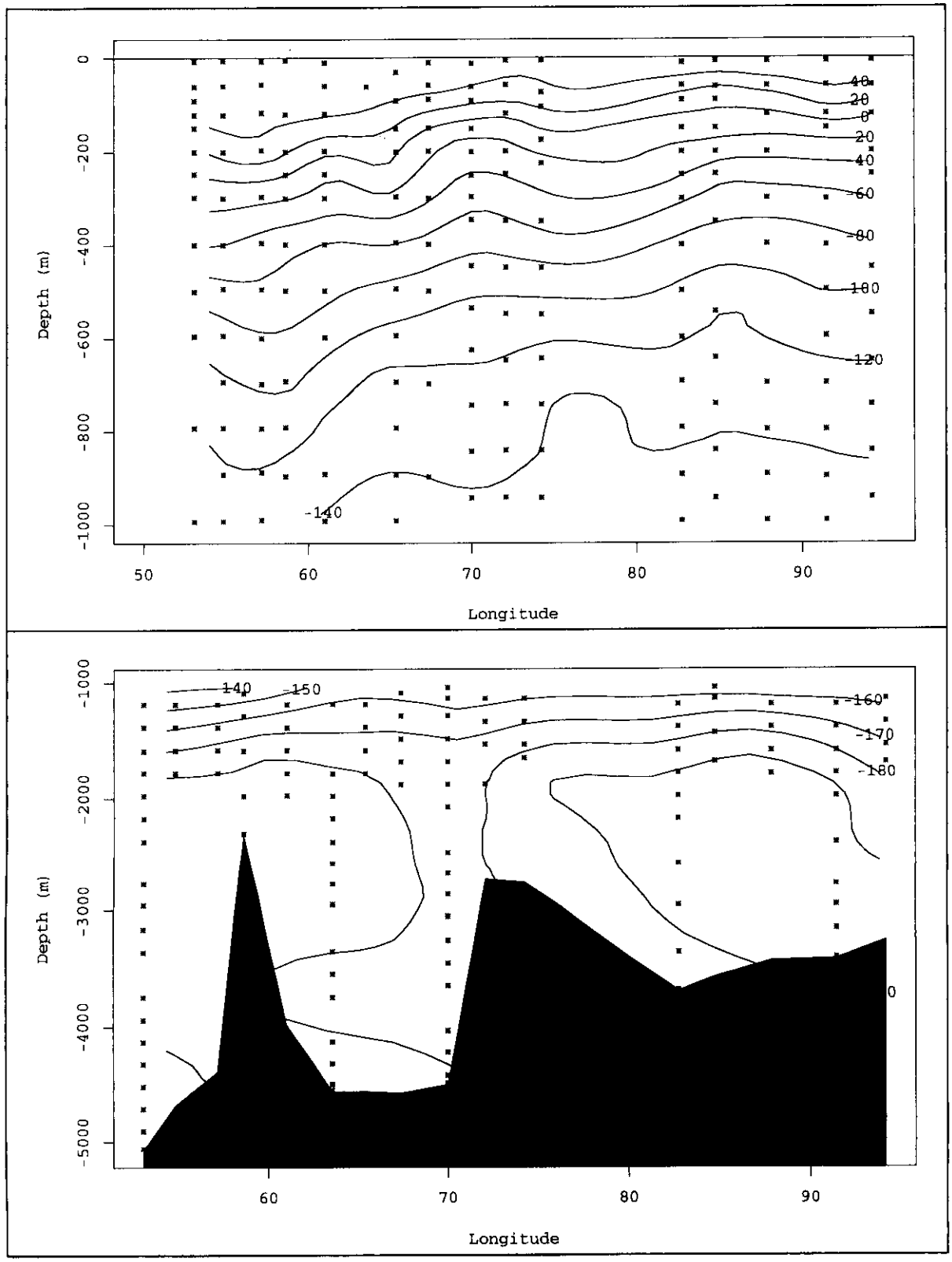

Figure 7: $\Delta^{14}C$ along 11 in the northern Indian Ocean.

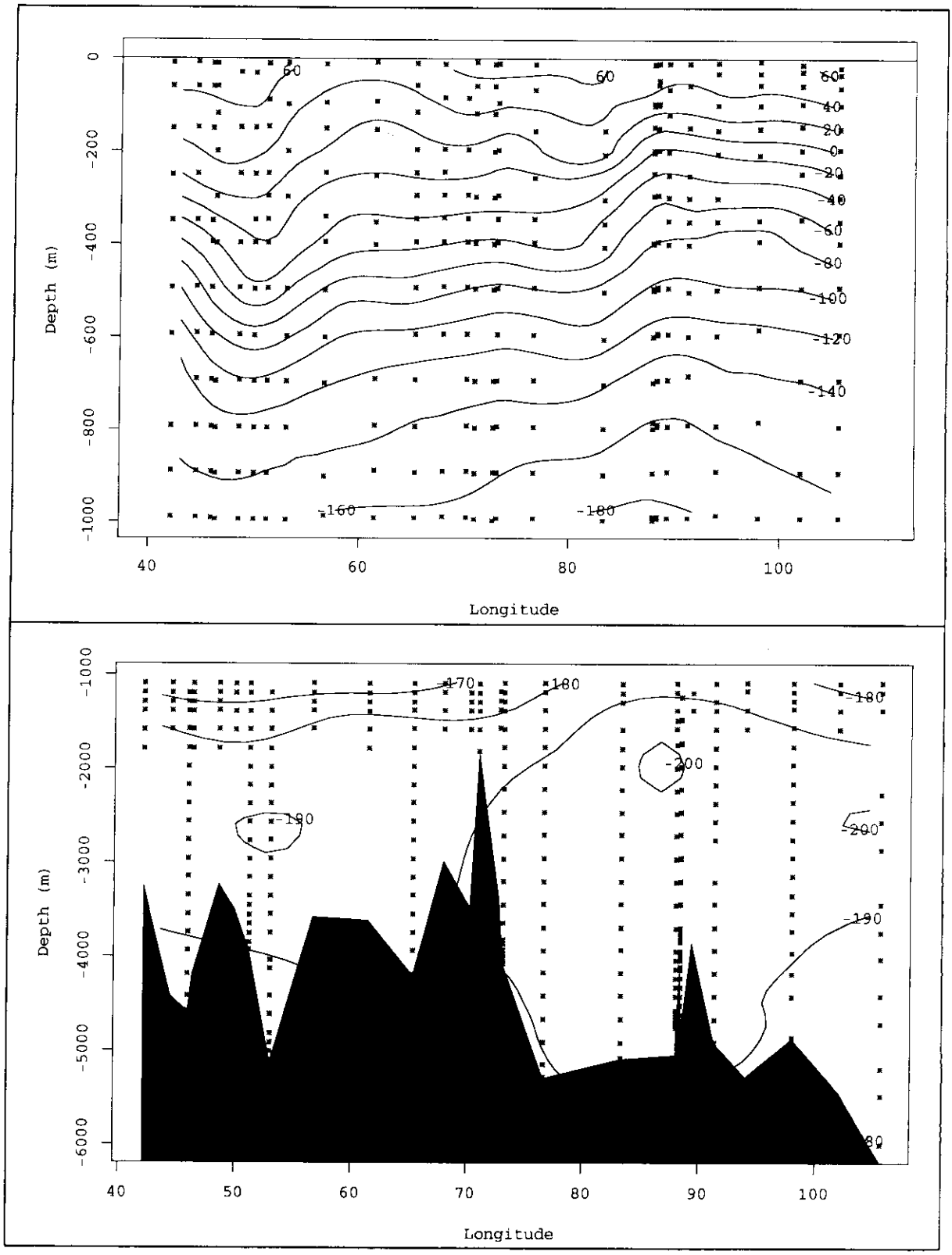

Figure 8: $\Delta^{14}C$ along I2 in the southern tropical Indian Ocean.

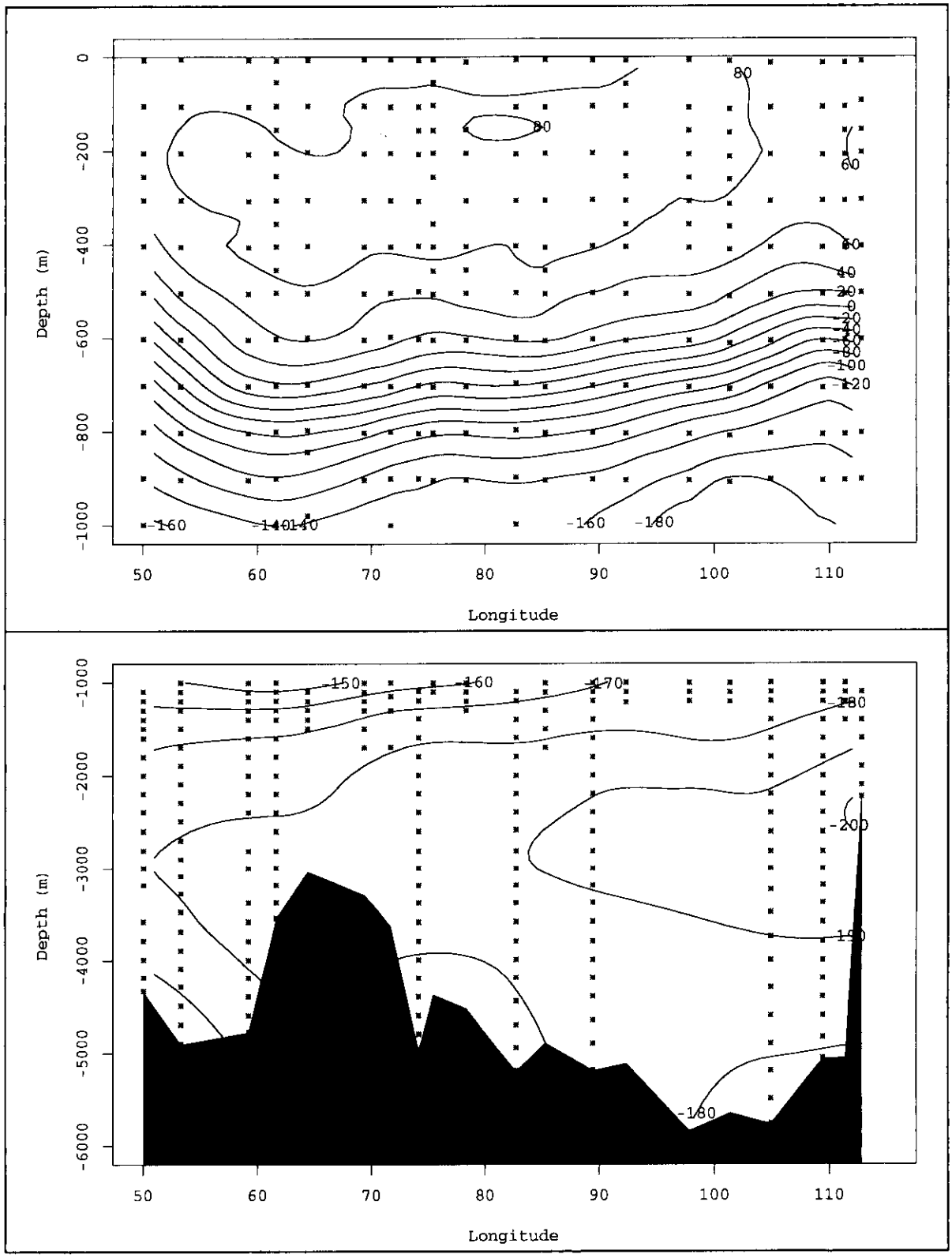

Figure 9: $\Delta^{14}C$ along I3 in the southern subtropical Indian Ocean at approximately 20°S.

equator due to the geography and difference in chemistry between the Bay of Bengal and Arabian Sea. Perhaps unexpected is the fact that the distributions differ significantly as far as 40°S. In the eastern section the maximum bomb $\Delta^{14}C$ values are found between 40°S and 20°S and more or less uniformly from the surface down to the level where σ_θ~26.5. The western section has a maximum in the same latitude range but in this case the maximum occurs as a subsurface lens.

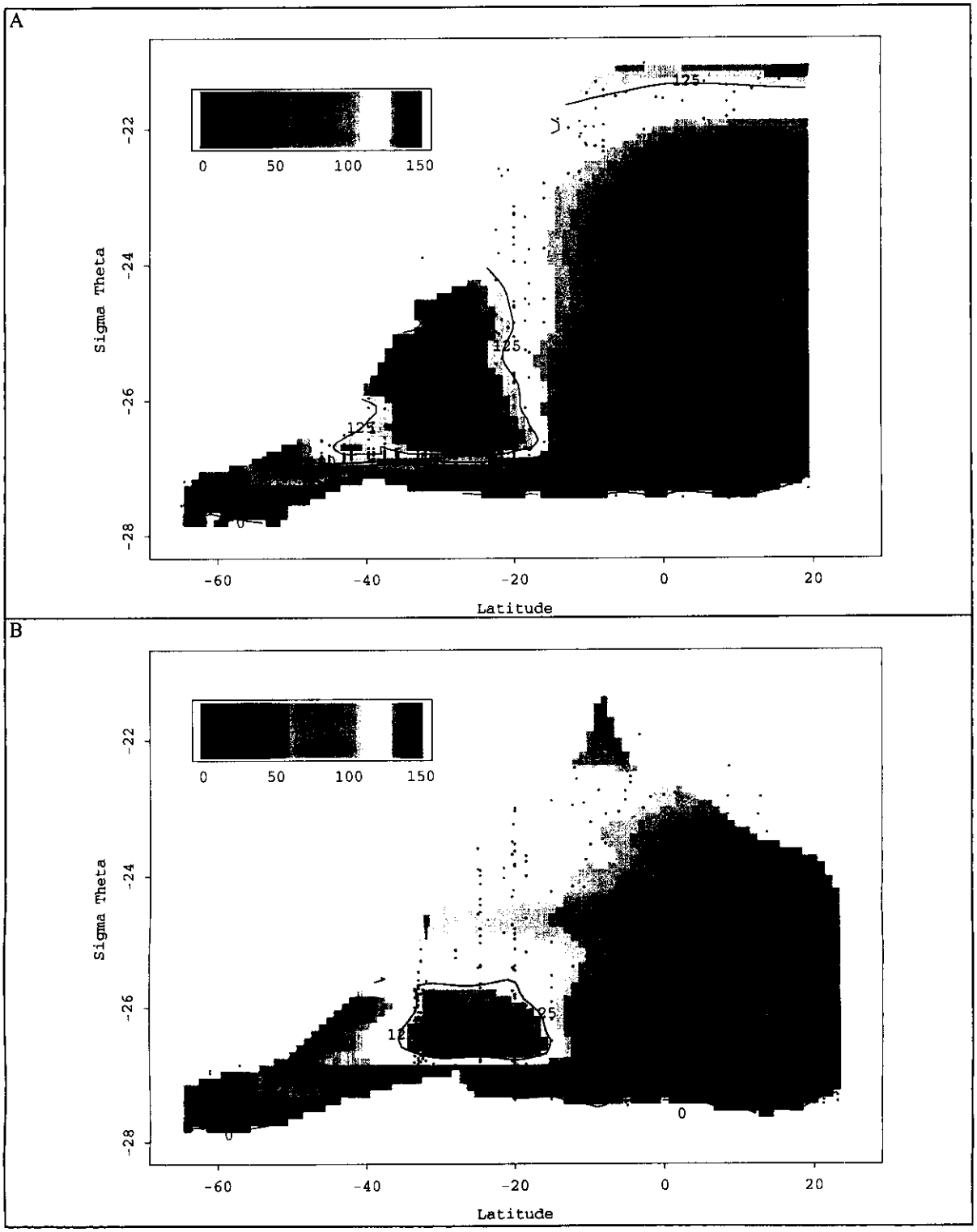

Figure 10: .Mean bomb-produced $\Delta^{14}C$ sections in the eastern (A) and western (B) Indian Ocean, shown in potential density space for samples from the upper 1000m.

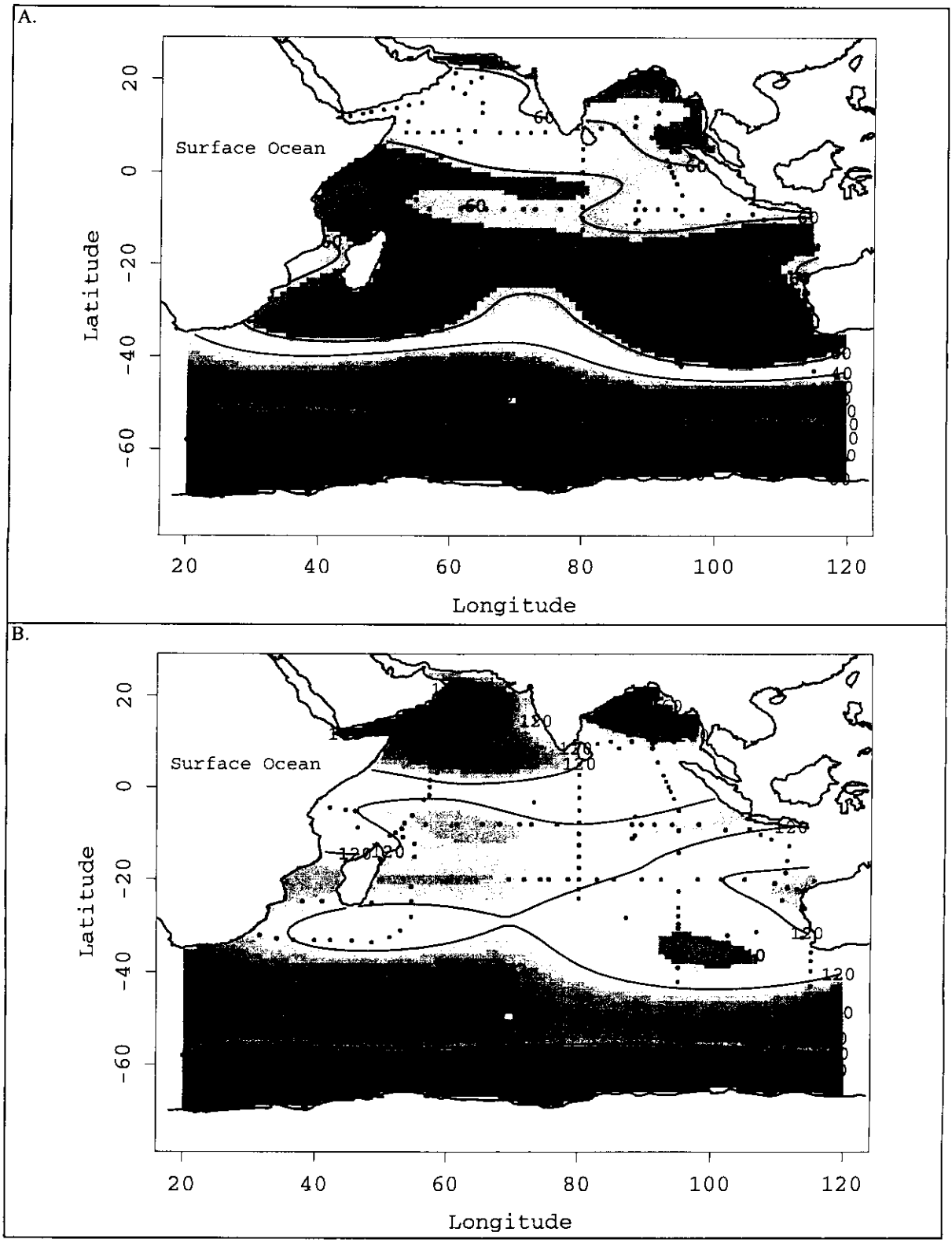

Figure 11: .(A) $\Delta^{14}C$ and (B) bomb-produced $\Delta^{14}C$ for the surface Indian Ocean from WOCE measurements.

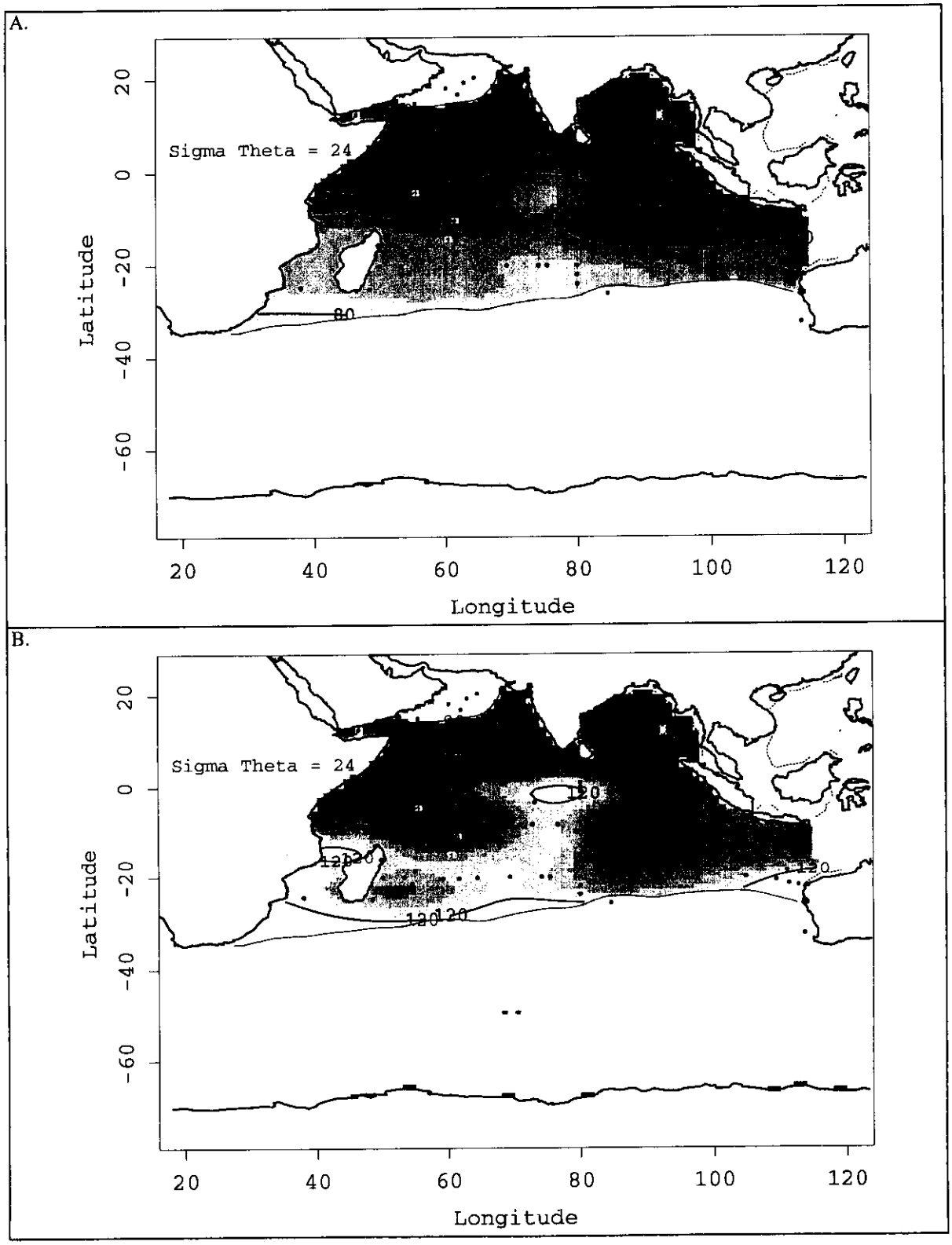

Figure 12: .(A) $\Delta^{14}C$ and (B) bomb-produced $\Delta^{14}C$ on σ_θ=24.0.

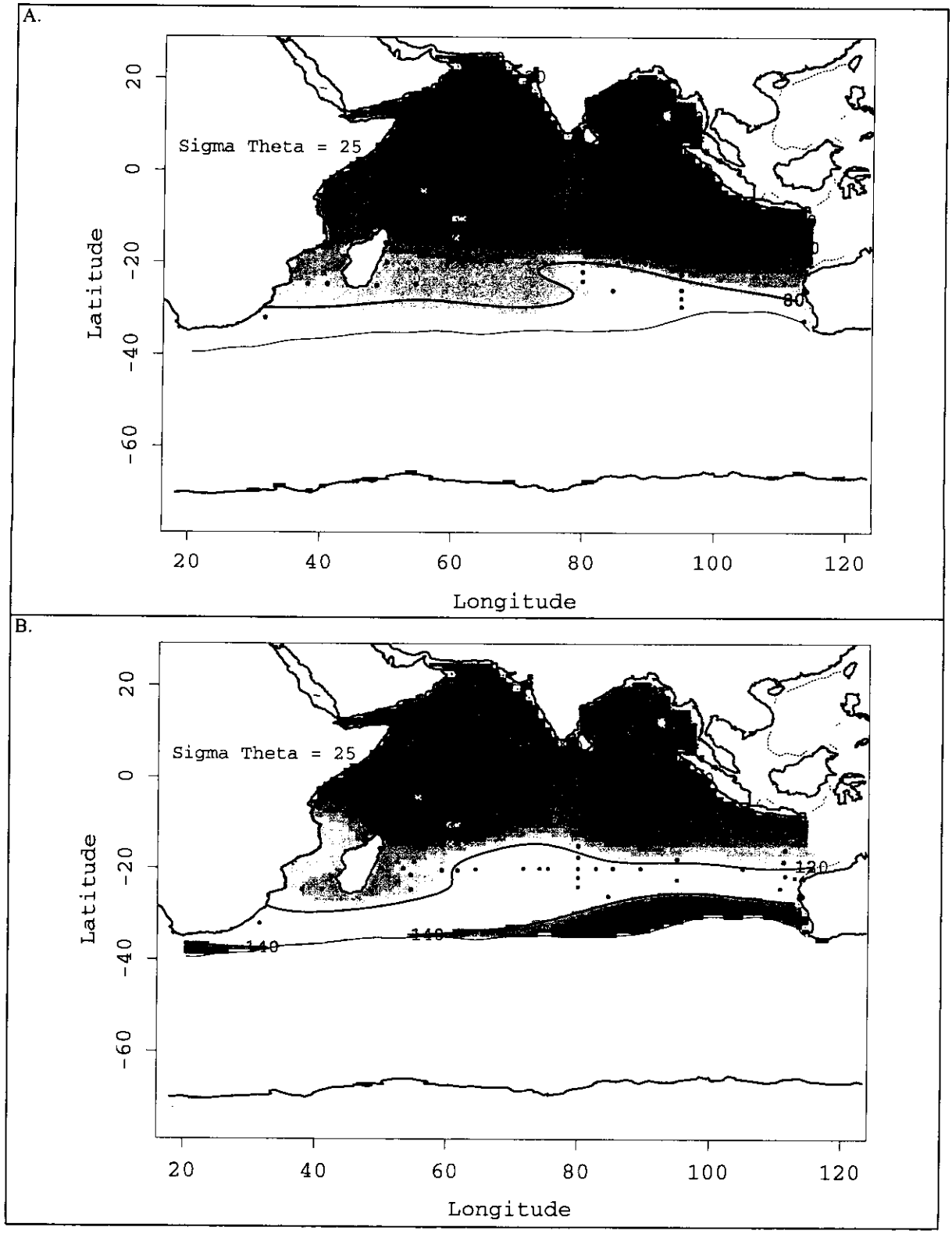

Figure 13: .(A) $\Delta^{14}C$ and (B) bomb-produced $\Delta^{14}C$ on σ_θ=25.0

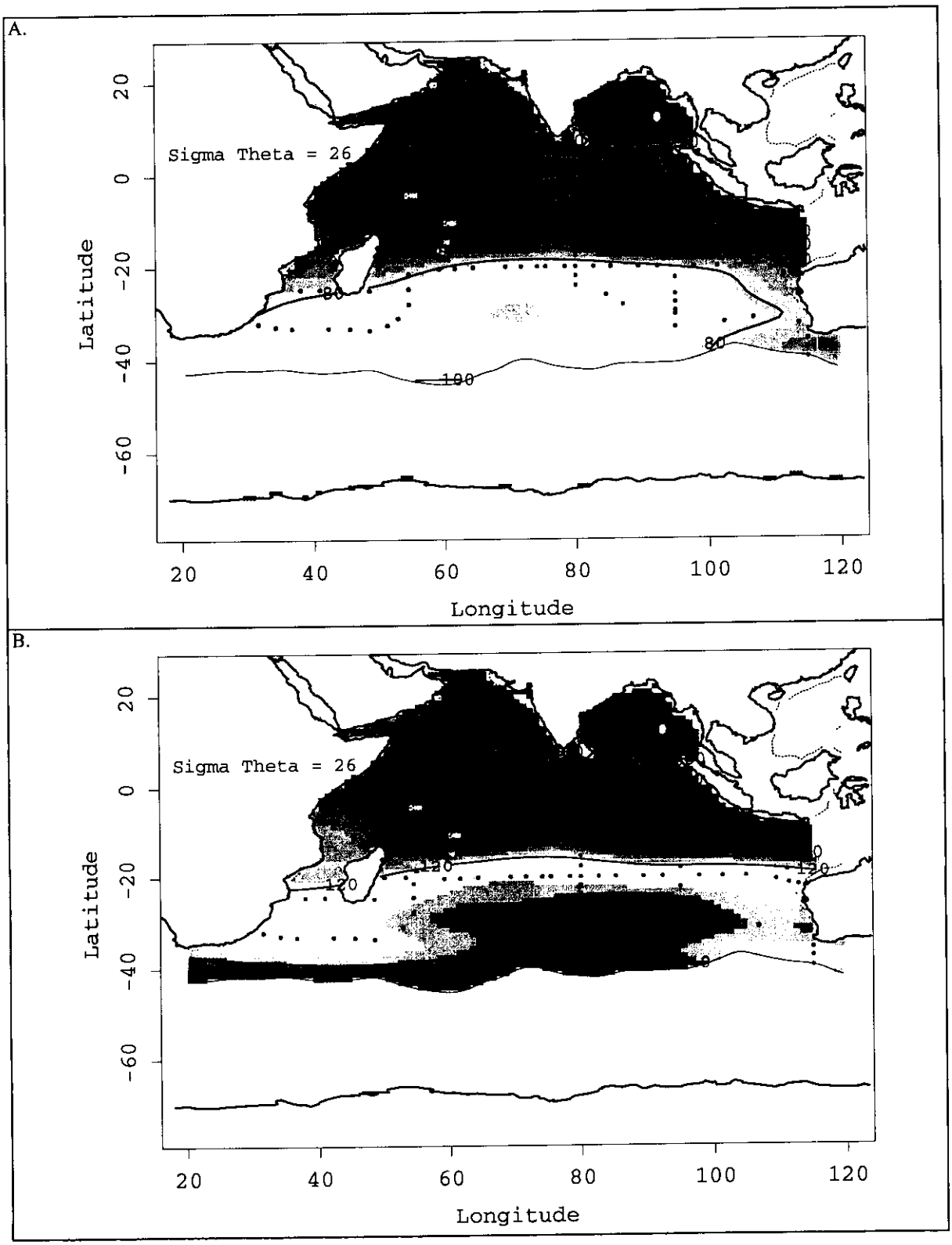

Figure 14: .(A) $\Delta^{14}C$ and (B) bomb-produced $\Delta^{14}C$ on σ_θ=26.0

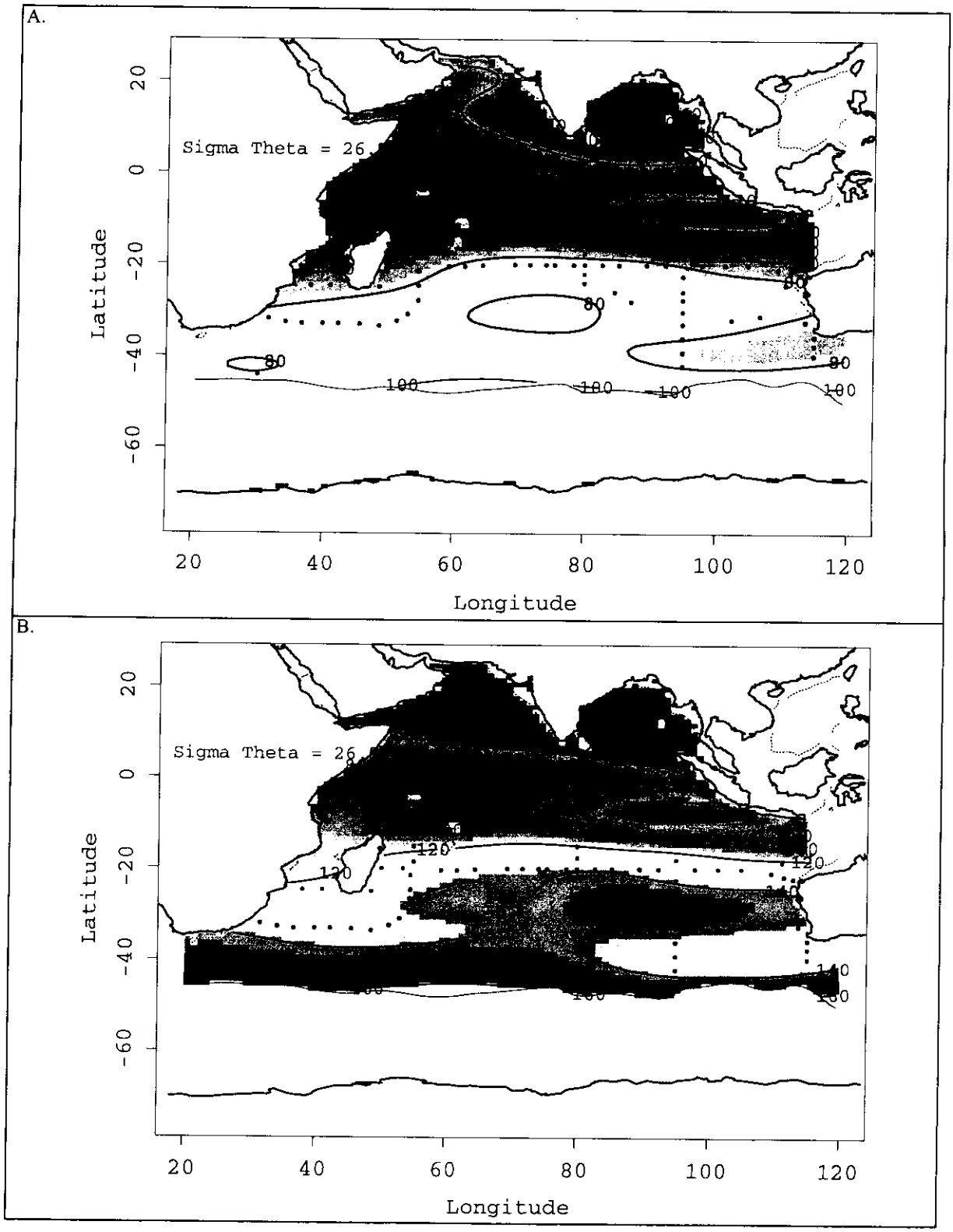

Figure 15: .(A) $\Delta^{14}C$ and (B) bomb-produced $\Delta^{14}C$ on σ_θ=26.5

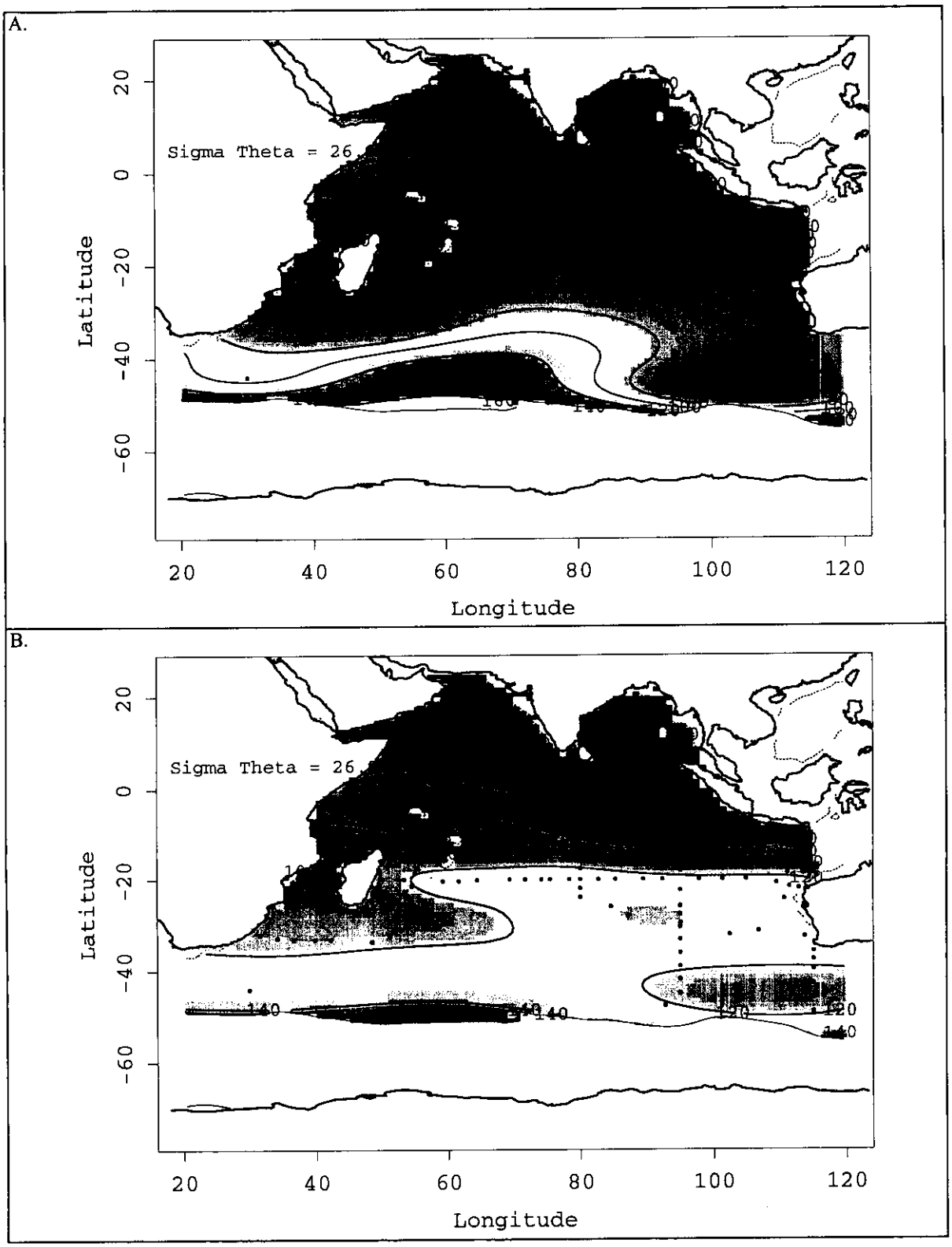

Figure 16: .(A) $\Delta^{14}C$ and (B) bomb-produced $\Delta^{14}C$ on σ_θ=26.8

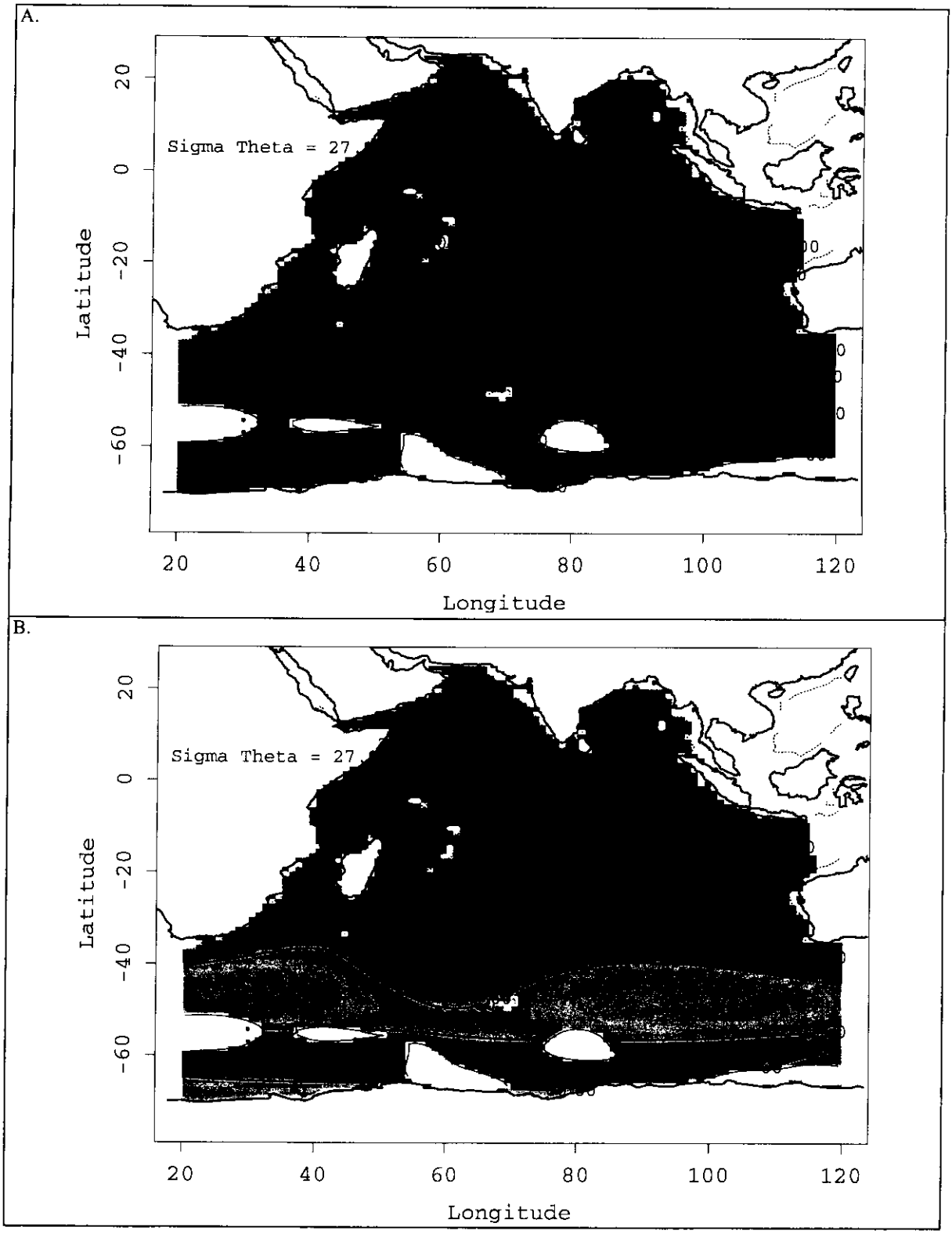

Figure 17: .(A) $\Delta^{14}C$ and bomb-produced (B) $\Delta^{14}C$ on σ_θ=27.1

5.0 References and Supporting Documentation

Bard, E., M. Arnold, H.G. Ostlund, P. Maurice, P. Monfray and J.-C. Duplessy, Penetration of bomb radiocarbon in the tropical Indian Ocean measured by means of accelerator mass spectrometry, *Earth Planet. Sci. Lett., 87*, 379-389, 1988.

Broecker, W.S., S. Sutherland and W. Smethie, Oceanic radiocarbon: Separation of the natural and bomb components, *Global Biogeochemical Cycles, 9(2)*, 263-288, 1995.

Chambers, J.M. and Hastie, T.J., 1991, Statistical Models in S, Wadsworth & Brooks, Cole Computer Science Series, Pacific Grove, CA, 608pp.

Chambers, J.M., Cleveland, W.S., Kleiner, B., and Tukey, P.A., 1983, Graphical Methods for Data Analysis, Wadsworth, Belmont, CA.

Cleveland, W.S., 1979, Robust locally weighted regression and smoothing scatterplots, J. Amer. Statistical Assoc., 74, 829-836.

Cleveland, W.S. and S.J. Devlin, 1988, Locally-weighted regression: An approach to regression analysis by local fitting, J. Am. Statist. Assoc, 83:596-610.

Elder, K.L. A.P. McNichol and A.R. Gagnon, Reproducibility of seawater, inorganic and organic carbon ^{14}C results at NOSAMS, *Radiocarbon, 40(1)*, 223-230, 1998

Joyce, T., and Corry, C., *eds*., Corry, C., Dessier, A., Dickson, A., Joyce, T., Kenny, M., Key, R., Legler, D., Millard, R., Onken, R., Saunders, P., Stalcup, M., *contrib*., Requirements for WOCE Hydrographic Programme Data Reporting, WHPO Pub. 90-1 Rev. 2, 145pp., 1994.

Key, R.M., WOCE Pacific Ocean radiocarbon program, *Radiocarbon, 38(3)*, 415-423, 1996.

Key, R.M., P.D. Quay, G.A. Jones, A.P. McNichol, K.F. Von Reden and R.J. Schneider, WOCE AMS Radiocarbon I: Pacific Ocean results; P6, P16 & P17, *Radiocarbon, 38(3)*, 425-518, 1996.

Key, R.M. and P. Schlosser, S4P: Final report for AMS ^{14}C samples, Ocean Tracer Lab Technical Report 99-1, January, 1999, 11pp.

Leboucher, V. J. Orr, P. Jean-Babtiste, M. Arnold, P. Monfrey, N. Tisnerat-Laborde, A. Poisson and J.C. Duplessey, Oceanic radiocarbon between Antarctica and South Africa along WOCE section I6 at 30°E, *Radiocarbon, 41*, 51-73, 1999.

McNichol, A.P., G.A. Jones, D.L. Hutton, A.R. Gagnon, and R.M. Key, Rapid analysis of seawater samples at the National Ocean Sciences Accelerator Mass Spectrometry Facility, Woods Hole, MA, *Radiocarbon,* **36** (2):237-246, 1994.

NOSAMS, National Ocean Sciences AMS Facility Data Report #99-043, Woods Hole Oceanographic Institution, Woods Hole, MA, 02543, 2/16/1999.

Osborne, E.A. A.P. McNichol, A.R. Gagnon, D.L. Hutton and G.A. Jones, Internal and external checks in the NOSAMS sample preparation laboratory for target quality and homogeneity, *Nucl. Instr. and Methods in Phys. Res., B92*, 158-161, 1994.

Rubin, S. and R.M. Key, Separating natural and bomb-produced radiocarbon in the ocean: The potential alkalinity method, *Global Biogeochem. Cycles, in press*, 2002.

Sabine, C.L. and R.M. Key, Surface Water and Atmospheric Underway Carbon Data Obtained During the World Ocean Circulation Experiment Indian Ocean Survey Cruises (R/V Knorr, December 1994-January 1996), ORNL/CDIAC-103, NDP-064, Carbon Dioxide Information Analysis Center, Oak Ridge National Laboratory, Oak Ridge TN, 89 pp., 1997.

Sabine, C.L., R. Wanninkhof, R.M. Key, C. Goyet, R. Millero, Seasonal CO_2 fluxes in the tropical Indian Ocean, *Mar. Chem., 72,* 33-53, 2000.

Schneider, R.J. A.P. McNichol, M.J. Nadeau and K.F. von Reden, Measurements of the oxalic acid I/oxalic acid II ratio as a quility control parameter at NOSAMS, *In* Proceedings of the 15th International ^{14}C Conference, *Radiocarbon, 37(2)*, 693-696, 1995.

Stuiver, M. and H.G. Ostlund, GEOSECS Indian Ocean and Mediterranean radiocarbon, *Radiocarbon, 25(1)*, 1-29, 1983.